

Clemson University

TigerPrints

All Dissertations

Dissertations

12-2022

Developmental Effects of Chronic Low-Level Arsenic Exposure in Mouse Embryonic Stem Cells and in Human Induced Pluripotent Stem Cells

M. Chiara Perego
mperego@g.clemson.edu

Follow this and additional works at: https://tigerprints.clemson.edu/all_dissertations



Part of the [Developmental Biology Commons](#), and the [Toxicology Commons](#)

Recommended Citation

Perego, M. Chiara, "Developmental Effects of Chronic Low-Level Arsenic Exposure in Mouse Embryonic Stem Cells and in Human Induced Pluripotent Stem Cells" (2022). *All Dissertations*. 3237.
https://tigerprints.clemson.edu/all_dissertations/3237

This Dissertation is brought to you for free and open access by the Dissertations at TigerPrints. It has been accepted for inclusion in All Dissertations by an authorized administrator of TigerPrints. For more information, please contact kokeefe@clemson.edu.

DEVELOPMENTAL EFFECTS OF CHRONIC LOW-LEVEL ARSENIC EXPOSURE
IN MOUSE EMBRYONIC STEM CELLS AND IN HUMAN INDUCED
PLURIPOTENT STEM CELLS

A Dissertation
Presented to
the Graduate School of
Clemson University

In Partial Fulfillment
of the Requirements for the Degree
Doctor of Philosophy
Biological Sciences

by
Maria Chiara Perego
December 2022

Accepted by:
Dr. Lisa Bain, Committee Chair
Dr. William Baldwin
Dr. Charles Rice
Dr. Yanzhang Wei

ABSTRACT

Arsenic is an environmental contaminant commonly found in food and drinking water. Exposure to arsenic during embryonic development has been linked to reduced muscle growth, disrupted muscle development and locomotor activity, impaired neurodevelopment, reduced IQ, impaired memory and learning deficits. While the mechanisms responsible for developmental changes following *in utero* exposure to arsenic are not well known, one possibility is that arsenic might disrupt proper cellular differentiation. Therefore, we aimed to investigate the mechanisms by which arsenic exposure could alter stem cell differentiation into neurons.

First, we continuously exposed P19 mouse embryonic stem (ES) cells to 0.1 μM (7.5 ppb) arsenic for 28 weeks to assess if chronic, low level arsenic exposure would delay cellular differentiation into neuronal cells. Importantly, this concentration is below the current drinking water standard of 10 ppb. The results show temporal changes of genes associated with pluripotency and cellular differentiation. Specifically, starting at week 12, transcript levels of the pluripotency markers *Sox2* and *Oct4* were increased by 1.9- to 2.5- fold in arsenic-exposed cells. By week 16, SOX2 protein expression was increased, and starting at week 20, the expression of a SOX2 target protein, N-cadherin, was also increased. Concurrently, by week 16, levels of the differentiation marker *Gdf3* were decreased by 3.4- fold, along with the reduced phosphorylation of the GDF3 target protein SMAD2/3.

To investigate the mechanisms responsible for maintaining pluripotency and hindering cellular differentiation into neurons, RNA sequencing was performed in control and arsenic-exposed cells at week 8, 16 and 24. This analysis revealed significant exposure-dependent changes in gene expression starting at week 16. Pathway analysis showed that arsenic exposure disrupts the Hippo signaling pathway, which is involved in pluripotency maintenance and embryonic development. Immunohistochemistry revealed that the ratios between nuclear (active) and

cytoplasmic (inactive) expression of the main effector YAP and the main transcription factor TEAD were significantly increased in arsenic-exposed cells at week 16 and 28. Consistently, expression of the Hippo pathway target genes *Ctgf* and *c-Myc* were also significantly upregulated following arsenic exposure. These results indicate that chronic arsenic exposure impairs the Hippo signaling pathway resulting in increased YAP activation, thereby reducing neuronal differentiation.

Previous studies have shown that P19 cells differentiate into sensory neurons, so we also wanted to investigate whether arsenic impaired differentiation into motor neurons. Thus, we switched to using human induced pluripotent stem (iPS) cells, which can differentiate into day 6 neuroepithelial progenitors (NEPs), day 12 motor neuron progenitors (MNPs), day 18 early motor neurons (MNs) and day 28 mature MNs. During this process, cells were exposed to arsenic concentrations up to 0.75 μM (56.25 ppb), and morphological alterations along with pluripotency and stage-specific neuronal markers were assessed. Day 6 NEPs exposed to arsenic had reduced levels of the neural progenitor/stem cell marker *NES* and neuroepithelial progenitor marker *SOX1*, while levels of these transcripts were increased in MNPs at day 12. Additionally, levels of the motor neuron progenitor marker *OLIG2* were increased in day 12 MNPs while levels of the cholinergic neuron marker *CHAT* were reduced by 2.5- fold in MNPs exposed arsenic. RNA sequencing and pathway analysis showed that the cholinergic synapse pathway was impaired following exposure to 0.5 μM arsenic, and that transcript levels of genes involved in acetylcholine synthesis (*CHAT*), transport (*SLC18A3* and *SLC5A7*) and degradation (*ACHE*) were all downregulated in early motor neurons at day 18. In mature motor neurons at day 28, expression of MAP2 and ChAT protein was significantly downregulated by 2.8- and 2.1- fold, respectively, concomitantly with a reduction in neurite length by 1.8- fold following exposure to 0.5 μM arsenic. Similarly, adult mice exposed to 100 ppb arsenic for five weeks had significantly reduced hippocampal ChAT levels. Taken all

together, the results of the dissertation show that environmentally relevant levels of arsenic have detrimental effects on neuronal differentiation.

DEDICATION

To my grandmother, always.

ACKNOWLEDGMENTS

I would like to acknowledge my advisor and mentor Dr. Lisa Bain for welcoming me in her research lab and for her endless support and encouragement. Dr. Bain has shown on numerous occasions that she is the best mentor I could have asked for and her experience and guidance have been a daily inspiration during my time at Clemson. I would also like to acknowledge my committee members, Dr. William Baldwin, Dr. Charles Rice, and Dr. Yanzhang Wei for serving on my committee and for all their encouragement, help and support. Thanks to Rhonda Reigers Powell for her expertise and support in confocal imaging and to Justin Scott for his assistance with flow cytometry. I would also like to thank our funding sources: NIH (R15ES027651), 2019 COSSAB-GIARD, 2021 and 2021 BSPDC-GIAR.

To my former lab mates Benjamin McMichael, Jordan Jatko and Michael Kellett for their mentoring, help, precious assistance, support and most importantly, friendship. I would have not made it without their support. To my newest lab mates Haley Jo Brashears, Binh Duong, and Scott Ventrello for being great supporters and for sharing the last part of this adventure with me. To my undergrad Nick McMurry, for his invaluable assistance in this project. To my “unofficial lab mates” and my lifetime and newly found friends for supporting, encouraging, and caring about me daily. To my Johnny for being the most dedicated player on my team and my compass when I get lost. To my family, Mom, Dad, and Aunt, for being the most loving, supportive, selfless, and fearless family and for giving me the biggest gift of all: wings to fly and roots to always remember where I come from.

TABLE OF CONTENTS

| | Page |
|--|------|
| TITLE PAGE | i |
| ABSTRACT..... | ii |
| DEDICATION | v |
| ACKNOWLEDGMENTS | vi |
| LIST OF TABLES | ix |
| LIST OF FIGURES..... | x |
| CHAPTER | |
| I. INTRODUCTION | 1 |
| Arsenic in the environment and its effects on human health..... | 1 |
| Arsenic-induced developmental toxicity | 3 |
| Neurotoxicity and muscle toxicity following arsenic exposure during development..... | 4 |
| Arsenic’s impairment of muscle and neuron development <i>in vitro</i> | 5 |
| Signaling pathways regulating pluripotency and differentiation | 6 |
| Cholinergic neurons and brain..... | 15 |
| Embryonic and induced pluripotent stem cells as <i>in vitro</i> models | 17 |
| Dissertation Goals and Objectives | 18 |
| References..... | 22 |
| II. LONG-TERM ARSENIC EXPOSURE IMPAIRS DIFFERENTIATION IN MOUSE EMBRYONAL STEM CELLS..... | 36 |
| Abstract..... | 37 |
| Introduction..... | 38 |
| Methods | 40 |
| Results | 44 |
| Discussion..... | 48 |
| Conclusion | 53 |
| Acknowledgements | 53 |
| References..... | 54 |
| Figures | 60 |

| Table of Contents (Continued) | Page |
|--|------|
| III. ARSENIC IMPAIRS STEM CELL DIFFERENTIATION VIA THE HIPPO SIGNALING PATHWAY | 76 |
| Abstract..... | 77 |
| Introduction..... | 78 |
| Methods | 81 |
| Results | 86 |
| Discussion..... | 89 |
| Conclusion | 95 |
| Acknowledgements | 95 |
| References..... | 96 |
| Figures | 103 |
| IV. ARSENIC IMPAIRS DIFFERENTIATION OF HUMAN INDUCED PLURIPOTENT STEM CELLS INTO CHOLINERGIC MOTOR NEURONS | 122 |
| Abstract..... | 123 |
| Introduction..... | 124 |
| Methods | 126 |
| Results | 133 |
| Discussion..... | 139 |
| Conclusion | 144 |
| Acknowledgements | 144 |
| References..... | 145 |
| Figures | 154 |
| V. CONCLUSION..... | 186 |
| Summary of the main findings..... | 186 |
| The importance of adequate drinking water standards..... | 188 |
| Impairment of the Hippo signaling pathway might have a role in improper neurogenesis following arsenic exposure..... | 189 |
| The effects of arsenic on motor neuron differentiation..... | 190 |
| Arsenic might disrupt synaptic transmission of cholinergic synapses by impairing ion channels | 192 |
| Conclusions..... | 193 |
| References..... | 194 |

LIST OF TABLES

| Table | | Page |
|-------|---|------|
| 2.1 | Cell lineage profiler array differential expression of selected genes | 61 |
| 2.2 | Area under the curve (AUC) measurements for transcript data | 66 |
| S2.3 | Primer sequences for qPCR..... | 72 |
| S3.1 | Primer sequences of genes quantified by qPCR..... | 121 |
| S4.1 | Supplements and growth factors used during differentiation of human iPS cells into motor neurons..... | 173 |
| S4.2 | Roles and chemical structures of supplements and growth factors used during differentiation of human iPS cells into motor neurons | 175 |
| S4.3 | Primer sequences of genes quantified by qPCR..... | 178 |
| S4.4 | Correlation between transcript levels of <i>SOX2</i> , <i>POU5F1</i> and <i>NANOG</i> in human iPS cells exposed to 0, 0.1 or 0.5 μ M arsenic for six days..... | 179 |
| S4.5 | Correlation between transcript levels of <i>SOX2</i> , <i>SOX1</i> and <i>NES</i> in day 6 NEPs exposed to 0, 0.1 or 0.5 μ M arsenic for six days | 180 |

LIST OF FIGURES

| Figure | Page |
|---|------|
| 1.1 TGF- β signaling pathway..... | 8 |
| 1.2 Hippo signaling pathway..... | 12 |
| 1.3 Crosstalk between the Hippo signaling pathway and TGF- β signaling pathway | 13 |
| 2.1 Morphology of day 9 cells exposed to 0 or 0.1 μ M arsenic | 60 |
| 2.2 Acute arsenic exposure alters the expression of neural and oxidative stress-related transcripts | 62 |
| 2.3 Chronic exposure to arsenic alters the expression of pluripotency markers..... | 64 |
| 2.4 SOX2 expression is increased due to arsenic exposure | 67 |
| 2.5 Arsenic exposure results in increased expression and altered patterning of N-cadherin | 69 |
| 2.6 Chronic arsenic exposure does not alter E-cadherin expression | 70 |
| 2.7 Arsenic impairs transcription of <i>Zeb1</i> | 71 |
| S2.1 <i>Gad2</i> and <i>Dcx</i> mRNA expression is not changed following a chronic arsenic exposure..... | 73 |
| S2.2 Gdf3 transcript and pSmad2/3 protein levels are reduced in arsenic exposed cells | 74 |
| S2.3 Changes in antioxidant response genes following acute and chronic arsenic exposure | 75 |
| 3.1 Arsenic exposure drives sample clustering and differential expression of several genes over time | 103 |
| 3.2 Chronic low-level arsenic exposure impairs biological processes related to embryonic development and cellular differentiation..... | 105 |

List of Figures (Continued)

| Figure | Page |
|--|------|
| 3.3 Arsenic impairs expression of key Hippo pathway components..... | 106 |
| 3.4 Arsenic exposure impairs protein expression of the Hippo pathway's core components | 108 |
| 3.5 Chronic low-level arsenic exposure impairs the cellular localization of YAP and TEAD over time | 110 |
| 3.6 Arsenic impairs transcript levels of the YAP1 target genes <i>c-Myc</i> and <i>Ctgf</i> | 112 |
| 3.7 Chronic low-level arsenic exposure impairs CTGF protein levels at week 28..... | 113 |
| S3.1 Chronic low-level arsenic exposure impairs pluripotency, Wnt and TGF- β signaling pathways..... | 115 |
| S3.2 Arsenic exposure does not impair protein levels of Hippo pathway's signal receiver MST1 | 117 |
| S3.3 Arsenic does not impair the expression of key Hippo pathway components at week 8 | 118 |
| S3.4 Arsenic impairs the expression of key Hippo pathway components at week 16..... | 119 |
| S3.5 Arsenic increases protein expression of LATS2 isoforms throughout the exposure | 120 |
| 4.1 Low arsenic levels induce cell death in human iPS cells, but not in neuroepithelial progenitor cells (NEPs) | 154 |
| 4.2 Differential gene expression of key markers during differentiation of human iPS cells into motor neurons | 157 |
| 4.3 Arsenic exposure leads to morphological alterations of MNPs and mature MNs | 158 |
| 4.4 Arsenic exposure impairs transcript levels of motor neuron differentiation markers | 160 |

List of Figures (Continued)

| Figure | Page |
|--|------|
| 4.5 Arsenic exposure drives sample clustering in NEPs and early MNs, and disrupts biological processes related to nervous system development and synapses..... | 163 |
| 4.6 Arsenic exposure downregulates genes involved in acetylcholine synthesis, transport, and degradation in day 18 early MNs..... | 166 |
| 4.7 Arsenic exposure alters MAP2 pattern in day 18 early MNs..... | 168 |
| 4.8 Arsenic exposure reduces neurite length and downregulates levels of MAP2 and ChAT in day 28 mature MNs..... | 170 |
| S4.1 Arsenic increases transcript levels of pluripotency markers <i>SOX2</i> , <i>POU5F1</i> and <i>NANOG</i> in human iPS cells | 181 |
| S4.2 Arsenic exposure impairs glutamatergic synapse, axon guidance and neuroactive ligand-receptors interaction pathway | 182 |
| S4.3 Arsenic exposure impairs ChAT protein levels in adult mice hippocampi | 185 |

CHAPTER ONE

INTRODUCTION

Arsenic in the environment and its effects on human health

Arsenic is a well-known environmental contaminant and one of the most abundant trace elements found in the Earth's crust (Shankar et al., 2014; Mochizuki, 2019). Arsenic can enter ground water through leaching from bedrock, but it can also originate from anthropogenic sources (Chung et al., 2014), including metallurgic and mining activities, pesticide use, and other industrial activities (Bundschuh et al., 2012; McClintock et al., 2012; Palma-Lara et al., 2020). Specifically, arsenic can be found in insecticides, pesticides, paints, wood preservatives and electric circuits (Palma-Lara et al., 2020). Moreover, arsenic not only has industrial and agricultural applications, but also chemical and medicinal ones as arsenic trioxide is used as chemotherapy drug in lymphoma and leukemia therapy (Novick and Warrell, 2000).

Arsenic is considered as one of the most hazardous chemicals in the world (Shankar et al., 2014) as millions of people in multiple countries are exposed to arsenic-contaminated groundwater (Ravenscroft et al., 2009; Mochizuki, 2019). Arsenic exposure results in serious health problems after both acute and chronic exposure. Adverse acute effects include weakness, nausea, diarrhea, vomiting, and abdominal pain as well as generalized vasodilation, cardiovascular collapse, and respiratory and kidney failure (Guha Mazumder, 2008; Mitra et al., 2019; Bjorklund et al., 2020). Chronic exposure has been strongly correlated with carcinogenesis, increased blood pressure, diabetes, increased production of reactive oxygen species and induced genomic instability through cytogenetic and epigenetic alterations (Kitchin, 2001; Kitchin and Conolly, 2010; Medeiros et al., 2012; Sarkar and Paul, 2016; Shankar et al., 2014; Mauro et al., 2016; Palma-Lara et al., 2020). The International Agency for Research on Cancer (IARC) has classified arsenic as a human and

rodent carcinogen as it increases the risk of skin, bladder, lung, and kidney tumors (IARC, 2012). For instance, chronic arsenic exposure can result in skin hyperpigmentation and hyperkeratosis (Rahman et al., 2006; Yajima et al., 2017; Yu et al., 2006; Yu et al., 2018; Zeng and Zhang, 2020) as well as skin cancers including squamous carcinoma and basal cell carcinoma (Wei et al., 2018a; Yu et al., 2006; Zeng and Zhang, 2020). Additionally, a positive correlation has been reported between urinary arsenic concentration and higher risk of squamous cell carcinoma in a study conducted in New Hampshire (Gossai et al., 2017). Similarly, an association between high arsenic concentrations and increased incidences of kidney (Jaafarzadeh et al., 2022), bladder and lung cancer (Mendez et al., 2017) has been reported.

The U.S. Environmental Protection Agency and the World Health Organization have established a concentration of 10 ppb arsenic as the drinking water standard; however, millions of people are currently exposed to arsenic concentrations not only above 10 ppb but also more than 50 ppb, which is the concentration limit established in several Asian countries (Ravenscroft et al., 2009; Shankar et al., 2014). Elevated arsenic concentrations have been documented in various countries including China, Mexico, Chile, Argentina, India, Bangladesh, and USA (Smith et al., 2000; Bundschuh et al., 2009; Bhattacharya et al., 2011; Bjorklund et al., 2020). These reports indicate that in the U.S., approximately 2.1 million people obtain drinking water from domestic wells with an arsenic concentration above 10 $\mu\text{g/L}$. States with high concentrations of arsenic include Maine, New Hampshire, Nevada, Arizona, California, and southern Texas (Ayotte et al., 2017). Additionally, it has been previously estimated that on average, an individual adult in the U.S. ingests 3.2 $\mu\text{g/kg}$ of arsenic daily, with a total dietary intake of 1.8-11.4 $\mu\text{g/day}$ for males and 1.3-9.4 $\mu\text{g/day}$ for females (Meacher et al., 2002; Sarkar and Paul, 2016). In addition to water, dietary intake of foods contaminated through irrigation or pesticide use such as vegetables, rice and rice products, grains, fruits, and juices is also associated with long-term arsenic exposure (Jackson

et al., 2012; Karagas et al., 2019). Consumption of rice has been increasing since the 1960's (FAO, 2002), and an average concentration of 0.2 mg/kg arsenic has been reported in rice grown in Europe and the U.S. (Zavala and Duxbury, 2008; Karagas et al., 2019).

Arsenic-induced developmental toxicity

Several human epidemiological and animal model studies have shown that arsenic can cause adverse effects during embryonic development including death, structural abnormalities, impaired growth, and functional deficiencies (Chattopadhyay et al., 2002; Milton et al., 2005; Rahman et al., 2007; Martinez-Finley et al., 2011; Jing et al., 2012, Pandey et al., 2017). Importantly, placental and cord blood arsenic concentrations are comparable with maternal blood levels, as arsenic can readily cross the placental barrier (Concha et al., 1998a; Hall et al., 2007; Henn et al., 2016). For instance, a study conducted in Argentina on eleven pregnant women exposed to arsenic concentrations of 200 µg/L through drinking water showed that median concentrations of arsenic in maternal blood and cord blood were 11 and 9 µg/L, respectively. Additionally, the authors reported that the median arsenic concentration in the placenta was 34 µg/kg (Concha et al., 1998b). Similarly, Hall et al. (2007) observed a strong correlation between arsenic concentration in cord blood (15.7 µg/L on average) and maternal blood (11.9 µg/L on average) in 101 pregnant women from Bangladesh exposed to an average arsenic concentration of 90 µg/L through drinking water. However, arsenic has been measured at lower concentrations in breast milk; in particular, a study conducted by Concha et al. (1998a) reported an average arsenic concentration in human milk of 2.3 µg/kg with an average maternal blood concentration of 10 µg/L.

Prenatal arsenic exposure and impaired fetal development play a central role in the adverse health outcomes reported in newborns following arsenic exposure. For instance, studies conducted in Bangladesh reported increased spontaneous abortion, stillbirth and preterm birth in women

chronically exposed to arsenic through drinking water (Ahmad et al., 2001; Milton et al., 2005). Similarly, Rahman et al. (2007) observed that drinking tube-well water with an arsenic concentration above 50 µg/L significantly increased the incidence of infant death and fetal loss by 1.17- and 1.14- fold, respectively. Additionally, a cohort study conducted in Antofagasta, Chile, showed that arsenic exposure during embryogenesis and early life is associated with increased risk of cancer and other diseases in adult life. The authors reported increased mortality for all cancers by 1.7-fold and increased mortality from circulatory diseases and diseases involving the genitourinary system by 1.7- and 2- fold, respectively (Smith et al., 2012). Moreover, perinatal exposure to inorganic arsenic has been linked with increased cardiovascular diseases (Rahman et al., 2013) as well as enhanced infection susceptibility and impaired lung function (Dauphine et al., 2011; Farzan et al., 2013).

Neurotoxicity and muscle toxicity following arsenic exposure during development

Studies conducted in children suggest that arsenic impairs proper neurological development as arsenic exposure is associated with impaired cognitive function, decreased verbal and full-scale IQ and disrupted learning and memory abilities (Hamadani et al., 2011; Thomas, 2013; Wasserman et al., 2014). Adverse effects of arsenic on myogenesis and muscle differentiation have also been reported. For instance, epidemiological studies have shown that perinatal and postnatal arsenic exposure is associated with low birth weight, reduced head, and chest circumferences at birth (Hopenhayn et al., 2003; Rahman et al., 2009; Saha et al., 2012; Almberg et al., 2017), as well as decreased body weight gain and length from birth to two years of age (Saha et al., 2012) and impaired motor function (Parvez et al., 2011).

Similar adverse effects have been reported using rodent models in which administration of inorganic arsenic to pregnant dams induces fetal malformations, impaired development, disrupted

locomotor activity and behavioral deficits (DeSesso et al., 1998; Chattopadhyay et al., 2002; Rodriguez et al., 2002; Wang et al., 2006). Chattopadhyay and his coworkers (2002) observed that 300 ppb of sodium arsenite administered through drinking water to pregnant rats resulted in decreased spontaneous behavior of neonatal pups and their brain cells had membrane damage, increased concentration of reactive oxygen and nitric oxide species along with reduced DNA and protein synthesis. Consistently, hippocampal neurogenesis, cell morphology and gene expression patterns have been impaired following exposure to 50 ppb arsenic during fetal development (Tyler and Allan, 2013). Tyler and Allan (2013) observed upregulation of genes involved in apoptosis and Alzheimer's disease such as *Apbb1* and *ApoE* and a downregulation of genes involved in neurite growth such as *Dcx* as well as growth factor *Fgf2* and transcription factor *Pax6*. Moreover, disrupted learning abilities and memory behavior have been reported in adult mice following *in utero* arsenic exposure to 50 ppb of arsenic as sodium arsenate (Martinez-Finley et al., 2009; Thomas, 2013). A recent study showed that perinatal arsenic exposure is associated with hypoactivity (decreased distance traveled and time moving), impaired memory functions and the disruption of the cholinergic system in the brain (Chandravanshi et al., 2019). Specifically, the authors observed a significant decrease in AChE activity and ChAT protein levels in the frontal cortex and the hippocampus of rats perinatally exposed to 2 or 4 mg/kg body weight of sodium arsenite. Similarly, Yadav et al. (2011) reported reduced AChE activity in the hippocampus and frontal cortex along with reduced ChAT protein expression and decreased memory and learning performance in adult rats exposed to sodium arsenite for four weeks.

Arsenic's impairment of muscle and neuron development *in vitro*

In vitro studies also show that arsenic exposure impairs neurogenesis and myogenesis. Arsenic inhibits neurogenesis and impairs neurite outgrowth in Neuro-2a and PC12 cells (Frankel

et al., 2009; Wang et al., 2010; Aung et al., 2013), in differentiated SH-SY5Y cells (Niyomchan et al., 2015) and in primary neurons (Maekawa et al., 2013). For example, exposure to 1 and 2 μM of arsenic for two days reduced neurite length of primary neurons (Maekawa et al., 2013). Similarly, the offspring of pregnant mice exposed to 1.13 mM sodium arsenite showed a significant decrease in neurite length in their prelimbic cortical neurons, along with impaired cognitive behavior and adaptation (Aung et al., 2016).

Additionally, impairment of muscular differentiation has been observed following arsenic exposure. Yen et al. (2010) reported that exposure to arsenic trioxide inhibits myotube formation, muscular differentiation and reduces myogenin expression in murine C2C12 myoblast cells. Consistently, C2C12 myoblasts exposed to 20 nM sodium arsenite had impaired myotube formation caused by inhibition of myogenic transcription factor expression (Steffens et al., 2011). P19 mouse embryonic stem (ES) cells acutely exposed to sodium arsenite presented suppressed skeletal muscle and neuronal differentiation (Hong and Bain, 2012; McCoy et al., 2015; Bain et al., 2016). Hong and Bain hypothesized that the observed reduced expression of β -catenin could be involved in the downregulated expression of neurogenic and myogenic markers through the Wnt/ β -catenin signaling pathway.

Signaling pathways regulating pluripotency and differentiation

Pluripotent embryonic stem cells are characterized by their ability to self-renew and differentiate into all functional cell types of the three germ layers. Maintenance of the stem cell phenotype is ensured by the essential transcriptional core formed by the transcription factors SOX2, OCT4 and NANOG (Rodda et al., 2005). This core regulates the expression of genes important for self-renewal and pluripotency and inhibits the expression of genes involved in differentiation (Swain et al., 2020). A known cooperative interaction exists between SOX2 and OCT4, and SOX2

and OCT4 bind to the NANOG promoter in human ES cells and mice, suggesting the presence of a pluripotency regulatory network (Rodda et al., 2005). Several signaling pathways are involved in the balance between pluripotency and differentiation (Tanabe, 2015). Here, I discuss the role of the TGF- β , GDF3 and the Hippo signaling pathway in pluripotency and cellular differentiation.

TGF- β signaling pathway

The mammalian transforming growth factor (TGF) β superfamily is composed of 33 members that regulate of many key processes of embryonic development. Members of this superfamily display distinct, sometimes opposite effects on target cells, depending on the cellular context, presence of other ligands, dosage, and identity of the cytokine (Massague, 2012; Tykwinska et al., 2013). The ligands of this superfamily include activins, inhibins, bone morphogenic proteins (BMPs), Nodal and growth differentiation factors (GDFs). They are synthesized as pre-propeptides, and cleavage results in a mature peptide that undergoes homo- or hetero-dimerization resulting in the production of signaling molecules. TGF- β signaling is involved in cell fate determination including germ cells (through activation of BMP/GDF signaling), muscle tissue (through activation of TGF- β /activin/nodal signal) and nervous tissue (through inhibition of BMP/GDF signaling) (Levine and Brivanlou, 2006a). Specifically, SMAD2/3 signaling promotes mesodermal differentiation along with neural induction, through BMP inhibition; while BMP signaling induces epidermis cell fate activation (Levine and Brivanlou, 2006a).

TGF- β signaling pathway ligands are functionally classified into two main categories based on their homology and which SMAD proteins they activate (Lander et al., 2001; Levine et al., 2009). As shown in Figure 1.1, TGF- β /activin/Nodal ligands activate Smad2/3 whereas BMPs/GDFs activate Smad1/5/8 (Shi and Massague, 2003; Levine et al., 2009); however, there are several atypical ligands that have been characterized in either category based on homology. The

high number of TGF- β ligands could indicate significant redundancy or reflect a subtle regulation and variation among these ligands (Levine et al., 2009). TGF- β signaling pathway receptors are transmembrane serine-threonine kinase glycoproteins that are divided into two groups: type I receptors that contain a kinase domain preceded by a GS domain, and type II receptors which contain a kinase domain (Wrana et al., 1994; Zamani and Brown, 2011). The order of receptors' activation differs for different ligands; for instance, ligands that activate SMAD2/3 proteins bind to type II receptors that then recruit and phosphorylate type I receptor, forming a complex that activate SMAD 2 or 3. On the other hand, some BMPs can form this tertiary complex by binding to either type I or type II receptors first (Chang et al., 2002; Zamani and Brown, 2011).

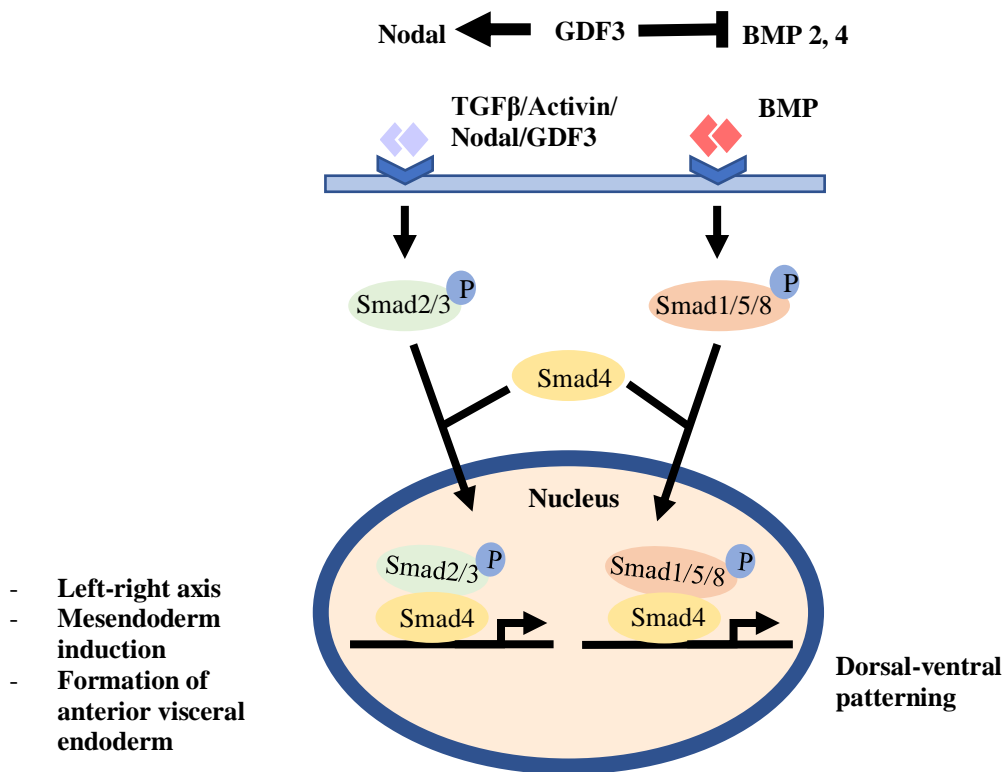


Figure 1.1. TGF- β signaling pathway. Dimeric ligands bind to type I and type II receptors triggering the phosphorylation of R-SMADS (SMADS 2/3 for TGF β /Activin/Nodal/GDF3 signaling and SMADS 1/5/8 for BMP signaling). Phosphorylated R-SMADS associate with Smad4 (common SMAD) forming a complex that translocates to the nucleus to regulate transcription of downstream target genes.

Once activated through phosphorylation, R-SMADs associate with SMAD4 (common SMAD) forming a complex that enters the nucleus to regulate transcription of target genes (Hill, 2009; Zamani and Brown, 2011) (Figure 1.1). The nuclear accumulation of this complex is partially regulated by the nuclear transporter TAZ (Varelas et al., 2008) while the signaling is terminated by nuclear phosphatases which dephosphorylate R-SMADs causing the complex dissociation and the recycling of SMADs in the cytoplasm (Lin et al., 2006).

Role of GDF3 during embryonic development

Growth and differentiation factor 3 (GDF3) is a member of the TGF- β superfamily and a pluripotency-associated factor. GDF3 possesses several unique characteristics compared to the other members of the TGF- β family; it lacks the 4th cysteine in the ligand's mature region, usually involved in intermolecular interactions between TGF- β ligands, is mostly found in cells in its unprocessed prepro form and has not been found in any non-mammalian species (Levine and Brivanlou, 2006a).

Previous studies have shown that GDF3 is expressed in ES cells and the early embryo where it regulates pluripotency and differentiation potential (McPherron et al., 1993; Clark et al., 2004; Levine and Brivanlou, 2006a,b; Han et al., 2016). Moreover, GDF3 appears to be required during embryonic development as GDF3-null mice have mispositioned or absent anterior visceral endoderm (Chen et al., 2006). Depending on the cellular context, GDF3 shows contradictory roles: it increases cell proliferation of B16 myeloma cells (Ehira et al., 2010), inhibits proliferation of breast cancer cells (Li et al., 2012a) and promotes PC12 neuronal cell differentiation (Li et al., 2012b; Han et al., 2016).

GDF3 can act as both a BMP signaling inhibitor and a TGF- β /Activin/ Nodal signaling activator (Bansho et al., 2017). In fact, it is involved in both canonical pathways triggered by TGF- β family members: (1) extracellular inhibition of BMPs (Levine and Brivanlou, 2006b) and (2) induction of Smad2/3 phosphorylation (Chen et al., 2006; Andersson et al., 2008; Tykwinska et al., 2013) (Figure 1). In 2003, Sato et al. conducted a global analysis of gene expression in undifferentiated vs differentiated human ES cells, which revealed that very few ligands are involved in early embryogenesis. Interestingly, GDF3 is one of the three TGF- β superfamily members that was highly expressed during pluripotency and dramatically decreased during differentiation. Additionally, two research groups have studied GDF3 function during embryogenesis, obtaining conflicting results regarding how it activates signaling pathways. One study demonstrated that exogenous GDF3 inhibits BMP signaling thereby blocking SMAD1/5/8 phosphorylation (Levine and Brivanlou, 2006a), and the other showed activation of TGF- β /activin/Nodal signaling through SMAD2/3 which induced BMPs antagonists and indirectly inhibited SMAD1/5/8 (Chen et al., 2006). There are also species differences. GDF3 overexpression in human ES cells maintained markers of pluripotency while, reduced GDF3 levels in mouse ES cells prevented *in vitro* differentiation by maintaining significant levels of OCT3/4, SOX2 and FGF5, a marker of pluripotent epiblast and decreasing levels of brachyury, a mesoderm marker (Levine and Brivanlou, 2006a).

Andersson et al. (2007) have argued that GDF3 is poorly processed and its signaling activity is only detectable when combined with other TGF- β ligands, such as Nodal. They hypothesized that the results obtained by Chen et al. (2006) showing that 35% of GDF3-null mice displayed embryonic defects while the remaining reached adulthood could suggest the presence of other ligands with redundant functions to GDF3 (Andersson et al., 2007; Ye et al., 2010). Consistently, more recent studies conducted in zebrafish have shown that GDF3 is an essential

cofactor in Nodal signaling during establishment of the embryonic axis (Bisgrove et al., 2017), head and trunk mesoderm and endoderm formation, and dorsal-ventral patterning (Pelliccia et al., 2017) while zygotic expression of GDF3 is necessary for embryonic development (Pelliccia et al., 2017). Additionally, GDF3 was identified as a potential driver of notochord differentiation in an *in vitro* study conducted using human ES cells (Diaz-Hernandez et al., 2019).

Hippo signaling pathway

The Hippo signaling pathway controls tissue homeostasis by regulating embryonic and organ development, tissue regeneration, cell proliferation, apoptosis, tumorigenesis, and maintenance of stem cell pluripotency (Yu et al., 2013; Wang et al., 2017; Chen et al., 2019). Various proteins are involved in the signaling and initiation of the Hippo pathway, including Merlin, KIBRA, RASSFs, and Ajuba, the Cadherin-Catenin complex, G-protein coupled receptors and Wnt/ β -catenin signal pathways (Li et al., 2013). Briefly, following upstream activation, the signal receiver MST1/2 phosphorylates LATS1/2, which then phosphorylates the major co-activators of the pathway, YAP and TAZ, at multiple residues (Piccolo et al., 2014; Papaspyropoulos et al., 2018). Phosphorylation of the YAP/TAZ complex results in cytoplasmic retention through binding of phosphorylatedSer112-YAP to 14-3-3 proteins, or in ubiquitination and subsequent degradation (Meng et al., 2016). Conversely, the un-phosphorylated YAP/TAZ complex translocates to the nucleus where it interacts with members of the transcriptional enhancer factor domain (TEAD) family to regulate transcriptional activation and the expression of target genes involved in cellular proliferation and apoptosis inhibition (Zhao et al., 2008; Stein et al., 2015; Chen et al., 2019) (Figure 1.2).

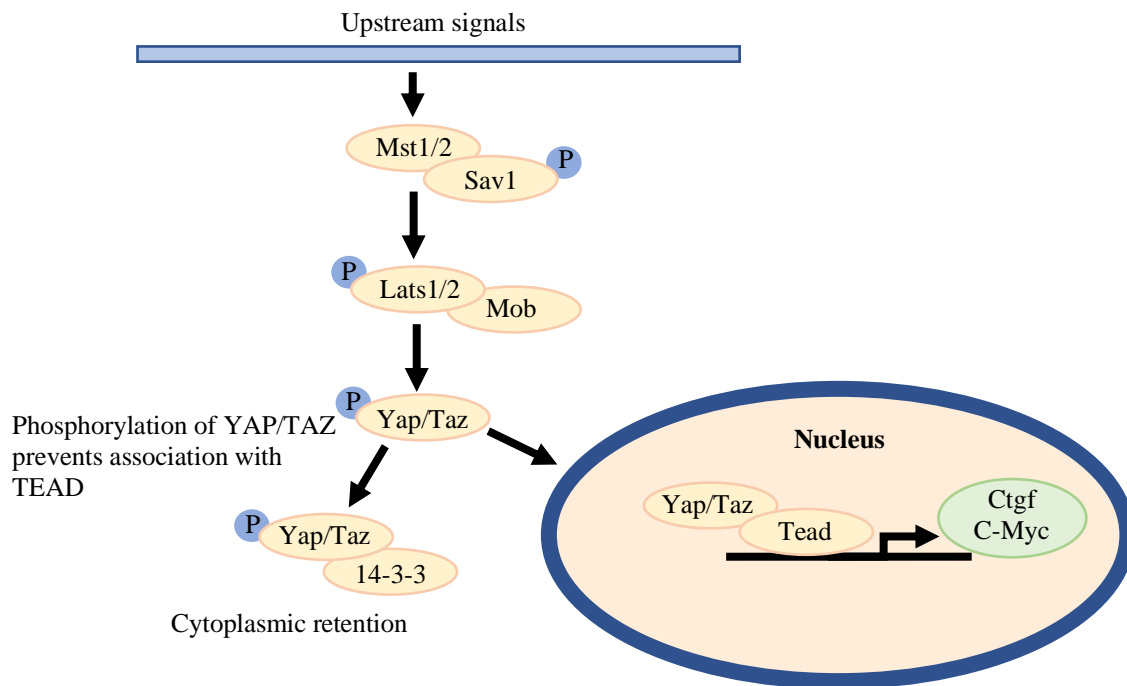


Figure 1.2. Hippo signaling pathway. Activation of the Hippo signaling through signal receiver Mst1/2 triggers a phosphorylation cascade, resulting in phosphorylation and cytoplasmic retention of the main effector Yap. Active (dephosphorylated) Yap enters the nucleus where it interacts with Tead transcription factors to regulate transcription of downstream target genes.

YAP and TAZ are WW domain proteins in the Hippo pathway; this domain recognizes proline-rich peptide motifs and phosphorylated serine/threonine-proline sites while mediating protein-protein interactions. Additionally, YAP and TAZ cannot directly bind to the DNA and consequently, they act as co-activators with DNA-binding transcriptional factors to regulate expression of target genes (Chen et al., 2019). The WW domain of both proteins recognizes and binds the transcriptional enhancer factor domain (TEAD) family, mainly TEAD1-4, to drive the expression of numerous genes involved in cell proliferation, survival and migration, including c-MYC, cyclin E, connective tissue growth factor (CTGF), AXL, and fibroblast growth factor (Figure 2) (Piccolo et al., 2014; Wang et al., 2014; Totaro et al., 2018; Chen et al., 2019; Shea et al., 2020).

Moreover, YAP/TAZ complex can regulate transcription through multiple mechanisms; for instance, it can work synergistically with other transcription factors such as RUNX1/2 and members of the SMAD family by forming a complex with phosphorylated SMAD2/3 (Fig. 1.3).

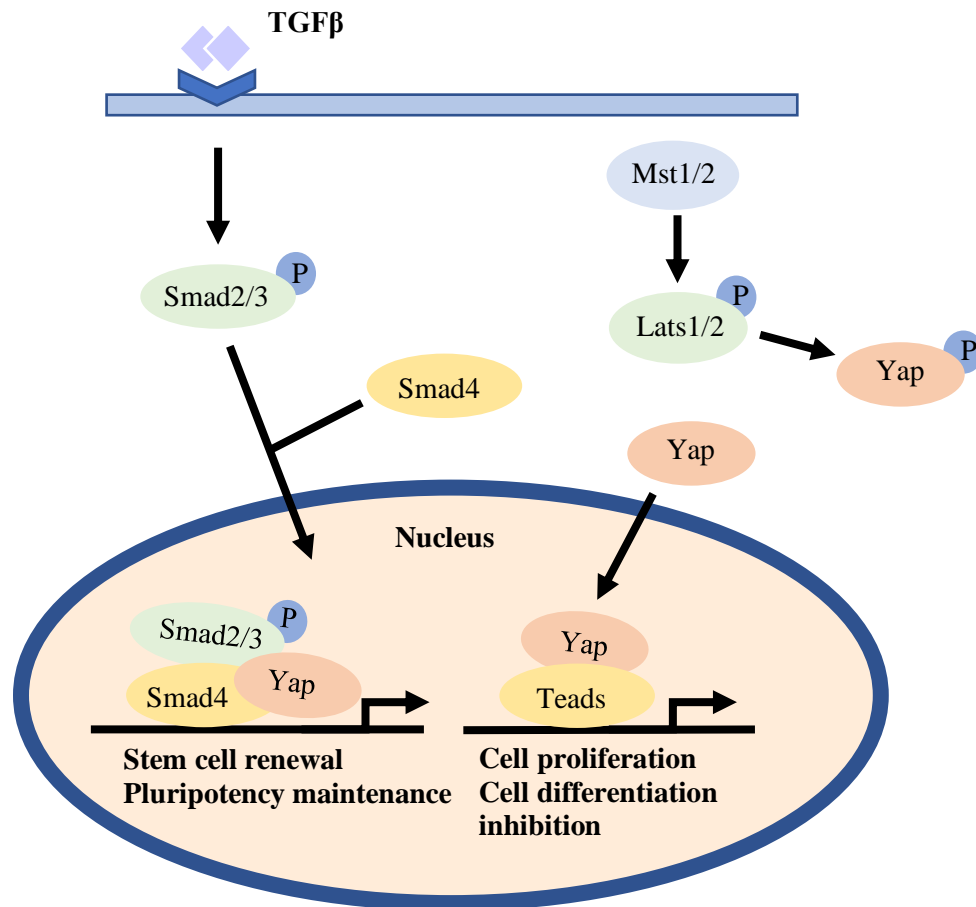


Figure 1.3. Crosstalk between the Hippo signaling pathway and TGF-β signaling pathway. When the Hippo signaling pathway is inactive, YAP is present in its non-phosphorylated form and is able to translocate to the nucleus where it promotes transcriptional activity by binding to TEAD or by forming a complex with phosphorylated SMAD2/3.

This complex translocates from the cytoplasm to the nucleus where it binds the pluripotency regulator OCT4 and TEAD transcription factors. To drive mesendoderm specification and differentiation, the TAZ/YAP-TEAD-OCT4 complex dissociates from SMAD2/3, allowing the latter to activate the forkhead transcription factor FOXH1 (Lian et al., 2010; Chen et al., 2019).

Additionally, YAP/TAZ can inhibit transcription of target genes by binding to nucleosome remodeling histone deacetylase (NuRD) (Kim et al., 2015). Further, YAP is involved in miRNA production by regulating miRNA processing enzymes (Chaulk et al., 2014; Mori et al., 2014); for instance, it enhances the production of miR-130a which represses vestigial-like family member 4, a known YAP/TAZ inhibitor (Shen et al., 2015); thus, forming a positive feedback loop to increase YAP activity (Chen et al., 2019).

Previous studies have shown that the Hippo pathway plays a role in early embryonic development and cell fate specification (Piccolo et al., 2014; Fu et al., 2017; Wang et al., 2017; Chen et al., 2019; Barzegari et al., 2020). For instance, embryonic death and cell division arrest at the blastomere stage has been reported in YAP knockout mice (Morin-Kensicki et al., 2006; Tamm et al., 2011; Chen et al., 2019). Similarly, defects in cell fate specification and embryonic lethality at the morula stage have been observed in YAP and TAZ double knockout mice (Nishioka et al., 2009; Yu et al., 2015; Chen et al., 2019). YAP is highly expressed in cultured ES cells and its activation leads to pluripotency maintenance, progenitor cell expansion, and inhibition of cellular differentiation (Camargo et al., 2007; Cao et al., 2008; Lian et al., 2010; Ramos and Camargo, 2012; Li et al., 2013; Piccolo et al., 2014; McKey et al., 2016; Chen et al., 2019). Conversely, during cellular differentiation, YAP is inactivated and sequestered in the cytoplasm leading to downregulation of pluripotency markers such as SOX2, OCT4 and NANOG (Lian et al., 2010; Chen et al., 2019). Recent *in vitro* studies have reported that YAP overexpression in ES cells results in upregulation of pluripotency markers and maintenance of stem cell phenotypes concomitant with inhibition of cellular differentiation even under differentiation culture conditions (Lian et al., 2010; Li et al., 2013) while YAP knockdown leads to decreased expression of genes associated with pluripotency, impaired stem cell phenotype and properties (Lian et al., 2010).

Previous studies have shown that the Hippo signaling pathway is involved in neuronal differentiation (Lin et al., 2012; Cheng et al., 2020) of human iPS cells (Musah et al., 2014; Sun et al., 2014) and that YAP overexpression inhibits neuronal differentiation in murine primary cortical progenitors (Lin et al., 2012) and P19 ES cells (Zhang et al., 2012). Similarly, exogenous GDF3 inhibited growth of PC12 while inducing neuronal differentiation (Li et al., 2012). Moreover, previous studies have shown that *GDF3* is abundantly transcribed in both murine and human brain, especially in the cerebral cortex, hippocampus, and cerebellum, suggesting that it may play an important role in the central nervous system (Hexige et al., 2005).

Cholinergic neurons and brain

A high density of cholinergic neurons has been reported in the cerebral cortex and the limbic system, including the hippocampus (Hampel et al., 2018). Additionally, cholinergic neurons (motor neurons) are also found at the neuromuscular junctions where they are involved in the regulation of skeletal muscle activity and contraction by the central nervous system (Tintignac et al., 2015). Specifically, spinal motor neurons convey signals from the central nervous system to the peripheral skeletal muscle to regulate complex movements. Sensory neurons are also involved in movement regulation by providing feedback loops necessary for movement tuning (Stifani, 2014). Formation of a functional and integrated neuronal circuitry between the central nervous system, motor neurons, skeletal muscle and sensory neurons is necessary to ensure proper motor activity and refined coordination. Consequently, impairment of the neuromuscular junctions results in loss of motor neuron activity, progressive muscle weakness and paralysis. A wide range of disorders have been linked to impairment of the neuromuscular junctions, which can be caused by structural changes in the entirety of the neuromuscular junctions or by presynaptic or postsynaptic defects. Genetic mutations, drugs or toxins can disrupt the proper function of essential proteins that regulate

the signaling between presynaptic motor neurons and postsynaptic muscle fiber (Verschuuren et al., 2016).

The main excitatory neurotransmitter used by cranial, spinal, and visceral motor neurons of the sympathetic and parasympathetic systems is acetylcholine (Moore, 1993). Studies have shown that acetylcholine in the brain plays a role in synaptic transmission and plasticity, neuronal network formation, neuronal excitability and memory and learning functions (Power, 2004; Picciotto et al., 2012; Hampel et al., 2018). Briefly, acetylcholine is synthesized in the cytoplasm of the nerve terminal by the enzyme choline acetyltransferase (ChAT), which transfers the acetyl group from acetyl-CoA to choline (Deutch and Roth, 2014). The neurotransmitter is then loaded through the vesicular acetylcholine transporter (VAChT) into presynaptic vesicles and stored until it is released in the synaptic cleft (Arvidsson et al., 1997; Fisher and Wonnacott, 2012), where it interacts with acetylcholine receptors located on the postsynaptic cell membrane to propagate the electrical signal (Richardson and Makhaeva, 2014). Acetylcholine activity is terminated by acetylcholinesterase (AChE), which rapidly hydrolyzes acetylcholine into choline and acetate (Trang and Khandhar, 2022). Lastly, the high-affinity choline transporter (ChT) is responsible for the choline re-uptake into the cholinergic neuron (Choudhary et al., 2017).

While extensive research has been conducted to investigate the impairment of cholinergic neurons and the inhibition of acetylcholinesterase activity as targets of pesticides, including organophosphate and carbamate (Kamanyire and Karalliedde, 2004; Chen, 2012; Carey et al., 2013; King and Aaron, 2015; Petreski et al., 2020), little is known about their role in arsenic-induced neurotoxicity and neurodevelopmental toxicity. Importantly, assessment of neurotoxicity in the human species has been challenging to investigate because of the inaccessibility of the human brain, the limited access to postmortem brain samples, the complex protocols and procedures

necessary to perform *ex vivo* techniques and to maintain live neurons *in vitro* and the differences in genetic background of non-primate species (Ochalek et al., 2016).

Embryonic and induced pluripotent stem cells as *in vitro* models

ES cells are pluripotent self-renewable cells derived from the inner cell mass of the early blastocyst embryos (Thomson et al., 1998; Dhara and Stice, 2008; Chuang et al., 2015). Under appropriate culture conditions, these cells possess the ability to differentiate into functional neural stem cells; which can further differentiate into various neural cell types including functional neurons, cholinergic neurons, oligodendrocytes, and glial cells (Shin et al., 2006; Dhara and Stice, 2008; Hong and Do, 2019; Hosseini et al., 2020). Importantly, differentiation of ES cells as adherent cultures accurately reproduces *in vivo* embryonic formation of the neuroectoderm (Noisa et al., 2015; Hosseini et al., 2020). Therefore, *in vitro* models using ES cells are a promising tool in toxicity assessment and to investigate neuronal differentiation and early developmental events (Kim et al., 2020). Species-specific developmental timing is retained in *in vitro* models. For instance, a recent study has shown that neuronal differentiation is accelerated in mouse epiblast stem cells compared to human ES cells under identical differentiation conditions (Barry et al., 2017). Consistently, Rayon et al. (2019) have reported that differentiation of ES cells into motor neurons is twice as fast in mouse cells compared with human cells. Additionally, although many developmental features and gene expression changes are conserved in early development of mouse and human embryonic cells (Gabdouline et al., 2015), differences in gene expression patterns have been reported (Fougerousse et al., 2000; Gabdouline et al., 2015). Therefore, these differences must be considered when performing developmental toxicity studies.

P19 cells are murine pluripotent stem cells derived from a teratocarcinoma (McBurney, 1993). These cells have the ability to differentiate the three germ layers (ectoderm, mesoderm and

endoderm) and are therefore a useful model to investigate early developmental stages and cell fate determination (McBurney, 1993; van der Heyden and Defize, 2003). To promote differentiation, three-dimensional cell aggregates, defined as embryoid bodies, are initially formed to resemble the embryonic inner cell mass (Martins and Evans, 1974; 1975; van der Heyden and Defize, 2003). With the use of chemicals or small molecules, the differentiation of P19 cells typically progresses to form cardiac myocytes, skeletal myocytes, and neurons (McBurney et al., 1982; McBurney, 1993; van der Heyden and Defize, 2003). This murine cell line provides a valuable and convenient model to perform developmental studies *in vitro*, as these cells are easy to maintain and culture and do not require basement membrane matrix and various supplements. However, known species-specific differences in the metabolism and whole-body retention of arsenic between mice and humans exist, with mice being able to methylate arsenic more rapidly and eliminate it through the urine (Vahter, 2002; Drobná et al., 2010; States et al., 2011). These differences in sensitivity to arsenic toxicity must be considered if one wants to develop a reliable and accurate risk assessment.

Therefore, I decided to use human iPS cells as second *in vitro* model. To our knowledge, few studies have been conducted using human iPS cells to assess the effects of arsenic exposure on cellular differentiation. Additionally, differentiation of P19 cells previously conducted in our lab typically lead to formation of sensory neurons; therefore, a different *in vitro* model was needed to generate motor neurons.

Dissertation Goals and Objectives

The overall goal of the proposed research is to determine whether environmentally relevant arsenic concentrations disrupt cellular differentiation into sensory and/or motor neurons, and to investigate the mechanisms by which this occurs. I hypothesize that the impaired neuronal development seen in rodent and epidemiological studies is due to alterations in pluripotency genes

and key signaling molecules involved in neurogenesis. The results will further our understanding about how *in utero* arsenic exposure impairs signaling pathways pivotal for proper fetal development. Notably, the concentrations used in this study represent a realistic embryonic exposure, as previous human epidemiological studies have reported similar arsenic concentrations in cord blood and placenta.

Aim 1: Determine whether chronic low level arsenic exposure impairs differentiation of mouse embryonic stem cells

Previous studies conducted in our lab have shown that acute exposure to 0.5 μM (37.5 ppb) arsenic inhibits skeletal muscle and neuronal differentiation in mouse ES cells. Nonetheless, it is unclear whether chronic exposure to a lower arsenic concentration could have similar effects. Murine P19 ES cells were previously exposed to 0 or 0.1 μM (7.5 ppb) arsenic as sodium arsenite for 28 weeks. Every four weeks, cells were induced to differentiate into skeletal myotubes and neuronal progenitor cells. RNA and proteins were extracted from day 9 differentiated cells for further analysis. To investigate if arsenic exposure impairs cellular differentiation, transcript levels of pluripotency markers *Sox2* and *Oct4* and of the neuronal progenitor marker *Gdf3* were assessed through qPCR analysis. GDF3 is a ligand of the TGF- β family, so Western blots were performed to evaluate the protein expression of downstream targets including SMAD1/5/9, SMAD2/3, and their phosphorylated forms.

Aim 2: Investigate the mechanisms involved in arsenic-induced cellular differentiation impairment

To further understand the effects of chronic low-level arsenic exposure on the differentiation of mouse ES cells in an unbiased way, RNA-Sequencing and bioinformatic analyses

were done. RNA extracted from day 9 differentiated cells at week 8, 16 and 24 was sequenced and differential expression analysis was conducted using DESeq2 to identify key regulators that are disrupted following chronic arsenic exposure. Differentially expressed genes were identified and used to determine biochemical pathways impaired after arsenic exposure through KEGG pathway analysis. These analyses confirmed the impairment of several pathways known to be disrupted following arsenic exposure, including the Wnt/ β -catenin and the TGF- β signaling pathway. Our results also indicated that the Hippo signaling pathway is impaired following arsenic exposure. This pathway is also involved in embryonic development and its role in arsenic-induced developmental toxicity has been poorly investigated. qPCR analysis was used to confirm the differential expression of key genes identified through RNA-sequencing, and to assess transcript expression of two downstream target genes - *c-Myc* and *Ctgf*. Immunoblotting and IHC were used to investigate protein expression and cellular localization of key regulators of the Hippo signaling pathway including LATS, YAP, TEAD and CTGF.

Aim 3: Determine the effects of low-level arsenic exposure during the differentiation of human motor neurons

Significant differences in the metabolism and whole-body retention of arsenic have been reported in different mammalian species (Vahter, 2002; Drobná et al., 2010; States et al., 2011). Therefore, we assessed whether the differentiation impairment seen in murine stem cells also occurs using human iPS cells. Human iPS cells were exposed to 0, 0.25, 0.5 or 0.75 μ M arsenic during their differentiation into neuroepithelial progenitors, motor neuron progenitors, early motor neurons, and mature motor neurons. Morphological changes were assessed, and qPCR analysis was conducted to determine transcript levels of pluripotency markers, including *SOX2* and *POU5F1* and differentiation markers, including *SOX1*, *NES*, *OLIG2* and *CHAT*. RNA sequencing followed

by bioinformatics was used to identify and investigate pathways that were altered in neuroepithelial progenitors and early motor neurons due to arsenic exposure. These analyses revealed that pathways associated with cholinergic and glutamatergic synapse were inhibited following arsenic exposure. Scholl tracings were used to measure neurite length in arsenic-exposed cells, while IHC was used to confirm the involvement of key proteins in cholinergic neuron development, including MAP2 and ChAT.

References

- Ahmad, S.A., Sayed, M.H., Barua, S., Khan, M.H., Faruquee, M.H., Jalil, A., Hadi, S.A., Talukder, H.K., 2001. Arsenic in drinking water and pregnancy outcomes. *Environ. Health Perspect.* 109, 629-631.
- Almberg, K.S., Turyk, M.E., Jones, R.M., Rankin, K., Freels, S., Graber, J.M., Stayner, L.T., 2017. Arsenic in drinking water and adverse birth outcomes in Ohio. *Environ. Res.* 157, 52-59.
- Andersson, O., Bertolino, P., Ibáñez, C.F., 2007. Distinct and cooperative roles of mammalian Vg1 homologs GDF1 and GDF3 during early embryonic development. *Dev. Biol.* 311, 500-511.
- Andersson, O., Korach-Andre, M., Reissmann, E., Ibáñez, C.F., Bertolino, P., 2008. Growth/differentiation factor 3 signals through ALK7 and regulates accumulation of adipose tissue and diet-induced obesity. *Proc. Natl. Acad. Sci. U. S. A.* 105, 7252-7256.
- Arvidsson, U., Riedl, M., Elde, R., Meister, B., 1997. Vesicular acetylcholine transporter (VACHT) protein: a novel and unique marker for cholinergic neurons in the central and peripheral nervous systems. *J. Comp. Neurol.* 378, 454-467.
- Aung, K.H., Kurihara, R., Nakashima, S., Maekawa, F., Nohara, K., Kobayashi, T., Tsukahara, S., 2013. Inhibition of neurite outgrowth and alteration of cytoskeletal gene expression by sodium arsenite. *Neurotoxicology* 34, 226-235.
- Aung, K.H., Kyi-Tha-Thu, C., Sano, K., Nakamura, K., Tanoue, A., Nohara, K., Kakeyama, M., Tohyama, C., Tsukahara, S., Maekawa, F., 2016. Prenatal Exposure to Arsenic Impairs Behavioral Flexibility and Cortical Structure in Mice. *Front. Neurosci.* 10, 137.
- Ayotte, J.D., Medalie, L., Qi, S.L., Backer, L.C., Nolan, B.T., 2017. Estimating the High-Arsenic Domestic-Well Population in the Conterminous United States. *Environ. Sci. Technol.* 51, 12443-12454.
- Bain, L.J., Liu, J.T., League, R.E., 2016. Arsenic inhibits stem cell differentiation by altering the interplay between the Wnt3a and Notch signaling pathways. *Toxicol. Rep.* 3, 405-413.
- Bansho, Y., Lee, J., Nishida, E., Nakajima-Koyama, M., 2017. Identification and characterization of secreted factors that are upregulated during somatic cell reprogramming. *FEBS letters* 591, 1584-1600.
- Barry, C., Schmitz, M.T., Jiang, P., Schwartz, M.P., Duffin, B.M., Swanson, S., Bacher, R., Bolin, J.M., Elwell, A.L., McIntosh, B.E., Stewart, R., Thomson, J.A., 2017. Species-specific developmental timing is maintained by pluripotent stem cells ex utero. *Dev. Biol.* 423, 101-110.
- Barzegari, A., Gueguen, V., Omid, Y., Ostadrahimi, A., Nouri, M., Pavon-Djavid, G., 2020. The role of Hippo signaling pathway and mechanotransduction in tuning embryoid body formation and differentiation. *J. Cell. Physiol.* 235, 5072-5083.

- Bhattacharya, P., Hossain, M., Rahman, S.N., Robinson, C., Nath, B., Rahman, M., Islam, M.M., Von Bromssen, M., Ahmed, K.M., Jacks, G., Chowdhury, D., Rahman, M., Jakariya, M., Persson, L.A., Vahter, M., 2011. Temporal and seasonal variability of arsenic in drinking water wells in Matlab, southeastern Bangladesh: a preliminary evaluation on the basis of a 4 year study. *J. Environ. Sci. Health. A. Tox. Hazard. Subst. Environ. Eng.* 46, 1177-1184.
- Bisgrove, B.W., Su, Y., Yost, H.J., 2017. Maternal Gdf3 is an obligatory cofactor in Nodal signaling for embryonic axis formation in zebrafish. *eLife* 6.
- Bjorklund, G., Tippairote, T., Rahaman, M.S., Aaseth, J., 2020. Developmental toxicity of arsenic: a drift from the classical dose-response relationship. *Arch. Toxicol.* 94, 67-75.
- Bundschuh, J., Armienta, M.A., Birkle, P., Bhattacharya, P., Matschullat, A.B., Mukherjee, A.B., 2009. *Natural Arsenic in Groundwater of Latin America — Occurrence, health impact and remediation.* CRC Press.
- Bundschuh, J., Litter, M.I., Parvez, F., Roman-Ross, G., Nicolli, H.B., Jean, J., Liu, C., Lopez, D., Armienta, M.A., Guilherme, L.R., Cuevas, A.G., Cornejo, L., Cumbal, L., Toujaguez, R., 2012. One century of arsenic exposure in Latin America: A review of history and occurrence from 14 countries. *Sci. Total Environ.* 429, 2-35.
- Camargo, F.D., Gokhale, S., Johnnidis, J.B., Fu, D., Bell, G.W., Jaenisch, R., Brummelkamp, T.R., 2007. YAP1 increases organ size and expands undifferentiated progenitor cells. *Curr. Biol.* 17, 2054-2060.
- Cao, X., Pfaff, S.L., Gage, F.H., 2008. YAP regulates neural progenitor cell number via the TEA domain transcription factor. *Genes Dev.* 22, 3320-3334.
- Carey, J.L., Dunn, C., Gaspari, R.J., 2013. Central respiratory failure during acute organophosphate poisoning. *Respiratory physiology & neurobiology* 189, 403-410.
- Chandravanshi, L.P., Gupta, R., Shukla, R.K., 2019. Arsenic-Induced Neurotoxicity by Dysfunctioning Cholinergic and Dopaminergic System in Brain of Developing Rats. *Biol. Trace Elem. Res.* 189, 118-133.
- Chang, H., Brown, C.W., Matzuk, M.M., 2002. Genetic analysis of the mammalian transforming growth factor-beta superfamily. *Endocr. Rev.* 23, 787-823.
- Chattopadhyay, S., Bhaumik, S., Nag Chaudhury, A., Das Gupta, S., 2002. Arsenic induced changes in growth development and apoptosis in neonatal and adult brain cells in vivo and in tissue culture. *Toxicol. Lett.* 128, 73-84.
- Chaulk, S.G., Lattanzi, V.J., Hiemer, S.E., Fahlman, R.P., Varelas, X., 2014. The Hippo pathway effectors TAZ/YAP regulate dicer expression and microRNA biogenesis through Let-7. *The Journal of biological chemistry* 289, 1886-1891.

- Chen, C., Ware, S.M., Sato, A., Houston-Hawkins, D.E., Habas, R., Matzuk, M.M., Shen, M.M., Brown, C.W., 2006. The Vg1-related protein Gdf3 acts in a Nodal signaling pathway in the pre-gastrulation mouse embryo. *Development* 133, 319-329.
- Chen, Y., 2012. Organophosphate-Induced Brain Damage: Mechanisms, Neuropsychiatric and Neurological Consequences, and Potential Therapeutic Strategies. *J. Agric. Saf. Health* 18, 246-247.
- Chen, Y.A., Lu, C.Y., Cheng, T.Y., Pan, S.H., Chen, H.F., Chang, N.S., 2019. WW Domain-Containing Proteins YAP and TAZ in the Hippo Pathway as Key Regulators in Stemness Maintenance, Tissue Homeostasis, and Tumorigenesis. *Front. Oncol.* 9, 60.
- Cheng, J., Wang, S., Dong, Y., Yuan, Z., 2020. The Role and Regulatory Mechanism of Hippo Signaling Components in the Neuronal System. *Frontiers in immunology* 11, 281.
- Choudhary, P., Armstrong, E.J., Jorgensen, C.C., Piotrowski, M., Barthmes, M., Torella, R., Johnston, S.E., Maruyama, Y., Janiszewski, J.S., Storer, R.I., Skerratt, S.E., Benn, C.L., 2017. Discovery of Compounds that Positively Modulate the High Affinity Choline Transporter. *Frontiers in Molecular Neuroscience*, n/a.
- Chuang, J., Tung, L., Lin, Y., 2015. Neural differentiation from embryonic stem cells in vitro: An overview of the signaling pathways. *World journal of stem cells* 7, 437-447.
- Chung, J.Y., Yu, S.D., Hong, Y.S., 2014. Environmental source of arsenic exposure. *J. Prev. Med. Public Health.* 47, 253-257.
- Clark, A.T., Rodriguez, R.T., Bodnar, M.S., Abeyta, M.J., Cedars, M.I., Turek, P.J., Firpo, M.T., Reijo Pera, R.A., 2004. Human STELLAR, NANOG, and GDF3 genes are expressed in pluripotent cells and map to chromosome 12p13, a hotspot for teratocarcinoma. *Stem Cells* 22, 169-179.
- Concha, G., Vogler, G., Lezcano, D., Nermell, B., Vahter, M., 1998. Exposure to inorganic arsenic metabolites during early human development. *Toxicol. Sci.* 44, 185-190.
- Concha, G., Vogler, G., Nermell, B., Vahter, M., 1998. Low-level arsenic excretion in breast milk of native Andean women exposed to high levels of arsenic in the drinking water. *Int. Arch. Occup. Environ. Health* 71, 42-46.
- Dauphine, D.C., Ferreccio, C., Guntur, S., Yuan, Y., Hammond, S.K., Balmes, J., Smith, A.H., Steinmaus, C., 2011. Lung function in adults following in utero and childhood exposure to arsenic in drinking water: preliminary findings. *Int. Arch. Occup. Environ. Health* 84, 591-600.
- DeSesso, J.M., Jacobson, C.F., Scialli, A.R., Farr, C.H., Holson, J.F., 1998. An assessment of the developmental toxicity of inorganic arsenic. *Reprod. Toxicol.* 12, 385-433.
- Deutch, A.Y., Roth, R.H., 2004. Chapter 9 – Pharmacology and biochemistry of synaptic transmission: classic transmitters. *From Molecules to Networks*: 245-278.

- Dhara, S.K., Stice, S.L., 2008. Neural differentiation of human embryonic stem cells. *J. Cell. Biochem.* 105, 633-640.
- Diaz-Hernandez, M.E., Khan, N.M., Trochez, C.M., Yoon, T., Maye, P., Presciutti, S.M., Gibson, G., Drissi, H., 2020. Derivation of notochordal cells from human embryonic stem cells reveals unique regulatory networks by single cell-transcriptomics. *J. Cell. Physiol.* 235, 5241-5255.
- Drobna, Z., Walton, F.S., Paul, D.S., Xing, W., Thomas, D.J., Styblo, M., 2010. Metabolism of arsenic in human liver: the role of membrane transporters. *Arch. Toxicol.* 84, 3-16.
- Ehira, N., Oshiumi, H., Matsumoto, M., Kondo, T., Asaka, M., Seya, T., 2010. An embryo-specific expressing TGF- β family protein, growth-differentiation factor 3 (GDF3), augments progression of B16 melanoma. *Journal of experimental & clinical cancer research : CR* 29, 135.
- Food and Agricultural Organization of the United Nations (FAO). *Rice Information*; FAO: Rome, Italy, 2002; Vol. 3.
- Farzan, S.F., Korrick, S., Li, Z., Enelow, R., Gandolfi, A.J., Madan, J., Nadeau, K., Karagas, M.R., 2013. In utero arsenic exposure and infant infection in a United States cohort: a prospective study. *Environ. Res.* 126, 24-30.
- Fisher, S.K., Wonnacott, S. (2012). Chapter 13 – Acetylcholine. *Basic neurochemistry (eight edition)*: 258-282.
- Fougerousse, F., Bullen, P., Herasse, M., Lindsay, S., Isabelle, R., Wilson, D., Suel, L., Durand, M., Robson, S., Abitbol, M., Beckmann, J.S., Strachan, T., 2000. Human-mouse differences in the embryonic expression patterns of developmental control genes and disease genes. *Hum. Mol. Genet.* 9, 165.
- Frankel, S., Concannon, J., Brusky, K., Pietrowicz, E., Giorgianni, S., Thompson, W.D., Currie, D.A., 2009. Arsenic exposure disrupts neurite growth and complexity in vitro. *Neurotoxicology* 30, 529-537.
- Fu, V., Plouffe, S.W., Guan, K.L., 2017. The Hippo pathway in organ development, homeostasis, and regeneration. *Curr. Opin. Cell Biol.* 49, 99-107.
- Gabdoulline, R., Kaisers, W., Gaspar, A., Meganathan, K., Doss, M.X., Jagtap, S., Hescheler, J., Sachinidis, A., Schwender, H., 2015. Differences in the Early Development of Human and Mouse Embryonic Stem Cells. *PloS one* 10, e0140803.
- Gossai, A., Zens, M.S., Punshon, T., Jackson, B.P., Perry, A.E., Karagas, M.R., 2017. Rice Consumption and Squamous Cell Carcinoma of the Skin in a United States Population. *Environ. Health Perspect.* 125, 097005.
- Guha Mazumder, D.N., 2008. Chronic arsenic toxicity & human health. *Indian J. Med. Res.* 128, 436-447.

- Hall, M., Gamble, M., Slavkovich, V., Liu, X., Levy, D., Cheng, Z., van Geen, A., Yunus, M., Rahman, M., Pilsner, J.R., Graziano, J., 2007. Determinants of arsenic metabolism: blood arsenic metabolites, plasma folate, cobalamin, and homocysteine concentrations in maternal-newborn pairs. *Environ. Health Perspect.* 115, 1503-1509.
- Hamadani, J.D., Tofail, F., Nermell, B., Gardner, R., Shiraji, S., Bottai, M., Arifeen, S.E., Huda, S.N., Vahter, M., 2011. Critical windows of exposure for arsenic-associated impairment of cognitive function in pre-school girls and boys: a population-based cohort study. *Int. J. Epidemiol.* 40, 1593-1604.
- Hampel, H., Mesulam, M., Cuello, A.C., Farlow, M.R., Giacobini, E., Grossberg, G.T., Khachaturian, A.S., Vergallo, A., Cavedo, E., Snyder, P.J., Khachaturian, Z.S., 2018. The cholinergic system in the pathophysiology and treatment of Alzheimer's disease. *Brain : a journal of neurology* 141, 1917-1933.
- Han, M., Park, S., Do, H., Chung, H., Song, H., Kim, J., Kim, N., Park, K., Kim, J., 2016. Growth and Differentiation Factor 3 Is Transcriptionally Regulated by OCT4 in Human Embryonic Carcinoma Cells. *Biol. Pharm. Bull.* 39, 1802-1808.
- Henn, B.C., Ettinger, A. S., Hopkins, M. R., Jim, R., Amarasiriwardena, C., Christiani, D. C., et al., 2016. Prenatal arsenic exposure and birth outcomes among a population residing near a mining-related superfund site. *Environmental Health Perspectives*, 124(8), 1308-1315.
- Hexige, S., Guo, J., Ma, L., Sun, Y., Liu, X., Ma, L., Yan, X., Li, Z., Yu, L., 2005. Expression pattern of growth/differentiation factor 3 in human and murine cerebral cortex, hippocampus as well as cerebellum. *Neurosci. Lett.* 389, 83-87.
- Hill, C.S., 2009. Nucleocytoplasmic shuttling of Smad proteins. *Cell Res.* 19, 36-46.
- Hong, G.M., Bain, L.J., 2012. Sodium arsenite represses the expression of myogenin in C2C12 mouse myoblast cells through histone modifications and altered expression of Ezh2, Glp, and Igf-1. *Toxicol. Appl. Pharmacol.* 260, 250-259.
- Hong, Y.J., Do, J.T., 2019. Neural Lineage Differentiation From Pluripotent Stem Cells to Mimic Human Brain Tissues. *Frontiers in bioengineering and biotechnology* 7, 400.
- Hopenhayn, C., Ferreccio, C., Browning, S.R., Huang, B., Peralta, C., Gibb, H., Hertz-Picciotto, I., 2003. Arsenic exposure from drinking water and birth weight. *Epidemiology* 14, 593-602.
- Hosseini, K., Lekholm, E., Ahemaiti, A., Fredriksson, R., 2020. Differentiation of Human Embryonic Stem Cells into Neuron, Cholinergic, and Glial Cells. *Stem cells international* 2020, 8827874.
- IARC Working Group on the Evaluation of Carcinogenic Risks to Humans. Arsenic, Metals, Fibres and Dusts. Lyon (FR): International Agency for Research on Cancer; 2012. (IARC Monographs on the Evaluation of Carcinogenic Risks to Humans, No. 100C.

- Jaafarzadeh, N., Poormohammadi, A., Almasi, H., Ghaedrahmat, Z., Rahim, F., Zahedi, A., 2022. Arsenic in drinking water and kidney cancer: a systematic review. *Rev. Environ. Health* .
- Jackson, B.P., Taylor, V.F., Punshon, T., Cottingham, K.L., 2012. Arsenic concentration and speciation in infant formulas and first foods. *Pure and Applied Chemistry.Chimie Pure et Appliquee* 84, 215-223.
- Jing, J., Zheng, G., Liu, M., Shen, X., Zhao, F., Wang, J., Zhang, J., Huang, G., Dai, P., Chen, Y., Chen, J., Luo, W., 2012. Changes in the synaptic structure of hippocampal neurons and impairment of spatial memory in a rat model caused by chronic arsenite exposure. *Neurotoxicology* 33, 1230-1238.
- Kamanyire, R., Karalliedde, L., 2004. Organophosphate toxicity and occupational exposure. *Occupational Medicine* 54, 69-75.
- Karagas, M.R., Punshon, T., Davis, M., Bulka, C.M., Slaughter, F., Karalis, D., Argos, M., Ahsan, H., 2019. Rice Intake and Emerging Concerns on Arsenic in Rice: a Review of the Human Evidence and Methodologic Challenges. *Current Environmental Health Reports* 6, 361-372.
- Kim, J.W., Im, I., Kim, H., Jeon, J.S., Kang, E.H., Jo, S., Chun, H.S., Yoon, S., Kim, J.H., Kim, S.K., Park, H.J., 2020. Live-cell screening platform using human-induced pluripotent stem cells expressing fluorescence-tagged cytochrome P450 1A1. *FASEB J.* 34, 9141-9155.
- Kim, M., Kim, T., Johnson, R.L., Lim, D., 2015. Transcriptional co-repressor function of the hippo pathway transducers YAP and TAZ. *Cell reports* 11, 270-282.
- King, A.M., Aaron, C.K., 2015. Organophosphate and carbamate poisoning. *Emerg. Med. Clin. North Am.* 33, 133-151.
- Kitchin, K.T., 2001. Recent advances in arsenic carcinogenesis: modes of action, animal model systems, and methylated arsenic metabolites. *Toxicol. Appl. Pharmacol.* 172, 249-261.
- Kitchin, K.T., Conolly, R., 2010. Arsenic-induced carcinogenesis--oxidative stress as a possible mode of action and future research needs for more biologically based risk assessment. *Chem. Res. Toxicol.* 23, 327-335.
- Lander, E.S., Linton, L.M., Birren, B., Nusbaum, C., Zody, M.C., Baldwin, J., Devon, K., Dewar, K., Doyle, M., FitzHugh, W., Funke, R., Gage, D., Harris, K., Heaford, A., Howland, J., Kann, L., Lehoczy, J., LeVine, R., McEwan, P., McKernan, K., Meldrim, J., Mesirov, J.P., et al., 2001. Initial sequencing and analysis of the human genome. *Nature* 409, 860-921.
- Levine, A.J., Brivanlou, A.H., 2006a. GDF3, a BMP inhibitor, regulates cell fate in stem cells and early embryos. *Development* 133, 209-216.
- Levine AJ, Brivanlou AH., 2006b. GDF3 at the crossroads of TGF-beta signaling. *Cell Cycle*;5(10):1069-73.

- Levine, A.J., Levine, Z.J., Brivanlou, A.H., 2009. GDF3 is a BMP inhibitor that can activate Nodal signaling only at very high doses. *Dev. Biol.* 325, 43-48.
- Li, C., Srivastava, R.K., Elmets, C.A., Afaq, F., Athar, M., 2013. Arsenic-induced cutaneous hyperplastic lesions are associated with the dysregulation of Yap, a Hippo signaling-related protein. *Biochem. Biophys. Res. Commun.* 438, 607-612.
- Li, P., Chen, Y., Mak, K.K., Wong, C.K., Wang, C.C., Yuan, P., 2013. Functional role of Mst1/Mst2 in embryonic stem cell differentiation. *PLoS One* 8, e79867.
- Li, Q., Liu, X., Wu, Y., An, J., Hexige, S., Ling, Y., Zhang, M., Yang, X., Yu, L., 2012a. The conditioned medium from a stable human GDF3-expressing CHO cell line, induces the differentiation of PC12 cells. *Mol. Cell. Biochem.* 359, 115-123.
- Li, Q., Ling, Y., Yu, L., 2012b. GDF3 inhibits the growth of breast cancer cells and promotes the apoptosis induced by Taxol. *Journal of Cancer Research & Clinical Oncology* 138, 1073-9.
- Lian, I., Kim, J., Okazawa, H., Zhao, J., Zhao, B., Yu, J., Chinnaiyan, A., Israel, M.A., Goldstein, L.S., Abujarour, R., Ding, S., Guan, K.L., 2010. The role of YAP transcription coactivator in regulating stem cell self-renewal and differentiation. *Genes Dev.* 24, 1106-1118.
- Lin, X., Duan, X., Liang, Y., Su, Y., Wrighton, K.H., Long, J., Hu, M., Davis, C.M., Wang, J., Brunnicardi, F.C., Shi, Y., Chen, Y., Meng, A., Feng, X., 2006. PPM1A functions as a Smad phosphatase to terminate TGFbeta signaling. *Cell* 125, 915-928.
- Lin, Y., Ding, J., Li, M., Yeh, T., Wang, T., Yu, J., 2012. YAP regulates neuronal differentiation through Sonic hedgehog signaling pathway. *Exp. Cell Res.* 318, 1877-1888.
- Maekawa, F., Tsuboi, T., Oya, M., Aung, K.H., Tsukahara, S., Pellerin, L., Nohara, K., 2013. Effects of sodium arsenite on neurite outgrowth and glutamate AMPA receptor expression in mouse cortical neurons. *Neurotoxicology* 37, 197-206.
- Martin, G.R., Evans, M.J., 1975. Differentiation of clonal lines of teratocarcinoma cells: formation of embryoid bodies in vitro. *Proc. Natl. Acad. Sci. U. S. A.* 72, 1441-1445.
- Martin, G.R., Evans, M.J., 1974. The morphology and growth of a pluripotent teratocarcinoma cell line and its derivatives in tissue culture. *Cell* 2, 163-172.
- Martinez-Finley, E.J., Ali, A.M., Allan, A.M., 2009. Learning deficits in C57BL/6J mice following perinatal arsenic exposure: consequence of lower corticosterone receptor levels? *Pharmacol. Biochem. Behav.* 94, 271-277.
- Martinez-Finley, E.J., Goggin, S.L., Labrecque, M.T., Allan, A.M., 2011. Reduced expression of MAPK/ERK genes in perinatal arsenic-exposed offspring induced by glucocorticoid receptor deficits. *Neurotoxicol. Teratol.* 33, 530-537.
- Massagué, J., 2012. TGF[beta] signalling in context. *Nature Reviews.Molecular Cell Biology* 13, 616-30.

- Mauro, M., Caradonna, F., Klein, C.B., 2016. Dysregulation of DNA methylation induced by past arsenic treatment causes persistent genomic instability in mammalian cells. *Environ. Mol. Mutagen.* 57, 137-150.
- McBurney, M.W., 1993. P19 embryonal carcinoma cells. *Int. J. Dev. Biol.* 37, 135-140.
- McBurney, M.W., Jones-Villeneuve, E.M., Edwards, M.K., Anderson, P.J., 1982. Control of muscle and neuronal differentiation in a cultured embryonal carcinoma cell line. *Nature* 299, 165-167.
- McClintock, T.R., Chen, Y., Bundschuh, J., Oliver, J.T., Navoni, J., Olmos, V., Edda Villaamil Lepori, Ahsan, H., Faruque Parvez, 2012. Arsenic exposure in Latin America: Biomarkers, risk assessments and related health effects. *Sci. Total Environ.* 429, 76-91.
- McCoy, C.R., Stadelman, B.S., Brumaghim, J.L., Liu, J.T., Bain, L.J., 2015. Arsenic and Its Methylated Metabolites Inhibit the Differentiation of Neural Plate Border Specifier Cells. *Chem. Res. Toxicol.* 28, 1409-1421.
- McKey, J., Martire, D., de Santa Barbara, P., Faure, S., 2016. LIX1 regulates YAP1 activity and controls the proliferation and differentiation of stomach mesenchymal progenitors. *BMC Biol.* 14, 34-016-0257-2.
- McPherron, A.C., Lee, S.J., 1993. GDF-3 and GDF-9: two new members of the transforming growth factor-beta superfamily containing a novel pattern of cysteines. *The Journal of biological chemistry* 268, 3444-3449.
- Meacher, D.M., Manzel, D.B., Dillencourt, M.D., Bic, L.F., Schoof, R.A., Yost, L.J., Farr, C.H., 2002. Estimation of multimedia inorganic arsenic intake in the US population. *Hum. Ecol. Risk Assess.*, 8(7), pp. 1697-1721
- Medeiros, M., Zheng, X., Novak, P., Wnek, S.M., Chyan, V., Escudero-Lourdes, C., Gandolfi, A.J., 2012. Global gene expression changes in human urothelial cells exposed to low-level monomethylarsonous acid. *Toxicology* 291, 102-112.
- Mendez, W.M., Jr, Eftim Sorina, Cohen, J., Warren, I., Cowden, J., Lee, J.S., Reeder, S., 2017. Relationships between arsenic concentrations in drinking water and lung and bladder cancer incidence in U.S. counties. *Journal of Exposure Science and Environmental Epidemiology* 27, 235-243.
- Meng, Z., Moroishi, T., Guan, K.L., 2016. Mechanisms of Hippo pathway regulation. *Genes Dev.* 30, 1-17.
- Milton, A.H., Smith, W., Rahman, B., Hasan, Z., Kulsum, U., Dear, K., Rakibuddin, M., Ali, A., 2005. Chronic arsenic exposure and adverse pregnancy outcomes in bangladesh. *Epidemiology* 16, 82-86.
- Mochizuki, H., 2019. Arsenic Neurotoxicity in Humans. *Int. J. Mol. Sci.* 20, 10.3390/ijms20143418.

- Mitra, A., Chatterjee, S., Gupta, D., 2019. Environmental arsenic exposure and human health risk. In: Fares A, Singh SK (eds) Arsenic water resources contamination: challenges and solutions. Springer International Publishing, Cham, pp 103–129.
- Moore RY. Principles of synaptic transmission., 1993. *Ann N Y Acad Sci.*;695:1-9.
- Mori, M., Triboulet, R., Mohseni, M., Schlegelmilch, K., Shrestha, K., Camargo, F.D., Gregory, R.I., 2014. Hippo signaling regulates microprocessor and links cell-density-dependent miRNA biogenesis to cancer. *Cell* 156, 893-906.
- Morin-Kensicki, E.M., Boone, B.N., Howell, M., Stonebraker, J.R., Teed, J., Alb, J.G., Magnuson, T.R., O'Neal, W., Milgram, S.L., 2006. Defects in yolk sac vasculogenesis, chorioallantoic fusion, and embryonic axis elongation in mice with targeted disruption of Yap65. *Mol. Cell. Biol.* 26, 77-87.
- Musah, S., Wrighton, P.J., Zaltsman, Y., Zhong, X., Zorn, S., Parlato, M.B., Hsiao, C., Palecek, S.P., Chang, Q., Murphy, W.L., Kiessling, L.L., 2014. Substratum-induced differentiation of human pluripotent stem cells reveals the coactivator YAP is a potent regulator of neuronal specification. *Proc. Natl. Acad. Sci. U. S. A.* 111, 13805-13810.
- Nishioka, N., Inoue, K., Adachi, K., Kiyonari, H., Ota, M., Ralston, A., Yabuta, N., Hirahara, S., Stephenson, R.O., Ogonuki, N., Makita, R., Kurihara, H., Morin-Kensicki, E.M., Nojima, H., Rossant, J., Nakao, K., Niwa, H., Sasaki, H., 2009. The Hippo signaling pathway components Lats and Yap pattern Tead4 activity to distinguish mouse trophectoderm from inner cell mass. *Dev. Cell.* 16, 398-410.
- Niyomchan, A., Watcharasit, P., Visitnonthachai, D., Homkajorn, B., Thiantanawat, A., Satayavivad, J., 2015. Insulin attenuates arsenic-induced neurite outgrowth impairments by activating the PI3K/Akt/SIRT1 signaling pathway. *Toxicol. Lett.* 236, 138-144.
- Noisa, P., Raivio, T., Cui, W., 2015. Neural Progenitor Cells Derived from Human Embryonic Stem Cells as an Origin of Dopaminergic Neurons. *Stem cells international* 2015, 647437.
- Novick, S.C., Warrell, R.P., 2000. Arsenicals in hematologic cancers. *Semin. Oncol.* 27, 495-501.
- Ochalek, A., Szczesna, K., Petazzi, P., Kobolak, J., Dinnyes, A., 2016. Generation of Cholinergic and Dopaminergic Interneurons from Human Pluripotent Stem Cells as a Relevant Tool for In Vitro Modeling of Neurological Disorders Pathology and Therapy. *Stem Cells International* 2016.
- Palma-Lara, I., Martinez-Castillo, M., Quintana-Perez, J.C., Arellano-Mendoza, M.G., Tamay-Cach, F., Valenzuela-Limon, O.L., Garcia-Montalvo, E.A., Hernandez-Zavala, A., 2020. Arsenic exposure: A public health problem leading to several cancers. *Regul. Toxicol. Pharmacol.* 110, 104539.
- Pandey, R., Rai, V., Mishra, J., Mandrah, K., Kumar Roy, S., Bandyopadhyay, S., 2017. From the Cover: Arsenic Induces Hippocampal Neuronal Apoptosis and Cognitive Impairments via

- an Up-Regulated BMP2/Smad-Dependent Reduced BDNF/TrkB Signaling in Rats. *Toxicol. Sci.* 159, 137-158.
- Papaspyropoulos, A., Bradley, L., Thapa, A., Leung, C.Y., Toskas, K., Koennig, D., Pefani, D.E., Raso, C., Grou, C., Hamilton, G., Vlahov, N., Grawenda, A., Haider, S., Chauhan, J., Buti, L., Kanapin, A., Lu, X., Buffa, F., Dianov, G., von Kriegsheim, A., Matallanas, D., Samsonova, A., Zernicka-Goetz, M., O'Neill, E., 2018. RASSF1A uncouples Wnt from Hippo signalling and promotes YAP mediated differentiation via p73. *Nat. Commun.* 9, 424-017-02786-5.
- Parvez, F., Wasserman, G.A., Factor-Litvak, P., Liu, X., Slavkovich, V., Siddique, A.B., Sultana, R., Sultana, R., Islam, T., Levy, D., Mey, J.L., van Geen, A., Khan, K., Kline, J., Ahsan, H., Graziano, J.H., 2011. Arsenic exposure and motor function among children in Bangladesh. *Environ. Health Perspect.* 119, 1665-1670.
- Pelliccia, J.L., Jindal, G.A., Burdine, R.D., 2017. Gdf3 is required for robust Nodal signaling during germ layer formation and left-right patterning. *eLife* 6.
- Petreski, T., Kit, B., Strnad, M., Grenc, D., Svenšek, F., 2020. Cholinergic syndrome: a case report of acute organophosphate and carbamate poisoning. *Arhiv za higijenu rada i toksikologiju*, 163-166.
- Picciotto, M.R., Higley, M.J., Mineur, Y.S., 2012. Acetylcholine as a neuromodulator: cholinergic signaling shapes nervous system function and behavior. *Neuron* 76, 116-129.
- Piccolo, S., Dupont, S., Cordenonsi, M., 2014. The biology of YAP/TAZ: hippo signaling and beyond. *Physiol. Rev.* 94, 1287-1312.
- Power, A.E., 2004. Slow-wave sleep, acetylcholine, and memory consolidation. *Proc. Natl. Acad. Sci. U. S. A.* 101, 1795-1796.
- Rahman, A., Vahter, M., Ekstrom, E.C., Rahman, M., Golam Mustafa, A.H., Wahed, M.A., Yunus, M., Persson, L.A., 2007. Association of arsenic exposure during pregnancy with fetal loss and infant death: a cohort study in Bangladesh. *Am. J. Epidemiol.* 165, 1389-1396.
- Rahman, A., Vahter, M., Smith, A.H., Nermell, B., Yunus, M., El Arifeen, S., Persson, L.A., Ekstrom, E.C., 2009. Arsenic exposure during pregnancy and size at birth: a prospective cohort study in Bangladesh. *Am. J. Epidemiol.* 169, 304-312.
- Rahman, M., Sohel, N., Yunus, M., Chowdhury, M.E., Hore, S.K., Zaman, K., Bhuiya, A., Streatfield, P.K., 2013. Increased childhood mortality and arsenic in drinking water in Matlab, Bangladesh: a population-based cohort study. *PLoS One* 8, e55014.
- Rahman, M., Vahter, M., Wahed, M.A., Sohel, N., Yunus, M., Streatfield, P.K., Arifeen, S.E., Bhuiya, A., Zaman, K., Chowdhury, A.M.R., Ekström, E., Persson, L.Å., 2006. Prevalence of arsenic exposure and skin lesions. A population based survey in Matlab, Bangladesh. *J. Epidemiol. Community Health* 60, 242.

- Ramos, A., Camargo, F.D., 2012. The Hippo signaling pathway and stem cell biology. *Trends Cell Biol.* 22, 339-346.
- Ravenscroft, P., Brammer, H., Richards, K., 2009. *Arsenic Pollution—A Global Synthesis*. Wiley-Blackwell; Oxford, UK.
- Rayon, T., Stamataki, D., Perez-Carrasco, R., Garcia-Perez, L., Barrington, C., Melchionda, M., Exelby, K., Tybulewicz, V., Elizabeth Mc Fisher, Briscoe, J., 2019. Species-specific developmental timing is associated with global differences in protein stability in mouse and human. *bioRxiv*, n/a.
- Richardson, R.J., Makhaeva, G.F., 2014. Organophosphorus Compounds. *Encyclopedia of Toxicology (Third Edition)*; 714-719
- Rodda, D.J., Chew, J., Lim, L., Loh, Y., Wang, B., Ng, H., Robson, P., 2005. Transcriptional Regulation of Nanog by OCT4 and SOX2. *J. Biol. Chem.* 280, 24731-24737.
- Rodriguez, V.M., Carrizales, L., Mendoza, M.S., Fajardo, O.R., Giordano, M., 2002. Effects of sodium arsenite exposure on development and behavior in the rat. *Neurotoxicol. Teratol.* 24, 743-750.
- Saha, K.K., Engström, A., Hamadani, J.D., Tofail, F., Rasmussen, K.M., Vahter, M., 2012. Pre- and Postnatal Arsenic Exposure and Body Size to 2 Years of Age: A Cohort Study in Rural Bangladesh. *Environ. Health Perspect.* 120, 1208-14.
- Sarkar, A., Paul, B., 2016. The global menace of arsenic and its conventional remediation - A critical review. *Chemosphere* 158, 37-49.
- Sato, M., Muragaki, Y., Saika, S., Roberts, A.B., Ooshima, A., 2003. Targeted disruption of TGF-beta1/Smad3 signaling protects against renal tubulointerstitial fibrosis induced by unilateral ureteral obstruction. *J. Clin. Invest.* 112, 1486-1494.
- Shankar, S., Shanker, U., Shikha, 2014. Arsenic contamination of groundwater: a review of sources, prevalence, health risks, and strategies for mitigation. *ScientificWorldJournal* 2014, 304524.
- Shea, C.A., Rolfe, R.A., McNeill, H., Murphy, P., 2020. Localization of YAP activity in developing skeletal rudiments is responsive to mechanical stimulation. *Dev. Dyn.* 249, 523-542.
- Shen, S., Guo, X., Yan, H., Lu, Y., Ji, X., Li, L., Liang, T., Zhou, D., Feng, X., Zhao, J.C., Yu, J., Gong, X., Zhang, L., Zhao, B., 2015. A miR-130a-YAP positive feedback loop promotes organ size and tumorigenesis. *Cell Res.* 25, 997-1012.
- Shi, Y., Massagué, J., 2003. Mechanisms of TGF-beta signaling from cell membrane to the nucleus. *Cell* 113, 685-700.
- Shin, S., Mitalipova, M., Noggle, S., Tibbitts, D., Venable, A., Rao, R., Stice, S.L., 2006. Long-term proliferation of human embryonic stem cell-derived neuroepithelial cells using defined adherent culture conditions. *Stem Cells* 24, 125-138.

- Smith, A.H., Arroyo, A.P., Mazumder, D.N., Kosnett, M.J., Hernandez, A.L., Beeris, M., Smith, M.M., Moore, L.E., 2000. Arsenic-induced skin lesions among Atacamenos people in Northern Chile despite good nutrition and centuries of exposure. *Environ. Health Perspect.* 108, 617-620.
- Smith, A.H., Marshall, G., Liaw, J., Yuan, Y., Ferreccio, C., Steinmaus, C., 2012. Mortality in young adults following in utero and childhood exposure to arsenic in drinking water. *Environ. Health Perspect.* 120, 1527-1531.
- States, J.C., Barchowsky, A., Cartwright, I.L., Reichard, J.F., Futscher, B.W., Lantz, R.C., 2011. Arsenic toxicology: translating between experimental models and human pathology. *Environ. Health Perspect.* 119, 1356-1363.
- Steffens, A.A., Hong, G.M., Bain, L.J., 2011. Sodium arsenite delays the differentiation of C2C12 mouse myoblast cells and alters methylation patterns on the transcription factor myogenin. *Toxicol. Appl. Pharmacol.* 250, 154-161.
- Stein, C., Bardet, A.F., Roma, G., Bergling, S., Clay, I., Ruchti, A., Agarinis, C., Schmelzle, T., Bouwmeester, T., Schubeler, D., Bauer, A., 2015. YAP1 Exerts Its Transcriptional Control via TEAD-Mediated Activation of Enhancers. *PLoS Genet.* 11, e1005465.
- Stifani, N., 2014. Motor neurons and the generation of spinal motor neurons diversity. *Frontiers in Cellular Neuroscience*, n/a.
- Sun, Y., Yong, K.M.A., Villa-diaz, L.G., Zhang, X., Chen, W., Philson, R., Weng, S., Xu, H., Krebsbach, P.H., Fu, J., 2014. Hippo/YAP-mediated rigidity-dependent motor neuron differentiation of human pluripotent stem cells. *Nature Materials* 13, 599-604.
- Swain, N., Thakur, M., Pathak, J., Swain, B., 2020. SOX2, OCT4 and NANOG: The core embryonic stem cell pluripotency regulators in oral carcinogenesis. *Journal of oral and maxillofacial pathology : JOMFP* 24, 368-373.
- Tamm, C., Bower, N., Anneren, C., 2011. Regulation of mouse embryonic stem cell self-renewal by a Yes-YAP-TEAD2 signaling pathway downstream of LIF. *J. Cell. Sci.* 124, 1136-1144.
- Tanabe, S., 2015. Signaling involved in stem cell reprogramming and differentiation. *World journal of stem cells* 7, 992-998.
- Thomas, D.J., 2013. The die is cast: arsenic exposure in early life and disease susceptibility. *Chem. Res. Toxicol.* 26, 1778-1781.
- Thomson, J.A., Itskovitz-Eldor, J., Shapiro, S.S., Waknitz, M.A., Swiergiel, J.J., Marshall, V.S., Jones, J.M., 1998. Embryonic stem cell lines derived from human blastocysts. *Science (New York, N.Y.)* 282, 1145-1147.
- Tintignac, L.A., Brenner, H., Rüegg, M.A., 2015. Mechanisms Regulating Neuromuscular Junction Development and Function and Causes of Muscle Wasting. *Physiol. Rev.* 95, 809-852.

- Totaro, A., Panciera, T., Piccolo, S., 2018. YAP/TAZ upstream signals and downstream responses. *Nat. Cell Biol.* 20, 888-899.
- Trang, A., Khandhar, P.B., 2022. Physiology, Acetylcholinesterase. StatPearls Publishing.
- Tykwinska, K., Lauster, R., Knaus, P., Rosowski, M., 2013. Growth and differentiation factor 3 induces expression of genes related to differentiation in a model of cancer stem cells and protects them from retinoic acid-induced apoptosis. *PLoS one* 8, e70612.
- Tyler, C.R., Allan, A.M., 2013. Adult hippocampal neurogenesis and mRNA expression are altered by perinatal arsenic exposure in mice and restored by brief exposure to enrichment. *PLoS One* 8, e73720.
- Vahter, M., 2002. Mechanisms of arsenic biotransformation. *Toxicology* 181-182, 211-217.
- van der Heyden, M.A., Defize, L.H., 2003. Twenty one years of P19 cells: what an embryonal carcinoma cell line taught us about cardiomyocyte differentiation. *Cardiovasc. Res.* 58, 292-302.
- Varelas, X., Sakuma, R., Samavarchi-Tehrani, P., Peerani, R., Rao, B.M., Dembowy, J., Yaffe, M.B., Zandstra, P.W., Wrana, J.L., 2008. TAZ controls Smad nucleocytoplasmic shuttling and regulates human embryonic stem-cell self-renewal. *Nat. Cell Biol.* 10, 837-848.
- Verschuuren, J., Strijbos, E., Vincent, A., 2016. Neuromuscular junction disorders. *Handbook of clinical neurology* 133, 447-466.
- Wang, A., Holladay, S.D., Wolf, D.C., Ahmed, S.A., Robertson, J.L., 2006. Reproductive and developmental toxicity of arsenic in rodents: a review. *Int. J. Toxicol.* 25, 319-331.
- Wang, X., Meng, D., Chang, Q., Pan, J., Zhang, Z., Chen, G., Ke, Z., Luo, J., Shi, X., 2010. Arsenic inhibits neurite outgrowth by inhibiting the LKB1-AMPK signaling pathway. *Environ. Health Perspect.* 118, 627-634.
- Wang, Y., Cui, M., Sun, B.D., Liu, F.B., Zhang, X.D., Ye, L.H., 2014. MiR-506 suppresses proliferation of hepatoma cells through targeting YAP mRNA 3'UTR. *Acta Pharmacol. Sin.* 35, 1207-1214.
- Wang, Y., Wang, Z., Li, H., Xu, W., Dong, L., Guo, Y., Feng, S., Bi, K., Zhu, C., 2017. Arsenic trioxide increases expression of secreted frizzled-related protein 1 gene and inhibits the WNT/beta-catenin signaling pathway in Jurkat cells. *Exp. Ther. Med.* 13, 2050-2055.
- Wasserman, G.A., Liu, X., Loiacono, N.J., Kline, J., Factor-Litvak, P., van Geen, A., Mey, J.L., Levy, D., Abramson, R., Schwartz, A., Graziano, J.H., 2014. A cross-sectional study of well water arsenic and child IQ in Maine schoolchildren. *Environ. Health* 13, 23-069X-13-23.
- Wei, B., Yu, J., Kong, C., Li, H., Yang, L., Xia, Y., Wu, K., 2018. A follow-up study of the development of skin lesions associated with arsenic exposure duration. *Environ. Geochem. Health* 40, 2729-2738.

- Wrana, J.L., Attisano, L., Wieser, R., Ventura, F., Massagué, J., 1994. Mechanism of activation of the TGF-beta receptor. *Nature* 370, 341-347.
- Yadav, R.S., Chandravanshi, L.P., Shukla, R.K., Sankhwar, M.L., Ansari, R.W., Shukla, P.K., Pant, A.B., Khanna, V.K., 2011. Neuroprotective efficacy of curcumin in arsenic induced cholinergic dysfunctions in rats. *Neurotoxicology* 32, 760-768.
- Yajima, I., Kumasaka, M.Y., Iida, M., Oshino, R., Tanihata, H., Aeorangajeb Al Hossain, Ohgami, N., Kato, M., 2017. Arsenic-mediated hyperpigmentation in skin via NF-kappa B/endothelin-1 signaling in an originally developed hairless mouse model. *Archives of Toxicology.Archiv für Toxikologie* 91, 3507-3516.
- Ye, M., Berry-Wynne, K.M., Asai-Coakwell, M., Sundaresan, P., Footz, T., French, C.R., Abitbol, M., Fleisch, V.C., Corbett, N., Allison, W.T., Drummond, G., Walter, M.A., Underhill, T.M., Waskiewicz, A.J., Lehmann, O.J., 2010. Mutation of the bone morphogenetic protein GDF3 causes ocular and skeletal anomalies. *Hum. Mol. Genet.* 19, 287-298.
- Yen, Y.P., Tsai, K.S., Chen, Y.W., Huang, C.F., Yang, R.S., Liu, S.H., 2010. Arsenic inhibits myogenic differentiation and muscle regeneration. *Environ. Health Perspect.* 118, 949-956.
- Yu, F.X., Zhang, Y., Park, H.W., Jewell, J.L., Chen, Q., Deng, Y., Pan, D., Taylor, S.S., Lai, Z.C., Guan, K.L., 2013. Protein kinase A activates the Hippo pathway to modulate cell proliferation and differentiation. *Genes Dev.* 27, 1223-1232.
- Yu, F.X., Zhao, B., Guan, K.L., 2015. Hippo Pathway in Organ Size Control, Tissue Homeostasis, and Cancer. *Cell* 163, 811-828.
- Yu, H., Liao, W., Chai, C., 2006. Arsenic carcinogenesis in the skin. *J. Biomed. Sci.* 13, 657-666.
- Yu, S., Liao, W., Lee, C., Chai, C., Yu, C., Yu, H., 2018. Immunological dysfunction in chronic arsenic exposure: From subclinical condition to skin cancer. *J. Dermatol.* 45, 1271-1277.
- Zamani, N., Brown, C.W., 2011. Emerging roles for the transforming growth factor- β superfamily in regulating adiposity and energy expenditure. *Endocr. Rev.* 32, 387-403.
- Zavala, Y.J., Duxbury, J.M., 2008. Arsenic in Rice: I. Estimating Normal Levels of Total Arsenic in Rice Grain. *Environ. Sci. Technol.* 42, 3856.
- Zeng, Q., Zhang, A., 2020. Assessing potential mechanisms of arsenic-induced skin lesions and cancers: Human and in vitro evidence. *Environmental pollution (Barking, Essex : 1987)* 260, 113919.
- Zhang, H., Deo, M., Thompson, R.C., Uhler, M.D., Turner, D.L., 2012. Negative regulation of Yap during neuronal differentiation. *Dev. Biol.* 361, 103-115.
- Zhao, B., Ye, X., Yu, J., Li, L., Li, W., Li, S., Yu, J., Lin, J.D., Wang, C.Y., Chinnaiyan, A.M., Lai, Z.C., Guan, K.L., 2008. TEAD mediates YAP-dependent gene induction and growth control. *Genes Dev.* 22, 1962-1971.

CHAPTER TWO

LONG-TERM ARSENIC EXPOSURE IMPAIRS DIFFERENTIATION IN MOUSE EMBRYONAL STEM CELLS

Benjamin D. McMichael, M. Chiara Perego, Caitlin L. Darling, Rebekah L. Perry, Sarah C. Coleman, Lisa J. Bain

This chapter was published in Journal of Applied Toxicology and is in the format required of that journal.

The citation is:

McMichael BD, Perego MC, Darling CL, Perry RL, Coleman SC, Bain LJ. (2020). Long-term arsenic exposure impairs differentiation in mouse embryonal stem cells. J Appl Toxicol.;41(7):1089-1102.

Abstract

Arsenic is a contaminant found in many foods and drinking water. Exposure to arsenic during development can cause improper neuronal progenitor cell development, differentiation, and function, while *in vitro* studies have determined that acute arsenic exposure to stem and progenitor cells reduced their ability to differentiate. In the current study, P19 mouse embryonal stem cells were exposed continuously to 0.1 μM (7.5 ppb) arsenic for 32 weeks. A cell lineage array examining mRNA changes after 8 and 32 weeks of exposure showed that genes involved in pluripotency were increased, while those involved in differentiation were reduced. Therefore, temporal changes of select pluripotency and neuronal differentiation markers throughout the 32-week chronic arsenic exposure were investigated. *Sox2* and *Oct4* mRNA expression were increased by 1.9- to 2.5-fold in the arsenic-exposed cells, beginning at week 12. *Sox2* protein expression was similarly increased starting at week 16 and remained elevated by 1.5- to 6-fold. One target of *Sox2* is N-cadherin, whose expression is a hallmark of epithelial-mesenchymal transitions (EMT). Exposure to arsenic significantly increased N-cadherin protein levels beginning at week 20, concurrent with increased grouping of N-cadherin positive cells at the perimeter of the embryoid body. Expression of *Zeb1*, which helps increase the expression of *Sox2* was also increased started at week 16. In contrast, *Gdf3* mRNA expression was reduced by 3.4- to 7.2-fold beginning at week 16, and expression of its target protein, phospho-Smad2/3, was also reduced. These results suggest that chronic, low-level arsenic exposure may delay neuronal differentiation and maintain pluripotency.

Introduction

Arsenic (As) is a ubiquitous groundwater toxicant found throughout the world, with the highest incidences of exposure seen in Bangladesh and India (Chakraborti et al., 2015; Kumar, Adak, Gurian, & Lockwood, 2010; Naujokas et al., 2013). Many people in these countries are exposed to arsenic concentrations higher than the World Health Organization (WHO) recommendation and U.S. Environmental Protection Agency (U.S. EPA) standard of 10 ppb in drinking water. In addition to the risk from drinking water, various vegetables, grains, and fruits can uptake arsenic from irrigation water and soil (Davis et al., 2012; Wilson et al., 2012; Zavala & Duxbury, 2008). Adult exposure is correlated with an increased incidence of cancer, hypertension, diabetes mellitus, and cardiovascular disease (Kuo et al., 2017). Arsenic can cross the placenta and has been found at similar concentrations in both cord and maternal blood (Concha et al., 1998). Consequently, epidemiological studies of populations exposed to arsenic report increased incidences of stillbirths, reduced birth weight and weight gain (Golmohammadi et al., 2019; Raqib et al., 2009; Shih et al., 2020; von Ehrenstein et al., 2006), altered locomotor activity, altered sensory ability, and learning deficits (Dakeishi et al., 2006; Markowski et al., 2012; Nahar et al., 2014; Tolins et al., 2014; Yorifuji et al., 2016).

In order to delineate the mechanisms through which arsenic induces these developmental deficiencies, *in vitro* studies using mouse and rat neuroblast cells acutely exposed to arsenic have reduced neurite length and branching compared to controls (Frankel et al., 2009; Wang et al., 2010). Similarly, C2C12 mouse myoblasts acutely exposed to low concentrations of arsenic have reduced differentiation, decreased myogenin levels, and reduced multi-nucleation (Steffens et al., 2011; Yen et al., 2010). Previous studies using P19 mouse embryonal stem cells have shown a reduction in both skeletal myotube and neuron formation, but not proliferation, following an acute 0.5 μM sodium arsenite exposure (Hong & Bain, 2012).

While these previous studies have shown that acute *in vitro* arsenic exposures can reduce cellular differentiation, several studies have also shown that fate-determined cells chronically exposed to arsenic can turn into a cancer stem cell-like phenotype. Human HaCaT keratinocytes exposed to 50 ppb arsenic for 18 weeks developed a cancer stem-like phenotype that showed higher rates of proliferation when compared to passage matched controls (Huang et al., 2013). Similarly, exposure of human urothelial (UROtsa) cells to 6.2 ppb of the inorganic arsenic metabolite, monomethylarsenous acid (MMA^{III}) for 52 weeks transformed them into malignant cells, showing anchorage-independence after 24 weeks, the formation of tumors in SCID mice after 52 weeks, and irreversible transformation after 12 weeks of exposure (Bredfeldt et al., 2006; Wnek et al., 2010). While the mechanism for transforming differentiated cells to cancer stem-cell like cells is not fully understood, this may be mediated through arsenic-induced transcriptional regulation of pluripotency markers. The transcription factors Sox2 and Oct4 have been shown in several different cancer stem cell lineages to increase cell stemness by acting synergistically to maintain pluripotency and drive the transcription of various target genes, including *Nanog*, *Oct3/4*, and *Sox2* (Boumahdi et al., 2014; Leis et al., 2012; Rodda et al., 2005). A study of human bronchial epithelial (HBE) cells exposed to 1.0 μ M arsenite for 15 weeks showed significant increases in *Oct4* transcript expression by week 5 of the exposure, although no significant increases in *Sox2* expression were observed (Xu et al., 2012). Another chronic *in vitro* study exposed human epithelial stem/progenitor cells (WPE-stem) to 5 μ M arsenite for 18 weeks and found that several markers of self-renewal, including *Bmi1*, *Notch1*, and *Oct4*, were decreased for the first several weeks of the arsenic exposure, before all markers began to increase later (Tokar et al., 2010).

The purpose of the current study was to examine whether long-term arsenic exposure, below the current drinking standard of 10 ppb, altered the differentiation of P19 stem cells and to investigate the mechanisms responsible. Our results demonstrate an increase in the transcription

factors *Sox2* and *Zeb1* starting at weeks 12 and 16 of arsenic exposure, respectively. Further, at approximately 20 weeks, we report an overall increase in N-cadherin protein expression, as well as increased groupings of N-cadherin positive cells at the perimeter of arsenic exposed embryoid bodies. Concomitantly, there is a decrease in *Gdf3*, a member of the TGF β family of ligands, starting at week 16 along with a reduction in its active target protein, phospho-Smad 2/3. These results suggest that chronic arsenic exposure hinders the ability of neural progenitor cells to properly differentiate.

Methods

Chronic exposure of P19 cells to arsenic

P19 mouse embryonal cells (Sigma-Aldrich, St. Louis, MO, USA) were grown in α -MEM media (ThermoFisher, Waltham, MA), containing 7.5% bovine calf serum (ThermoFisher), 2.5% fetal bovine serum (ThermoFisher), and 0.1% L-glutamine (ThermoFisher,) (McBurney, 1993). To start the chronic exposure, cells were cultured in medium containing 0 or 0.1 μ M arsenic as sodium arsenite (Sigma-Aldrich), equivalent to 7.5 ppb arsenic, for up to 32 weeks. Both the control and the arsenic exposed samples were cultured as three independent replicates (n=3 for each treatment). The cells were passaged every two to three days to maintain low confluency and avoid premature cellular differentiation.

P19 cell differentiation

At eight time points (once every four weeks of the 32-week exposure), the six separate cultures of cells (n=3 for each treatment) were differentiated via the hanging drop method (500 cells/drop) using medium containing 1% DMSO (ThermoFisher), but without any arsenic (Wang & Yang, 2008). After two days of hanging drop culture, individual embryoid bodies were

transferred to 96-well ultralow attachment plates (Greiner Bio-One, Monroe, NC) for another three days. Representative images of day 5 embryoid bodies were captured using a VWR VistaVision microscope camera (Radnor, PA). After imaging, embryoid bodies from one 96-well plate were pooled together, washed in PBS, and placed in 10% neutral buffered formalin (NBF, ThermoFisher) overnight at 4°C for immunohistochemical analyses. An additional set of day 5 embryoid bodies were transferred to four 0.1% gelatin-coated 48-well plates, and medium was refreshed every other day. On day 9, representative pictures were taken. Afterwards, two plates of the day 9 cells were pooled and stored in Trizol (ThermoFisher) at -80°C for RNA extraction, while the cells from the other two plates were pooled and stored in RIPA lysis buffer at -80°C for protein extraction.

An additional set of naïve P19 cells was exposed acutely to 0, 0.1, or 0.5 M arsenic during the nine-day differentiation process as described above (n=6 for controls and n=3 for each exposure group). Day 9 cells were stored at Trizol at -80°C for RNA extraction.

Cell lineage profiler array

To initially assess changes over the continuous exposure, RNA from differentiated control and arsenic-exposed P19 cells at weeks 8 and 32 were analyzed using a Qiagen RT² Profiler Cell Lineage PCR Profiler Array (Germantown, MD). This array detects expression of a suite of 84 genes involved in cellular differentiation. RNA was extracted using Trizol, and RNA concentration and purity were determined on a Nanodrop (ThermoFisher). A Qiagen RT² First Strand Kit was used to synthesize cDNA from 2 µg of RNA from control and arsenic-exposed treatments, respectively (n=3). Quantitative PCR was then conducted with SYBR Green PCR Master Mix (Applied Biosystems, Foster City, CA). Array data was analyzed using Qiagen's GeneGlobe

(<https://geneglobe.qiagen.com/us/analyze/>), and fold changes were calculated between control and arsenic-exposed cells at each time point.

Gene expression analysis using quantitative PCR

RNA was extracted using Trizol, and RNA concentration and purity were determined on a Nanodrop (ThermoFisher) and stored at -80°C. RNA (2 µg) was reverse transcribed into cDNA and gene expression determined by qPCR on an Applied Biosystems StepOnePlus. qPCR was performed using SYBR Green PCR Master Mix (Applied Biosystems), 40ng cDNA, and 10 µM forward and reverse primers for genes of interest (Supplementary Table 1; obtained from IDTDNA, Coralville, IA). All samples were run in triplicate and melt curves were used to verify gene-specific binding. PCR efficiency and linearity were determined using a standard curve generated by serial dilutions of five concentration points (10^{-3} to 10^{-7} ng DNA) of the gene of interest. The geometric mean of Gapdh and β2-microglobulin was used for normalization, as the expression of these reference genes does not vary due to arsenic exposure (Liu & Bain, 2018). Relative fold expression was compared to the week 0 controls and quantified by the Delta-Delta Ct method (Schmittgen & Livak, 2008). Statistical significance between the control and arsenic-exposed replicates at each time point were assessed using Student's t-test ($p \leq 0.05$). Area under the curve (AUC) was used to determine gene expression changes over time (GraphPad, La Jolla, CA) and statistical differences between control and arsenic-exposed cells were analyzed using Student's t-test ($p \leq 0.05$).

Determining protein expression by immunohistochemistry

Following fixation in NBF, day 5 embryoid bodies were dehydrated, embedded in paraffin, and sectioned at 5 µm. Slides were deparaffinized and antigen retrieval was carried out in Tris-

EDTA buffer (pH 9). Primary antibodies for Sox2 (1:2000, Abcam, Cambridge, MA, #ab97959), N-cadherin (1:250, Santa Cruz Biotechnology, Santa Cruz, CA, #sc-59987), and E-cadherin (1:250, Novus, St. Charles, MO, #NBP2-19051) were incubated overnight at 4°C. After incubation with Alexa Fluor 488 secondary antibodies (1:1000, anti-rabbit, #A11034 and 1:500, anti-mouse, #A11001; Life Technologies, Rockville, MD), nuclei were counterstained with DAPI (Invitrogen, Carlsbad, CA). All samples were imaged on a Leica SPE Confocal microscope (Wetzlar, Germany) equipped with traditional PMT detectors and a 20x objective. Excitation wavelength for all antibodies was 488 nm with emission wavelength between 500-560 nm, while the excitation wavelength for DAPI was 405 nm with an emission wavelength of 430-480 nm. Imaging parameters (laser power, gain, and offset) for each antibody were held consistent between control and arsenic-exposed groups at each individual time point for each antibody.

Images were analyzed in ImageJ to determine protein expression (pixel intensity). Sox2 expression was determined by counting the number of cells using the particle analyzer function, and then dividing the integrated density by cell count to get an integrated density value (IDV) per cell. This analysis was done to account for differences in embryoid body sizes. Since N-cadherin was predominantly expressed at the periphery of embryoid bodies, protein expression in ~5 cells of the outer border only were included in the analysis. The outer edge of the embryoid body and an inner ring were traced, and fluorescence within these borders was analyzed and is reported as the IDV. Expression of E-cadherin was more evenly spread though embryoid bodies, therefore an IDV was determined for each embryoid body. IDVs were averaged for each treatment group, and statistical differences between the control and arsenic exposed replicates of each time point were determined using Student's t-test ($p \leq 0.05$) (n=3).

Analyzing protein expression by immunoblotting

Day 9 cells were lysed in RIPA buffer containing protease and phosphatase inhibitors (Thermo Fisher) and then centrifuged at 12,000 g for 20 minutes. Protein concentration of the supernatants was determined using a BCA protein assay kit (ThermoFisher), with BSA as a standard. Proteins (10 µg) were electrophoresed onto 5-20% TBX gels (Bio-Rad, Hercules, CA). Immunoblotting was performed according to standard methods, using primary antibodies for Sox2 (1:1000, Abcam, #ab97959), Smad2/3 (1:1000; Cell Signaling Technology, Danvers, MA #8685), or phospho-Smad2/3 (1:1000; Cell Signaling Technology, #8828) and goat anti-rabbit-HRP secondary antibody (1:2000 - 1:5000, Santa Cruz Biotechnology, #sc-2004). Protein expression was examined by chemiluminescence (Luminol, Santa Cruz Biotechnology) on a Bio-Rad ChemiDoc imaging system. Densitometry values were determined using BioRad ImageLab software and normalized to Gapdh (1:1000, GeneTex, Irvine, CA, #GTX627408) as a loading control using goat anti-mouse-HRP secondary antibody (1:2000 – 1:5000, Invitrogen, #62-6520). Densitometry values were compared to the average control value to calculate individual fold changes. Statistical differences were determined using Student's t-test ($p \leq 0.05$) (n=3).

Results

Chronic, low-level arsenic exposure impairs cellular differentiation

The goal of this study was to assess the impacts of long-term, low-level arsenic exposure on cellular differentiation. Thus, P19 mouse embryonic stem cells were continuously cultured in six independent flasks exposed to either 0 or 0.1 µM (7.5 ppb) arsenic for up to 32 weeks. Every four weeks, a portion of the cells from each flask were differentiated via hanging drops into embryoid bodies (EBs) after five days (D5), and then into differentiated cells after nine days (D9). During the differentiation process, no arsenic was placed in the medium to assess the permanence

of changes. Examining cell morphological changes across the time course, no differences in D5 embryoid body morphology or the number of viable embryoid bodies were seen (data not shown). Images taken of Day 9 cells show no morphological differences between the control and arsenic-exposed cells at any of the time points examined (Figure 1).

To better understand if a low-level, chronic arsenic exposure resulted in impairment of cellular differentiation, Qiagen's Mouse Cell Lineage PCR array was used to examine transcript levels of 84 genes. Analysis of differential gene expression in the week 8 and week 32 cells indicates that transcript levels of genes involved in maintaining pluripotency, including *Sox2* and *Oct4* were upregulated in the arsenic-exposed cells (Table 1). Similarly, transcripts of ectodermal and neuroectodermal germ cells were increased in the arsenic-exposed cells. These genes included *Fibroblast growth factor 5 (Fgf5)*, *Forkhead box D3 (FoxD3)*, *zinc finger protein of the cerebellum 1 (Zic1)*, and *gastrulation brain homeobox 2 (Gbx2)*. However, genes that were indicative of neuronal progenitors, such as *Doublecortin (Dcx)* and *growth and differentiation factor 3 (Gdf3)*, and those of more differentiated neurons, including *Prominin 1 (Prom1)*, were decreased in the arsenic-exposed cells (Table 1). Genes involved in mesoderm formation were either not changed or downregulated (Table 1), while those involved in endoderm formation were either not expressed or were expressed at low levels, but not different between the groups (data not shown).

Using this data, expression of select differentially-expressed genes were examined in P19 cells exposed acutely for nine days to 0.1 and 0.5 μM arsenic, to ensure that the changes in differential gene expression were likely due to arsenic exposure, rather than long-term culture. Transcripts required for the maintenance of pluripotency, such as *Sox2* and *Oct4* (Takahashi & Yamanaka, 2006) were examined, but these were not changed in either one of the exposure groups (Figure 2A and B). Markers for neuronal progenitor cells, including *Dcx* and *Ascl1* (Patel et al, 2006; Vasconcelos & Castro, 2014) were not different between control and the 0.1 μM exposed

cells. However, exposure to 0.5 μ M arsenic significantly reduced *Ascl1* expression by 10-fold (Figure 2C) and *Dcx* expression by 4-fold (Figure 2E). Similarly, the expression of *Gad2*, an indicator of more differentiated neurons (Francis et al., 1999), was also reduced by 2-fold in the 0.5 μ M-arsenic exposed cells (Figure 2F). In contrast, the expression of *Gdf3*, a signaling molecule involved in early neuronal differentiation (Li et al., 2012) was increased by nearly 5-fold in the 0.5 μ M-arsenic exposed cells (Figure 2D). Thus, while an acute exposure to the lower concentration of 0.1 μ M did not alter transcript expression, a higher concentration of arsenic significantly altered a number of genes.

To assess whether long-term culture in 0.1 μ M (7.5 ppb) arsenic altered transcript levels, the expression of several genes was determined in each individual chronically-exposed flask of cells over the 28-week exposure period. After 4 weeks of exposure, there are few changes between the control and arsenic-exposed cells (Figure 3). Starting at week 12, *Sox2* expression in the arsenic-exposed cells was increased by 1.9-fold compared to the control cells (Figure 3A), and *Oct4* expression was increased by 2.5-fold (Figure 3B). While *Sox2* expression remained elevated throughout most of the remaining exposure period (Figure 3A), *Oct4* expression was not different between control and arsenic-exposed cells (Figure 3B). Growth and differentiation factor 3 (*Gdf3*) is a signaling molecule expressed in embryonic stem cells that promotes mesodermal and neuronal differentiation in mice (Chen et al., 2006; Levine & Brivanlou, 2006a; Levine & Brivanlou, 2006b). Transcript levels of *Gdf3* are non-significantly ($p = 0.08$) reduced by 4-fold in the arsenic-exposed cells at week 16 (Figure 3C). By week 24 and continuing to week 28, *Gdf3* expression was significantly reduced in the arsenic-exposed cells by 3.4- to 7.2-fold, respectively (Figure 3C). In contrast, levels of *Dcx* and *Gad2* did not change during the exposure (Figure S1).

Transcript levels from each individual flask were then used to calculate the area under the curve (AUC) for each gene. Average *Sox2* AUCs were approximately 2-fold higher in the arsenic-exposed cells (Table 2), while *Gdf3* expression was significantly reduced in the arsenic-exposed cells (Table 2). These results suggest that chronic, low-level arsenic exposure reduces neuronal differentiation and allows cells to remain in a more pluripotent state.

Gdf3 and pSmad2/3 expression is reduced in the cells chronically exposed to arsenic

We then wanted to examine whether reductions in *Gdf3* mRNA expression in the arsenic-exposed cells led to effects on downstream target proteins. During the differentiation of mouse embryonic stem cells, *Gdf3* binds to the receptor complex comprised of type I receptor ALK4, type II receptor ActRIIA or B and co-receptor Cripto, resulting in phosphorylation and nuclear translocation of Smad2/3 (Andersson et al., 2007; Andersson et al., 2008; Chen et al., 2006). We examined protein levels of both total Smad2/3 and phosphorylated Smad2/3 by immunoblotting. At all time points examined during the chronic exposure, the ratio of phosphorylated Smad 2/3 to total Smad2/3 was consistently lower in the arsenic exposed cells (Figure S2A), ranging between 1.75- to 2-fold lower values (Figure S2B).

Arsenic exposure increases the expression of Sox2, Zeb1, and N-cadherin over time

Next, we wanted to confirm *Sox2* mRNA changes by examining *Sox2* protein levels and assessing expression of its target proteins. First, *Sox2* protein expression was examined by immunohistochemistry in day 5 embryoid bodies derived from cells chronically exposed to 0 or 0.1 μM arsenic for up to 32 weeks. While some *Sox2* was present in the cytoplasm, the majority of it localized to the nucleus (Figure 4A). No differences in *Sox2* expression were seen between control and arsenic-exposed cells at week 0 (Figure 4A). However, *Sox2* expression was increased by week

16 and remained elevated in cells chronically exposed to arsenic at weeks 24 and 32 (Figure 4A). Quantifying Sox2 expression revealed that arsenic-exposed cells had between 1.4- and 2.1-fold higher expression than controls, depending on the week examined (Figure 4B). Immunoblots revealed a similar pattern of Sox2 expression, this time using day 9 differentiated cells (Figure 4C). Sox2 expression is upregulated by 2.2-fold in the arsenic-exposed cells starting at week 16 (Figure 4D), and its levels remained increased, reaching a 4-fold difference by week 24 (Figure 4D).

Previous studies have described the role of Sox2 in regulating epithelial-mesenchymal transitions (EMT), and the expression of cadherin proteins (Herrerros-Villanueva et al., 2013; Yang, Hui, Wang, Yang, & Jiang, 2014). To examine the downstream effects of Sox2, expression of both N-cadherin and E-cadherin were analyzed by immunohistochemistry. The data indicate that chronic arsenic exposure results in a temporal increase in the expression of N-cadherin along with clustering of N-cadherin positive cells at the periphery of embryoid bodies (Figure 5A). While there were no differences in N-cadherin expression early in the exposure, arsenic-exposed cells at weeks 20, 28, and 32 showed significant increases in N-cadherin levels between 1.3- and 1.8-fold (Figure 5B). The E-cadherin protein expression was also examined by IHC (Figure 6A), but its levels did not differ between control and arsenic-exposed cells at any time point (Figure 6B). The transcription factor Zeb1 is also part of a feedback loop between Sox2, EMT, and maintained stemness (Wellner et al., 2009). Its expression in day 5 embryoid bodies was increased by 1.4- to 2-fold, starting at week 16 (Figure 7).

Discussion

The results demonstrate that a chronic, environmentally-relevant arsenic exposure impairs cellular differentiation and maintains stemness through the induction of markers commonly

indicative of epithelial-mesenchymal transition (EMT). This increased pluripotency appears to result in decreased neural differentiation.

Arsenic maintains pluripotency of stem cells

To investigate the reasons why chronic arsenic impaired differentiation, the expression pluripotency-associated transcription factors Oct4 and Sox2 were assessed. A known positive feedback loop exists between Oct4 and Sox2, and their expression is directly related to increased pluripotency (Masui et al., 2007; Rodda et al., 2005). Though well-known to play a role in the general pluripotency maintenance of totipotent cells, Sox2 is also commonly expressed in multipotent lineages including embryonic neural stem cells (Ferri et al., 2004). *Oct4* transcript levels were only significantly increased at week 12. These findings are in line with a previous study demonstrating that human urothelial cells chronically exposed to 1 μM arsenic for 12 months only had moderate increases in expression of *Oct4* (Ooki et al., 2018). However, *Sox2* mRNA expression was significantly elevated starting at week 12 and remained elevated throughout most of the remaining arsenic exposure. Sox2 protein expression was first upregulated in chronic arsenic-exposed samples at week 16, as determined by both immunoblotting and immunohistochemistry.

Expression of Sox2 remained elevated throughout the remaining weeks of exposure. Protein levels were not assessed at week 12, so it is unknown whether Sox2 protein expression would have been increased at this time point, similar to the mRNA levels. The findings do suggest that between week 12 and 16 of exposure, there exists a point at which the differentiation of P19 cells remains impaired by arsenic exposure. Previous studies exposing differentiated cells to arsenic support a similar time frame. For example, rat hepatocytes exposed to 0.5 μM arsenic or human prostate epithelial progenitor cell exposed to 5 μM arsenic were permanently transformed after 18 weeks of exposure (Tokar et al., 2010; Zhao et al., 1997). There is one flask of arsenic-exposed

P19 cells that had consistently low mRNA levels of *Sox2*. The reasons for the variability in transcript expression between the independent flasks is unknown, but this did not translate into variability in protein expression since levels of *Sox2* and cadherin protein expression were similar between all three arsenic-exposed cell lines. These results highlight the need for maintaining independent populations of cells during a chronic exposure study.

To our knowledge, the current study is the first to demonstrate that chronic arsenic exposure impairs differentiation and maintains stemness in an embryonic stem cell population. However, several previous studies have shown *Sox2* to be an important mediator of stemness during transformation of adult cells into cancer stem cells. For example, a chronic exposure of 0.25 μM arsenic for six months reprogrammed human bronchial epithelial cells (BEAS-2B) into cancer stem cells that exhibited elevated *Sox2* expression levels (Chang et al., 2014), while a study of human urothelial cells (HUC1) chronically exposed to 1 μM arsenic trioxide for 6 to 12 months had highly increased *Sox2* expression and self-renewal properties (Ooki et al., 2018).

To determine possible mechanisms that linked chronic arsenic exposure to altered pluripotency, two markers of oxidative stress, *Hmox1* and *Nrf2*, were examined. While *Hmox1* levels were increased in the 0.5 μM acute arsenic exposure (Figure S3A), they were not changed at 0.1 μM (Figure S3A) nor in the chronically exposed cells (Figure S3C). *Nrf2* transcripts were not changed in either the acute (Figure S3B) or chronically exposed cells (Figure S3D). The expression of several early neural markers was also investigated. Previous studies focusing on acute arsenic exposure have shown a reduction in *Ascl1*, a transcription factor needed for neural differentiation (Liu & Bain, 2014, 2018). While *Ascl1* mRNA expression was reduced at an acute 0.5 μM arsenic exposure, it was not altered at the lower 0.1 μM level. Rather, profiler array data indicated that expression of several other neural differentiation genes was reduced, including *Gdf3*, a gene encoding a signaling molecule that can induce neuronal differentiation (Li et al., 2012). It has been

demonstrated that Gdf3 is expressed in embryonic stem cells and the early embryo where it regulates both pluripotency and differentiation (Han et al., 2016; Levine & Brivanlou, 2006; Levine & Brivanlou, 2006), in part by inducing a panel of genes identified as important regulators of ectoderm formation and neurogenesis in human NCCIT cells, an *in vitro* model of cancer stem cells (Tykwinska et al., 2013).

Consistent with our findings, mouse ES cells with reduced Gdf3 protein levels maintained significant levels of Oct3/4 and Sox2 while showing reduced levels of brachyury, a mesoderm marker (Levine & Brivanlou, 2006). Gdf3 is a known regulator of Smad2/3, and previous studies have reported impairment of TGF- β signaling following arsenic exposure. For instance, mouse coronary progenitor cells exposed to 1.3 μ M arsenite had reduced levels and nuclear localization of phosphorylated Smad2/3 (Allison et al., 2013). In addition, arsenic trioxide inhibited the activation and expression of TGF- β and Smad signaling pathway in human prostate cancer *in vivo* and in human adenocarcinoma cells *in vitro* (Ji et al., 2014). Similarly, according to our results, protein levels of phosphorylated Smad2/3 were downregulated at week 16 following arsenic exposure. Taken together these results suggest that neural differentiation is reduced and pluripotency is maintained in embryonic stem cells following chronic arsenic exposure.

Arsenic alters N-cadherin protein expression and patterning within embryoid bodies

During proper embryonic development, the expression of a family of cell-to-cell adhesion molecules known as cadherins, are highly regulated. In particular, epithelial and neural cadherins (E- and N-cadherin, respectively) regulate embryonic gastrulation and neurulation (Brayshaw & Price, 2016). Following chronic arsenic exposure, the expression of N-cadherin and E-cadherin were assessed by immunohistochemistry. N-cadherin protein expression was significantly increased in the arsenic-treated samples starting at week 20 and remained elevated for the rest of

the exposure. Further, N-cadherin protein in the arsenic-treated samples clustered together, resulting in altered patterning. The implications of this clustering is not known.

A number of other chronic arsenic exposure studies have also seen increases in N-cadherin expression. For example, six different human urothelial UROtsa cell isolates transformed with 1 μ M arsenic all showed increased N-cadherin mRNA and protein expression. E-cadherin mRNA expression in these isolates was varied, but there were no changes in E-cadherin protein expression (Sandquist et al., 2016). Human hepatic L-02 cells cultured in 2 μ M arsenic for 15 weeks and human bronchial epithelial cells cultured in 1 μ M arsenic for 15 weeks also had increased N-cadherin protein levels (Chen et al., 2018; Xu et al., 2012).

Typically, there is an inverse relationship in the expression of N-cadherin and E-cadherin during EMT due to a process known as cadherin switching. During cadherin switching, expression of the epithelial-associated E-cadherin is reduced, while expression of the mesenchymal-associated N-cadherin is increased, leading to the promotion of cellular motility and invasion. This process is reversible and known to play a crucial role in proper embryonic development as well as cancer formation (Brayshaw & Price, 2016). Interestingly, throughout the chronic arsenic exposure, as N-cadherin expression was temporally increased, E-cadherin levels remained static. N-cadherin may be in part regulated by Sox2, as its expression is thought to be governed by several Sox-dependent enhancers (Matsumata et al., 2005). It has been shown that Sox2 overexpression promotes an EMT phenotype through increased expression of mesenchymal markers, such as N-cadherin, vimentin, and fibronectin (Yang et al., 2014).

Another important transcription factor in regulating EMT and stem cell-like properties is the zinc finger E-box binding homeobox 1 (Zeb1) (Zhang et al., 2015). Zeb1 helps to maintain stemness by increasing the expression of Sox2 through inhibition of miR-200c, -203, -141, and -183 (Burk et al., 2008; Wellner et al., 2009). In the current study, arsenic-exposed P19 cells have

increased *Zeb1* expression starting at week 16 and remaining elevated by 1.5- and 2-fold throughout the chronic exposure. The expression pattern is similar to that of *Sox2*, which is concordant with other chronic arsenic exposure studies. For example, human urothelial cells chronically exposed to 1 μ M arsenic for up to months had increased expression of *Sox2* and *Zeb1* (Ooki et al., 2018), while *Zeb1* expression was increased in HBE cells exposed to 1 μ M arsenic starting at 10 weeks of chronic exposure (Xu et al., 2012).

Conclusion

A chronic arsenic exposure of 0.1 μ M inorganic arsenic for 32 weeks was shown to impair cellular differentiation and induce an EMT-like phenotype in P19 mouse embryonic stem cells. Consistently elevated *Sox2* and *Zeb1* expression, in conjunction with decreased *Gdf3* and *pSmad2/3* levels is indicative of pluripotency maintenance and diminished differentiation. Further, arsenic exposure led to increased protein expression and altered patterning of the EMT marker, N-cadherin. Taken as a whole, chronic, low-level arsenic exposure appears to induce an EMT-like mechanism to impair neural differentiation and maintain pluripotency.

Acknowledgements

The authors thank Laine Chambers in Clemson's Histology Core Facility. This work was supported by the National Institutes of Health (ES027651) and by Clemson COSSAB funding

References

- Allison, P., Huang, T., Broka, D., Parker, P., Barnett, J. V., & Camenisch, T. D. (2013). Disruption of canonical TGF β -signaling in murine coronary progenitor cells by low level arsenic. *Toxicology and Applied Pharmacology*, *272*, 147-153.
- Andersson, O., Bertolino, P., & Ibáñez, C. F. (2007). Distinct and cooperative roles of mammalian Vg1 homologs GDF1 and GDF3 during early embryonic development. *Developmental Biology*, *311*, 500-511.
- Andersson, O., Korach-Andre, M., Reissmann, E., Ibáñez, C. F., & Bertolino, P. (2008). Growth/differentiation factor 3 signals through ALK7 and regulates accumulation of adipose tissue and diet-induced obesity. *Proceedings of the National Academy of Sciences USA*, *105*, 7252-7256.
- Boumahdi, S., Driessens, G., Lapouge, G., Rorive, S., Nassar, D., Le Mercier, M., . . . Blanpain, C. (2014). SOX2 controls tumour initiation and cancer stem-cell functions in squamous-cell carcinoma. *Nature*, *511*, 246-250.
- Brayshaw, L. L., & Price, S. R. (2016). Cadherins in Neural Development. In S. Suzuki & S. Hirano (Eds.), *The Cadherin Superfamily* (pp. 315-340). Tokyo: Springer.
- Bredfeldt, T. G., Jagadish, B., Eblin, K. E., Mash, E. A., & Gandolfi, A. J. (2006). Monomethylarsonous acid induces transformation of human bladder cells. *Toxicology and Applied Pharmacology*, *216*, 69-79.
- Burk, U., Schubert, J., Wellner, U., Schmalhofer, O., Vincan, E., Spaderna, S., & Brabletz, T. (2008). A reciprocal repression between ZEB1 and members of the miR-200 family promotes EMT and invasion in cancer cells. *EMBO Reports*, *9*, 582-589.
- Chakraborti, D., Rahman, M. M., Mukherjee, A., Alauddin, M., Hassan, M., Dutta, R. N., . . . Hossain, M. M. (2015). Groundwater arsenic contamination in Bangladesh-21 Years of research. *Journal of Trace Elements in Medicine and Biology*, *31*, 237-248.
- Chang, Q., Chen, B., Thakur, C., Lu, Y., & Chen, F. (2014). Arsenic-induced sub-lethal stress reprograms human bronchial epithelial cells to CD61- cancer stem cells. *Oncotarget*, *5*, 1290-1303.
- Chen, C., Ware, S. M., Sato, A., Houston-Hawkins, D. E., Habas, R., M.M., Shen, M. M., & Brown, C. W. (2006). The Vg1-related protein Gdf3 acts in a Nodal signaling pathway in the pre-gastrulation mouse embryo. *Development*, *133*, 319-329.
- Chen, C., Yang, Q., Wang, D., Luo, F., Liu, X., Xue, J., . . . Liu, Q. (2018). MicroRNA-191, regulated by HIF-2 α , is involved in EMT and acquisition of a stem cell-like phenotype in arsenite-transformed human liver epithelial cells. *Toxicology In Vitro*, *48*, 128-136.
- Concha, G., Vogler, G., Lezcano, D., Nermell, B., & Vahter, M. (1998). Exposure to inorganic arsenic metabolites during early human development. *Toxicology Sciences*, *44*, 185-190.

- Dakeishi, M., Murata, K., & Grandjean, P. (2006). Long-term consequences of arsenic poisoning during infancy due to contaminated milk powder. *Environmental Health*, *5*, 31.
- Davis, M. A., Mackenzie, T. A., Cottingham, K. L., Gilbert-Diamond, D., Punshon, T., & Karagas, M. R. (2012). Rice consumption and urinary arsenic concentrations in U.S. children. *Environmental Health Perspectives*, *120*, 1418-1424.
- Ferri, A. L. M., Cavallaro, M., Braidà, D., Di Cristofano, A., Canta, A., Vezzani, A., . . . Nicolis, S. K. (2004). Sox2 deficiency causes neurodegeneration and impaired neurogenesis in the adult mouse brain. *Development*, *131*, 3805–3819.
- Francis, F., Koulakoff, A., Boucher, D., Chafey, P., Schaar, B., Vinet, M. C., . . . Chelly, J. (1999). Doublecortin is a developmentally regulated, microtubule-associated protein expressed in migrating and differentiating neurons. *Neuron*, *23*, 247-256.
- Frankel, S., Concannon, J., Brusky, K., Pietrowicz, E., Giorgianni, S., Thompson, W. D., & Currie, D. A. (2009). Arsenic exposure disrupts neurite growth and complexity *in vitro*. *NeuroToxicology*, *30*, 529-537.
- Golmohammadi, J., Jahanian-Najafabadi, A., & Aliomrani, M. (2019). Chronic oral arsenic exposure and its correlation with serum S100B concentration. *Biology and Trace Elements Research*, *189*, 172-179.
- Han, M. H., Park, S. W., Do, H. J., Chung, H. J., Song, H., Kim, J. H., . . . Kim, J. H. (2016). Growth and Differentiation Factor 3 Is transcriptionally regulated by OCT4 in human embryonic carcinoma cells. *Biology and Pharmacology Bulletin*, *39*, 1802-1808.
- Herreros-Villanueva, M., Zhang, J. S., Koenig, A., Abel, E. V., Smyrk, T. C., Bamlet, W. R., . . . Billadeau, D. D. (2013). SOX2 promotes dedifferentiation and imparts stem cell-like features to pancreatic cancer cells. *Oncogenesis*, *2*, e61.
- Hong, G.-M., & Bain, L. J. (2012). Arsenic exposure inhibits myogenesis and neurogenesis in P19 stem cells through repression of the b-catenin signaling pathway. *Toxicological Sciences*, *129*, 146-156.
- Huang, S., Guo, Guo, F., Yang, Q., Xiao, X., Murata, M., . . . Ma, N. (2013). CD44v6 expression in human skin keratinocytes as a possible mechanism for carcinogenesis associated with chronic arsenic exposure. *European Journal of Histochemistry*, *57*, e1.
- Ji, H., Li, Y., Jiang, F., Wang, X., Zhang, J., Shen, J., & Yang, X. (2014). Inhibition of transforming growth factor beta/SMAD signal by MiR-155 is involved in arsenic trioxide-induced anti-angiogenesis in prostate cancer. *Cancer Science*, *105*, 1541-1549.
- Kumar, A., Adak, P., Gurian, P. L., & Lockwood, J. R. (2010). Arsenic exposure in US public and domestic drinking water supplies: a comparative risk assessment. *Journal of Exposure Science and Environmental Epidemiology*, *20*, 245-254.

- Kuo, C. C., Moon, K. A., Wang, S. L., Silbergeld, E., & Navas-Acien, A. (2017). The association of arsenic metabolism with cancer, cardiovascular disease, and diabetes: a systematic review of the epidemiological evidence. *Environmental Health Perspectives*, *125*, 087001.
- Leis, O., Eguiara, A., Lopez-Arribillaga, E., Alberdi, M. J., Hernandez-Garcia, S., Elorriaga, K., . . . Martin, A. G. (2012). Sox2 expression in breast tumours and activation in breast cancer stem cells. *Oncogene*, *31*, 1354-1365.
- Levine, A. J., & Brivanlou, A. H. (2006). GDF3 at the crossroads of TGF- β signaling. *Cell Cycle*, *5*, 1069-1073.
- Levine, A. J., & Brivanlou, A. H. (2006). GDF3, a BMP inhibitor, regulates cell fate in stem cells and early embryos. *Development*, *133*, 209-216.
- Li, Q., Liu, X., Wu, Y., An, J., Hexige, S., Ling, Y., . . . Yu, L. (2012). The conditioned medium from a stable human GDF3-expressing CHO cell line, induces the differentiation of PC12 cells. *Molecular and Cellular Biochemistry*, *359*, 115-123.
- Liu, J.-T., & Bain, L. J. (2014). Arsenic inhibits hedgehog signaling during P19 cell differentiation. *Toxicology and Applied Pharmacology*, *281*, 243-253.
- Liu, J.-T., & Bain, L. J. (2018). Arsenic induces members of the mmu-miR-466-669 cluster which reduces NeuroD1 expression. *Toxicological Sciences*, *162*, 67-78.
- Markowski, V. P., Reeve, E. A., Onos, K., Assadollahzadeh, M., & McKay, N. (2012). Effects of prenatal exposure to sodium arsenite on motor and food-motivated behaviors from birth to adulthood in C57BL6/J mice. *Neurotoxicology and Teratology*, *34*, 221-231.
- Masui, S., Nakatake, Y., Toyooka, Y., Shimosato, D., Yagi, R., Takahashi, K., . . . Niwa, H. (2007). Pluripotency governed by Sox2 via regulation of Oct3/4 expression in mouse embryonic stem cells. *Nature Cell Biology*, *9*, 625-635.
- Matsumata, M., Uchikawa, M., Kamachi, Y., & Kondoh, H. (2005). Multiple N-cadherin enhancers identified by systematic functional screening indicate its Group B1 SOX-dependent regulation in neural and placodal development. *Developmental Biology*, *286*, 601-617.
- McBurney, M. W. (1993). P19 embryonal carcinoma cells. *International Journal of Developmental Biology*, *37*, 135-140.
- Nahar, M. N., Inaoka, T., Fujimura, M., Watanabe, C., Shimizu, H., Tasmin, S., & Sultana, N. (2014). Arsenic contamination in groundwater and its effects on adolescent intelligence and social competence in Bangladesh with special reference to daily drinking/cooking water intake. *Environmental Health and Preventative Medicine*, *19*, 151-158.
- Naujokas, M. F., Anderson, B., Ahsan, H., Aposhian, H. V., Graziano, J. H., Thompson, C., & Suk, W. A. (2013). The broad scope of health effects from chronic arsenic exposure: update on a worldwide public health problem. *Environmental Health Perspectives*, *121*, 295-302.

- Ooki, A., Begum, A., Marchionni, L., VandenBussche, C. J., Mao, S., Kates, M., & Hoque, M. O. (2018). Arsenic promotes the COX2/PGE2-SOX2 axis to increase the malignant stemness properties of urothelial cells. *International Journal of Cancer*, *143*, 113-126.
- Patel, A. B., De Graaf, R. A., Martin, D. L., Battaglioli, G., & Behar, K. L. (2006). Evidence that GAD65 mediates increased GABA synthesis during intense neuronal activity *in vivo*. *Journal of Neurochemistry*, *97*, 385-396.
- Raqib, R., Ahmed, S., Sultana, R., Wagatsuma, Y., Mondal, D., Hoque, A. M., . . . Vahter, M. (2009). Effects of in utero arsenic exposure on child immunity and morbidity in rural Bangladesh. *Toxicology Letters*, *185*, 197-202.
- Rodda, D. J., Chew, J. L., Lim, L. H., Loh, Y. H., Wang, B., Ng, H. H., & Robson, P. (2005). Transcriptional regulation of Nanog by OCT4 and SOX2. *Journal of Biological Chemistry*, *280*, 24731–24737.
- Sandquist, E. J., Somji, S., Dunlevy, J. R., Garrett, S. H., Zhou, X. D., Slusser-Nore, A., & Sens, D. A. (2016). Loss of N-Cadherin expression in tumor transplants produced from As+3- and Cd+2-transformed human irothelial (UROtsa) cell lines. *PLoS ONE*, *11*, e0156310.
- Schmittgen, T. D., & Livak, K. J. (2008). Analyzing real-time PCR data by the comparative CT method. *Nature Protocols*, *3*, 1101–1108.
- Shih, Y. H., Scannell Bryan, M., & Argos, M. (2020). Association between prenatal arsenic exposure, birth outcomes, and pregnancy complications: An observational study within the National Children's Study cohort. *Environmental Research*, *183*, 109182.
- Steffens, A. A., Hong, G.-M., & Bain, L. J. (2011). Sodium arsenite delays the differentiation of C2C12 mouse myoblast cells and alters methylation patterns on the transcription factor myogenin. *Toxicology and Applied Pharmacology*, *250*, 154-161.
- Takahashi, K., & Yamanaka, S. (2006). Induction of pluripotent stem cells from mouse embryonic and adult fibroblast cultures by defined factors. *Cell*, *126*, 663-676.
- Tokar, E. J., Diwan, B. A., & Waalkes, M. P. (2010). Arsenic exposure transforms human epithelial stem/progenitor cells into a cancer stem-like phenotype. *Environmental Health Perspectives*, *118*, 108-115.
- Tokar, E. J., Qu, W., Liu, J., Liu, W., Webber, M. M., Phang, J. M., & Waalkes, M. P. (2010). Arsenic-specific stem cell selection during malignant transformation. *Journal of the National Cancer Institute*, *102*, 638-649.
- Tolins, M., Ruchirawat, M., & Landrigan, P. (2014). The developmental neurotoxicity of arsenic: cognitive and behavioral consequences of early life exposure. *Annals of Global Health*, *80*, 303-314.

- Tykwinska, K., Lauster, R., Knaus, K., & Rosowski, M. (2013). Growth and differentiation factor 3 induces expression of genes related to differentiation in a model of cancer stem cells and protects them from retinoic acid-induced apoptosis *PLoS ONE*, *8*, e70612.
- Vasconcelos, F. F., & Castro, D. S. (2014). Transcriptional control of vertebrate neurogenesis by the proneural factor *Ascl1*. *Frontiers in Cellular Neurosciences*, *8*, 412.
- von Ehrenstein, O. S., Guha Mazumder, D. N., Hira-Smith, M., Ghosh, N., Yuan, Y., Windham, G., . . . Smith, A. H. (2006). Pregnancy outcomes, infant mortality, and arsenic in drinking water in West Bengal, India. *American Journal of Epidemiology*, *163*, 662-669.
- Wang, X., Meng, D., Chang, Q., Pan, J., Zhang, Z., Chen, G., . . . Shi, X. (2010). Arsenic inhibits neurite outgrowth by inhibiting the LKB1-AMPK signaling pathway. *Environmental Health Perspectives*, *118*, 627-634.
- Wang, X., & Yang, P. (2008). *In vitro* differentiation of mouse embryonic stem (mES) cells using the hanging drop method. *JoVE*, *17*, <http://www.jove.com/index/details.stp?id=825>, doi: 810.3791/3825.
- Wellner, U., Schubert, J., Burk, U. C., Schmalhofer, O., Zhu, F., Sonntag, A., . . . Brabletz, T. (2009). The EMT-activator ZEB1 promotes tumorigenicity by repressing stemness-inhibiting microRNAs. *Nature Cell Biology*, *11*, 1487-1495.
- Wilson, D., Hooper, C., & Shi, X. (2012). Arsenic and lead in juice: Appliede, citrus, and Appliede-base. *Journal of Environmental Health*, *75*, 14-20.
- Wnek, S. M., Jensen, T. J., Severson, P. L., Futscher, B. W., & Gandolfi, A. J. (2010). Monomethylarsonous acid produces irreversible events resulting in malignant transformation of a human bladder cell line following 12 weeks of low-level exposure. *Toxicological Sciences*, *116*, 44-57.
- Xu, Y., Li, Y., Pang, Y., Ling, M., Shen, L., Yang, X., . . . Liu, Q. (2012). EMT and stem cell-like properties associated with HIF-2 α are involved in arsenite-induced transformation of human bronchial epithelial cells. *PLoS ONE*, *7*, e37765.
- Yang, N., Hui, L., Wang, Y., Yang, H., & Jiang, X. (2014). Overexpression of SOX2 promotes migration, invasion, and epithelial-mesenchymal transition through the Wnt/ β -catenin pathway in laryngeal cancer Hep-2 cells. *Tumour Biology*, *35*, 7965-7973.
- Yen, Y. P., Tsai, K. S., Chen, Y. W., Huang, C. F., Yang, R. S., & Liu, S. H. (2010). Arsenic inhibits myogenic differentiation and muscle regeneration. *Environmental Health Perspectives*, *118*, 949-956.
- Yorifuji, T., Kato, T., Ohta, H., Bellinger, D. C., Matsuoka, K., & Grandjean, P. (2016). Neurological and neuropsychological functions in adults with a history of developmental arsenic poisoning from contaminated milk powder. *Neurotoxicology and Teratology*, *53*, 75-80.

- Zavala, Y. J., & Duxbury, J. M. (2008). Arsenic in rice: I. Estimating normal levels of total arsenic in rice grain. *Environmental Science and Technology*, *42*, 3856-3860.
- Zhang, P., Sun, Y., & Ma, L. (2015). ZEB1: at the crossroads of epithelial-mesenchymal transition, metastasis and therapy resistance. *Cell Cycle*, *14*, 481-487.
- Zhao, C. Q., Young, M. R., Diwan, B. A., Coogan, T. P., & Waalkes, M. P. (1997). Association of arsenic-induced malignant transformation with DNA hypomethylation and aberrant gene expression. *Proceedings of the National Academy of Sciences USA*, *94*, 10907-10912.

Figures

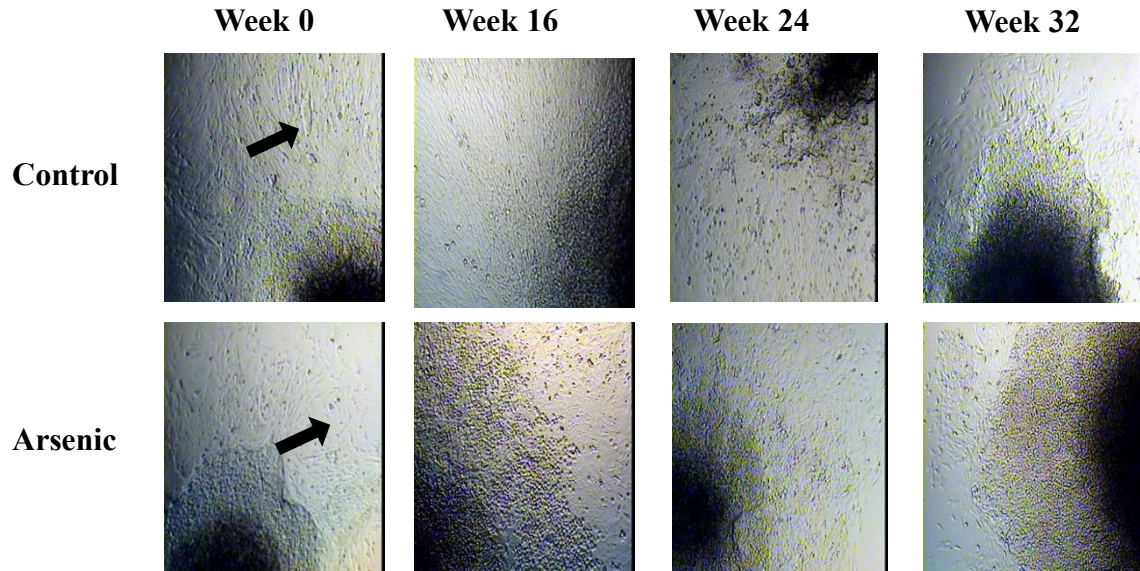


Figure 2.1. Morphology of day 9 cells exposed to 0 or 0.1 μM arsenic. Representative images of day 9 cells at weeks 0, 16, 24, and 32 of exposure are shown. Arrows show elongating and differentiating cells.

| | Week 8 | Week 32 | |
|--|--|--|--|
| Gene symbol and function | Expression in arsenic/control cells | Expression in arsenic/control cells | Change in arsenic-exposed cells |
| Pluripotency | | | |
| Sox2 | 1.9 | 3.3 | ↑ |
| Oct4 | 2.7 | 0.7 | ↑ |
| Nanog | 0.8 | 0.8 | ▬ |
| Ectoderm and neuroectoderm germ cells | | | |
| Fgf5 | 2.2 | 1.4 | ↑ |
| FoxD3 | 1.5 | 1.2 | ↑ |
| Otx2 | 1.5 | 0.5 | ▬ |
| Zic1 | 1.5 | 1.0 | ↑ |
| Gbx2 | 3.7 | 1.3 | ↑ |
| Differentiated neurons | | | |
| Dcx | 0.1 | 0.4 | ↓ |
| Prom1 | 0.1 | 0.7 | ↓ |
| Gad2 | 0.1 | 0.1 | ↓ |
| Gdf3 | 0.1 | 0.5 | ↓ |
| Mesoderm germ cells | | | |
| Gata2 | 0.6 | 1.8 | ▬ |
| Tbxt | 0.1 | 0.6 | ↓ |
| Differentiated muscles | | | |
| Myh1 | ND | 0.1 | ↓ |
| Myh7 | 3.3 | 0.6 | ▬ |

ND = not detectable

Table 2.1. Cell lineage profiler array differential expression of select genes

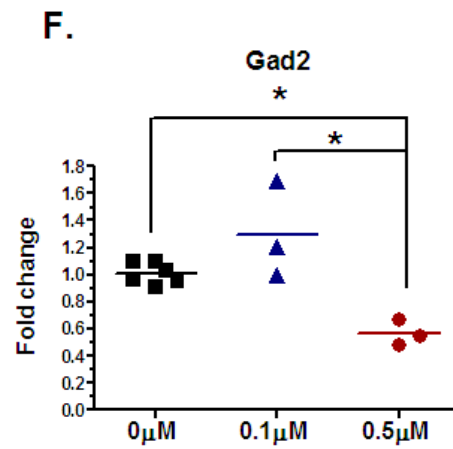
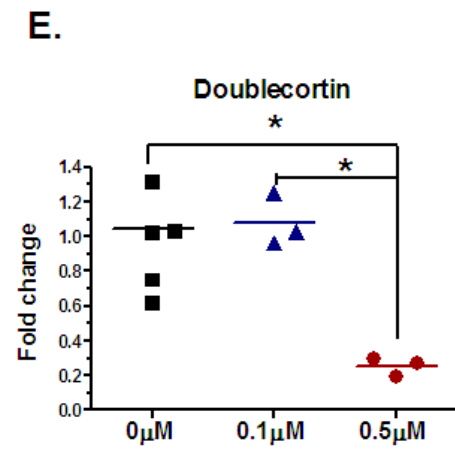
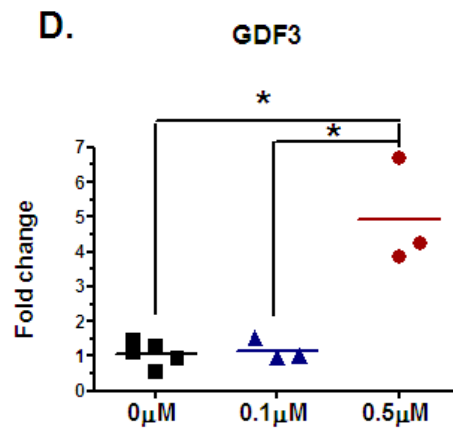
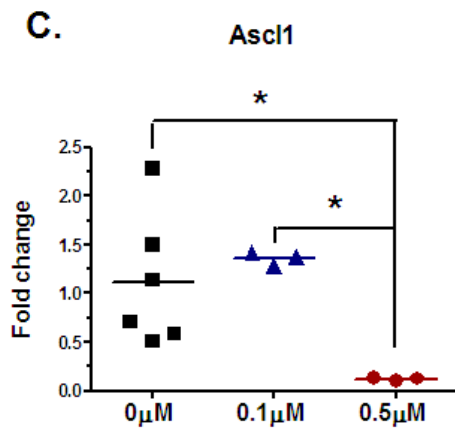
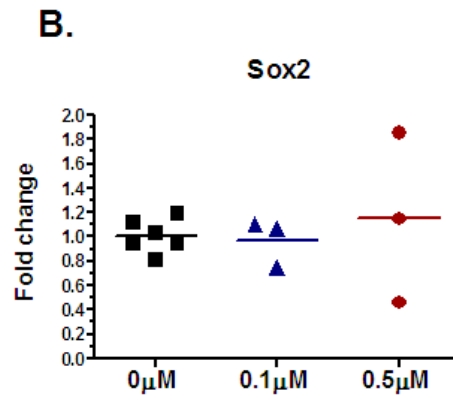
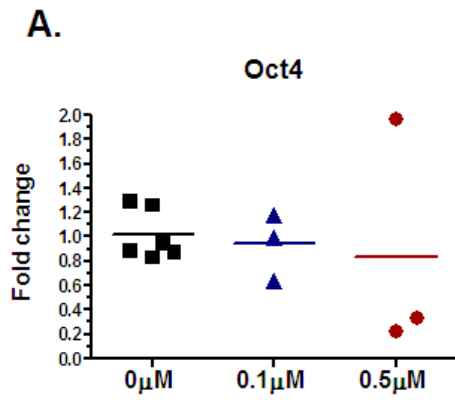
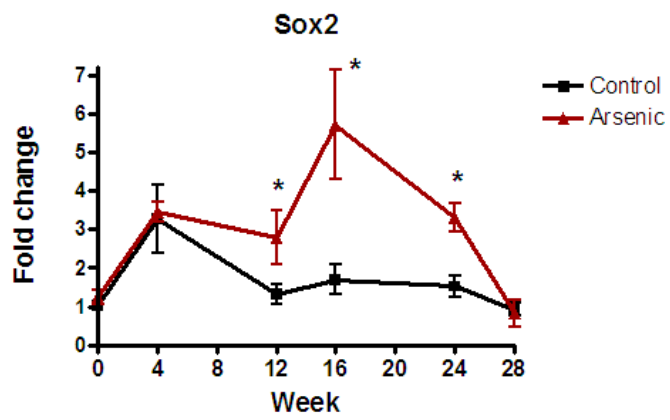
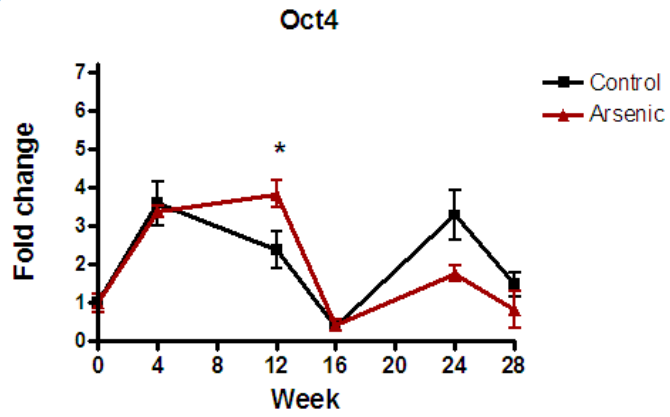


Figure 2.2 Acute arsenic exposure alters the expression of neural and oxidative stress-related transcripts. Levels of mRNA following a nine-day acute exposure to 0.1 and 0.5 μ M arsenic exposure was quantified by qPCR for *Oct4* (A), *Sox2* (B), *Ascl1* (C), *Gdf3* (D), *Dcx* (E), and *Gad2* (F). Data was normalized to the geometric mean of *Gapdh* and β 2-microglobulin and is expressed as the average $2^{-\Delta\Delta Ct}$ for each group (n=6 for controls and n=3 for each exposure group). Statistical differences (*) were determined using ANOVA followed by Bonferroni's test ($p \leq 0.05$).

A.



B.



C.

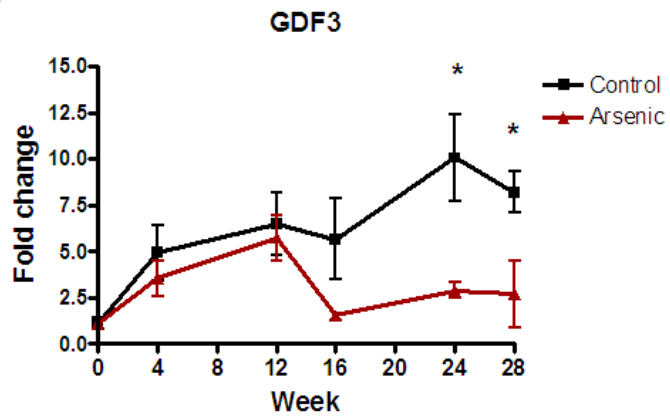
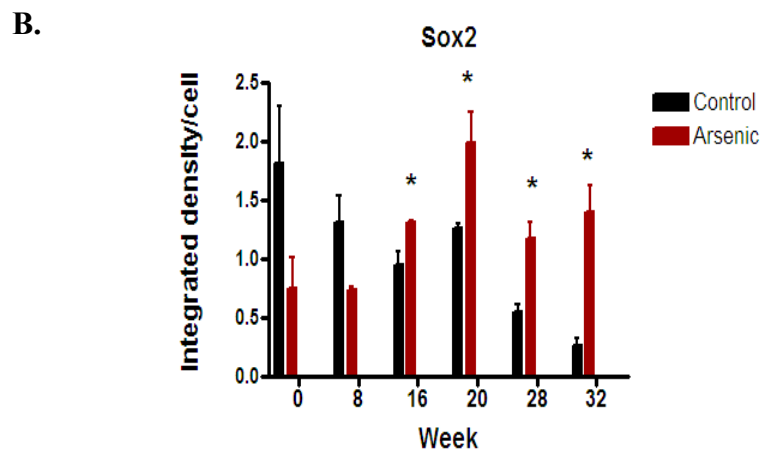
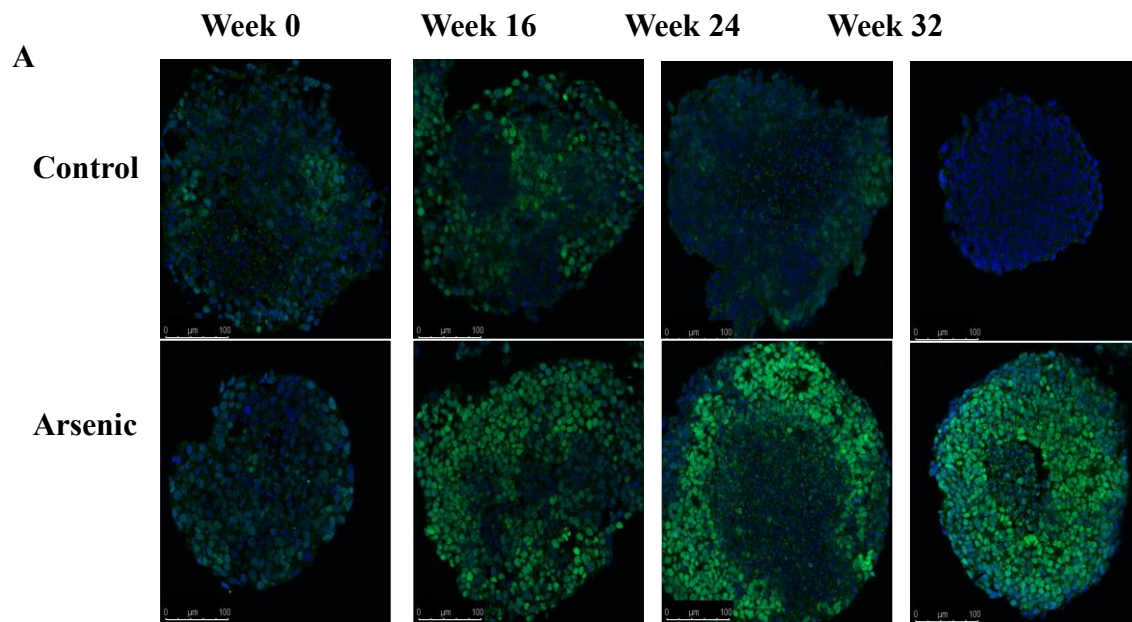


Figure 2.3 Chronic exposure to arsenic alters the expression of pluripotency markers.

Transcript levels from day 9 differentiated cells after 0, 4, 12, 16, 24, and 28 weeks of continuous exposure to 0.1 μ M arsenic were quantified by qPCR for *Sox2* (A), *Oct4* (B), and *Gdf3* (C). At each time point, data were normalized to the geometric mean of *Gapdh* and β 2-microglobulin using the ddCt method. Expression fold changes were compared to transcript levels at week 0 (n=3 flasks per exposure group). Statistical differences (*) were determined using Student's t-test ($p \leq 0.05$).

| Transcript name | Control AUC Average \pm S.D. | Arsenic AUC Average \pm S.D. |
|------------------------|--|--|
| Oct4 | 70.7 \pm 10.8 | 68.4 \pm 8.9 |
| Sox2 | 60.1 \pm 22.1 | 114.3 \pm 11.6 * |
| Gdf3 | 160 \pm 22.5 | 75.5 \pm 12.3 * |
| Dcx | 142.1 \pm 9.3 | 132.2 \pm 52.6 |
| Gad2 | 73.0 \pm 11.8 | 81.0 \pm 13.3 |
| Hmox | 41.2 \pm 11.5 | 36.4 \pm 18.6 |
| Nrf2 | 87.3 \pm 31.8 | 51.3 \pm 6.0 |

Table 2.2. Area under the curve (AUC) measurements for transcript data



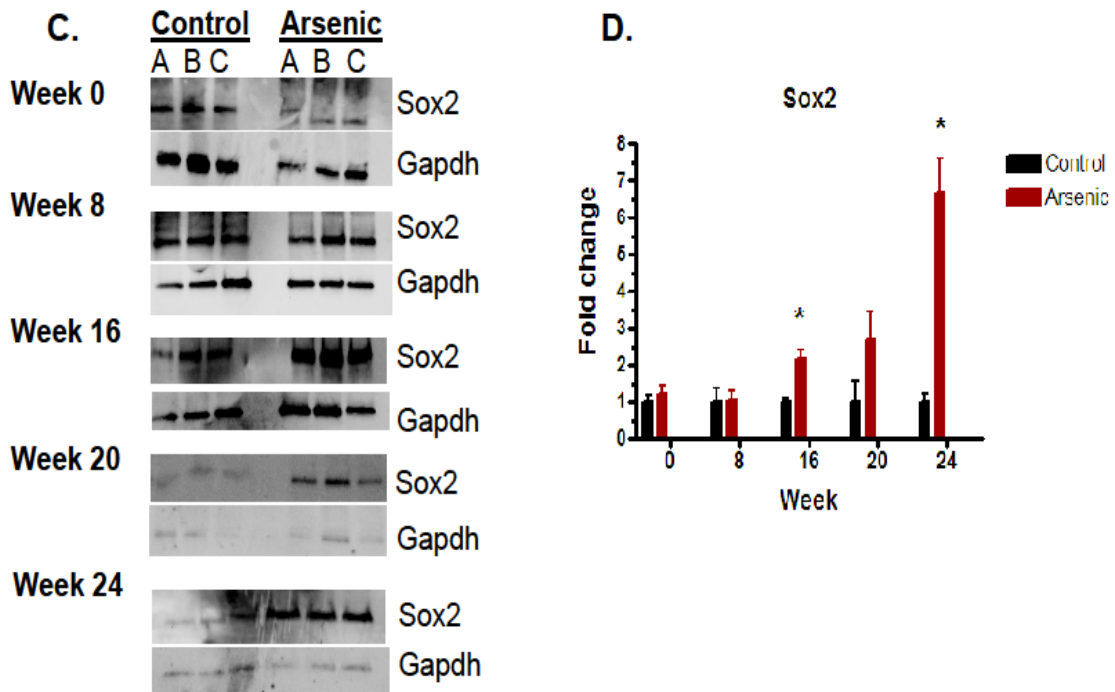


Figure 2.4 Sox2 expression is increased due to arsenic exposure. Representative images of Sox2 expression in day 5 control and 0.1 μM arsenic exposed embryoid bodies at weeks 0, 16, 24, and 32 of exposure (A). Relative fluorescence was determined in ImageJ and is expressed as the integrated density per cell ($n=3$ per exposure group). Statistical differences (*) were determined using Student's t-test at $p \leq 0.05$ (B). Immunoblotting of Sox2 and Gapdh protein expression in the day 9 control and 0.1 μM arsenic exposed cells (C). Protein levels were assessed by densitometry, normalized to Gapdh, and relative fold-expression ($n=3$ per exposure group) was assessed using the integrated density function in BioRad ImageLab (D). Statistical differences (*) were determined using Student's t-test ($p < 0.05$).

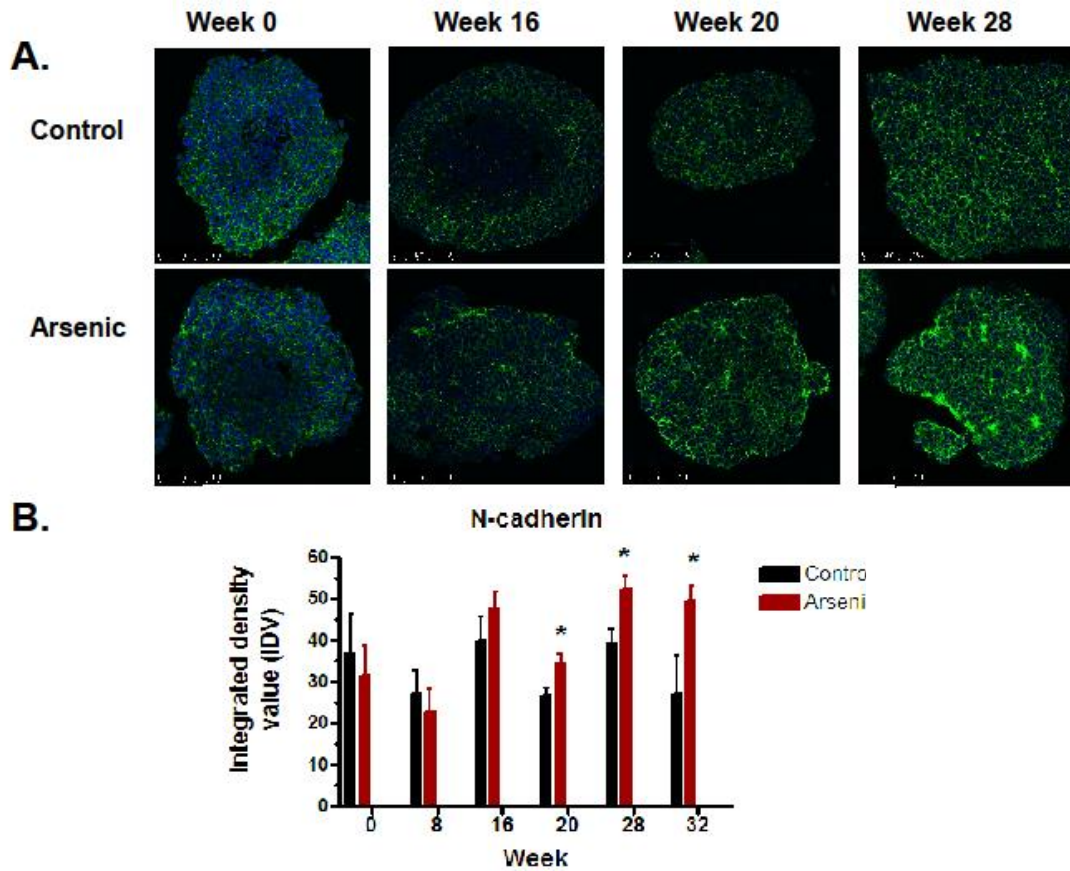


Figure 2.5 Arsenic exposure results in increased expression and altered patterning of N-cadherin. (a) Representative images of N-cadherin expression in day 5 control and 0.1 μ M arsenic exposed embryoid bodies at weeks 0, 16, 20, and 28 of exposure. (b) Relative fluorescence was determined in ImageJ and is expressed as an integrated density value (IDV) (n=3 per exposure group). Statistical differences (*) were determined using Student's t-test at $p \leq 0.05$.

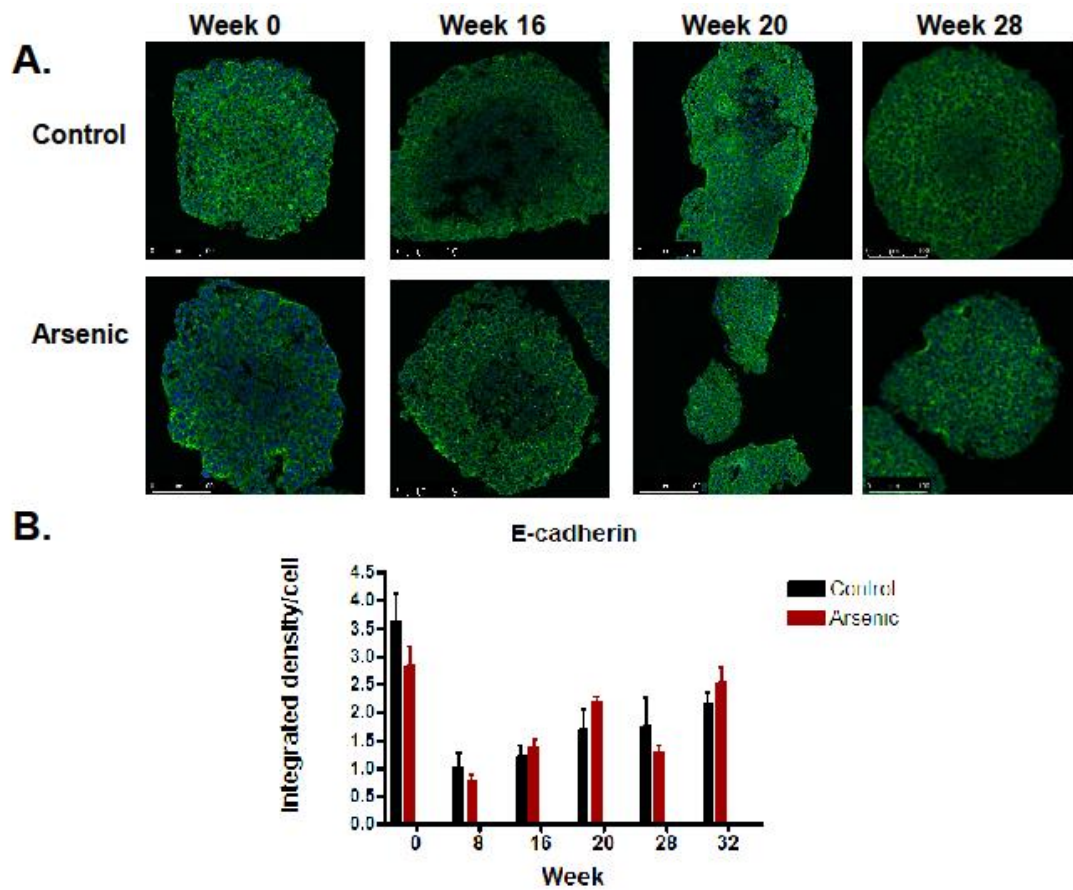


Figure 2.6 Chronic arsenic exposure does not alter E-cadherin expression. (a) Representative images of E-cadherin expression in day 5 control and 0.1 μ M arsenic exposed embryoid bodies at weeks 0, 16, 20, and 28 of exposure. (b) Relative fluorescence was determined in ImageJ and is expressed as the integrated density per cell ($n=3$ per exposure group). Statistical differences (*) were determined using Student's t-test at $p \leq 0.05$.

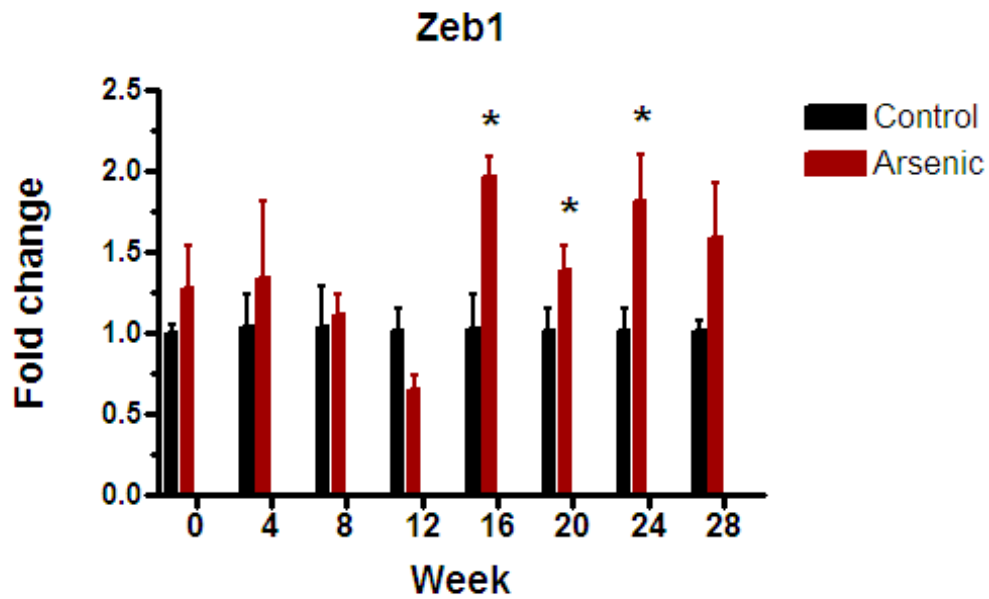


Figure 2.7 Arsenic impairs transcription of Zeb1. Transcript levels in day 5 embryoid bodies after 0, 4, 8, 12, 16, 20, 24, and 28 weeks of continuous exposure to 0.1 μM arsenic were quantified by qPCR. At each time point, *Zeb1* levels were normalized to the geometric mean of *Gapdh* and $\beta 2$ -microglobulin using the ddCt method. Expression fold changes were compared to transcript levels at week 0 (n=3 flasks per exposure group). Statistical differences (*) were determined using Student's t-test ($p \leq 0.05$).

| <u>Gene</u> | <u>Primer Sequence</u> | |
|-------------------------|-------------------------------|--------------------------------|
| | <u>Forward</u> | <u>Reverse</u> |
| <i>Sox2</i> | 5'-AGGCAGAGAAGAGAGTGTGG-3' | 5'-CTTCTCTCCTTTCTTTCTCTCTCC-3' |
| <i>Oct4</i> | 5'-CCTACAGCAGATCACTCACATC-3' | 5'-TGTCCCTGTAGCCTCATACT-3' |
| <i>Gad2</i> | 5'-GTCTGCTTCTGGTTTGTACCT-3' | 5'-GTGGTCCCATACTCCATCATTC-3' |
| <i>Gdf3</i> | 5'-GGTGGTAACCCTCA TCCTAAA-3' | 5'-GTGGCAGAAGTTCCTACAGAA-3' |
| <i>Dcx</i> | 5'-GGTGACGGATGAATGGACTT-3' | 5'-CGTACCTTCTTGGCCTTCTT-3' |
| <i>Ascl1</i> | 5' ACTTGAACTCTATGGCGGGTT -3' | 5'-CCAGTTGGTAAAGTCCAGCAG -3' |
| <i>Hmox</i> | 5'-GTACACATCCAAGCCGAGAA-3' | 5'-TGGTACAAGGAAGCCATCAC-3' |
| <i>Nrf2</i> | 5'-CTCCGTGGAGTCTTCCATTAC-3' | 5'-GCACTATCTAGCTCCTCCATTTC-3' |
| <i>Zeb1</i> | 5'-CTTACGGATTACAGTGGAGAG-3' | 5'-GTGAGCTATAGGAGCCAGAATG-3' |
| <i>Gapdh</i> | 5'-TGCGACTTCAACAGCAACTC-3' | 5'-ATGTAGGCCATGAGGTCCAC-3' |
| <i>β2-microglobulin</i> | 5'-CAGCAAGGACTGGTCTTTCTAT -3' | 5'-AACTCTGCAGGCGTATGTATC-3' |

Table S2.1: Primer sequences for qPCR.

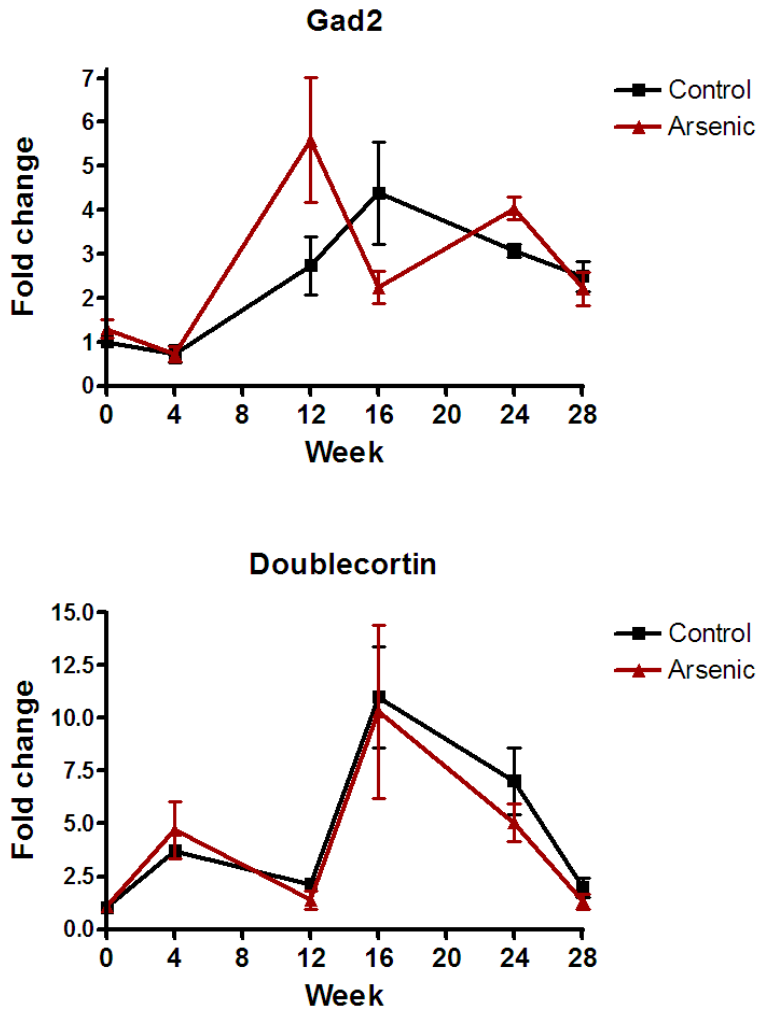


Figure S2.1. Gad2 and Dcx mRNA expression is not changed following a chronic arsenic exposure. Transcript levels of *Gad2* and *Dcx* were quantified in day 9 differentiated cells after 0, 4, 12, 16, 24, and 28 weeks of continuous exposure to 0.1 μ M arsenic by qPCR. At each time point, data were normalized to the geometric mean of *Gapdh* and β 2-microglobulin using the ddCt method. Expression fold changes were compared to transcript levels at week 0 (n=3 flasks per exposure group). Statistical differences (*) were determined using ANOVA followed by Bonferroni's test ($p \leq 0.05$).

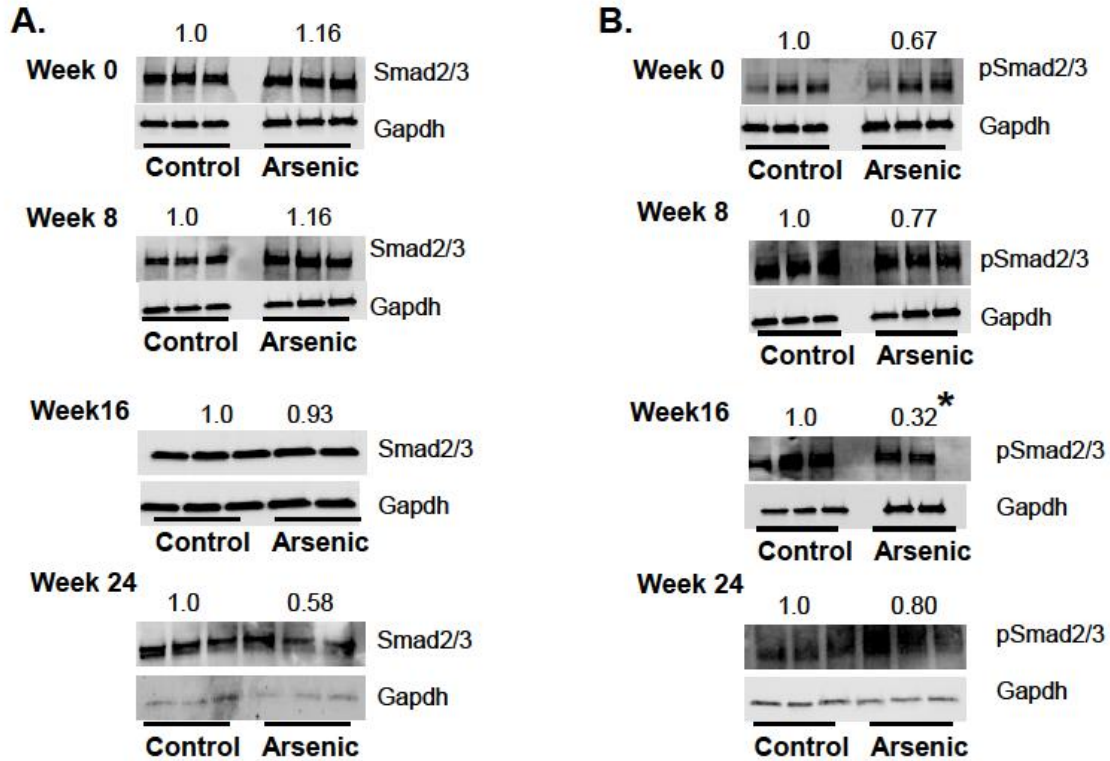


Figure S2.2. Gdf3 transcripts and pSmad2/3 protein levels are reduced in arsenic exposed cells. Protein expression of Smad2/3 (A) and phospho-Smad2/3 (B) in the day 9 control and 0.1 μ M arsenic exposed cells were determined by immunoblotting (n=2 3 independent flasks). Protein levels were assessed by densitometry, normalized to Gapdh, and relative fold-expression was assessed using the integrated density function in BioRad ImageLab. Fold-expression values are shown above the bands in each blot. Statistical differences (*) were determined using Student's t-test ($p \leq 0.05$).

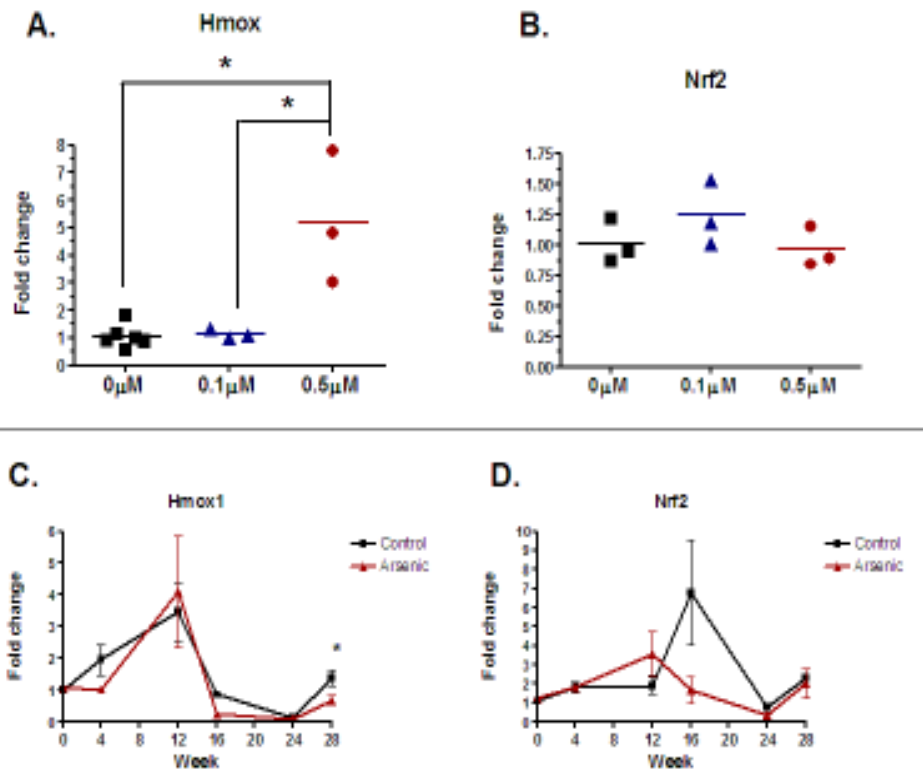


Figure S2.3. Changes in antioxidant response genes following acute and chronic arsenic exposure. Levels of mRNA following a nine-day acute exposure to 0.1 and 0.5 μM arsenic exposure was quantified by qPCR for *Hmox* (A) and *Nrf2* (B). Data was normalized to the geometric mean of *Gapdh* and *$\beta 2$ -microglobulin* and is expressed as the average $2^{\Delta\Delta\text{Ct}}$ for each group ($n=6$ for controls and $n=3$ for each exposure group). Transcript levels of *Hmox* (C) and *Nrf2* (D) were quantified by qPCR in day 9 differentiated cells after 0, 4, 12, 16, 24, and 28 weeks of continuous exposure to 0.1 μM arsenic. At each time point, data were normalized to the geometric mean of *Gapdh* and *$\beta 2$ -microglobulin* using the $\Delta\Delta\text{Ct}$ method. Expression fold changes were compared to transcript levels at week 0 ($n=3$ flasks per exposure group). Statistical differences (*) were determined using ANOVA followed by Bonferroni's test ($p \leq 0.05$).

CHAPTER THREE

ARSENIC IMPAIRS STEM CELL DIFFERENTIATION VIA THE HIPPO SIGNALING PATHWAY

M. Chiara Perego, Benjamin D. McMichael, Lisa J. Bain

This chapter has been submitted to Toxicology Research and is in the format required of that journal.

Abstract

Arsenic is a ubiquitous toxic metalloid, with over 150 million people exposed to arsenic concentrations above the current 10 ppb drinking water standard through contaminated food and water. Arsenic is a known developmental toxicant as neuronal and muscle development are disrupted following arsenic exposure during embryogenesis. In this study, murine embryonic stem cells were chronically exposed to 0.1 μ M (7.5 ppb) arsenic for 32 weeks. RNA sequencing showed that the Hippo signaling pathway, which is involved in embryonic development and pluripotency maintenance, is impaired following arsenic exposure. Thus, temporal changes in the Hippo pathway's core components and its downstream target genes *Ctgf* and *c-Myc* were investigated. Protein expression of the pathway's main effector YAP in its active form was significantly upregulated by 3.7-fold in arsenic-exposed cells at week 8, while protein expression of inactive phosphorylated YAP was significantly downregulated by 2.5- and 2- fold at week 8 and 16. Exposure to arsenic significantly increased the ratio between nuclear and cytoplasmic YAP by 1.9-fold at weeks 16 and 28. The ratio between nuclear and cytoplasmic TEAD was similarly increased in arsenic-treated samples by 3.4- and 1.6- fold at week 16 and 28, respectively. Levels of *Ctgf* and *c-Myc* were also upregulated following arsenic exposure. These results suggest that chronic exposure to an environmentally relevant arsenic concentration might hinder cellular differentiation and maintain pluripotency through the impairment of the Hippo signaling pathway resulting in increased YAP activation.

Introduction

Arsenic is a ubiquitous toxic metalloid found in soil and groundwater that is well known for its hazardous effects on health. Arsenic can originate from natural sources as well as anthropogenic activities (Dakeishi et al., 2006; Sarkar and Paul, 2016). Its main route of exposure is through ingestion of contaminated food and drinking water, threatening more than 150 million people in 70 countries. The current drinking water standard is 10 ppb arsenic, which was established by the U.S. Environmental Protection Agency and the World Health Organization (Ravenscroft et al., 2009; Shankar et al., 2014). Elevated arsenic concentrations have been documented in various countries including China, Mexico, Chile, Argentina, India, Bangladesh and the United States (Smith et al., 2000; Bundschuh et al., 2009; Bhattacharya et al., 2011; Bjorklund et al., 2020). Reports indicate that in the U.S., approximately 2.1 million people obtain drinking water from domestic wells with arsenic concentrations above 10 $\mu\text{g/L}$ (Ayotte et al., 2017). Additionally, it has been previously estimated that on average, an individual adult in the U.S ingests 3.2 μg of arsenic daily, with a total dietary intake ranging from of 1.3-11.4 $\mu\text{g/day}$ (Meacher et al., 2002; Sarkar and Paul, 2016). Epidemiological studies have shown that placental and cord blood arsenic concentrations are comparable, indicating that arsenic can readily cross the placental barrier (Concha et al., 1998; Hall et al., 2007; Henn et al., 2016). Consequently, exposure during pregnancy and embryonic development can cause both immediate and delayed effects, including increased spontaneous abortion and stillbirths, low birth weight, reduced weight gain, impaired muscle development and locomotor activity, learning and memory deficits, and neurobehavioral alterations (Concha et al., 1998; Dakeishi et al., 2006; Von Ehrenstein et al., 2006; Hall et al., 2007; Raqib et al., 2009).

Previous studies conducted using rodent models have shown that administration of inorganic arsenic to pregnant dams induces fetal malformations, impaired development, disrupted

locomotor activity and behavioral deficits (DeSesso et al., 1998; Chattopadhyay et al., 2002; Rodriguez et al., 2002; Wang et al., 2006). In particular, Chattopadhyay and colleagues (2002) observed that 300 ppb of sodium arsenite administered through drinking water to pregnant rats resulted in offspring with decreased responsiveness to a new environment, along with reduced locomotion and limb movement. Consistently, hippocampal neurogenesis, cell morphology and gene expression patterns have been impaired following exposure to 50 ppb arsenic during fetal development (Tyler and Allan, 2013). Moreover, disrupted learning abilities and memory behavior have been reported in adult mice following *in utero* arsenic exposure to 50 ppb of arsenic as these mice performed poorly in new object identification tests and failed to show improvements in hippocampal-dependent learning tasks compared with control mice (Martinez-Finley et al., 2009; Thomas, 2013).

While the mechanisms responsible for developmental changes in offspring are not fully understood, one possibility is that arsenic impairs proper cellular development and differentiation. For instance, C2C12 myoblasts exposed to 20 nM sodium arsenite showed impaired differentiation and myotube formation caused by inhibition of myogenic transcription factor expression (Steffens et al., 2011). Similarly, exposure of P19 mouse embryonic stem cells to 0.5 μ M sodium arsenite suppressed skeletal muscle and neuronal differentiation (Hong and Bain, 2012). Neuronal differentiation and neurite outgrowth was also impaired in Neuro-2a cells when exposed to < 5 μ M arsenic trioxide (Wang et al., 2010) or to 5 μ M sodium arsenite (Aung et al., 2013). Moreover, chronic low-level arsenic exposure can increase expression of genes involved in pluripotency maintenance and decrease the expression of genes involved in cellular differentiation (McMichael et al., 2020).

Signaling pathways help regulate the balance between pluripotency and cellular differentiation. Arsenic exposure is known to impair several signaling pathways, including TGF- β

(Allison et al., 2013; Ji et al., 2014; McMichael et al., 2020) and Wnt/ β -catenin (Hong and Bain, 2012; Wang et al., 2017; Jatko et al., 2021). Another pathway involved in regulating cellular differentiation and stem cell maintenance is the Hippo signaling pathway (Liu et al., 2012; Chen et al., 2019). In the Hippo pathway following upstream activation, the signal receiver MST1/2 phosphorylates LATS1/2, which then phosphorylates YAP when it is bound to TAZ, (Piccolo et al., 2014; Papaspyropoulos et al., 2018). Phosphorylation of the YAP/TAZ complex results in cytoplasmic retention, or in ubiquitination and subsequent degradation (Meng et al., 2016). Conversely, the un-phosphorylated YAP/TAZ complex translocates to the nucleus where it interacts with members of the transcriptional enhancer factor domain (TEAD) family to regulate expression of target genes (Zhao et al., 2008; Stein et al., 2015; Chen et al., 2019), including connective tissue growth factor (*Ctgf*), *Axl*, and *c-Myc* (Piccolo et al., 2014; Wang et al., 2014; Totaro et al., 2018; Chen et al., 2019; Shea et al., 2019). Interestingly, unlike other signaling pathways, its role in arsenic-induced developmental toxicity has been poorly investigated.

The purpose of the current study was to determine whether a long-term arsenic exposure to P19 embryonic stem cells disrupted the Hippo pathway, thereby inhibiting cellular differentiation. Our results showed an increased expression of YAP at week 8 along with a decreased expression of its phosphorylated (inactive) form at week 8 and 16. Transcript levels of *Lats2* were significantly upregulated at week 24, and protein levels of LATS2 were significantly increased at week 8 and 16 of arsenic exposure. Further, at week 16 and 28, the ratio of nuclear (active) and cytoplasmic (inactive) YAP and TEAD was increased concomitantly with upregulated expression of YAP's target genes *Ctgf* and *c-Myc* resulting in pluripotency maintenance. These results suggest that the Hippo signaling pathway plays a role in arsenic-induced developmental toxicity and is involved in the disruption of proper cellular differentiation following arsenic exposure.

Methods

Cell culture

P19 mouse embryonic stem cells (Sigma-Aldrich St. Louis, MO, USA) were cultured in α -MEM media (Hyclone, Logan, UT, USA) with 7.5 % bovine calf serum (Hyclone), 2.5 % fetal bovine serum (Sigma-Aldrich) and 1 % L-glutamine (Thermo Fisher Scientific, Waltham, MA, USA). Cells were cultured in a humidified incubator at 37 °C and 5% CO₂ and passaged every two to three days to maintain low confluency and avoid premature cellular differentiation. Cells were exposed to 0 or 0.1 μ M arsenic as sodium arsenite (Sigma-Aldrich) for up to 32 weeks as previously described (McMichael et al., 2020). The concentration chosen for this study (0.1 μ M or 7.5 ppb) is lower than the current drinking water standard of 10 ppb and is a relevant concentration for an embryonic exposure study (Concha et al., 1998; Henn et al., 2016). Control and arsenic-exposed samples were cultured as three independent replicates (n = 3 for each treatment).

Cell Differentiation

Every four weeks, the control and arsenic-exposed cells were differentiated as previously described (McMichael et al., 2020). In brief, cells were exposed to 1 % DMSO and cultured as hanging drops for two days, with the newly formed embryoid bodies (EBs) transferred to 96-well ultralow attachment plates and cultured for an additional 3 days. At day 5, half the EBs were harvested, washed in PBS and incubated overnight at 4 °C in 10 % neutral buffered formalin (NBF) for subsequent immunohistochemistry. The remaining EBs were transferred to 48-well plates coated with 0.1 % gelatin and cultured for 4 days to promote differentiation into skeletal myoblasts and neural progenitors. Culture medium was refreshed every 48 hours. At day 9, cells were collected and stored at -80 °C in Trizol (Thermo Fisher) for subsequent RNA extraction, or in RIPA buffer for subsequent protein analysis.

Quantitative PCR

Extracted RNA (2µg) was converted into cDNA using M-MLV Reverse Transcriptase (Promega, Madison, Wisconsin, USA). Gene expression was assessed by Real-Time quantitative PCR on a Bio-Rad iQ5 thermocycler (Hercules, CA, USA) using RT² SYBR Green (Applied Biosystems, Foster City, CA, USA) and gene specific primers (Supplementary Table 1). Samples were run in triplicate and a standard curve was generated with five concentration points (10^{-3} - 10^{-7} ng cDNA) to determine run efficiency. A melt curve was obtained for each analysis to ensure the absence of non-specific primer binding. Gapdh and β 2-microglobulin were used as housekeeping genes to normalize data. Gene expression was analyzed using the delta-delta Ct method (Schmittgen and Livak, 2008).

Immunohistochemistry analysis

Day 5 EBs were fixed overnight in NBF, dehydrated in ethanol, embedded in paraffin, and sectioned at 5 µm. Slides were deparaffinized and Tris-EDTA buffer (pH 9) was used for antigen retrieval. Primary antibodies for YAP (1:100, Cell Signaling, #12395), TEAD4 (1:50, Sigma-Aldrich, #AV38276) and CTGF (1:200, Genetex, #GTX124232) were incubated overnight at 4 °C. After incubation with Alexa Fluor 488 secondary antibodies (1:200, anti-rabbit, Invitrogen #A11034) and Alexa Fluor 546 (1:200 anti-mouse, Invitrogen, #A11003), nuclei were counterstained with TO-PRO-3 (1:1000, Thermo Fisher, #T3605).

Samples double labelled with YAP and TEAD4 were imaged using a Leica SP8X confocal microscope (Leica Microsystems, Buffalo Grove, IL), equipped with a tunable white light laser, HyD detectors, and time gating. Samples were imaged using a 63X objective (N.A.= 1.4) and a zoom of 1.5. To image TO-PRO-3, we used an excitation wavelength of 635 nm and collected emission wavelengths of 650 to 700 nm, with a time gate of 0.5 to 6.0 ns, and a frame average of

2. To image Alexa Fluor 546, we used an excitation wavelength of 557 nm and collected emission wavelengths of 562 to 620 nm, with a time gate of 0.5 to 6.0 ns and a frame average of 4. To image Alexa Fluor 488, we used an excitation wavelength of 499 nm and collected emission wavelengths of 504 to 550 nm, with a time gate of 0.5 to 6.0 ns and a frame average of 4. Additional overview images were collected using a 20X objective (N.A. = 0.75) and a zoom of 1.0 using the settings outlined above, but with frame averages of 1 (TO-PRO-3), 2 (AF546), and 2 (AF488).

Samples labelled with CTGF were imaged using a Leica SPE confocal microscope (Leica Microsystems, Buffalo Grove, IL), using a 63X objective (N.A.= 1.3) and a zoom of 1.5. To image TO-PRO-3, we used an excitation wavelength of 635 nm and collected emission wavelengths of 650 to 700 nm, with a frame average of 2. To image Alexa Fluor 488, we used an excitation wavelength of 488 nm and collected emission wavelengths of 495 to 550 nm, with a frame average of 4. Additional overview images were collected using a 20X objective (N.A. = 0.6) and a zoom of 1.0 using the settings outlined above, but with frame averages of 2 for both TO-PRO-3 and AF488. Images were analyzed in ImageJ to determine protein expression and cellular localization. CTGF, YAP and TEAD expression was determined by assessing the integrated density value (IDV), which was normalized to area. For YAP and TEAD, a section at the outer edge of the EBs containing 30-40 cells was identified, and IDV were determined for the total section and for the nuclei. Protein expression in the cytoplasm was determined by subtracting the nuclei IDV from the IDV of the whole tissue section. Both were used to calculate a nuclear/cytoplasmic ratio for YAP and TEAD expression.

Immunoblotting Analysis

EBs were harvested at day 9 and proteins were extracted using RIPA buffer supplemented with protease inhibitor cocktail (Thermo Fisher Scientific). Total protein concentration was

quantified using the BCA protein assay kit (Thermo Fisher Scientific). Equal amounts of protein (10 µg) were electrophoresed on 5-20 % TBX gels (Bio-Rad) and immunoblotting was performed. Primary antibodies included: active YAP1 (1:1000, Abcam, #ab205270), phosphorylated-YAP1 (1:1000, Cell Signaling, #13008S), LATS2 (1:1000, Proteintech, #20276-1-AP), MST1 (1:1000, Cell Signaling, #3682S), GAPDH (1:1000, GeneTex, #GTX627408), and acetylated tubulin (1:1000, Sigma-Aldrich, #T7451). HRP-conjugated anti-rabbit (1:5000, Abcam, #ab6721) and anti-mouse (1:5000, Invitrogen, #62-6520) secondary antibodies were used. Protein expression was assessed by chemiluminescence (Luminol, Santa Cruz, Santa Cruz, CA, USA) using a Bio-Rad ChemiDoc imaging system.

RNA Sequencing

RNA sequencing and subsequent quality control and genome alignment were performed by Novogene (Sacramento, CA) on rRNA-depleted RNA extracted from day 9 differentiated cells at weeks 8, 16 and 24 (n=3 for each treatment). Paired-end sequencing was performed via the Illumina platform, and reads were checked for quality metrics and trimmed for low quality bases. Indexes of the reference genome were built using STAR (Dobin et al., 2013), and paired-end clean reads were aligned to the *Mus musculus* (mm10) reference genome using STAR (v2.5). HTSeq v0.6.1 (Anders et al., 2014; Putri et al., 2021) was used to count the mapped reads for each gene. Differential expression analysis was performed using the DESeq2 (v1.29.7) R package (Love et al., 2014) which can be used to identify genes that react in a condition-specific manner in time course experiments. Specifically, we performed a Wald test at week 16 and week 24 to compare control and arsenic-treated samples at those specific time points. The Wald test is a hypothesis test commonly used to detect differentially expressed genes when comparing two groups. Gene counts were normalized to library size using DESeq2. The p-values resulting from the differential

expression analysis were subjected to the Benjamini-Hochberg adjustment to control for the False Discovery Rate (FDR). Genes with a resulting adjusted p-value < 0.05 were considered differentially expressed and used for subsequent functional annotation analysis. Differentially expressed genes were annotated using the R package *annotables* (Steinbaugh et al., 2017). The samples were clustered using the hierarchical clustering distance method with the *heatmap* package in R (Kolde, 2012). Gene Ontology (GO) over-representation analysis and gene set enrichment analysis (GSEA) of differentially expressed genes were performed using the R package *clusterProfiler* (Yu et al., 2012; Wu et al., 2021) that adjusted for gene length bias. GO terms with adjusted p-value < 0.05 were considered significantly enriched by differentially expressed genes. To assess and investigate the biochemical pathways impaired following chronic low-level arsenic exposure, the *clusterProfiler* package was also used to test the over-representation and statistical enrichment of differential gene expression in KEGG pathways.

Statistical Analysis

Results are expressed as mean \pm SE. Statistical significance for differential gene expression was calculated by Student's t-test. Protein expression for immunoblotting analysis was conducted using Image Lab software (Bio-Rad) to determine densitometry values and normalized to GAPDH and acetylated tubulin as loading control. Protein expression and cellular localization for immunohistochemistry analysis were determined using ImageJ. Statistical significance for average protein expression and localization in control and arsenic-treated biological replicates was assessed by Student's t-test. $P < 0.05$ was considered statistically significant.

Results

Chronic low level arsenic exposure drives differential expression of several genes over time

P19 mouse embryonic stem cells were chronically cultured as previously described (McMichael et al., 2020) for 32 weeks and exposed to 0 or 0.1 μM (7.5 ppb) arsenic as sodium arsenite. Cells were differentiated in clean medium every four weeks via hanging drop to form skeletal myoblasts and neural progenitors. The arsenic-exposed cells were shown to have increased expression of genes involved in pluripotency, such as *Sox2* and *Oct4*, and decreased expression of genes involved in differentiation, such as *Dcx*, *Gdf3* and *Prom1* (McMichael et al., 2020). To investigate the mechanisms responsible for the impaired differentiation, RNA sequencing was performed on day 9 differentiated cells at weeks 8, 16 and 24. Expression analysis shows that differences in RNA expression between the independent control and arsenic-exposed cell lines increases over time, becoming exposure-dependent at week 16 and 24 (Fig. 1A-C). Conversely, sample clustering at week 8 indicates a partial divergence in expression between control and arsenic treated samples (Fig. 1A).

Additionally, principal component analysis (PCA) indicates that arsenic-exposed embryonic stem cells express different genes than their control counterparts and that these differences accumulate throughout the exposure (Fig. 1D). Arsenic samples at different time points are mainly distributed along the x-axis (PC1), which accounts for 39% of the variation reported. Conversely, control samples at different time points are mainly distributed along the y-axis (PC2), which account for 20% of the variation. Interestingly, the distance between control and arsenic treated samples is minimal at week 8 while progressively increasing along the x-axis at week 16 and 24 suggesting that the differences in gene expression profile accumulate throughout time (Fig. 1D).

Gene ontology (GO) indicates that the most significantly enriched functional annotations in arsenic treated samples were related to embryonic development, regulation of neuron differentiation, pattern specification processes, and regulation of cell adhesion (Fig. 2A-B). Additionally, gene set enrichment analysis (GSEA) was performed to investigate the biological processes in which differentially expressed genes (DEGs) were enriched between control and arsenic samples. This analysis revealed that DEGs with high enrichment scores were associated with cell fate commitment, embryonic skeletal system development, neuron fate commitment and forebrain neuron differentiation (Fig. 2C).

Hippo signaling pathway is disrupted following chronic low level arsenic exposure

Pathway analysis was performed to assess DEGs that are enriched in KEGG pathways. Our results indicated that signaling pathways regulating pluripotency in stem cells are overall upregulated in arsenic-treated samples (Fig. S1A). Moreover, the results also confirm that arsenic exposure impairs the Wnt/ β -catenin signaling pathway (Fig. S1B) and TGF- β signaling pathway (Fig. S1C), as has been previously described (Hong and Bain, 2012; Allison et al., 2013; Ji et al., 2014; Wang et al., 2017; McMichael et al., 2020; Jatko et al., 2021) Interestingly, our results suggest that the Hippo signaling pathway might also be disrupted over time following chronic, low-level arsenic exposure (Fig. 3A).

The Hippo signaling pathway regulates embryonic and organ development, tissue regeneration, tumorigenesis, and maintenance of stem cell pluripotency (Yu et al., 2013; Wang et al., 2017; Chen et al., 2019) and Yap is highly expressed in embryonic stem cells. *In vitro* studies have shown that during cellular differentiation, YAP is inactivated and sequestered in the cytoplasm, resulting in downregulation of pluripotency markers such as Nanog, Oct4 and Sox2. Transcript expression of the Hippo pathway's key components, *Lats2*, *Tead3* and *Tead4*, were all

significantly upregulated by 1.7-, 2.1- and 2.5- fold in arsenic treated samples at week 24 respectively (Fig. 3B-D), while transcript levels of *E-cadherin*, an upstream regulator of the Hippo pathway, were significantly downregulated by 2.7-fold in arsenic treated samples at week 24 (Fig. 3E). Read counts of these genes were consistent in the control samples throughout the exposure and, while no differences were reported at week 8, increased levels of *Lats2*, *Tead4* and *E-cadherin* were observed at week 16 (Fig. S3, S4).

Chronic arsenic exposure impairs protein expression of key components of the Hippo signaling pathway

Immunoblotting was performed to investigate the effects of arsenic exposure on key proteins in the Hippo signaling pathway including the signal receiver MST1, LATS2 and the main effector YAP1. No significant differences were seen in the protein levels of MST1 (Fig. S2) throughout the exposure. Immunoblotting of LATS2 revealed multiple bands suggesting the presence of alternative splicing or post translational modifications (Fig. 4A). Analysis of the strongest band suggested that arsenic exposure increased the protein expression of LATS2 throughout the exposure, with protein levels of LATS2 significantly upregulated by 6.4-fold and 3.6-fold at weeks 8 and 16, respectively (Fig. 4A-B). Interestingly, significant upregulation of LATS2 expression was reported when analyzing the weakest bands at all time points (Fig S5). Protein levels of active YAP1 were significantly upregulated by 3.8-fold in arsenic treated samples at week 8. Conversely, protein expression of inactive phosphorylated YAP1 was significantly downregulated by 2.1-fold at week 16 in arsenic-treated cells while it was significantly upregulated at week 24 by 1.7-fold (Fig. 4C-D).

We also examined YAP's nuclear translocation and co-localization with its nuclear effector TEAD through immunohistochemistry in Day 5 EBs derived from cells exposed to 0 or 0.1 μ M

arsenic. Both YAP and TEAD4 were present in the cytoplasm and nucleus (Fig. 5). While no differences in total YAP and TEAD4 expression were observed between control and arsenic exposed EBs at week 16 (Fig. 5A), the ratio between nuclear and cytoplasmic YAP expression was significantly upregulated in arsenic-treated samples by 1.2- and 1.4- fold at week 16 and 28, respectively (Fig. 5A-C). Similarly, the ratio between nuclear and cytoplasmic TEAD was also significantly increased in arsenic-treated samples by 1.2- fold at week 16 and 28 (Fig. 5A-B, D). This data implies that the Hippo signaling pathway is dysregulated due to chronic arsenic exposure, leading to YAP activation.

Chronic low level arsenic exposure increases the expression of YAP's target genes

Finally, we investigated levels of two YAP1 target genes, *c-Myc* and *Ctgf*. *C-Myc* mRNA levels were upregulated in arsenic-exposed samples at week 16 and week 24 by 2.5- and 3.6-fold, respectively (Fig. 6A). Similarly, *Ctgf* transcript levels were upregulated by 6.9-fold in arsenic-treated samples at week 24 (Fig. 6B). While CTGF protein expression was not significantly altered at week 16 in arsenic treated EBs (Fig. 7A, C), it was significantly upregulated by 1.4- fold at week 28 along with clustering of CTGF positive cells at the EBs' periphery (Fig. 7B-C). These results suggest that chronic, low-level arsenic exposure enhances YAP activation and nuclear translocation, thereby promoting interaction with TEAD to increase transcription of target genes.

Discussion

The results of this study suggest that chronic exposure to an environmentally relevant arsenic concentration delays cellular differentiation by disrupting the Hippo signaling pathway. This occurs by enhancing the activation and nuclear translocation of YAP, the main effector in the Hippo signaling pathway, but also of its transcription factor TEAD. This increased nuclear

accumulation of YAP and TEAD results in increased expression of YAP's target genes, which are involved in pluripotency activation and maintenance.

Arsenic maintains stem cell pluripotency through impairment of the Hippo signaling pathway

The Hippo pathway is a conserved signaling pathway that controls tissue homeostasis through regulation of apoptosis, cell proliferation, migration, cellular differentiation and stem cell renewal. Previous studies have shown that the Hippo pathway plays a role in early embryonic development and cell fate specification (Piccolo et al., 2014; Fu et al., 2017; Wang et al., 2017; Chen et al., 2019; Barzegari et al., 2020). YAP is the main effector protein of the Hippo signaling pathway, and when it is phosphorylated by LATS1/2 kinases upon activation, YAP remains in the cytoplasm and is ultimately degraded. Conversely, when the Hippo pathway is inhibited, active un-phosphorylated YAP is able to translocate in the nucleus and regulate transcription of downstream target genes through interaction with TEAD. Yap knockout mice are embryonic lethal, as cell division is arrested at the blastomere stage (Morin-Kensicki et al., 2006; Tamm et al., 2011; Chen et al., 2019). Similarly, double knockout of Yap and Taz results in cell fate specification defects and embryo death at the morula stage (Nishioka et al., 2009; Yu et al., 2015; Chen et al., 2019). Yap is highly expressed in cultured stem cells and its activation leads to pluripotency maintenance, progenitor cell expansion, and inhibition of cellular differentiation (Camargo et al., 2007; Cao et al., 2008; Lian et al., 2010; Ramos and Camargo, 2012; Li et al., 2013; Piccolo et al., 2014; McKey et al., 2016; Chen et al., 2019). Conversely, during embryonic stem cell differentiation, YAP is retained in the cytoplasm, resulting in downregulation of genes involved in pluripotency such as *Sox2*, *Oct4* and *Nanog* (Lian et al., 2010; Chen et al., 2019). Recent *in vitro* studies have shown that overexpression of YAP in embryonic stem cells not only upregulates pluripotency markers but also maintains stem cell phenotype and inhibits differentiation even under differentiation culture

conditions (Lian et al., 2010; Li et al., 2013). Conversely, YAP knockdown results in decreased stem cell properties and impaired phenotype (Lian et al., 2010).

In the current study, RNA sequencing and KEGG analysis suggest that the Hippo signaling pathway is impaired following chronic arsenic exposure. Other studies have shown that arsenic exposure inhibits neuronal and muscle differentiation, in part by maintaining cells in their pluripotent state (Wang et al., 2010; Yen et al., 2010; Steffens et al. 2011; Hong and Bain, 2012; Aung et al. 2013; Ivanov and Hei, 2013; Bain et al., 2016; McMichael et al., 2020). For example, gene expression of the pluripotency markers *Sox2* and *Oct4* were increased in differentiating embryonic stem cells that had been exposed to arsenic for 12 weeks (McMichael et al., 2020). Consistently, our results indicate that chronic arsenic exposure upregulates signaling pathways involved in pluripotency regulation and maintenance.

Our findings also indicate that differential gene expression between independent control and arsenic-exposed samples increases throughout the time course as few differences are observed at week 8 while RNA expression becomes exposure-dependent at week 16 and 24. A similar time frame was reported by previous chronic studies conducted exposing stem cells (McMichael et al., 2020), progenitor cells (Tokar et al., 2010, 2013), and differentiated cells (Xu et al., 2014) to arsenic.

Arsenic impairs protein levels and cellular localization of Hippo pathway's core proteins

Yap is crucial in the response to oxidative stress induced by exposure to different xenobiotics and in the resistance to cytotoxic agents and heavy metals, including arsenic (Toone and Jones, 1999; Michel-Ramirez et al., 2017). Li and coworkers (2013) reported that arsenic activated Yap independently of the canonical Hippo signaling pathway and induced a Yap-mediated disruption of tight and adherens junctions in the skin. Mice exposed to up to 200 ppm

arsenic for one month through their drinking water had increased phosphorylation of LATS which, however, did not result in YAP inactivation (Li et al., 2013). Conversely, our results did not report significant differences in phosphorylated LATS protein levels following arsenic exposure while we observed downregulation of LATS protein levels at week 24. Importantly, the cadherin/catenin complex is involved in the initiation of the Hippo pathway (Kim et al., 2011; Piccolo et al., 2014; McCrea et al., 2015; Kourtidis et al., 2017; Chen et al., 2019). According to our results, transcript expression of *E-cadherin* was significantly downregulated in arsenic-exposed cells at week 24 and we have previously shown that arsenic treatment significantly increased N-cadherin protein levels (McMichael et al., 2020). These results suggest that the dysregulation of cadherin/catenin complex following chronic, low-level arsenic exposure could be involved in the activation of the Hippo signaling pathway.

Hepatocellular carcinoma cells exposed to extracellular vesicles obtained from THP-1 cells treated with arsenite had increased colony formation, migration, and invasion capacity along with reduced LATS1 and phosphorylated YAP protein levels and elevated protein expression of unphosphorylated YAP and TAZ (Li et al., 2021). Our findings show that arsenic exposure significantly upregulated YAP protein expression at week 8 and significantly inhibited phosphorylated YAP protein levels at week 16. Additionally, the ratio between nuclear (active) and cytoplasmic (inactive) YAP was significantly upregulated at weeks 16 and 28 in arsenic-exposed samples, as determined by immunohistochemistry analysis. We observed upregulation of *Lats2* transcript levels at week 24 and increased LATS2 protein expression at week 8 and 16. Importantly, previous studies have shown that *Lats2* overexpression increased phosphorylation of Yap and induced Yap's nuclear to cytoplasm translocation (Reuven et al., 2013; Guo et al., 2019). These results are in line with Li and coworkers' findings and suggest that arsenic exposure might suppress

the activation of the Hippo signaling pathway through the impairment of Lats expression and subsequently enhance YAP activation and nuclear translocation.

Arsenic-induced Yap activation enhances transcription of Yap's target genes

To confirm our hypothesis that arsenic exposure increases YAP activation and nuclear translocation, we investigated the expression of YAP's known downstream target genes, *c-Myc* and *Ctgf* (Piccolo et al., 2014; Totaro et al., 2018; Shea et al., 2019). *C-Myc* transcript levels were significantly upregulated at week 16 and 24 while *Ctgf* transcript levels were significantly increased at week 24. Immunohistochemistry analysis confirmed upregulation of CTGF protein levels at week 28 in arsenic-treated EBs. Various studies have previously reported that arsenite exposure increases c-Myc levels in cells (Chen et al., 2001; Liu et al., 2006; Ruiz-Ramos et al., 2009; Nakareangrit et al., 2016), and in lung (Xiao et al., 2021) and intestinal tissues (Jatko et al., 2021) of mice exposed to arsenite through drinking water. However, little is known about the changes in *Ctgf* transcript and protein levels following arsenic exposure. Consistent with our findings, Li and coworkers reported increased *Ctgf* mRNA levels in the skin of mice exposed to 100ppm of sodium arsenite for 30 days (Li et al., 2013); similarly, elevated CTGF protein levels were observed in aortal tissues of rats exposed to 50 ppm of sodium arsenite for 90 days (Khuman et al., 2016). These results indicate that arsenic exposure might enhance YAP activation and nuclear translocation resulting in upregulated expression of downstream target genes. Conversely, Zhou et al. (2020) hypothesized that arsenic promotes YAP degradation as they observed increased ubiquitination mediated degradation of YAP in esophageal squamous cell carcinoma cells exposed to arsenic nano-complexes. While these contrasting results could be explained by the different *in vitro* models used, further studies are needed to clarify the role of arsenic in the dysregulation of the Hippo signaling pathway.

Arsenic may enhance Yap activation through a non-canonical Hippo pathway

YAP is a transcription co-activator and changes in the expression of its target genes are regulated through interaction with members of the TEAD family of transcription factors in the nucleus. While the role of TEAD in the regulation of the Hippo pathway has been largely overlooked, recent studies have shown that TEAD mediates the expression of YAP's target genes and is involved in the regulation of YAP's biological functions (Zhao et al., 2008). Additionally, Lin and coworkers (2017) investigated the effects of TEAD nuclear-cytoplasmic translocation on YAP activation showing that TEAD cellular localization plays an essential role in regulating YAP's activity and the output of the Hippo signaling pathway. Specifically, *Tead* knockout cells had normal YAP dephosphorylation upon Hippo pathway inhibition, yet YAP did not accumulate in the nucleus. Similarly, inhibition of TEAD and increased cytoplasmic localization prevented YAP nuclear accumulation (Lin et al., 2017).

To our knowledge, the current study is the first to investigate the effects of arsenic exposure on TEAD expression and cellular localization. Our results show that *Tead* transcript levels are significantly upregulated following arsenic exposure at week 24 along with increased ratio between nuclear and cytoplasmic TEAD at week 16 and 28. These results, compounded by the findings of Lin et al. (2017), suggest that chronic low level arsenic exposure impairs the expression and nuclear localization of YAP not only by impairing the canonical Hippo signaling pathway, but also by regulating the subcellular localization of TEAD. Further studies are needed in order to clarify the role of YAP and TEAD and their interplay in arsenic-induced impairment of the Hippo signaling pathway.

Conclusion

A chronic 0.1 μ M arsenic exposure for 32 weeks impaired the Hippo signaling pathway in P19 mouse embryonic stem cells. Lats downregulation along with an increased ratio between nuclear and cytoplasmic YAP and TEAD suggest that arsenic impairs the Hippo signaling pathway and enhances YAP activation resulting in increased expression of YAP's target genes *Ctgf* and *c-Myc*. Taken together, these results suggest that the impairment of the Hippo signaling pathway and increased YAP activation play a role in pluripotency maintenance and delayed cellular differentiation following arsenic exposure.

Acknowledgments

This work was supported by National Institutes of Health (ES027651). We thank Rhonda Reigers Powell from the Clemson Light Imaging Facility (CLIF) for assistance with the confocal microscopy. CLIF is supported, in part, by the NIH P20GM109094 NIH 1P30GM131959, NSF MRI 1126407 and 1920095, and 2020 BSPDC-GIAR.

References

- Allison, P., Huang, T., Broka, D., Parker, P., Barnett, J.V., Camenisch, T.D., 2013. Disruption of canonical TGFbeta-signaling in murine coronary progenitor cells by low level arsenic. *Toxicol. Appl. Pharmacol.* 272, 147-153.
- Anders, S., Pyl, P.T., Huber, W., 2015. HTSeq--a Python framework to work with high-throughput sequencing data. *Bioinformatics* 31, 166-169.
- Aung, K.H., Kurihara, R., Nakashima, S., Maekawa, F., Nohara, K., Kobayashi, T., Tsukahara, S., 2013. Inhibition of neurite outgrowth and alteration of cytoskeletal gene expression by sodium arsenite. *Neurotoxicology* 34, 226-235.
- Ayotte, J.D., Medalie, L., Qi, S.L., Backer, L.C., Nolan, B.T., 2017. Estimating the High-Arsenic Domestic-Well Population in the Conterminous United States. *Environ. Sci. Technol.* 51, 12443-12454.
- Bain, L.J., Liu, J.T., League, R.E., 2016. Arsenic inhibits stem cell differentiation by altering the interplay between the Wnt3a and Notch signaling pathways. *Toxicol. Rep.* 3, 405-413.
- Barzegari, A., Gueguen, V., Omid, Y., Ostadrahimi, A., Nouri, M., Pavon-Djavid, G., 2020. The role of Hippo signaling pathway and mechanotransduction in tuning embryoid body formation and differentiation. *J. Cell. Physiol.* 235, 5072-5083.
- Bhattacharya, P., Hossain, M., Rahman, S.N., Robinson, C., Nath, B., Rahman, M., Islam, M.M., Von Bromssen, M., Ahmed, K.M., Jacks, G., Chowdhury, D., Rahman, M., Jakariya, M., Persson, L.A., Vahter, M., 2011. Temporal and seasonal variability of arsenic in drinking water wells in Matlab, southeastern Bangladesh: a preliminary evaluation on the basis of a 4 year study. *J. Environ. Sci. Health. A. Tox. Hazard. Subst. Environ. Eng.* 46, 1177-1184.
- Bjorklund, G., Tippairote, T., Rahaman, M.S., Aaseth, J., 2020. Developmental toxicity of arsenic: a drift from the classical dose-response relationship. *Arch. Toxicol.* 94, 67-75.
- Bundschuh, J., Armenta, M.A., Birkle, P., Bhattacharya, P., Matschullat, A.B., Mukherjee, A.B., 2009. *Natural Arsenic in Groundwater of Latin America - Occurrence, health impact and remediation.* CRC Press.
- Camargo, F.D., Gokhale, S., Johnnidis, J.B., Fu, D., Bell, G.W., Jaenisch, R., Brummelkamp, T.R., 2007. YAP1 increases organ size and expands undifferentiated progenitor cells. *Curr. Biol.* 17, 2054-2060.
- Cao, X., Pfaff, S.L., Gage, F.H., 2008. YAP regulates neural progenitor cell number via the TEA domain transcription factor. *Genes Dev.* 22, 3320-3334.
- Chattopadhyay, S., Bhaumik, S., Nag Chaudhury, A., Das Gupta, S., 2002. Arsenic induced changes in growth development and apoptosis in neonatal and adult brain cells in vivo and in tissue culture. *Toxicol. Lett.* 128, 73-84.

- Chen, H., Liu, J., Zhao, C.Q., Diwan, B.A., Merrick, B.A., Waalkes, M.P., 2001. Association of c-myc overexpression and hyperproliferation with arsenite-induced malignant transformation. *Toxicol. Appl. Pharmacol.* 175, 260-268.
- Chen, Y.A., Lu, C.Y., Cheng, T.Y., Pan, S.H., Chen, H.F., Chang, N.S., 2019. WW Domain-Containing Proteins YAP and TAZ in the Hippo Pathway as Key Regulators in Stemness Maintenance, Tissue Homeostasis, and Tumorigenesis. *Front. Oncol.* 9, 60.
- Concha, G., Vogler, G., Lezcano, D., Nermell, B., Vahter, M., 1998. Exposure to inorganic arsenic metabolites during early human development. *Toxicol. Sci.* 44, 185-190.
- Dakeishi, M., Murata, K., Grandjean, P., 2006. Long-term consequences of arsenic poisoning during infancy due to contaminated milk powder. *Environ. Health* 5, 31-069X-5-31.
- DeSesso, J.M., Jacobson, C.F., Scialli, A.R., Farr, C.H., Holson, J.F., 1998. An assessment of the developmental toxicity of inorganic arsenic. *Reprod. Toxicol.* 12, 385-433.
- Dobin, A., Davis, C.A., Schlesinger, F., Drenkow, J., Zaleski, C., Jha, S., Batut, P., Chaisson, M., Gingeras, T.R., 2013. STAR: ultrafast universal RNA-seq aligner. *Bioinformatics* 29, 15-21.
- Fu, V., Plouffe, S.W., Guan, K.L., 2017. The Hippo pathway in organ development, homeostasis, and regeneration. *Curr. Opin. Cell Biol.* 49, 99-107.
- Guo, C., Liang, C., Yang J., Hu, H., Fan, B., Liu, X. 2019. LATS2 inhibits cell proliferation and metastasis through the Hippo signaling pathway in glioma. *Oncol Rep.* 41(5):2753-2761.
- Hall, M., Gamble, M., Slavkovich, V., Liu, X., Levy, D., Cheng, Z., van Geen, A., Yunus, M., Rahman, M., Pilsner, J.R., Graziano, J., 2007. Determinants of arsenic metabolism: blood arsenic metabolites, plasma folate, cobalamin, and homocysteine concentrations in maternal-newborn pairs. *Environ. Health Perspect.* 115, 1503-1509.
- Henn, B.C., Ettinger, A. S., Hopkins, M. R., Jim, R., Amarasiriwardena, C., Christiani, D. C., Coull, B.A., Bellinger, D.C., Wright, R. O. 2016. Prenatal arsenic exposure and birth outcomes among a population residing near a mining-related superfund site. *Environmental Health Perspectives*, 124(8), 1308-1315.
- Hong, G.M., Bain, L.J., 2012. Sodium arsenite represses the expression of myogenin in C2C12 mouse myoblast cells through histone modifications and altered expression of Ezh2, Glp, and Igf-1. *Toxicol. Appl. Pharmacol.* 260, 250-259.
- Ivanov, V.N., Hei, T.K., 2013. Induction of apoptotic death and retardation of neuronal differentiation of human neural stem cells by sodium arsenite treatment. *Exp. Cell Res.* 319, 875-887.
- Jatko, J.T., Darling, C.L., Kellett, M.P., Bain, L.J., 2021. Arsenic exposure in drinking water reduces Lgr5 and secretory cell marker gene expression in mouse intestines. *Toxicol. Appl. Pharmacol.* 422, 115561.

- Ji, H., Li, Y., Jiang, F., Wang, X., Zhang, J., Shen, J., Yang, X., 2014. Inhibition of transforming growth factor beta/SMAD signal by MiR-155 is involved in arsenic trioxide-induced anti-angiogenesis in prostate cancer. *Cancer. Sci.* 105, 1541-1549.
- Khuman, M.W., Harikumar, S.K., Sadam, A., Kesavan, M., Susanth, V.S., Parida, S., Singh, K.P., Sarkar, S.N., 2016. Candesartan ameliorates arsenic-induced hypertensive vascular remodeling by regularizing angiotensin II and TGF-beta signaling in rats. *Toxicology* 374, 29-41.
- Kim, N.G., Koh, E., Chen, X., Gumbiner, B.M., 2011. E-cadherin mediates contact inhibition of proliferation through Hippo signaling-pathway components. *Proc. Natl. Acad. Sci. U. S. A.* 108, 11930-11935.
- Kolde, R. 2012. Pheatmap: pretty heatmaps. R package version 1.2: 747.
- Kourtidis, A., Lu, R., Pence, L.J., Anastasiadis, P.Z. 2017. A central role for cadherin signaling in cancer. *Exp Cell Res*, 358(1):78-85.
- Li, C., Srivastava, R.K., Elmets, C.A., Afaq, F., Athar, M., 2013. Arsenic-induced cutaneous hyperplastic lesions are associated with the dysregulation of Yap, a Hippo signaling-related protein. *Biochem. Biophys. Res. Commun.* 438, 607-612.
- Li, J., Xue, J., Ling, M., Sun, J., Xiao, T., Dai, X., Sun, Q., Cheng, C., Xia, H., Wei, Y., Chen, F., Liu, Q., 2021. MicroRNA-15b in extracellular vesicles from arsenite-treated macrophages promotes the progression of hepatocellular carcinomas by blocking the LATS1-mediated Hippo pathway. *Cancer Lett.* 497, 137-153.
- Li, P., Chen, Y., Mak, K.K., Wong, C.K., Wang, C.C., Yuan, P., 2013. Functional role of Mst1/Mst2 in embryonic stem cell differentiation. *PLoS One* 8, e79867.
- Lian, I., Kim, J., Okazawa, H., Zhao, J., Zhao, B., Yu, J., Chinnaiyan, A., Israel, M.A., Goldstein, L.S., Abujarour, R., Ding, S., Guan, K.L., 2010. The role of YAP transcription coactivator in regulating stem cell self-renewal and differentiation. *Genes Dev.* 24, 1106-1118.
- Lin, K.C., Moroishi, T., Meng, Z., Jeong, H.S., Plouffe, S.W., Sekido, Y., Han, J., Park, H.W., Guan, K.L., 2017. Regulation of Hippo pathway transcription factor TEAD by p38 MAPK-induced cytoplasmic translocation. *Nat. Cell Biol.* 19, 996-1002.
- Liu, H., Jiang, D., Chi, F., Zhao, B., 2012. The Hippo pathway regulates stem cell proliferation, self-renewal, and differentiation. *Protein Cell.* 3, 291-304.
- Liu, J., Benbrahim-Tallaa, L., Qian, X., Yu, L., Xie, Y., Boos, J., Qu, W., Waalkes, M.P., 2006. Further studies on aberrant gene expression associated with arsenic-induced malignant transformation in rat liver TRL1215 cells. *Toxicol. Appl. Pharmacol.* 216, 407-415.
- Love, M.I., Huber, W., Anders, S., 2014. Moderated estimation of fold change and dispersion for RNA-seq data with DESeq2. *Genome Biol.* 15, 550-014-0550-8.

- Martinez-Finley, E.J., Ali, A.M., Allan, A.M., 2009. Learning deficits in C57BL/6J mice following perinatal arsenic exposure: consequence of lower corticosterone receptor levels? *Pharmacol. Biochem. Behav.* 94, 271-277.
- Meacher, D.M., Manzel, D.B., Dillencourt, M.D., Bic, L.F., Schoof, R.A., Yost, L.J., Farr, C.H. 2002. Estimation of multimedia inorganic arsenic intake in the US population. *Hum. Ecol. Risk Assess.*, 8(7), pp. 1697-1721
- McCrea, P.D., Maher, M.T., Gottardi C.G. 2015. Nuclear signaling from cadherin adhesion complexes. *Curr Top Dev Biol*,112:129-96.
- McKey, J., Martire, D., de Santa Barbara, P., Faure, S., 2016. LIX1 regulates YAP1 activity and controls the proliferation and differentiation of stomach mesenchymal progenitors. *BMC Biol.* 14, 34-016-0257-2.
- McMichael, B.D., Perego, M.C., Darling, C.L., Perry, R.L., Coleman, S.C., Bain, L.J., 2020. Long-term arsenic exposure impairs differentiation in mouse embryonal stem cells. *J. Appl. Toxicol.* .
- Meng, Z., Moroishi, T., Guan, K.L., 2016. Mechanisms of Hippo pathway regulation. *Genes Dev.* 30, 1-17.
- Michel-Ramirez, G., Recio-Vega, R., Ocampo-Gomez, G., Palacios-Sanchez, E., Delgado-Macias, M., Delgado-Gaona, M., Lantz, R.C., Gandolfi, J., Gonzalez-Cortes, T., 2017. Association between YAP expression in neoplastic and non-neoplastic breast tissue with arsenic urinary levels. *J. Appl. Toxicol.* 37, 1195-1202.
- Morin-Kensicki, E.M., Boone, B.N., Howell, M., Stonebraker, J.R., Teed, J., Alb, J.G., Magnuson, T.R., O'Neal, W., Milgram, S.L., 2006. Defects in yolk sac vasculogenesis, chorioallantoic fusion, and embryonic axis elongation in mice with targeted disruption of Yap65. *Mol. Cell. Biol.* 26, 77-87.
- Nakareangrit, W., Thiantanawat, A., Visitnonthachai, D., Watcharasit, P., Satayavivad, J., 2016. Sodium arsenite inhibited genomic estrogen signaling but induced pERalpha (Ser118) via MAPK pathway in breast cancer cells. *Environ. Toxicol.* 31, 1133-1146.
- Nishioka, N., Inoue, K., Adachi, K., Kiyonari, H., Ota, M., Ralston, A., Yabuta, N., Hirahara, S., Stephenson, R.O., Ogonuki, N., Makita, R., Kurihara, H., Morin-Kensicki, E.M., Nojima, H., Rossant, J., Nakao, K., Niwa, H., Sasaki, H., 2009. The Hippo signaling pathway components Lats and Yap pattern Tead4 activity to distinguish mouse trophectoderm from inner cell mass. *Dev. Cell.* 16, 398-410.
- Papaspyropoulos, A., Bradley, L., Thapa, A., Leung, C.Y., Toskas, K., Koennig, D., Pefani, D.E., Raso, C., Grou, C., Hamilton, G., Vlahov, N., Grawenda, A., Haider, S., Chauhan, J., Buti, L., Kanapin, A., Lu, X., Buffa, F., Dianov, G., von Kriegsheim, A., Matallanas, D., Samsonova, A., Zernicka-Goetz, M., O'Neill, E., 2018. RASSF1A uncouples Wnt from Hippo signalling and promotes YAP mediated differentiation via p73. *Nat. Commun.* 9, 424-017-02786-5.

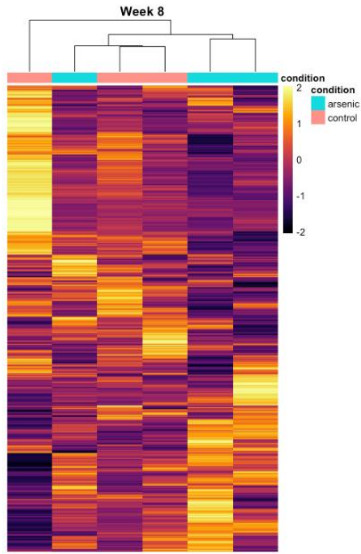
- Piccolo, S., Dupont, S., Cordenonsi, M., 2014. The biology of YAP/TAZ: hippo signaling and beyond. *Physiol. Rev.* 94, 1287-1312.
- Putri, G., Anders, S., Pyl, P.T., Pimanda, J.E., Zanini, F. 2021. Analysing high-throughput sequencing data with HTSeq 2.0. arXiv:2112.00939.
- Ramos, A., Camargo, F.D., 2012. The Hippo signaling pathway and stem cell biology. *Trends Cell Biol.* 22, 339-346.
- Raqib, R., Ahmed, S., Sultana, R., Wagatsuma, Y., Mondal, D., Hoque, A.M., Nermell, B., Yunus, M., Roy, S., Persson, L.A., Arifeen, S.E., Moore, S., Vahter, M., 2009. Effects of in utero arsenic exposure on child immunity and morbidity in rural Bangladesh. *Toxicol. Lett.* 185, 197-202.
- Ravenscroft, P., Brammer, H., Richards, K. 2009. *Arsenic Pollution—A Global Synthesis*. Wiley-Blackwell; Oxford, UK.
- Reuven, N., Adler, J., Meltser, V., Shaul, Y. 2013. The Hippo pathway kinase Lats2 prevents DNA damage induced apoptosis through inhibition of the tyrosine kinase c-Abl. *Cell Death Differ.* 20(10):1330-40.
- Rodriguez, V.M., Carrizales, L., Mendoza, M.S., Fajardo, O.R., Giordano, M., 2002. Effects of sodium arsenite exposure on development and behavior in the rat. *Neurotoxicol. Teratol.* 24, 743-750.
- Ruiz-Ramos, R., Lopez-Carrillo, L., Rios-Perez, A.D., De Vizcaya-Ruiz, A., Cebrian, M.E., 2009. Sodium arsenite induces ROS generation, DNA oxidative damage, HO-1 and c-Myc proteins, NF-kappaB activation and cell proliferation in human breast cancer MCF-7 cells. *Mutat. Res.* 674, 109-115.
- Sarkar, A., Paul, B., 2016. The global menace of arsenic and its conventional remediation - A critical review. *Chemosphere* 158, 37-49.
- Schmittgen, T.D., Livak, K.J., 2008. Analyzing real-time PCR data by the comparative C(T) method. *Nat. Protoc.* 3, 1101-1108.
- Shankar, S., Shanker, U., Shikha, 2014. Arsenic contamination of groundwater: a review of sources, prevalence, health risks, and strategies for mitigation. *ScientificWorldJournal* 2014, 304524.
- Shea, C.A., Rolfe, R.A., McNeill, H., Murphy, P., 2020. Localization of YAP activity in developing skeletal rudiments is responsive to mechanical stimulation. *Dev. Dyn.* 249, 523-542.
- Smith, A.H., Arroyo, A.P., Mazumder, D.N., Kosnett, M.J., Hernandez, A.L., Beeris, M., Smith, M.M., Moore, L.E., 2000. Arsenic-induced skin lesions among Atacameño people in Northern Chile despite good nutrition and centuries of exposure. *Environ. Health Perspect.* 108, 617-620.

- Steffens, A.A., Hong, G.M., Bain, L.J., 2011. Sodium arsenite delays the differentiation of C2C12 mouse myoblast cells and alters methylation patterns on the transcription factor myogenin. *Toxicol. Appl. Pharmacol.* 250, 154-161.
- Stein, C., Bardet, A.F., Roma, G., Bergling, S., Clay, I., Ruchti, A., Agarinis, C., Schmelzle, T., Bouwmeester, T., Schubeler, D., Bauer, A., 2015. YAP1 Exerts Its Transcriptional Control via TEAD-Mediated Activation of Enhancers. *PLoS Genet.* 11, e1005465.
- Steinbaugh, M., Turner, S., Wolen, A. 2017. stephenturner/annotables: Ensembl 90 (v0.1.90). Zenodo. <https://doi.org/10.5281/zenodo.996854>
- Tamm, C., Bower, N., Anneren, C., 2011. Regulation of mouse embryonic stem cell self-renewal by a Yes-YAP-TEAD2 signaling pathway downstream of LIF. *J. Cell. Sci.* 124, 1136-1144.
- Thomas, D.J., 2013. The die is cast: arsenic exposure in early life and disease susceptibility. *Chem. Res. Toxicol.* 26, 1778-1781.
- Tokar, E.J., Diwan, B.A., Waalkes, M.P., 2010. Arsenic exposure transforms human epithelial stem/progenitor cells into a cancer stem-like phenotype. *Environ. Health Perspect.* 118, 108-115.
- Tokar, E.J., Person, R.J., Sun, Y., Perantoni, A.O., Waalkes, M.P., 2013. Chronic exposure of renal stem cells to inorganic arsenic induces a cancer phenotype. *Chem. Res. Toxicol.* 26, 96-105.
- Toone, W.M., Jones, N. 1999. AP-1 transcription factors in yeast. *Curr Opin Gene Dev.* 9:55–61.
- Totaro, A., Panciera, T., Piccolo, S., 2018. YAP/TAZ upstream signals and downstream responses. *Nat. Cell Biol.* 20, 888-899.
- Tyler, C.R., Allan, A.M., 2013. Adult hippocampal neurogenesis and mRNA expression are altered by perinatal arsenic exposure in mice and restored by brief exposure to enrichment. *PLoS One* 8, e73720.
- von Ehrenstein, O.S., Guha Mazumder, D.N., Hira-Smith, M., Ghosh, N., Yuan, Y., Windham, G., Ghosh, A., Haque, R., Lahiri, S., Kalman, D., Das, S., Smith, A.H., 2006. Pregnancy outcomes, infant mortality, and arsenic in drinking water in West Bengal, India. *Am. J. Epidemiol.* 163, 662-669.
- Wang, A., Holladay, S.D., Wolf, D.C., Ahmed, S.A., Robertson, J.L., 2006. Reproductive and developmental toxicity of arsenic in rodents: a review. *Int. J. Toxicol.* 25, 319-331.
- Wang, X., Meng, D., Chang, Q., Pan, J., Zhang, Z., Chen, G., Ke, Z., Luo, J., Shi, X., 2010. Arsenic inhibits neurite outgrowth by inhibiting the LKB1-AMPK signaling pathway. *Environ. Health Perspect.* 118, 627-634.

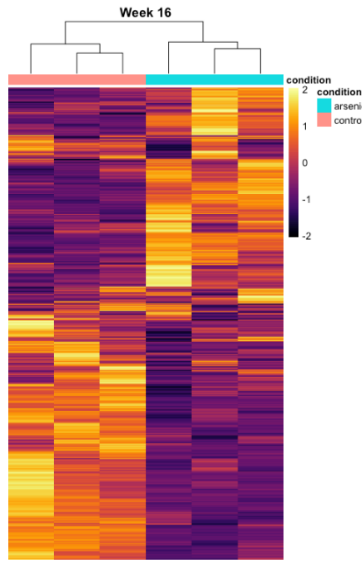
- Wang, Y., Cui, M., Sun, B.D., Liu, F.B., Zhang, X.D., Ye, L.H., 2014. MiR-506 suppresses proliferation of hepatoma cells through targeting YAP mRNA 3'UTR. *Acta Pharmacol. Sin.* 35, 1207-1214.
- Wang, Y., Wang, Z., Li, H., Xu, W., Dong, L., Guo, Y., Feng, S., Bi, K., Zhu, C., 2017. Arsenic trioxide increases expression of secreted frizzled-related protein 1 gene and inhibits the WNT/beta-catenin signaling pathway in Jurkat cells. *Exp. Ther. Med.* 13, 2050-2055.
- Wang, Z., Liu, P., Zhou, X., Wang, T., Feng, X., Sun, Y.P., Xiong, Y., Yuan, H.X., Guan, K.L., 2017. Endothelin Promotes Colorectal Tumorigenesis by Activating YAP/TAZ. *Cancer Res.* 77, 2413-2423.
- Wu, T., Hu, E., Xu, S., Chen, M., Guo, P., Dai, Z., Feng, T., Zhou, L., Tang, W., Zhan, L., Fu, X., Liu, S., Bo, X., Yu, G., 2021. clusterProfiler 4.0: A universal enrichment tool for interpreting omics data. *Innovation (N. Y)* 2, 100141.
- Xiao, T., Zou, Z., Xue, J., Syed, B.M., Sun, J., Dai, X., Shi, M., Li, J., Wei, S., Tang, H., Zhang, A., Liu, Q., 2021. LncRNA H19-mediated M2 polarization of macrophages promotes myofibroblast differentiation in pulmonary fibrosis induced by arsenic exposure. *Environ. Pollut.* 268, 115810.
- Xu, Y., Tokar, E.J., Waalkes, M.P., 2014. Arsenic-induced cancer cell phenotype in human breast epithelia is estrogen receptor-independent but involves aromatase activation. *Arch. Toxicol.* 88, 263-274.
- Yen, Y.P., Tsai, K.S., Chen, Y.W., Huang, C.F., Yang, R.S., Liu, S.H., 2010. Arsenic inhibits myogenic differentiation and muscle regeneration. *Environ. Health Perspect.* 118, 949-956.
- Yu, F.X., Zhang, Y., Park, H.W., Jewell, J.L., Chen, Q., Deng, Y., Pan, D., Taylor, S.S., Lai, Z.C., Guan, K.L., 2013. Protein kinase A activates the Hippo pathway to modulate cell proliferation and differentiation. *Genes Dev.* 27, 1223-1232.
- Yu, F.X., Zhao, B., Guan, K.L., 2015. Hippo Pathway in Organ Size Control, Tissue Homeostasis, and Cancer. *Cell* 163, 811-828.
- Yu, G., Wang, L.G., Han, Y., He, Q.Y., 2012. clusterProfiler: an R package for comparing biological themes among gene clusters. *OMICS* 16, 284-287.
- Zhao, B., Ye, X., Yu, J., Li, L., Li, W., Li, S., Yu, J., Lin, J.D., Wang, C.Y., Chinnaiyan, A.M., Lai, Z.C., Guan, K.L., 2008. TEAD mediates YAP-dependent gene induction and growth control. *Genes Dev.* 22, 1962-1971.
- Zhou, W., Liu, M., Li, X., Zhang, P., Li, J., Zhao, Y., Sun, G., Mao, W., 2020. Arsenic nano complex induced degradation of YAP sensitized ESCC cancer cells to radiation and chemotherapy. *Cell. Biosci.* 10, 146-020-00508-x.

Figures

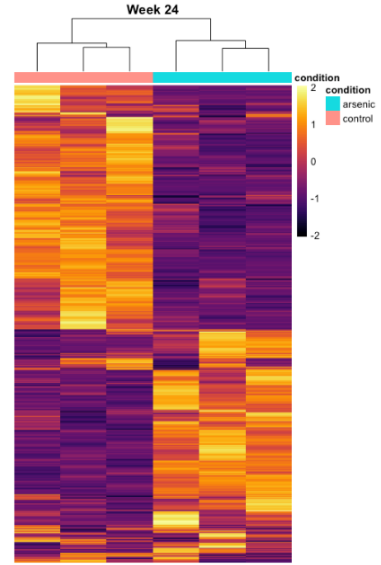
A



B



C



D

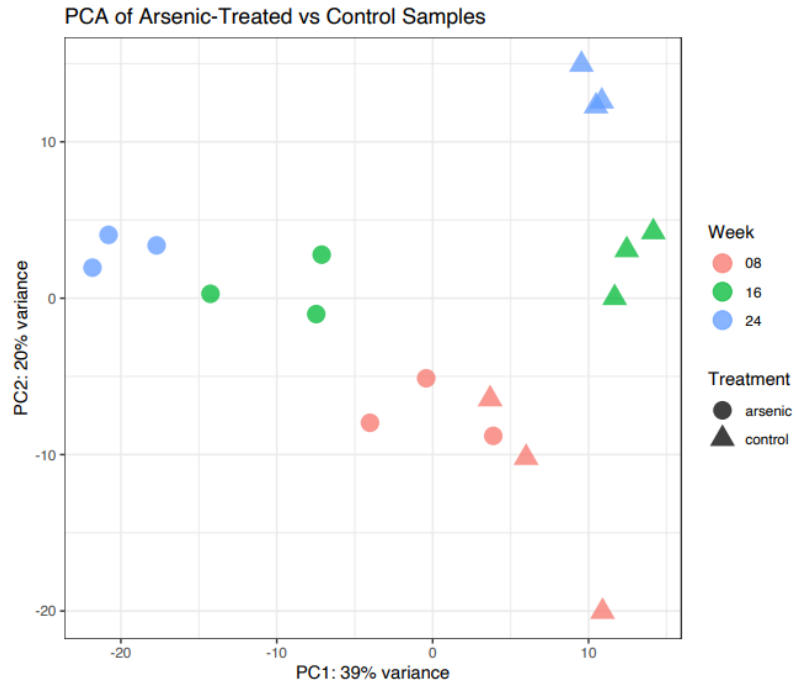


Figure 3.1. Arsenic exposure drives sample clustering and differential expression of several genes over time. (A-C) Heat map representations of normalized read counts of differentially expressed transcripts from day 9 differentiated cells exposed to 0 (pink bars) or 0.1 μM arsenic (blue bars) at week 8 (A), 16 (B) and 24 (C). (D) Principal component analysis (PCA) from embryonic stem cells exposed to 0 (blue circles) or 0.1 μM arsenic (pink circles) at week 8 (pink dots), 16 (green dots) and 24 (blue dots). The differences in gene expression profile are represented by the distance between the samples. (n=3 per exposure group).

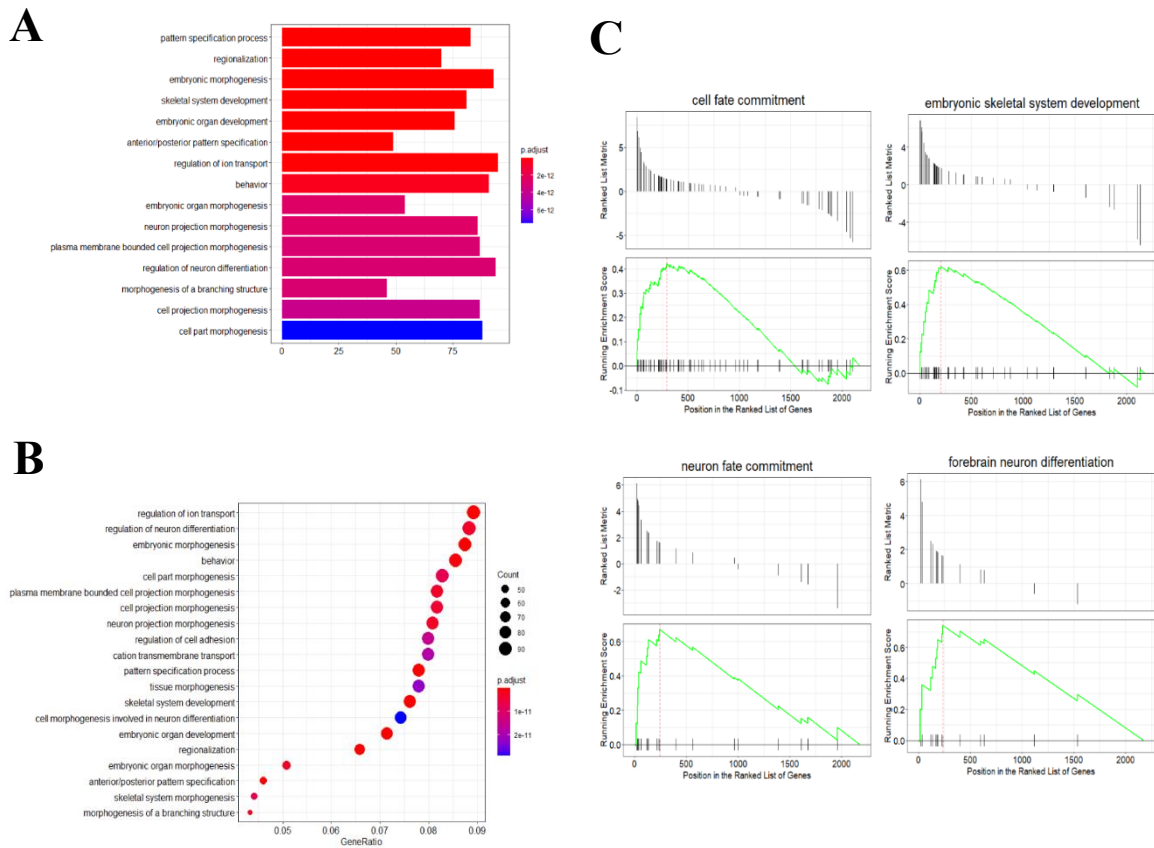
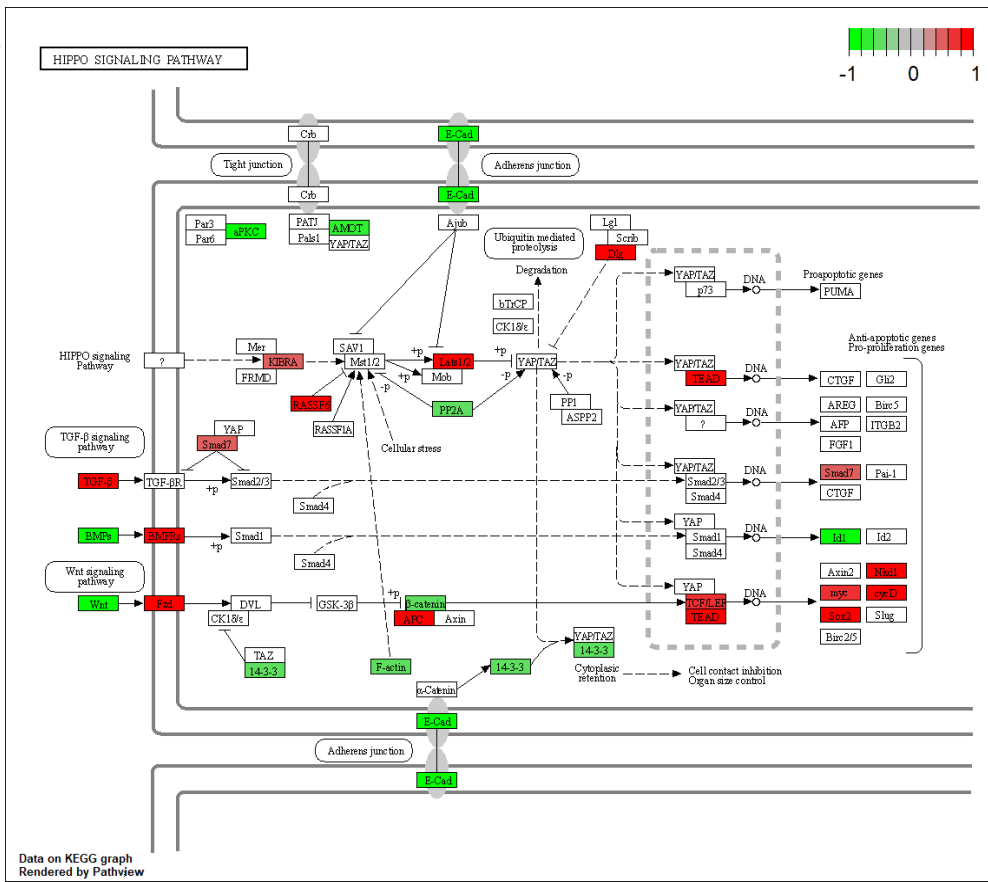


Figure 3.2. Chronic low level arsenic exposure impairs biological processes related to embryonic development and cellular differentiation. (A) GO pathway enrichment analysis performed on differentially expressed genes (DEGs) of arsenic-treated samples at week 24. Bar plot showing the 15 most enriched GO pathways. (B) Dot plot representing the ratio of enriched genes according to the number of DEGs. (C) Significantly enriched GO pathways ($FDR \leq 0.05$) are presented. Gene set enrichment analysis (GSEA) performed on DEGs of arsenic-treated samples at week 24. Gene sets for cell fate commitment, embryonic skeletal system development, neuron fate commitment and forebrain neuron differentiation were significantly enriched in arsenic treated samples. The genes are represented on the x-axis (vertical black lines) while the enrichment score is identified on the y-axis. Significance threshold was set at $FDR \leq 0.05$.

A



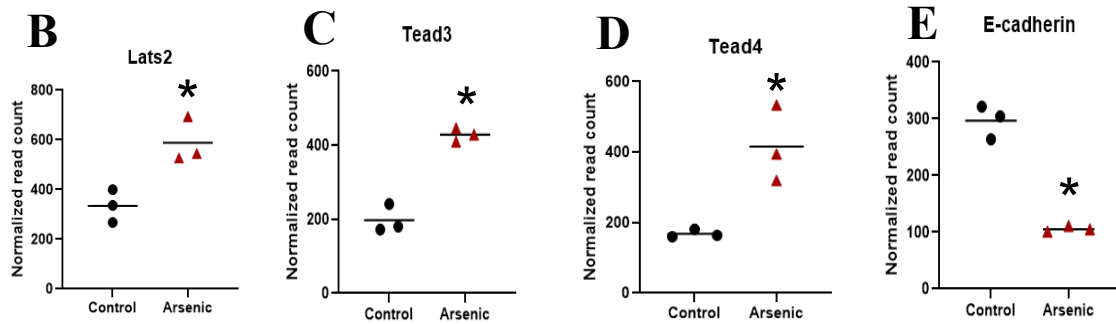
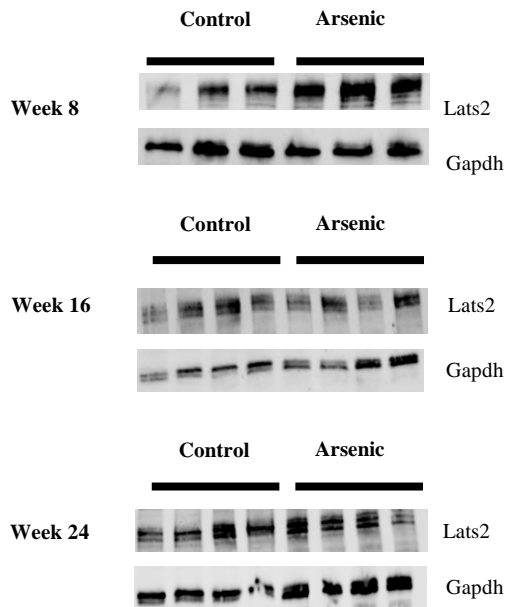
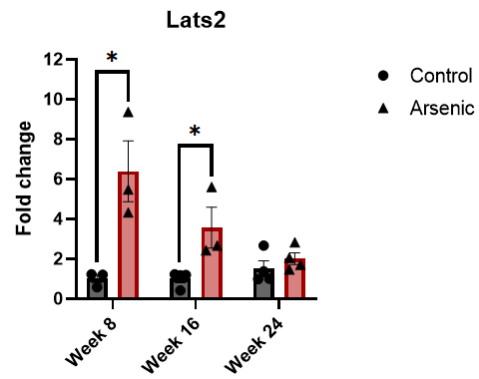
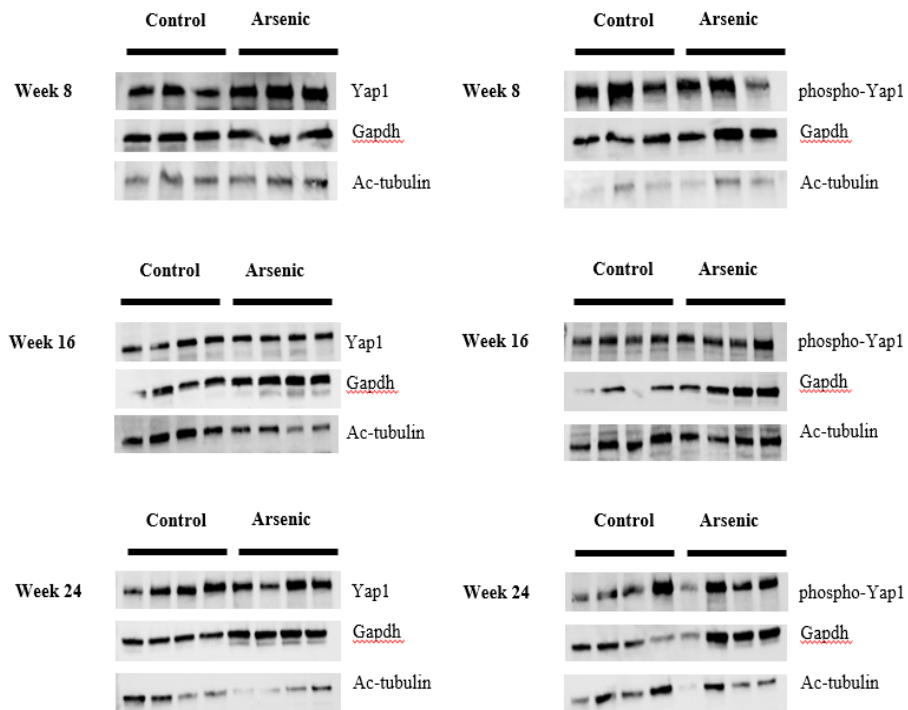


Figure 3.3. Arsenic impairs expression of key Hippo pathway components. (A) KEGG pathway analysis of the Hippo signaling shows several downregulated (green) and upregulated (red) genes in arsenic-treated samples at week 24. (B-E) RNA sequencing normalized read counts of *Lats2* (B), *Tead3* (C), *Tead4* (D) and *E-cadherin* (E) at week 24. Data is presented as read count \pm SE. Statistical differences (*) were determined using the adjusted P-value ($FDR \leq 0.05$).

A**B****C**

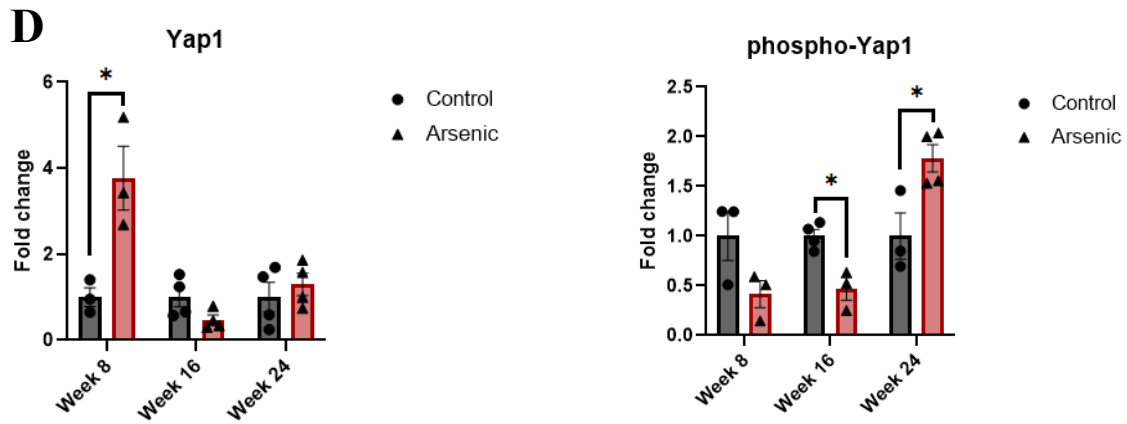


Figure 3.4. Arsenic exposure impairs protein expression of the Hippo pathway's core components. (A) Protein expression of LATS2 of differentiated cells exposed to 0 or 0.1 μM arsenic at week 8, 16 and 24. (B) Protein expression of LATS2 expressed as fold change. (C) Protein expression of YAP1 (left) and phosphorylated YAP1 (right) of differentiated cells exposed to 0 or 0.1 μM arsenic at week 8, 16 and 24. (D) Protein expression of YAP1 (left) and phosphorylated YAP1 (right) expressed as fold change. Protein levels were determined by immunoblotting analysis, assessed by densitometry and normalized to GAPDH, or to GAPDH and acetylated tubulin. Statistical differences were determined using Student's t-test (* $p \leq 0.05$).

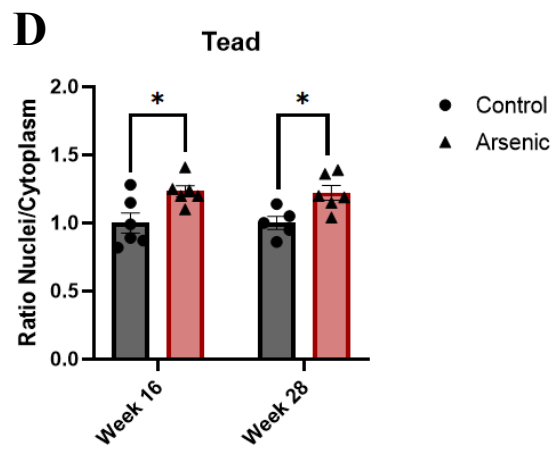
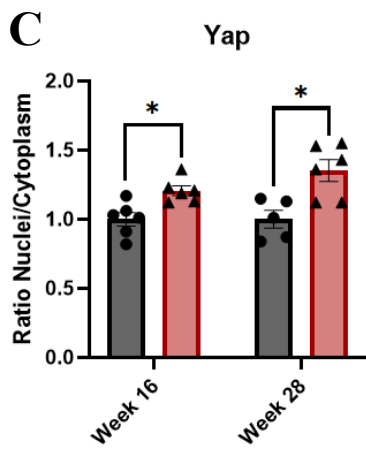
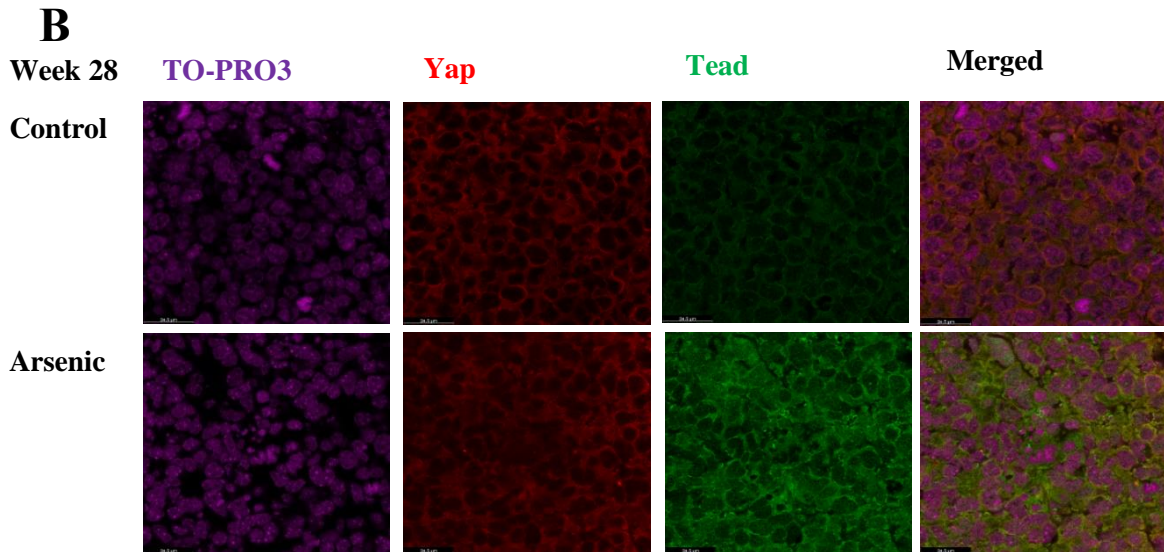
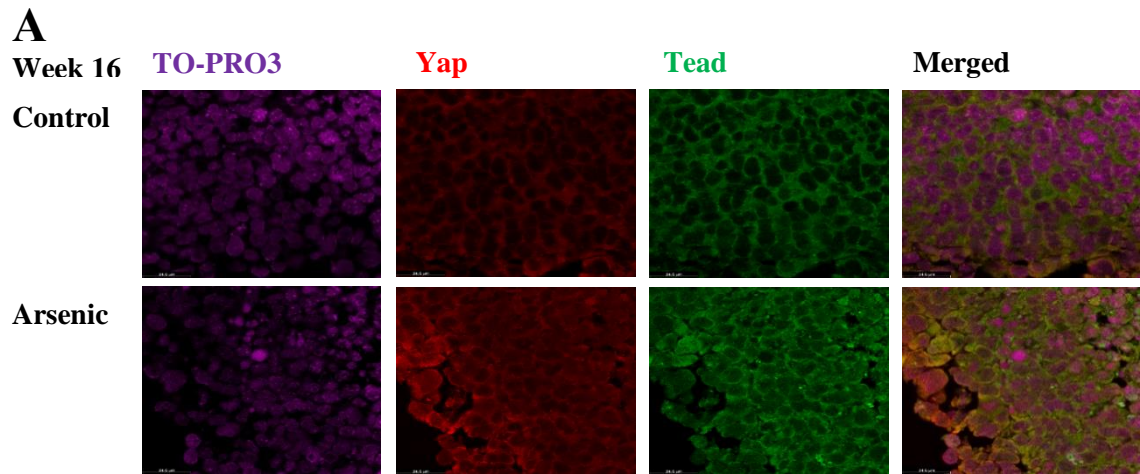


Figure 3.5. Chronic low level arsenic exposure impairs the cellular localization of Yap and Tead over time. (A-B) Representative images of YAP (red) and TEAD (green) expression and cellular localization in Day 5 control and 0.1 μ M arsenic-exposed EBs at Weeks 16 (A) and 28 (B) of exposure. (C-D) Relative fluorescence and nuclear or cytoplasmic localization of YAP (C) and TEAD (D) were determined in imageJ and expressed as ratio of integrated density value (IDV) of nuclear protein and IDV of cytoplasmic protein (n=4-6 per exposure group). Statistical differences were determined using Student's t-test (* $p \leq 0.05$).

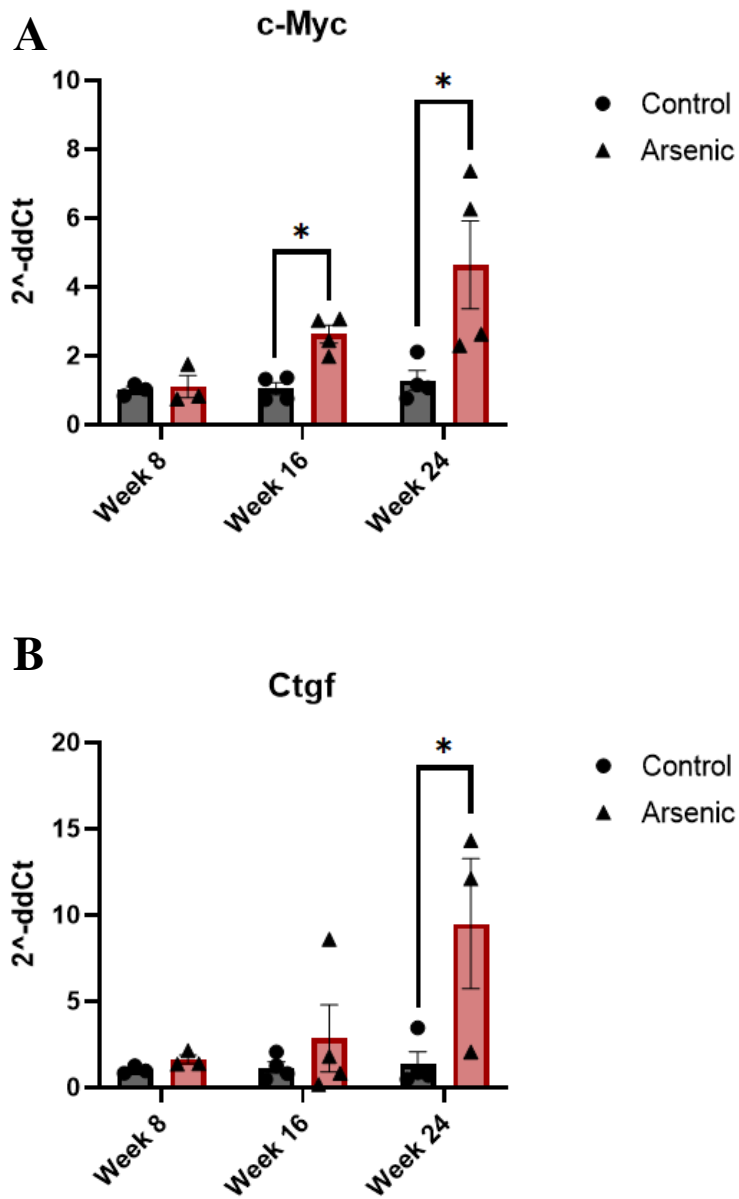
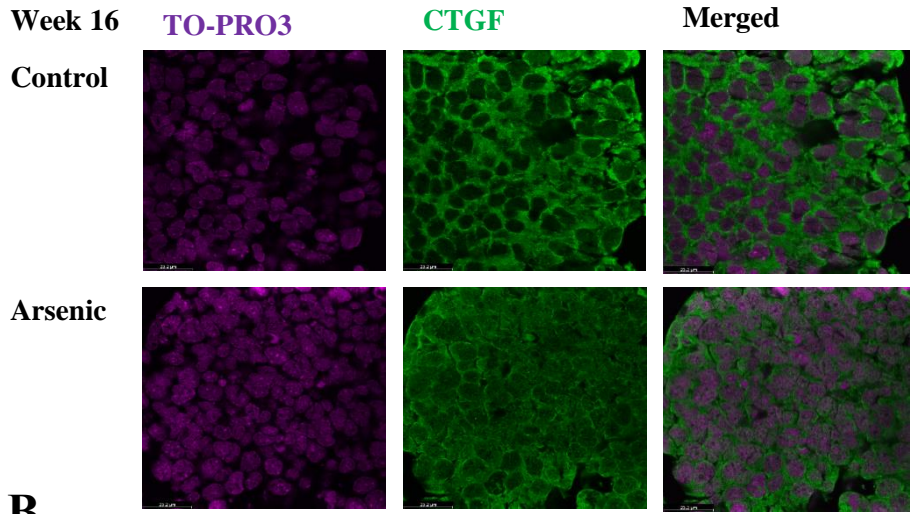
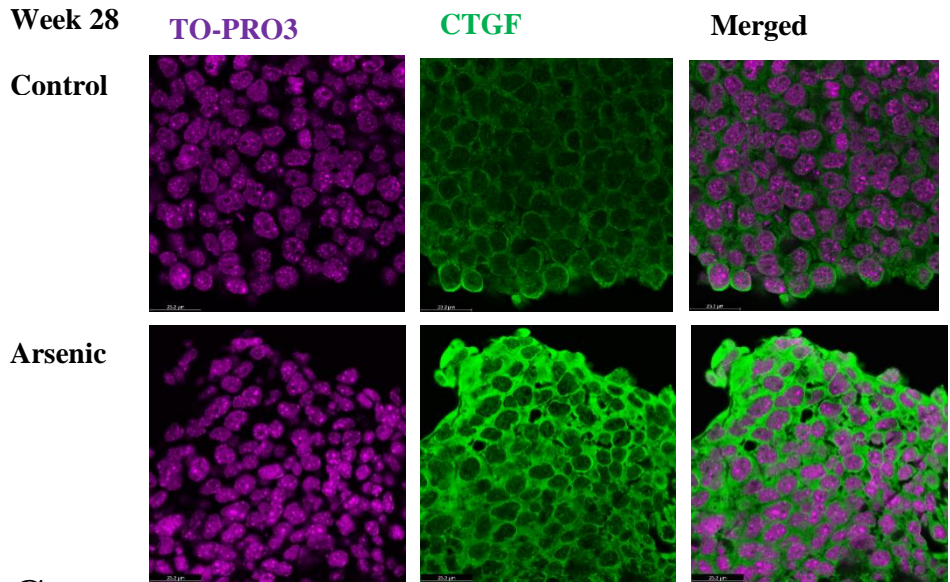


Figure 3.6. Arsenic impairs transcript levels of the YAP1 target genes *c-Myc* and *Ctgf*. (A-B) Transcript levels of *c-Myc* (A) and *Ctgf* (B) were assessed in day 9 differentiated cells exposed to 0 or 0.1 μM arsenic at week 8, 16 and 24 through qPCR analysis. Fold change was determined using the ddCt method and results were normalized to geometric mean of *Gapdh* and β -*microglobulin*. Statistical differences were determined using Student's t-test (* $p \leq 0.05$).

A



B



C

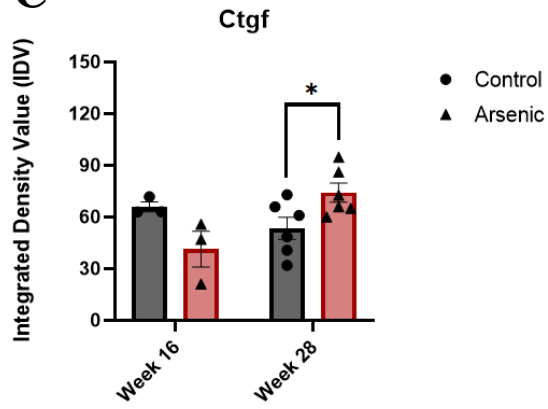


Figure 3.7. Chronic low level arsenic exposure impairs CTGF protein levels at week 28. (A-B) Representative images of CTGF (green) in Day 5 control and 0.1 μ M arsenic-exposed EBs at Weeks 16 (A), and 28 (B) of exposure. (C) Relative fluorescence was determined in imageJ and is presented as integrated density value (IDV) \pm SE. (n=3-6 per exposure group). Statistical differences were determined using Student's t-test (* $p \leq 0.05$).

C

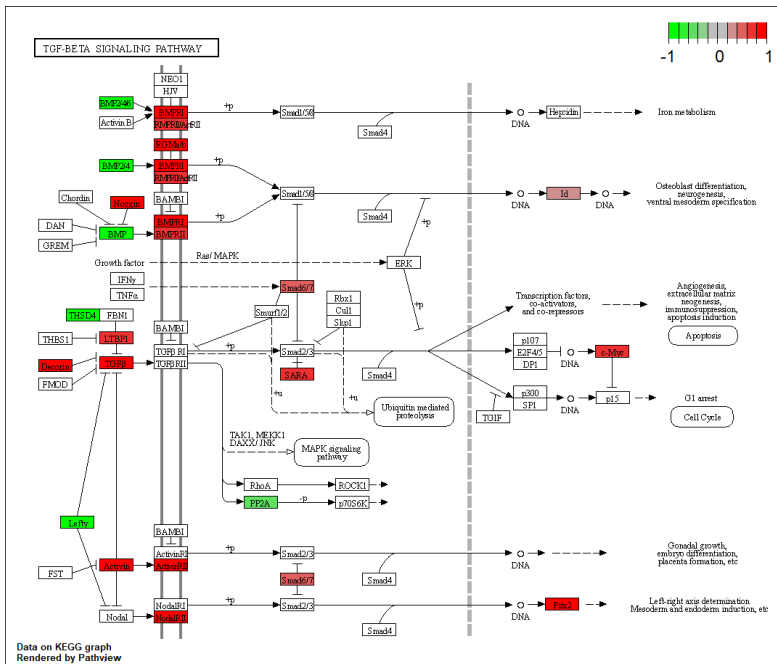


Figure S3.1. Chronic low-level arsenic impairs pluripotency, Wnt and TGF- β signaling pathways. KEGG pathway analysis of signaling pathways regulating pluripotency in stem cells (A), Wnt signaling pathway (B) and TGF- β signaling pathway (C) shows several genes downregulated (green box) and upregulated (red box) in arsenic-treated samples at week 24.

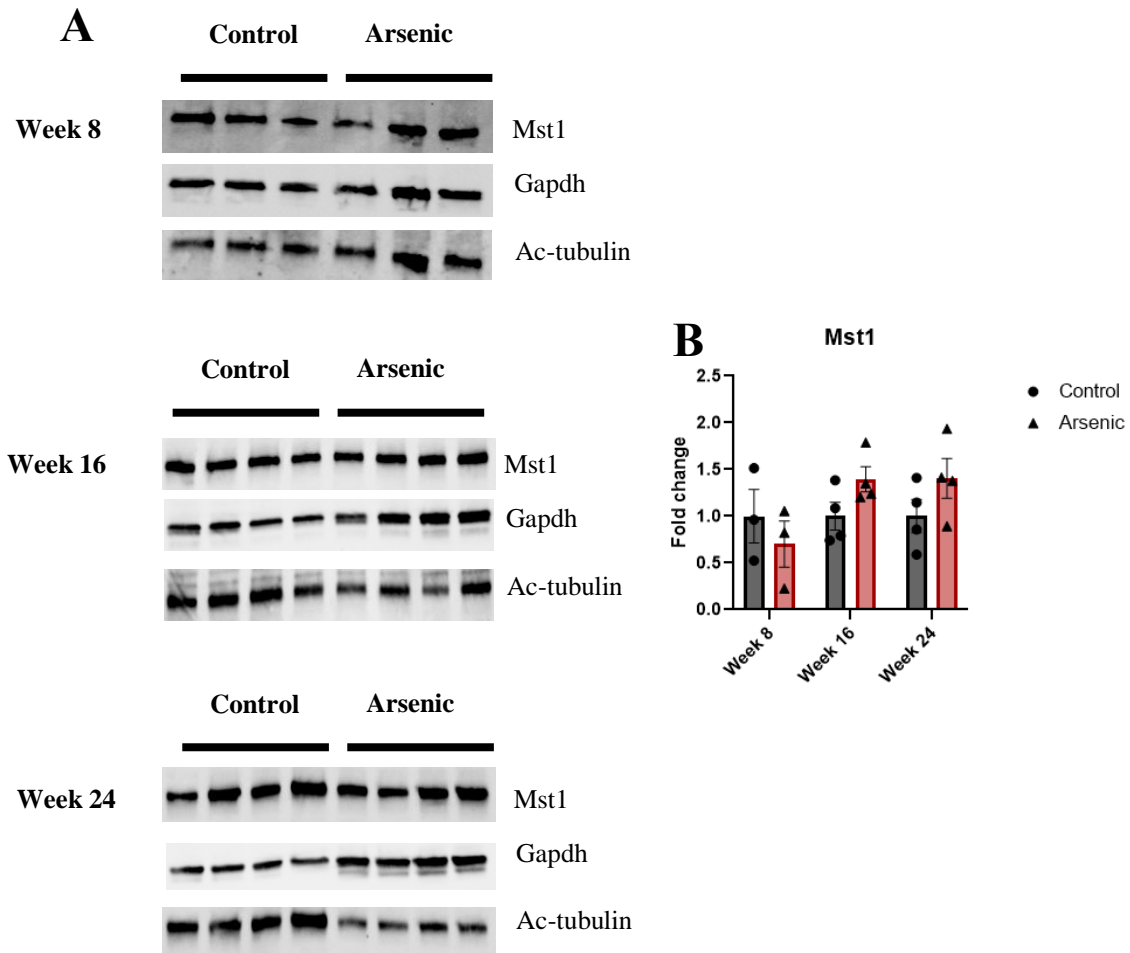


Figure S3.2. Arsenic exposure does not impair protein levels of Hippo pathway's signal receiver MST1. Protein expression of MST1 of differentiated cells exposed to 0 or 0.1 μ M arsenic at week 0, 8, 16 and 24 (A). Protein expression of MST1 expressed as fold change (B). Protein levels were determined by immunoblotting analysis, assessed by densitometry and normalized to GAPDH and acetylated tubulin. Statistical differences were determined using Student's t-test (* $p \leq 0.05$).

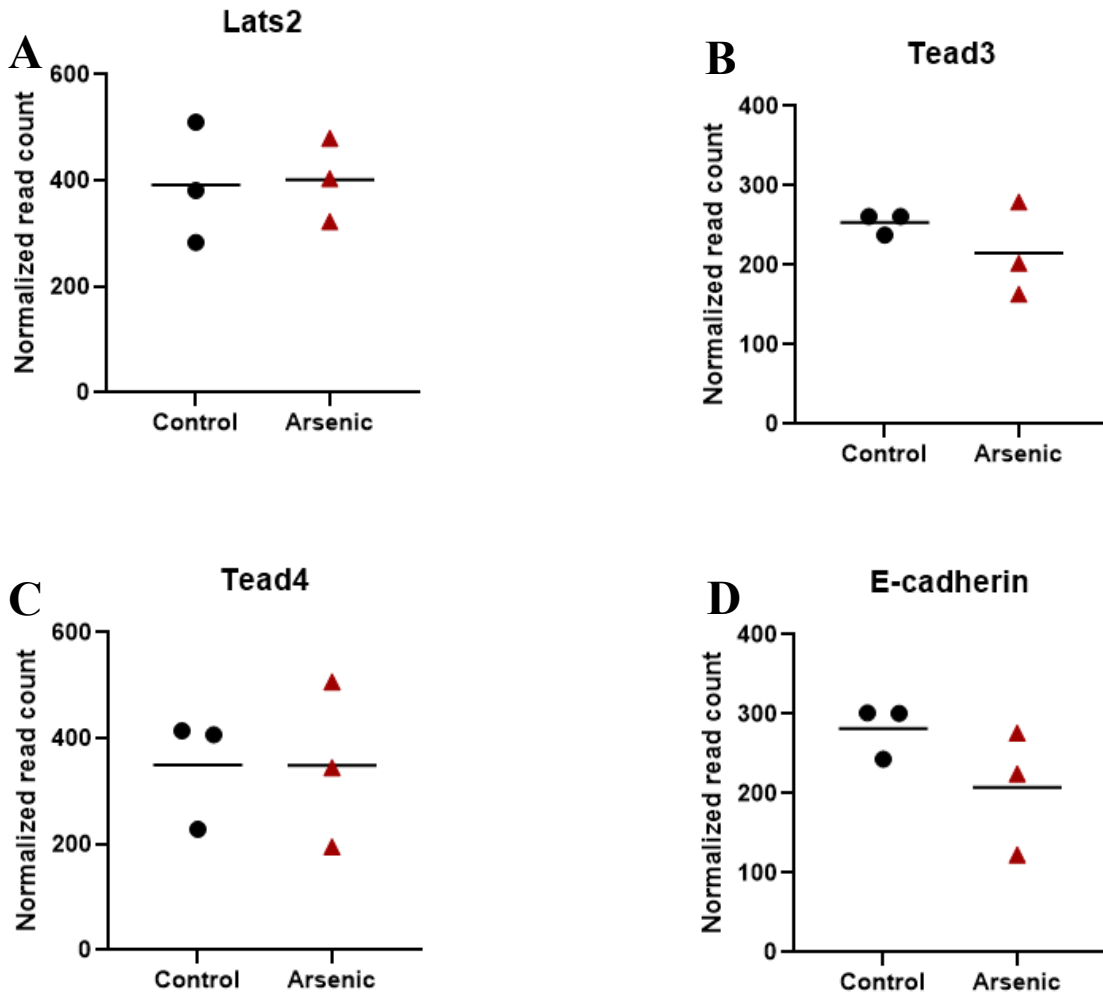


Figure S3.3. Arsenic does not impair the expression of key Hippo pathway components at week 8. RNA sequencing normalized read counts of *Lats2* (A), *Tead3* (B), *Tead4* (C) and *E-cadherin* (D) at week 8. Data is presented as read count \pm SE. Statistical differences (*) were determined using the adjusted P-value ($p \leq 0.05$).

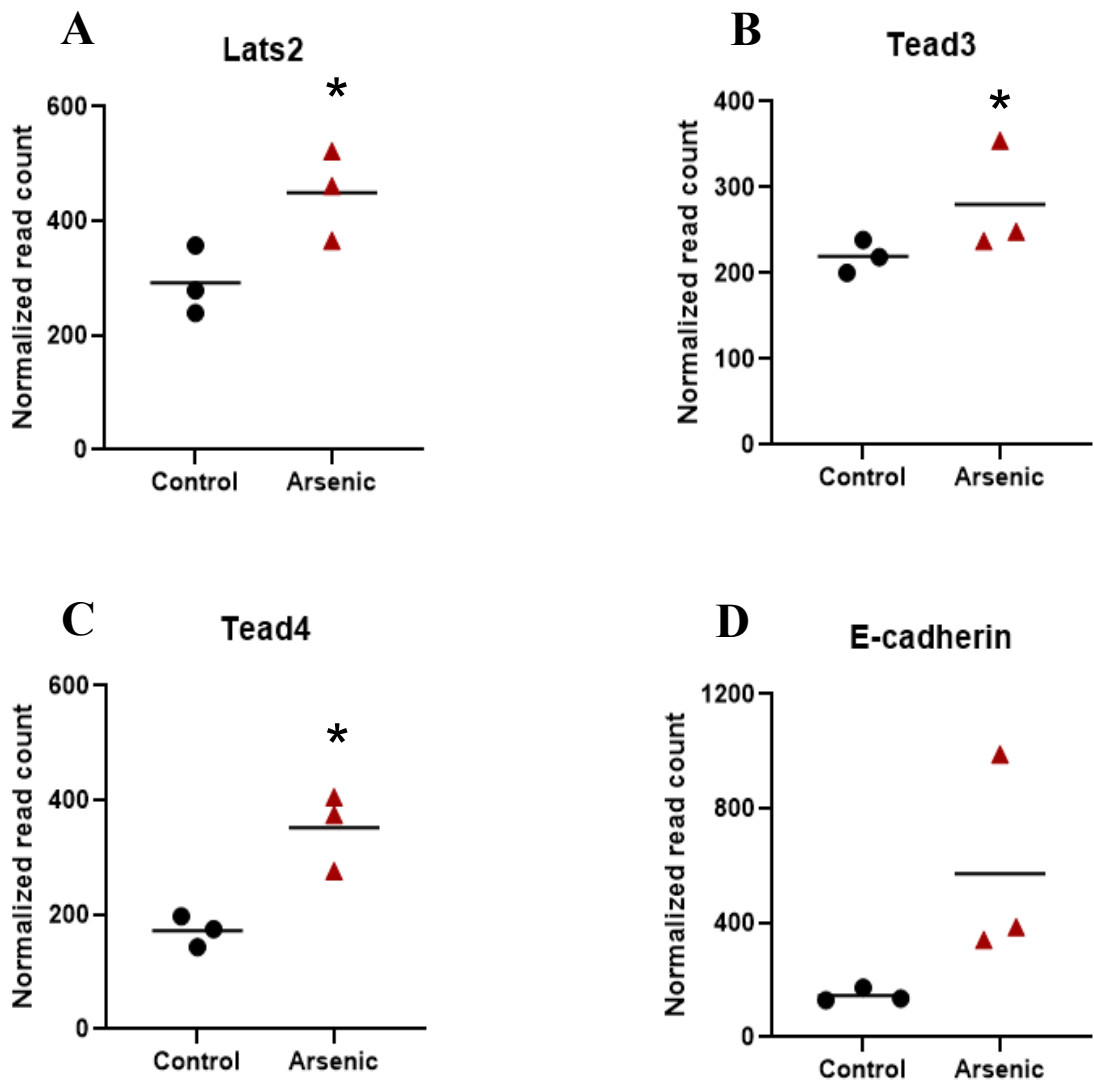


Figure S3.4. Arsenic impairs the expression of key Hippo pathway components at week 16.

RNA sequencing normalized read counts of *Lats2* (A), *Tead3* (B), *Tead4* (C) and *E-cadherin* (D) at week 16. Data is presented as read count \pm SE. Statistical differences (*) were determined using the adjusted P-value ($p \leq 0.05$).

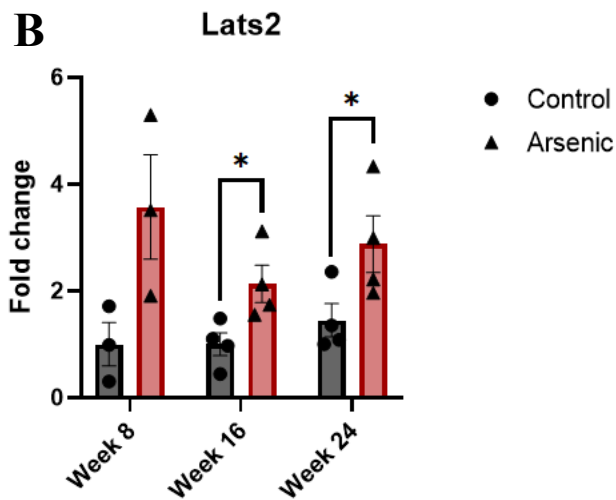
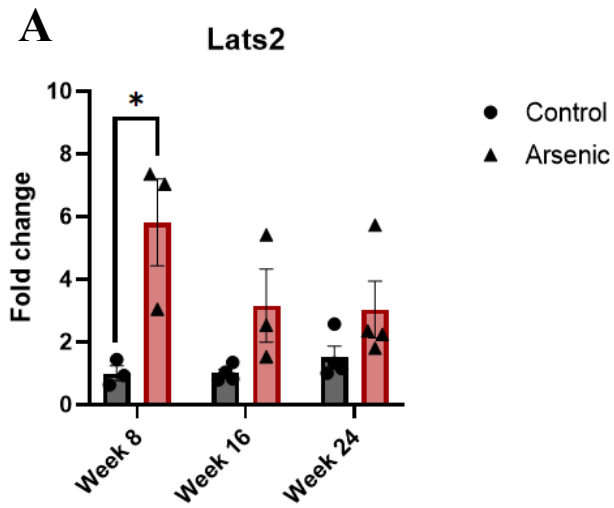


Figure S3.5. Arsenic increases protein expression of LATS2 isoforms throughout the exposure. (A) Protein expression of LATS2 upper weaker band expressed as fold change (B) Protein expression of LATS2 lower weaker band expressed as fold change. Protein levels were determined by immunoblotting analysis, assessed by densitometry and normalized to GAPDH. Statistical differences were determined using Student's t-test (* $p \leq 0.05$).

| Gene Name | Primer Sequence | |
|-------------------------|------------------------|------------------------|
| | Forward (5'-3') | Reverse (5'-3') |
| <i>Gapdh</i> | TGCGACTTCAACAGCAACTC | ATGTAGGCCATGAGGTCCAC |
| <i>β2-microglobulin</i> | GGTCTTTCTGGTGCTTGTCT | TATGTTCGGCTTCCCATTCTC |
| <i>c-Myc</i> | CTCCGTACAGCCCTATTCAT | TGGGAAGCAGCTCGAATTT |
| <i>Ctgf</i> | TGCGAAGCTGACCTGGAGGAAA | CCGCAGAACTTAGCCCTGTATG |

Table S3.1. Primer sequences of genes quantified by qPCR

CHAPTER FOUR

ARSENIC IMPAIRS DIFFERENTIATION OF HUMAN INDUCED PLURIPOTENT STEM CELLS INTO CHOLINERGIC MOTOR NEURONS

M. Chiara Perego, Benjamin D. McMichael, Nick R. McMurry, Scott W. Ventrello, Lisa J. Bain

This chapter has been submitted to Toxicological Sciences and is in the format required of that journal.

Abstract

Exposure to arsenic, a ubiquitous toxic metalloid, during embryogenesis can lead to improper neurodevelopment and locomotor activity. *In vitro* studies have also shown that arsenic inhibits differentiation of sensory neurons and skeletal muscle. In the current study, human induced pluripotent stem (iPS) cells were differentiated into motor neurons over 28 days, while being exposed to up to 0.75 μM (56.3 ppb) arsenic. On day 6, neuroepithelial progenitor cells (NEPs) exposed to arsenic had reduced transcript levels of the neural progenitor/stem cell marker *NES* and neuroepithelial progenitor marker *SOX1*, while levels of these transcripts were increased in motor neuron progenitors (MNPs) at day 12. In early motor neurons on day 18, the marker gene *CHAT* was reduced by 1.5-fold in cells exposed to 0.5 μM arsenic. RNA sequencing showed that the cholinergic synapse pathway was impaired following exposure to 0.5 μM arsenic, and that transcript levels of genes involved in acetylcholine synthesis (*CHAT*), its transport (*SLC18A3* and *SLC5A7*) and degradation (*ACHE*) were all downregulated in early motor neurons at day 18. Thus, protein expression of the neural marker MAP2, and the motor neuron marker ChAT, was investigated. In mature motor neurons at day 28, arsenic significantly downregulated the expression of MAP2 and ChAT by 2.8- and 2.1- fold, respectively, concomitantly with a reduction in neurite length. These results show that exposure to environmentally relevant arsenic concentrations hinders the differentiation of human iPS cells into motor neurons and impairs the cholinergic synapse pathway, suggesting that exposure impairs cholinergic function in motor neurons.

Introduction

Arsenic is a well-known environmental contaminant and one of the most abundant trace elements found in the Earth's crust (Shankar et al., 2014; Mochizuki, 2019). Arsenic has been classified as one of the most hazardous chemicals in the world (Shankar et al., 2014) as it poses a threat to 150 million people that are exposed to arsenic through drinking contaminated groundwater (Ravenscroft et al., 2009; Mochizuki, 2019). High arsenic concentrations have been reported in China, Mexico, Chile, Argentina, India, Bangladesh, and USA (Smith et al., 2000; Bundschuh et al., 2009; Bhattacharya et al., 2011; Shankar et al., 2014; Ayotte et al., 2017; Bjorklund et al., 2020). The current drinking water standard established by the World Health Organization and US Environmental Protection Agency is 10 ppb.

Epidemiological studies have reported that arsenic concentrations are similar in maternal blood, placental tissue, and cord blood, suggesting that arsenic can readily cross the placental barrier (Concha et al., 1998; Hall et al., 2007; Henn et al., 2016). Several human epidemiological studies have shown that arsenic exposure during pregnancy and embryonic development impairs proper neurodevelopment and leads to neurobehavioral alterations (Von Ehrenstein et al., 2006; Hamadani et al., 2011; Wang et al., 2018; Skogheim et al., 2021). Additionally, perinatal exposure to arsenic in children is associated with impaired cognitive function, decreased IQ and disrupted memory and learning skills (Hamadani et al., 2011; Wasserman et al., 2014). Impaired development and behavioral alterations have also been observed in rat and mouse pups when dams were exposed to inorganic arsenic during pregnancy (Chattopadhyay et al., 2002; Rodriguez et al., 2002; Wang et al., 2006). For instance, Tyler and Allan (2013) observed that exposure to 50 ppb arsenic during embryonic development led to impaired hippocampal neurogenesis and altered cell morphology as well as downregulation of genes involved in neurite elongation. Studies conducted *in vitro* confirm the neurogenesis impairment following arsenic exposure. For example, neuronal differentiation

inhibition and reduced neurite outgrowth following arsenic exposure were shown in PC12 cells and Neuro-2a cells (Frankel et al., 2009; Wang et al., 2010; Aung et al., 2013), in differentiated SH-SY5Y cells (Niyomchan et al., 2015), and in primary neurons (Maekawa et al., 2013). Neuronal differentiation impairment was also observed in P19 mouse embryonic stem cells exposed to 0.5 μ M of arsenic as sodium arsenite (Hong and Bain, 2012).

We have previously reported that exposure to sodium arsenite inhibits differentiation of sensory neurons and skeletal muscle of mouse embryonic stem cells (McCoy et al., 2015; McMichael et al., 2020). Similarly, reduced differentiation and myotube formation was observed in murine C2C12 myoblast cells following exposure to sodium arsenite (Steffens et al., 2011) and arsenic trioxide (Yen et al., 2010). Arsenic-induced impairment of myogenesis and skeletal muscle functions has also been reported in studies conducted using rodent models (Chattopadhyay et al., 2002; Rodriguez et al., 2002; Ambrosio et al., 2014).

While extensive research has shown that arsenic impairs neuronal differentiation in primary neurons and in neural cell lines, little is known about the effects of arsenic on the differentiation of motor neurons, which are anatomically and physiologically connected with skeletal muscle. A recent epidemiological study analyzed the link between motor neuron disease and heavy metals released into rivers showing a 16.7% higher risk of mortality associated with motor neuron disease in arsenic-contaminated areas (Sánchez-Díaz et al., 2018). Additionally, a significant decrease in ChAT protein expression and AChE activity has been reported in the brain of developing rats following perinatal arsenic exposure, suggesting that arsenic could disrupt the cholinergic system (Chandravanshi et al., 2019).

The purpose of the current study was to determine the effects of environmentally relevant arsenic exposure to human induced pluripotent stem (iPS) cells throughout their differentiation into motor neurons. Our results showed that exposure to arsenic during motor neuron differentiation led

to morphological changes along with decreased transcript levels of neural progenitor marker *SOX1* and neural progenitor/stem cell marker *NES* at day 6. Transcript levels of *SOX1*, *NES* and motor neuron progenitor marker *OLIG2* were increased by day 12 in MNPs. Transcript levels of genes involved in acetylcholine synthesis (*CHAT*), its transport (*SLC18A3* and *SLC5A7*) and degradation (*ACHE*) were downregulated at day 18. Further, at day 28, expression of neural marker MAP2 and motor neuron marker ChAT was decreased concomitantly with a reduction in neurite length. These results suggest that arsenic exposure delays the differentiation of human iPS cells into motor neurons and could impair the proper activity of acetylcholine leading to disrupted cholinergic function in motor neurons.

Methods

Human iPS cell culture and arsenic exposure

Human iPS cells (DYS0100, ATCC, Manassas, VA, USA) were cultured in mTeSR1 medium (StemCell, Vancouver, BC, Canada) on Matrigel (Corning, Corning, NY, USA)-coated 6-well plates (Thermo Fisher, Waltham, MA, USA) performing a daily media change. Cells were maintained in a humidified incubator at 37°C and 5% CO₂ and passaged every 3-5 days using ReLeSR (StemCell).

HiPS cells were exposed to 0, 0.1, 0.25 or 0.5 µM arsenic as sodium arsenite (Sigma Aldrich, St. Louis, MO, USA) for six days. On Day -1, human iPS cells were dissociated with ReLeSR and plated on 6-well Matrigel coated plates (2 x 10⁵ cells/well) with mTeSR1 medium containing 10 µM Y-27632 ROCK inhibitor (Tocris, Bristol, UK). From day 0 to day 6, cells were cultured in mTeSR1 medium, which was refreshed every 24 hours. At day 6, cells were collected for flow cytometry or stored at -80 °C in TRIzol (Sigma Aldrich) for subsequent RNA extraction.

Control and arsenic-exposed samples were cultured as independent replicates (n = 3-6 for each treatment).

Cell differentiation

To investigate arsenic effects on motor neurons differentiation, human iPS cells were induced to differentiate into motor neurons as previously described (Du et al., 2015; Solomon et al., 2021). Briefly, cells were dissociated with Dispase (1mg/ml) (Millipore Sigma, St. Louis, MO, USA) and split 1:6 onto Matrigel-coated 6-well plates (day -1). Cells were allowed to attach for 24 hours and cultured in mTeSR1 medium supplemented with 10 μ M Y-27632 ROCK inhibitor. The medium was switched, and cells were cultured in neural medium composed of DMEM/F12 (Gibco, Waltham, MA, USA) and Neurobasal medium (Gibco) at 1:1, 0.5x B27 (Gibco), 0.5x N2 (Gibco), 0.1 mM ascorbic acid (Fisher, Waltham, MA, USA), 1x glutamine (Gibco) and 1x Pen/Strep (Corning) for 28 days supplemented with different growth factors (Supplementary Table 1-2). To induce neuroepithelial progenitors (NEPs; Day 6), cells were cultured in the neural medium supplemented with 3 μ M CHIR99021 (StemCell), 2 μ M DMH-1 (Tocris) and 2 μ M SB431542 (Sigma Aldrich) for 6 days performing a media change every other day. To induce motor neuron progenitors (MNPs; Day 12), NEPs were dissociated with Dispase (1mg/ml) and split 1:6 onto Matrigel-coated 6-well plates. Cells were cultured in the neural medium supplemented by 0.1 μ M retinoic acid (Acros Organics, Geel, Belgium), 0.5 μ M purmorphamine (Millipore Sigma), 1 μ M CHIR99021, 2 μ M DMH-1 and 2 μ M SB431542 for an additional 6 days, performing a media change every other day. Subsequently, to induce early motor neurons (early MNs; Day 18), MNPs were dissociated with Dispase (1mg/ml), split 1:6 onto Matrigel-coated 6-well plates and cultured in neural medium supplemented with 0.5 μ M retinoic acid and 0.1 μ M purmorphamine for 6 days performing a media change every other day. Finally, to induce mature motor neurons (mature MNs;

Day 28), early MNs were dissociated with Accumax (eBioscience, San Diego, CA, USA), plated on Matrigel-coated 6-well plates and cultured for 10 days in neural medium supplemented by 0.5 μ M retinoic acid, 0.1 μ M purmorphamine, 0.1 μ M Compound E (Millipore Sigma), 10 ng/ml insulin-like growth factor 1 (IGF-1) (Sigma Aldrich), 10 ng/ml brain-derived neurotrophic factor (BDNF) (R&D Systems, Minneapolis, MN, USA) and 10 ng/ml ciliary neurotrophic factor (CNTF) (R&D Systems). Throughout the differentiation process, cells were exposed to 0, 0.1, 0.25 and 0.5 μ M arsenic as sodium arsenite. NEPs, Olig2+ MNPs and early MNs were harvested and stored at -80 °C in TRIzol for subsequent transcript analysis and RNA sequencing, while early MN and mature MNs were fixed in 4% paraformaldehyde for subsequent immunohistochemical analysis. Control and arsenic-exposed samples were cultured as independent replicates (n = 3-6 for each treatment).

In vivo arsenic exposure and hippocampi collection

Adult C57/BL6 mice (Taconic) were exposed to 0 or 100 ppb of arsenic as sodium arsenite in their drinking water for five weeks as previously described (Jatko et al., 2021; n = 6 per exposure group). Approval to conduct this study was obtained from Clemson's Institutional Animal Care and Use Committee (IACUC). Following five weeks of exposure, mice were euthanized, the hippocampi harvested, fixed in formalin, and embedded in paraffin for subsequent immunohistochemical analysis.

Quantitative PCR

RNA was extracted using TRIzol and a Nanodrop (Thermo Fisher) used to determine RNA concentration and purity. M-MLV Reverse Transcriptase (Promega, Madison, WI, USA) was used to convert extracted RNA (2 μ g) into cDNA. Gene expression was assessed by Real-Time

quantitative PCR on a Bio-Rad iQ5 thermocycler (Hercules, CA, USA) using RT² SYBR Green (Applied Biosystems, Foster City, CA, USA) and 10 μ M forward and reverse gene specific primers (Supplementary Table 3). Samples were run in triplicate and qPCR run efficiency was determined using a standard curve generated with five concentration points (10^{-3} - 10^{-7} ng cDNA). Absence of non-specific primer binding was verified through a melt curve obtained for each analysis. Data was normalized to housekeeping genes GAPDH and β 2-microglobulin. Gene expression was analyzed using the delta-delta Ct method (Schmittgen and Livak, 2008).

Immunohistochemistry

Day 18 early MNs and day 28 mature MNs were exposed to 0.5 μ M arsenic and cultured on Matrigel-coated glass-bottom culture dishes as described above. Cells were fixed in 4 % paraformaldehyde, permeabilized with 0.2 % Triton X-100 in PBS, and blocked in PBST with 5 % BSA and 10 % donkey serum for one hour at room temperature. Primary antibodies for ChAT (1:100, Millipore Sigma, #AB144P) and MAP2 (1:200, Millipore Sigma, #AB5622) were incubated overnight at 4 °C. After incubation with Alexa Fluor 488 secondary antibodies (1:500, anti-goat, Invitrogen, Waltham, MA, USA#A11055) and Alexa Fluor 594 (1:500 anti-rabbit, Invitrogen, #A21207), nuclei were counterstained with DAPI (1:1000, Invitrogen, #D1306). Samples were imaged using a Leica DMI8 widefield microscope system (Leica Microsystems, Buffalo Grove, IL), equipped with a Leica DFC9000 GTC camera and a 20X dry objective (N.A.= 0.4). To image DAPI, we used a LED_405 filter cube with excitation wavelength of 405/60 and emission wavelength of 470/40 nm. To image Alexa Fluor 488, we used a GFP-T filter cube with excitation wavelength of 475/40 nm and emission wavelength of 530/50 nm. To image Alexa Fluor 594, we used a Cherry-T filter cube with excitation wavelength of 560/40 and emission wavelength of 630/75 nm. Camera exposure times and gain settings for imaging Alexa Fluor 488 and Alexa

Fluor 594 were kept consistent within each experiment time point, although there is some variability between experiment time points. Similarly, all images within each time point were exported as .TIF using the same lookup table settings. The system software was Leica LAS-X, Version 3.6.0.20104 (Leica Microsystems). Images were analyzed in ImageJ to determine protein expression. For day 18 MNs, ChAT and MAP2 expression was determined by assessing the integrated density value (IDV), which was normalized to area. For day 28 MNs, the cell aggregates were located and manually selected, and IDVs were determined for the selected areas. Protein expression was assessed for two to six cell aggregates per biological replicate.

Hippocampi harvested from adult mice were fixed overnight in NBF, dehydrated in ethanol, embedded in paraffin, and sectioned at 10 μ m. Slides were deparaffinized and Tris-EDTA buffer (pH 9) was used for antigen retrieval. Primary antibodies for ChAT (1:200, Millipore Sigma, #AB144P) and MAP2 (1:500, Millipore Sigma, #AB5622) were incubated overnight at 4°C. After incubation with Alexa Fluor 488 secondary antibodies (1:500, anti-goat, Invitrogen, #A11055) and Alexa Fluor 594 (1:500 anti-rabbit, Invitrogen, #A21207), nuclei were counterstained with TO-PRO-3 (1:1000, Thermo Fisher, #T3605). Samples were imaged using a Leica DM2500 confocal microscope (Leica Microsystems, Buffalo Grove, IL) using a 20X objective (N.A.= 1.4) and a zoom of 1.0. To image TO-PRO-3, we used an excitation wavelength of 635 nm and collected emission wavelengths of 641 to 699 nm, with a time gate of 0.5 to 6.0 ns, and a frame average of 2. To image Alexa Fluor 488, we used an excitation wavelength of 488 nm and collected emission wavelengths of 504 to 568 nm, with a time gate of 0.5 to 6.0 ns and a frame average of 4. To image Alexa Fluor 594, we used an excitation wavelength of 532 nm and collected emission wavelengths of 590 to 633 nm, with a time gate of 0.5 to 6.0 ns and a frame average of 4. Images were analyzed in ImageJ to determine protein expression and distribution. Integrated density value (IDV), normalized to the area, was used to determine the expression of ChAT and MAP2.

Sholl analysis

To assess neurite length and dendritic patterns, Fiji (ImageJ) was used. Neural processes of MAP2+ day 28 MNs were traced, and their length was measured using Simple Neurite Tracer (SNT) plug-in (one to two cells per biological replicate). Sholl analysis was performed to investigate neuronal branching and assess the number of dendritic intersections at 1 μm intervals, using the Sholl plug-in (one to two cells per biological replicate).

RNA Sequencing

RNA sequencing was performed by Novogene (Sacramento, CA, USA) on rRNA-depleted RNA extracted from day 6 NEPs and day 18 early MNs (n=3 for each treatment). Paired-end sequencing was performed via the Illumina platform and reads of 150bp length were checked for quality metrics and trimmed using BBDuk from BBDuk (v38.96) (Bushnell, 2014) for low quality bases using a quality score of 20. Reference genome index was built using GENCODE Release 40/GRCh38 (Frankish et al., 2018), and paired-end clean reads were aligned to the *Homo sapiens* reference genome GRCh38 using STAR (v2.7.7a) (Dobin et al., 2013). Reads mapping to genes were counted using featureCounts (v.2.0.3) (Liao et al., 2014). Differential expression analysis was conducted using the DESeq2 (v1.29.7) R package (Love et al., 2014) using the Wald test to compare control and arsenic-exposed cells at day 6 and day 18. The Benjamini-Hochberg adjustment was used to control for False Discovery Rate (FDR). Functional annotation analysis was performed using the R package annotables (Steinbaugh et al., 2017) on differentially expressed genes with an adjusted $p < 0.05$. The hierarchical clustering distance method was performed to cluster samples using the pheatmap package in R (Kolde, 2012). The R package clusterProfiler was used to run Gene Ontology (GO) gene set enrichment analysis (GSEA) of differentially expressed genes (Yu et al., 2012; Wu et al., 2021). GO terms with adjusted $p < 0.05$ were considered significantly

enriched by differentially expressed genes. Lastly, biochemical pathways disrupted following arsenic exposure during motor neuron differentiation were identified using the clusterProfiler package to assess the statistical enrichment and over-representation of differential gene expression in KEGG pathways.

Flow cytometry

Annexin V and SyTox green staining was performed to determine cell viability and apoptosis in human iPS cells and NEPs following arsenic exposure. Briefly, cells were incubated in Accumax at 37 °C for 10 minutes to create a single cell suspension, and resuspended in FACS buffer (1X PBS, 1 % BSA, 0.1 % sodium azide). Cells were incubated with Annexin V (1:200, Santa Cruz, Santa Cruz, CA, USA #sc-74438) at 4°C for 30 minutes followed by incubation with Alexa Fluor 568 secondary antibody (1:400, anti-mouse, Invitrogen, #A11004) at 4°C for 30 minutes. Subsequently, cells were washed in FACS buffer and incubated with SyTox Green (1:1000, Invitrogen, #S34860) for 20 minutes. Flow cytometry was performed using a Bio-Rad S3e Cell Sorter. SyTox green fluorescence was assessed at 488 nm excitation and 504 nm emission while Annexin V fluorescence was assessed at 561 nm excitation and 603 nm emission.

Statistical analysis

Results are expressed as mean \pm SE. Statistical significance for differential gene expression was calculated by Student's t-test or by ANOVA followed by Tukey's multiple comparison test. Protein expression for immunohistochemistry were determined using ImageJ. Statistical significance for average protein expression in control and arsenic-treated biological replicates was assessed by Student's t-test. Neurite length was determined using neurite tracer plug-in to examine MAP2⁺ neural processes of one to two cells per biological replicate. Sholl analysis was conducted

at 1 μm intervals, using the Sholl plug-in for one to two cells per biological replicate. Statistical significance for average neurite length and number of dendritic intersections in control and arsenic-treated samples was assessed by Student's t-test. Percentage of live, apoptotic, and necrotic cells was investigated by flow cytometry. Statistical significance for average percentage of live, apoptotic, and necrotic cells in control and arsenic-treated samples was assessed by two-way ANOVA followed by Tukey's multiple comparison test. Data was analyzed for normal distribution and $p < 0.05$ was considered statistically significant.

Results

Human iPS cells are sensitive to arsenic exposure

To determine appropriate arsenic concentrations to use during differentiation, human iPS cells were first cultured for six days in mTeSR medium to maintain them as stem cells in their pluripotent state. During this maintenance phase, cells were treated with 0, 0.1, 0.25 and 0.5 μM arsenic (equivalent to 7.5 – 37.5 ppb). Morphological analysis indicates that 0.25 and 0.5 μM concentrations result in significant cell death starting at day 4 and continuing through the rest of the exposure (Fig. 1A). qPCR analysis of the cells exposed to 0.5 μM As showed increased expression of pluripotency transcripts, including *SOX2* (Fig. S1A), *POU5F1* (Fig. S1B) and *NANOG* (Fig. S1C). Consistently, we observed a strong positive correlation of *SOX2*, *POU5F1* and *NANOG* transcript levels in human iPS cells (Supplementary Table 4). A recent study conducted using mouse embryonic stem cells also reported an increased transcript expression of *Pou5f1* and *Nanog* at arsenic concentrations lower than 1 μM , while higher concentrations led to downregulation of *Sox2*, *Pou5f1* and *Nanog* transcription along with differentiation (Beeravolu et al., 2017).

Next, iPS cells were differentiated into neuroepithelial progenitors (NEPs) for six days while being exposed to 0, 0.25, 0.5, or 0.75 μM arsenic. There were no morphological differences between exposure groups (Fig. 1B). Consistently, flow cytometry with Annexin V and Sytox green did not indicate significant differences in the percentage of live, apoptotic, and necrotic cells following exposure to 0.25 or 0.5 μM arsenic for six days (Fig. 1C-D). Therefore, considering the absence of morphological alterations, compared with human iPS cells (Fig. 1A), and no significant changes in cell viability or death from the flow cytometry analysis, we decided to use concentrations of up to 0.75 μM arsenic for the remainder of the study.

Differential gene expression of key pluripotency and differentiation markers confirms generation of motor neurons (MNs)

To confirm the differentiation of human iPS cells into NEPs, motor neuron progenitors (MNPs), and early motor neurons (MNs), we analyzed the differential gene expression of key pluripotency and stage-specific markers in control samples throughout the differentiation process (day 0 to day 18). Transcript levels of the pluripotency marker *POU5F1* are significantly reduced by day 6 (Fig. 2A), while the NEP marker *SOX1* (Fig. 2B) and neural stem cell marker *NES* (Fig. 2C) are both significantly increased. Transcript levels of the MNP marker *OLIG2* were significantly increased starting at day 12, which should be the peak time of MNP generation. During the stage of differentiation into day 18 early MNs, the expression of *OLIG2* was significantly reduced (Fig. 2D). Expression of motor neuron specification marker *CHAT* was not different at the day 6 MNP stage, but its levels continued to increase by 3-fold in day 12 MNPs and by 5.5-fold in day 18 early MNs (Fig. 2E). The marker transcript data confirms the generation of NEPs, MNPs and early MNs, while suggesting phenotypic heterogeneity and the presence of a subpopulation of neural stem and progenitor cells even at later time points.

Key markers of motor neuron differentiation are disrupted following arsenic exposure

Previous studies have shown that exposure to low arsenic concentrations inhibits sensory neuron and skeletal muscle differentiation from mouse embryonic stem cells (Hong and Bain, 2012; McMichael et al., 2020). Therefore, we hypothesized that the differentiation into motor neurons, which are anatomically and physiologically connected with skeletal muscle, would also be impaired. To test this hypothesis, human iPS cells were exposed to 0, 0.25, 0.5 or 0.75 μM arsenic during their differentiation into neuroepithelial progenitors (NEPs) and motor neuron progenitors (MNPs), and to 0 or 0.5 μM arsenic during their differentiation into early and mature motor neurons (MNs). Arsenic treatment does not cause morphological changes in NEPs (Fig. 1B). However, transcript levels of the NEP marker *SOX1* were significantly downregulated by 1.4-, 2.7- and 1.6-fold in NEPs treated with 0.25, 0.5 and 0.75 μM As, respectively (Fig. 4A). Similarly, transcript levels of neural progenitor/stem cell marker *NES* were significantly decreased in NEPs exposed to 0.25, 0.5 and 0.75 μM As, by 1.3-, 1.4- and 1.3- fold, respectively (Fig. 4B). *SOX2* transcript levels were also significantly reduced by 1.3-, 1.7- and 1.5- fold, in NEPs exposed to 0.25, 0.5 and 0.75 μM As, respectively (Fig. 4C) while no differences were observed for *POU5F1* gene expression (Fig. 4D). Previous studies have suggested that expression of Nestin, encoded by the *NES* gene, positively correlates with the expression of Sox2 (Laga et al., 2011, Luo et al., 2013). Furthermore, Sox binding sites have been identified on the Nestin enhancer indicating the existence of a regulatory network and of a synergistic interaction between Sox and Nestin (Tanaka et al., 2004). Similarly, we have reported a positive correlation of *SOX2*, *SOX1* and *NES* transcript levels in NEPs (Supplementary Table 5).

At the next stage of motor neuron formation, we observed morphological differences in arsenic-treated day 12 MNPs, which are less elongated and lose their spatial organization compared with control MNPs (Figure 3A). Transcript levels of the MNP marker *OLIG2* were significantly

upregulated in MNPs exposed to 0.25 and 0.5 μM As by 2- and 1.3- fold, respectively (Fig. 4E). Interestingly, a recent study demonstrates that transgenic mice with *Olig2* overexpression in Nestin-positive neural progenitor cells had decreased brain thickness, increased neuronal cell death, and impaired locomotion (Liu et al., 2015; Szu et al., 2021). Transcript levels of *NES* (Fig. 4F) and *SOX1* (Fig. 4G) were also significantly upregulated in arsenic-treated MNPs, suggesting that arsenic exposure might be responsible for the maintenance of a stem/neuronal progenitor cell population. Conversely, transcript levels of *CHAT* were significantly downregulated in MNPs exposed to 0.5 and 0.75 μM As by 2.6- and 2.5- fold, respectively (Fig. 4H).

Lastly, while no morphological changes in arsenic-treated early MNs were noted (Fig. 3B), mature MNs exposed to arsenic possess shorter neural processes and less defined cell aggregates (Fig. 3C). Interestingly, *CHAT* expression was significantly downregulated by 1.5- fold in early MNs exposed to 0.5 μM As (Fig. 4I). Taken together, these results indicate that arsenic exposure reduces the differentiation of human iPS cells into motor neurons, leading to altered cellular morphology and neuronal process formation.

Differential gene expression due to arsenic exposure in day 6 NEPs and day 18 early MNs

To identify the signaling pathways responsible for the impairment of key markers involved in motor neuron differentiation, we performed RNA sequencing and pathway analysis in day 6 NEPs and day 18 early MNs. Differential expression analysis suggests that arsenic exposure is driving gene expression changes in both day 6 NEPs (Fig. 5A) and day 18 early MNs (Fig. 5B). Principal component analysis (PCA) confirms these results showing that cells exposed to arsenic express different genes than control samples at both time points (Fig. 5C-D). For instance, control and arsenic samples are heavily separated along the x-axis (PC1), which accounts for 82% and 77% of the variation in day 6 NEPs (Fig. 5C) and day 18 early MNs (Fig. 5D), respectively. Interestingly,

PCA analysis for both time points indicate that control and arsenic samples at different times are separated along the x-axis (PC1) which accounts for 98% of the variation (Fig. 5E), suggesting that NEPs and early MNs-like cells are also generated in arsenic treated-samples.

Gene set enrichment analysis (GSEA) indicates that some of the most significantly suppressed categories in arsenic-treated samples were related to synaptic signaling and nervous system process in day 6 NEPs, and to synapse, neuron projection and nervous system processes in day 18 early MNs (Fig. 5F). Consistently, biological processes in which DEGs presented high enrichment scores were associated with nervous system development, neurogenesis, neurotransmitter transport, synapse organization and synaptic signaling in day 18 early MNs (Fig. 5G).

Arsenic reduces expression of genes in cholinergic synapses involved in acetylcholine synthesis, transport, and degradation

To investigate potential mechanisms disrupted due to arsenic exposure during motor neuron differentiation, pathway analysis was conducted to identify DEGs enriched in KEGG pathways. Our results suggest that neuronal pathways, such as axon guidance (Fig. S2A) and neuroactive ligand-receptor interaction (Fig. S2B), are disrupted following arsenic exposure in day 18 early MNs. Additionally, we confirmed the impairment of signaling pathways we have previously reported to be disrupted following arsenic exposure. These pathways include the Wnt signaling pathway and the Hippo signaling pathway through upregulation of YAP and TEAD transcript levels (data not shown). However, while we have previously hypothesized that chronic low level arsenic exposure disrupts the TGF- β signaling pathway by reducing Gdf3 transcript levels in mouse embryonic stem cells, no significant changes were observed for GDF3 transcript levels in arsenic-treated day 6 NEPs and day 18 early MNs (data not shown).

Mammalian motor neurons can release both acetylcholine and glutamate (Nishimaru et al., 2005); in particular, upper motor neurons form glutamatergic synapses with lower motor neurons, which are cholinergic neurons (Stifani, 2014). Interestingly, both pathways associated with glutamatergic synapses (Fig. S2C) and cholinergic synapses (Fig. 6A) were overall downregulated in arsenic-treated day 18 early MNs. In addition, transcript expression of cholinergic pathway genes *CHAT*, *SLC18A3* (encoding for VACHT), *ACHE* and *SLC5A7* (encoding for ChT) was also downregulated in arsenic-treated day 18 early MNs by 1.4-, 2-, 2.2- and 1.3- fold, respectively (Fig. 6B - E). Briefly, ChAT is the enzyme involved in the biosynthesis of neurotransmitter acetylcholine, which is loaded into presynaptic vesicles by the transporter VACHT and released into the synaptic cleft where it is hydrolyzed by AChE into acetate and choline, which is transported back into the presynaptic nerve terminal by transporter ChT.

Read counts of these genes were consistently increased in day 18 early MNs as compared to day 6 NEPs, confirming the formation of cholinergic neurons during the differentiation process (Fig. 6B - E). These data, coupled with the observed morphological changes, suggests that arsenic exposure may disrupt the proper formation and function of cholinergic synapses in MNs.

Arsenic exposure downregulates protein expression of MAP2 and ChAT, and reduces neurite length in day 28 mature MNs

The effects of arsenic exposure on protein expression of the neuronal marker MAP2, and cholinergic marker ChAT, were investigated through immunohistochemical analysis. MAP2 plays a role in stabilization of microtubules, the development of neuronal processes, dendrite elongation and synaptic plasticity (Morrison et al., 1998; Sánchez et al., 2000; Harada et al., 2002). While no differences in MAP2 and ChAT protein expression were noted in day 18 early MNs (Fig. 7A-B), fewer MAP2+ neuronal extensions can be seen in arsenic-exposed day 18 early MNs (Fig. 7A).

However, protein expression of MAP2 and ChAT in the cell aggregates of day 28 mature MNs was significantly downregulated in arsenic-exposed samples by 2.8- and 2.1- fold, respectively (Fig. 8A-B). Moreover, morphological differences were observed in arsenic-treated MAP2+ neurites, which are less elongated (Fig. 8A). To further analyze arsenic's effects on neurite length and dendritic pattern, neurite tracing and Sholl analysis were conducted. Our results confirmed that arsenic significantly reduces neurite length by 1.8 -fold while increasing the number of intersections (Fig. 8C - E).

Arsenic exposure in vivo downregulated ChAT protein expression in adult mice hippocampi

To confirm the effects of arsenic exposure on ChAT and MAP2, we evaluated their expression in hippocampi of adult male mice exposed to 0 or 100 ppb arsenic for five weeks. Adult neurogenesis occurs in the dentate gyrus of the hippocampus, which is involved in memory, learning, and cognitive flexibility (Shors et al., 2002; Deng et al., 2010; Tyler and Allan, 2013; Toda et al., 2019). Cholinergic neurons are distributed in the hippocampus as acetylcholine modulates hippocampal-dependent memory function and learning (Haam and Yakel, 2017; Maurer and Williams, 2017; Haam et al., 2018). Immunohistochemical analysis confirms the presence of MAP2+ neurofilaments and ChAT+ cholinergic neurons in hippocampi collected from adult mice. While no differences were observed in protein expression of MAP2, arsenic treatment significantly reduced hippocampal ChAT levels (Fig. S3). Taken together, these results suggest that arsenic downregulation of ChAT expression could lead to impaired cholinergic functions in motor neurons.

Discussion

The results of this study suggest that motor neuron differentiation is disrupted following arsenic exposure, as gene expression of several differentiation markers, including *SOX1*, *NES*, *OLIG2* and

CHAT is impaired throughout the differentiation process. Expression of genes involved in the acetylcholine cycle such as *CHAT*, *SLC18A3* (encoding for VAChT), *SLC5A7* (encoding for ChT) and *ACHE* is also reduced, suggesting that arsenic might impair proper function of the cholinergic synapse. Consistently, arsenic exposure also downregulates ChAT protein expression in mature MNs while reducing neurite length and in hippocampi collected from adult mice exposed to 100 ppb of arsenic for five weeks.

Arsenic impairs transcript levels of key motor neuron differentiation markers

Species-specific responses in the metabolism and whole-body retention of arsenic have been reported. For instance, humans are more susceptible than mice to arsenic as they have reduced levels of arsenic methyltransferase (As3MT) and increased body retention (Vahter, 2002; Drobná et al., 2010; States et al., 2011). To our knowledge, few studies have investigated the effects of arsenic on cellular differentiation using human iPS cells as *in vitro* model. Most studies investigating impairment of neuronal differentiation or neurotoxicity due to arsenic exposure have been conducted using rodents (Liu et al., 2012; Li et al., 2018; Xiong et al., 2021; Pandey et al., 2022), murine cell lines (Frankel et al., 2009; Liu and Bain, 2014; McCoy et al., 2015; Bain et al., 2016), human neuroblastoma cell lines (Jung et al., 2006; Cheung et al., 2007; Petit et al., 2013; Stern et al., 2014) or differentiated human neuroblastoma cells (Niyomchan et al., 2015, 2018; Wisessaowapak et al., 2021a,b). Although a recent study has reported neurite damage following exposure to 50 μ M of arsenic as sodium arsenate for 48 hours in neural progenitor cells derived from human iPS cells (Jahan et al., 2022), the current study is the first to assess the effects of environmentally relevant arsenic concentrations on the cellular differentiation of human iPS cells-derived motor neurons.

Human iPS cells were differentiated into motor neurons and transcript levels of known motor neuron differentiation markers, including *SOX1*, *NES*, *OLIG2* and *CHAT*, were measured throughout the exposure. The transcription factor Sox1 is the earliest and most specific marker for neuroepithelial cells and is expressed by progenitor cells in the nervous system during fetal neurodevelopment (Aubert et al., 2003; Park et al., 2021). Nestin is an intermediate filament protein, encoded by the *NES* gene, highly expressed in multipotent stem cells and neural progenitor cells of the developing brain (Chen et al., 2010; Krishnasamy et al., 2017). Nestin was first described as a neuroepithelial stem cell marker and it is commonly used to identify progenitor populations (do Valle et al., 2022). Together, Sox1 and Nestin represent early markers of neural stem cells, those that have the potential to differentiate into functional neurons and other neuronal cell types (Feng et al., 2014). Our findings show that transcript levels of both *SOX1* and *NES* are significantly downregulated in NEPs after six days of exposure while increasing after 12 days of exposure in MNPs. These results indicate the presence of a significant neural stem cell/progenitor cell population (Nestin⁺, Sox1⁺ cells) in MNPs, suggesting that arsenic exposure hinders differentiation of human iPS cells into motor neuron progenitors. To our knowledge, this is the first study to show that arsenic exposure disrupts the early stages of motor neuron differentiation using human iPS cells. However, neuronal differentiation impairment following arsenic exposure has been previously reported in sensory neurons derived from P19 mouse ES cells (Hong and Bain, 2012; McCoy et al., 2015; Bain et al., 2016; McMichael et al., 2020), murine neuronal N2a and PC12 cells (Frankel et al., 2009; Wang et al., 2010; Chou et al., 2015).

The differentiation of stem and progenitor cells into motor neurons is characterized by changes in gene expression. For instance, *Olig2* is a transcription factor essential for establishing the identity of MNPs and for promoting neuronal differentiation into MNPs (Ortega et al., 2013; Sagner et al., 2018). Our data indicates that arsenic exposure enhances *OLIG2* transcript levels in

MNPs. Recently, a link between neurodevelopmental disorders, including Down syndrome and autism spectrum disorder, and Olig2 overexpression has been suggested (Szu et al., 2021), as overexpression of Olig2 was reported in neural progenitor cells collected from human patients affected by Down syndrome (Lu et al., 2012). Additionally, transgenic mice with Olig2 overexpression in neuronal progenitor cells showed enhanced neuronal cell death, reduced brain thickness and impaired locomotion (Liu et al., 2015; Szu et al., 2021).

Arsenic downregulates ChAT expression and inhibits genes involved in acetylcholine transport and degradation.

To confirm the hypothesis that arsenic exposure disrupts the function of cholinergic synapses, we investigated the expression of genes involved in the synthesis and breakdown of acetylcholine, including *CHAT*, *SLC18A3*, *SLC5A7* and *ACHE*. Briefly, acetylcholine is synthesized in the cytoplasm of cholinergic neurons by the enzyme choline acetyltransferase (ChAT), which transfers an acetyl group from acetyl-CoA to choline (Deutch and Roth, 2014). The neurotransmitter is then loaded through vesicular acetylcholine transporter (VAChT) (encoded by *SLC18A3*)-mediated transfer into presynaptic vesicles and stored until it is released in the synaptic cleft (Arvidsson et al., 1997; Fisher and Wonnacott, 2012). After being released, acetylcholine is hydrolyzed into choline and acetate by the enzyme acetylcholinesterase (AChE) to terminate neuronal signaling (Trang and Khandhar, 2022). Lastly, the high-affinity choline transporter (ChT) (encoded by *SLC5A7*) is responsible for the choline re-uptake into the cholinergic neuron (Choudhary et al., 2017). In the current study, RNA sequencing and KEGG analysis suggest that the cholinergic synapse pathway is impaired and show that transcript levels of *CHAT*, *SLC18A3*, *ACHE* and *SLC5A7* are all reduced in early motor neurons following arsenic exposure.

A high density of cholinergic synapses has been reported in the cerebral cortex and the hippocampus, suggesting that cholinergic function is also important for brain activity (Hampel et al., 2018). For instance, acetylcholine in the brain plays a role in synaptic transmission and plasticity and is involved in neuronal network formation and neuronal excitability (Picciotto et al., 2012). Additionally, cholinergic transmission is critical for many cognitive functions including memory and learning (Power, 2004; Hampel et al., 2018). A recent study has suggested that perinatal arsenic exposure leads to cholinergic system impairment in the brain of developing rats (Chandravanshi et al., 2019). Specifically, Chandravanshi and coworkers observed a significant decrease in AChE activity and ChAT protein levels in the frontal cortex and the hippocampus of rats perinatally exposed to sodium arsenite. Similarly, Yadav et al. (2011) reported reduced AChE activity in the hippocampus and frontal cortex along with decreased ChAT protein expression in adult rats exposed to sodium arsenite for four weeks. Consistently, our results show decreased protein expression of ChAT in mature motor neurons following exposure to 0.5 μM arsenic for 28 days and in the hippocampi collected from adult mice exposed to 100 ppb arsenic for five weeks.

Arsenic reduces neurite length in mature MNs

To further assess the morphological alterations observed in mature MNs following arsenic exposure for 28 days, neurite tracing analysis was conducted. Several studies conducted *in vivo* and *in vitro* have reported decreased neurite length following arsenic exposure. For instance, neurite length was significantly reduced by 1 μM sodium arsenite in primary cultured neurons (Maekawa et al., 2013) by 5 μM sodium arsenite and 0.5 μM arsenic trioxide in Neuro-2a cells (Wang et al., 2010; Aung et al., 2013), and by 5 μM sodium arsenite in differentiated neurons derived from mouse embryonic forebrains (Li et al., 2018). Similarly, treatment with sodium arsenite caused a dose-dependent inhibition of neurite length in differentiated human neuroblastoma SH-SY5Y cells

(Niyomchan et al., 2015). Additionally, neurite length reduction has been observed in mice following prenatal exposure to sodium arsenite from gestational day 8 to 18 (Aung et al., 2016). Consistently, our results show that following arsenic exposure, the length of MAP2+ neurites was reduced in day 28 MNs.

Conclusion

Exposure to 0.5 μ M arsenic during motor neuron differentiation impaired the cholinergic pathway. Downregulation of genes involved in acetylcholine synthesis (*CHAT*), transport (*SLC18A3* and *SLC5A7*) and degradation (*ACHE*) along with reduced ChAT protein expression and neurite outgrowth suggest that proper function of cholinergic neurons might be impaired following arsenic exposure. Taken together, these results suggest that arsenic-induced impairment of cholinergic functions could be responsible for the memory and learning deficits along with the locomotor and neurological alterations reported by epidemiological and *in vivo* studies.

Acknowledgements

This work was supported by National Institute of Environmental Health Sciences (ES027651), the National Institute of General Medical Sciences through SCBioCRAFT (GM131959), and 2021 BSPDC-GIAR. We thank Rhonda Reigers Powell and Justin Scott from the Clemson Light Imaging Facility (CLIF) for assistance with the confocal microscopy and flow cytometry analysis. CLIF is supported by funds from the Clemson University Division of Research and the National Institute of General Medical Sciences (GM146584). The authors thank Victoria Riley for assistance with the Sholl analysis and Dr. Aidan Sokolov for assistance with hippocampi collection.

References

- Ambrosio, F., Brown, E., Stolz, D., Ferrari, R., Goodpaster, B., Deasy, B., Distefano, G., Roperti, A., Cheikhi, A., Garciafigueroa, Y., Barchowsky, A., 2014. Arsenic induces sustained impairment of skeletal muscle and muscle progenitor cell ultrastructure and bioenergetics. *Free Radic. Biol. Med.* 74, 64-73.
- Arvidsson, U., Riedl, M., Elde, R., Meister, B., 1997. Vesicular acetylcholine transporter (VACHT) protein: a novel and unique marker for cholinergic neurons in the central and peripheral nervous systems. *J. Comp. Neurol.* 378, 454-467.
- Aubert, J., Stavridis, M.P., Tweedie, S., O'Reilly, M., Vierlinger, K., Li, M., Ghazal, P., Pratt, T., Mason, J.O., Roy, D., Smith, A., 2003. Screening for mammalian neural genes via fluorescence-activated cell sorter purification of neural precursors from Sox1-gfp knock-in mice. *Proc. Natl. Acad. Sci. U. S. A.* 100 Suppl 1, 11836-11841.
- Aung, K.H., Kurihara, R., Nakashima, S., Maekawa, F., Nohara, K., Kobayashi, T., Tsukahara, S., 2013. Inhibition of neurite outgrowth and alteration of cytoskeletal gene expression by sodium arsenite. *Neurotoxicology* 34, 226-235.
- Aung, K.H., Kyi-Tha-Thu, C., Sano, K., Nakamura, K., Tanoue, A., Nohara, K., Kakeyama, M., Tohyama, C., Tsukahara, S., Maekawa, F., 2016. Prenatal Exposure to Arsenic Impairs Behavioral Flexibility and Cortical Structure in Mice. *Front. Neurosci.* 10, 137.
- Ayotte, J.D., Medalie, L., Qi, S.L., Backer, L.C., Nolan, B.T., 2017. Estimating the High-Arsenic Domestic-Well Population in the Conterminous United States. *Environ. Sci. Technol.* 51, 12443-12454.
- Bain, L.J., Liu, J.T., League, R.E., 2016. Arsenic inhibits stem cell differentiation by altering the interplay between the Wnt3a and Notch signaling pathways. *Toxicol. Rep.* 3, 405-413.
- Beeravolu, N., McKee, C., Chaudhry, G.R. 2017. Mechanism of arsenite toxicity in embryonic stem cells. *J Appl Toxicol.*;37(10):1151-1161.
- Bhattacharya, P., Hossain, M., Rahman, S.N., Robinson, C., Nath, B., Rahman, M., Islam, M.M., Von Bromssen, M., Ahmed, K.M., Jacks, G., Chowdhury, D., Rahman, M., Jakariya, M., Persson, L.A., Vahter, M., 2011. Temporal and seasonal variability of arsenic in drinking water wells in Matlab, southeastern Bangladesh: a preliminary evaluation on the basis of a 4 year study. *J. Environ. Sci. Health. A. Tox. Hazard. Subst. Environ. Eng.* 46, 1177-1184.
- Bjorklund, G., Tippairote, T., Rahaman, M.S., Aaseth, J., 2020. Developmental toxicity of arsenic: a drift from the classical dose-response relationship. *Arch. Toxicol.* 94, 67-75.
- Bundschuh, J., Armienta, M.A., Birkle, P., Bhattacharya, P., Matschullat, A.B., Mukherjee, A.B. (2009). *Natural Arsenic in Groundwater of Latin America — Occurrence, health impact and remediation.* CRC Press.

- Bushnell, B. 2014. BBMap: A Fast, Accurate, Splice-Aware Aligner. United States. <https://www.osti.gov/servlets/purl/1241166>.
- Chandravanshi, L.P., Gupta, R., Shukla, R.K., 2019. Arsenic-Induced Neurotoxicity by Dysfunctioning Cholinergic and Dopaminergic System in Brain of Developing Rats. *Biol. Trace Elem. Res.* 189, 118-133.
- Chattopadhyay, S., Bhaumik, S., Nag Chaudhury, A., Das Gupta, S., 2002. Arsenic induced changes in growth development and apoptosis in neonatal and adult brain cells in vivo and in tissue culture. *Toxicol. Lett.* 128, 73-84.
- Chen, H., Yuh, C., Wu, K.K., 2010. Nestin is essential for zebrafish brain and eye development through control of progenitor cell apoptosis. *PLoS one* 5, e9318.
- Cheung, W.M.W., Chu, P.W.K., Kwong, Y.L., 2007. Effects of arsenic trioxide on the cellular proliferation, apoptosis and differentiation of human neuroblastoma cells. *Cancer Lett.* 246, 122-128.
- Chou, C., Lin, H., Hwang, P., Wang, S., Hsieh, C., Hwang, D., 2015. Taurine resumed neuronal differentiation in arsenite-treated N2a cells through reducing oxidative stress, endoplasmic reticulum stress, and mitochondrial dysfunction. *Amino Acids* 47, 735-744.
- Choudhary, P., Armstrong, E.J., Jorgensen, C.C., Piotrowski, M., Barthmes, M., Torella, R., Johnston, S.E., Maruyama, Y., Janiszewski, J.S., Storer, R.I., Skerratt, S.E., Benn, C.L., 2017. Discovery of Compounds that Positively Modulate the High Affinity Choline Transporter. *Frontiers in Molecular Neuroscience*, n/a.
- Concha, G., Vogler, G., Lezcano, D., Nermell, B., Vahter, M., 1998. Exposure to inorganic arsenic metabolites during early human development. *Toxicol. Sci.* 44, 185-190.
- Deng, W., Aimone, J.B., Gage, F.H., 2010. New neurons and new memories: how does adult hippocampal neurogenesis affect learning and memory? *Nature reviews.Neuroscience* 11, 339-350.
- Deutch, A.Y., Roth, R.H., 2004. Chapter 9 – Pharmacology and biochemistry of synaptic transmission: classic transmitters. *From Molecules to Networks*: 245-278.
- Dobin, A., Davis, C.A., Schlesinger, F., Drenkow, J., Zaleski, C., Jha, S., Batut, P., Chaisson, M., Gingeras, T.R., 2013. STAR: ultrafast universal RNA-seq aligner. *Bioinformatics* 29, 15-21.
- do Valle, I.B., Gomes, N.A., Diniz, I.M.A., de Arruda, J.A.A., Almeida, T.F.A., Santos, M.S., Birbrair, A., von Zeidler, S.V., Silva, T.A., 2022. Nestin and Neuron-gliial antigen 2 transgenes unveil progenitor units in murine salivary glands. *Arch. Oral Biol.* 134, 105344.
- Drobna, Z., Walton, F.S., Paul, D.S., Xing, W., Thomas, D.J., Styblo, M., 2010. Metabolism of arsenic in human liver: the role of membrane transporters. *Arch. Toxicol.* 84, 3-16.

- Du, Z., Chen, H., Liu, H., Lu, J., Qian, K., Huang, C., Zhong, X., Fan, F., Zhang, S., 2015. Generation and expansion of highly pure motor neuron progenitors from human pluripotent stem cells. *Nature communications* 6, 6626.
- Feng, N., Han, Q., Li, J., Wang, S., Li, H., Yao, X., Zhao, R.C., 2014. Generation of highly purified neural stem cells from human adipose-derived mesenchymal stem cells by Sox1 activation. *Stem cells and development* 23, 515-529.
- Fisher, S.K., Wonnacott, S., 2012. Chapter 13 – Acetylcholine. *Basic neurochemistry* (eight edition): 258-282.
- Frankel, S., Concannon, J., Brusky, K., Pietrowicz, E., Giorgianni, S., Thompson, W.D., Currie, D.A., 2009. Arsenic exposure disrupts neurite growth and complexity in vitro. *Neurotoxicology* 30, 529-537.
- Frankish, A., Diekhans, M., Ferreira, A.M., Johnson, R., Jungreis, I., Loveland, J. et. al. 2019. GENCODE reference annotation for the human and mouse genomes. *Nucleic Acids Res.*;47(D1):D766-D773.
- Haam, J., Yakel, J.L., 2017. Cholinergic modulation of the hippocampal region and memory function. *J. Neurochem.* 142 Suppl 2, 111-121.
- Haam, J., Zhou, J., Cui, G., Yakel, J.L., 2018. Septal cholinergic neurons gate hippocampal output to entorhinal cortex via oriens lacunosum moleculare interneurons. *Proc. Natl. Acad. Sci. U. S. A.* 115, E1886-E1895.
- Hall, M., Gamble, M., Slavkovich, V., Liu, X., Levy, D., Cheng, Z., van Geen, A., Yunus, M., Rahman, M., Pilsner, J.R., Graziano, J., 2007. Determinants of arsenic metabolism: blood arsenic metabolites, plasma folate, cobalamin, and homocysteine concentrations in maternal-newborn pairs. *Environ. Health Perspect.* 115, 1503-1509.
- Hamadani, J.D., Tofail, F., Nermell, B., Gardner, R., Shiraji, S., Bottai, M., Arifeen, S.E., Huda, S.N., Vahter, M., 2011. Critical windows of exposure for arsenic-associated impairment of cognitive function in pre-school girls and boys: a population-based cohort study. *Int. J. Epidemiol.* 40, 1593-1604.
- Hampel, H., Mesulam, M., Cuello, A.C., Farlow, M.R., Giacobini, E., Grossberg, G.T., Khachaturian, A.S., Vergallo, A., Cavedo, E., Snyder, P.J., Khachaturian, Z.S., 2018. The cholinergic system in the pathophysiology and treatment of Alzheimer's disease. *Brain : a journal of neurology* 141, 1917-1933.
- Harada, A., Teng, J., Takei, Y., Oguchi, K., Hirokawa, N., 2002. MAP2 is required for dendrite elongation, PKA anchoring in dendrites, and proper PKA signal transduction. *J. Cell Biol.* 158, 541-549.
- Henn, B.C., Ettinger, A. S., Hopkins, M. R., Jim, R., Amarasiriwardena, C., Christiani, D. C., . . . Wright, R. O. (2016). Prenatal arsenic exposure and birth outcomes among a population

- residing near a mining-related superfund site. *Environmental Health Perspectives*, 124(8), 1308-1315.
- Hong, G.M., Bain, L.J., 2012. Sodium arsenite represses the expression of myogenin in C2C12 mouse myoblast cells through histone modifications and altered expression of Ezh2, Glp, and Igf-1. *Toxicol. Appl. Pharmacol.* 260, 250-259.
- Jahan, S., Ansari, U.A., Siddiqui, A.J., Iqbal, D., Khan, J., Banawas, S., Alshehri, B., Alshahrani, M.M., Alsagaby, S.A., Redhu, N.S., Pant, A.B., 2022. Nobiletin Ameliorates Cellular Damage and Stress Response and Restores Neuronal Identity Altered by Sodium Arsenate Exposure in Human iPSCs-Derived hNPCs. *Pharmaceuticals (Basel, Switzerland)* 15.
- Jatko, J.T., Darling, C.L., Kellett, M.P., Bain, L.J., 2021. Arsenic exposure in drinking water reduces *Lgr5* and secretory cell marker gene expression in mouse intestines. *Toxicol. Appl. Pharmacol.* 422, 115561.
- Jung, H.S., Kim, H., Lee, M., Shin, H.Y., Ahn, H.S., Ryu, K., Seoh, J., Kim, C.J., Jang, J.J., 2006. Arsenic trioxide concentration determines the fate of Ewing's sarcoma family tumors and neuroblastoma cells in vitro. *FEBS Lett.* 580, 4969-4975.
- Kolde, R. 2012. Pheatmap: pretty heatmaps. R package version 1.2: 747.
- Krishnasamy, S., Weng, Y., Thammisetty, S.S., Phaneuf, D., Lalancette-Hebert, M., Kriz, J., 2017. Molecular imaging of nestin in neuroinflammatory conditions reveals marked signal induction in activated microglia. *Journal of neuroinflammation* 14, 45.
- Laga, A.C., Zhan, Q., Weishaupt, C., Ma, J., Frank, M.H., Murphy, G.F., 2011. SOX2 and nestin expression in human melanoma: an immunohistochemical and experimental study. *Exp. Dermatol.* 20, 339-345.
- Li, M., Zhao, X., Wang, W., Shi, H., Pan, Q., Lu, Z., Sonia Peña Perez, Suganthan, R., He, C., Bjørås, M., Klungland, A., 2018. Ythdf2-mediated m6A mRNA clearance modulates neural development in mice. *Genome Biol.* 19, n/a.
- Liao, Y., Smyth, G.K., Shi, W., 2014. featureCounts: an efficient general purpose program for assigning sequence reads to genomic features. *Bioinformatics* 30, 923-930.
- Liu, J.T., Bain, L.J., 2014. Arsenic inhibits hedgehog signaling during P19 cell differentiation. *Toxicol. Appl. Pharmacol.* 281, 243-253.
- Liu, S., Piao, F., Sun, X., Bai, L., Peng, Y., Zhong, Y., Ma, N., Sun, W., 2012. Arsenic-induced inhibition of hippocampal neurogenesis and its reversibility. *Neurotoxicology* 33, 1033-1039.
- Liu, W., Zhou, H., Liu, L., Zhao, C., Deng, Y., Chen, L., Wu, L., Mandrycky, N., McNabb, C.T., Peng, Y., Fuchs, P.N., Lu, J., Sheen, V., Qiu, M., Mao, M., Lu, Q.R., 2015. Disruption of neurogenesis and cortical development in transgenic mice misexpressing *Olig2*, a gene in the Down syndrome critical region. *Neurobiol. Dis.* 77, 106-116.

- Love, M.I., Huber, W., Anders, S., 2014. Moderated estimation of fold change and dispersion for RNA-seq data with DESeq2. *Genome Biol.* 15, 550-014-0550-8.
- Lu, J., Lian, G., Zhou, H., Esposito, G., Steardo, L., Delli-Bovi, L.C., Hecht, J.L., Lu, Q.R., Sheen, V., 2012. OLIG2 over-expression impairs proliferation of human Down syndrome neural progenitors. *Hum. Mol. Genet.* 21, 2330-2340.
- Luo, W., Li, S., Peng, B., Ye, Y., Deng, X., Yao, K., 2013. Embryonic Stem Cells Markers SOX2, OCT4 and Nanog Expression and Their Correlations with Epithelial-Mesenchymal Transition in Nasopharyngeal Carcinoma. *PLoS One* 8, e56324.
- Maekawa, F., Tsuboi, T., Oya, M., Aung, K.H., Tsukahara, S., Pellerin, L., Nohara, K., 2013. Effects of sodium arsenite on neurite outgrowth and glutamate AMPA receptor expression in mouse cortical neurons. *Neurotoxicology* 37, 197-206.
- Maurer, S.V., Williams, C.L., 2017. The Cholinergic System Modulates Memory and Hippocampal Plasticity via Its Interactions with Non-Neuronal Cells. *Frontiers in immunology* 8, 1489.
- McCoy, C.R., Stadelman, B.S., Brumaghim, J.L., Liu, J.T., Bain, L.J., 2015. Arsenic and Its Methylated Metabolites Inhibit the Differentiation of Neural Plate Border Specifier Cells. *Chem. Res. Toxicol.* 28, 1409-1421.
- McMichael, B.D., Perego, M.C., Darling, C.L., Perry, R.L., Coleman, S.C., Bain, L.J., 2020. Long-term arsenic exposure impairs differentiation in mouse embryonal stem cells. *J. Appl. Toxicol.* .
- Mochizuki, H., 2019. Arsenic Neurotoxicity in Humans. *Int. J. Mol. Sci.* 20, 10.3390/ijms20143418.
- Morrison, J.H., Hof, P.R., Huntley, G.W. (1998). Chapter II – Neurochemical organization of the primate visual cortex. *Handbook of Chemical Neuroanatomy*, 14: 299-430.
- Nishimaru, H., Restrepo, C.E., Ryge, J., Yanagawa, Y., Kiehn, O., 2005. Mammalian motor neurons corelease glutamate and acetylcholine at central synapses. *Proc. Natl. Acad. Sci. U. S. A.* 102, 5245-5249.
- Niyomchan, A., Watcharasit, P., Visitnonthachai, D., Homkajorn, B., Thiantanawat, A., Satayavivad, J., 2015. Insulin attenuates arsenic-induced neurite outgrowth impairments by activating the PI3K/Akt/SIRT1 signaling pathway. *Toxicol. Lett.* 236, 138-144.
- Niyomchan, A., Visitnonthachai, D., Suntararuks, S., Ngamsiri, P., Watcharasit, P., Satayavivad, J., 2018. Arsenic impairs insulin signaling in differentiated neuroblastoma SH-SY5Y cells. *Neurotoxicology* 66, 22-31.
- Ortega, J.A., Radonjic, N.V., Zecevic, N., 2013. Sonic hedgehog promotes generation and maintenance of human forebrain Olig2 progenitors. *Frontiers in Cellular Neuroscience* , n/a.

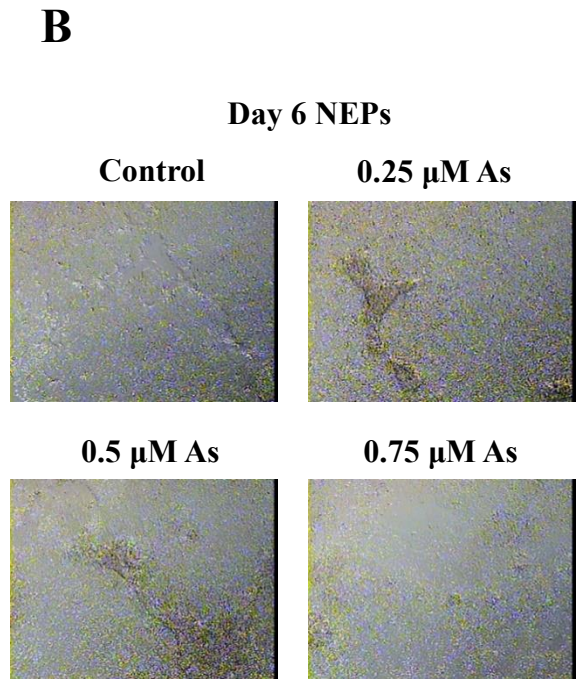
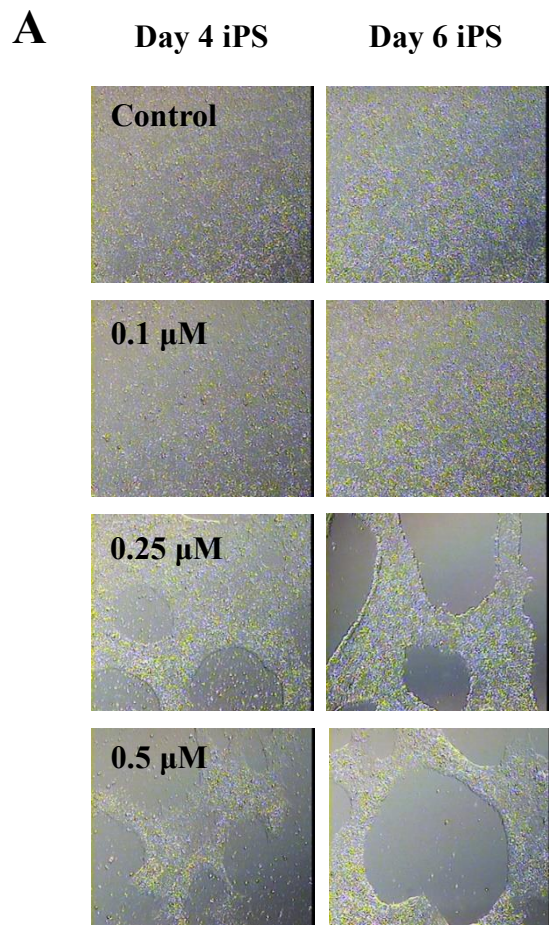
- Pandey Rukmani, Garg Asmita, Gupta Keerti, Shukla Pallavi, Mandrah Kapil, Somendu, R., Chattopadhyay Naibedya, Bandyopadhyay Sanghamitra, 2022. Arsenic Induces Differential Neurotoxicity in Male, Female, and E2-Deficient Females: Comparative Effects on Hippocampal Neurons and Cognition in Adult Rats. *Mol. Neurobiol.* 59, 2729-2744.
- Park, S.M., Jo, N.R., Lee, B., Jung, E., Lee, S.D., Jeung, E., 2021. Establishment of a developmental neurotoxicity test by Sox1-GFP mouse embryonic stem cells. *Reprod. Toxicol.* 104, 96-105.
- Petit, A., Delaune, A., Falluel-Morel, A., Goullé, J., Vannier, J., Dubus, I., Vasse, M., 2013. Importance of ERK activation in As₂O₃-induced differentiation and promyelocytic leukemia nuclear bodies formation in neuroblastoma cells. *Pharmacological research* 77, 11-21.
- Picciotto, M.R., Higley, M.J., Mineur, Y.S., 2012. Acetylcholine as a neuromodulator: cholinergic signaling shapes nervous system function and behavior. *Neuron* 76, 116-129.
- Power, A.E., 2004. Slow-wave sleep, acetylcholine, and memory consolidation. *Proc. Natl. Acad. Sci. U. S. A.* 101, 1795-1796.
- Ravenscroft, P., Brammer, H., Richards, K. (2009). *Arsenic Pollution—A Global Synthesis*. Wiley-Blackwell; Oxford, UK.
- Rodriguez, V.M., Carrizales, L., Mendoza, M.S., Fajardo, O.R., Giordano, M., 2002. Effects of sodium arsenite exposure on development and behavior in the rat. *Neurotoxicol. Teratol.* 24, 743-750.
- Sagner, A., Gaber, Z.B., Delile, J., Kong, J.H., Rousso, D.L., Pearson, C.A., Weicksel, S.E., Melchionda, M., Mousavy Gharavy, S.N., Briscoe, J., Novitch, B.G., 2018. Olig2 and Hes regulatory dynamics during motor neuron differentiation revealed by single cell transcriptomics. *PLoS biology* 16, e2003127.
- Sánchez, C., Díaz-Nido, J., Avila, J., 2000. Phosphorylation of microtubule-associated protein 2 (MAP2) and its relevance for the regulation of the neuronal cytoskeleton function. *Prog. Neurobiol.* 61, 133-168.
- Sánchez-Díaz, G., Escobar, F., Badland, H., Arias-Merino, G., Manuel Posada de la Paz, Alonso-Ferreira, V., 2018. Geographic Analysis of Motor Neuron Disease Mortality and Heavy Metals Released to Rivers in Spain. *International Journal of Environmental Research and Public Health* 15, 2522.
- Schmittgen, T. D., & Livak, K. J. (2008). Analyzing real-time PCR data by the comparative C(T) method. *Nature Protocols*, 3(6), 1101-1108.
- Shankar, S., Shanker, U., Shikha, 2014. Arsenic contamination of groundwater: a review of sources, prevalence, health risks, and strategies for mitigation. *ScientificWorldJournal* 2014, 304524.

- Shors, T.J., Townsend, D.A., Zhao, M., Kozorovitskiy, Y., Gould, E. (2002). Neurogenesis may relate to some but not all types of hippocampal-dependent learning. *Hippocampus*, 12(5):578-84.
- Skogheim, T.S., Weyde, K.V.F., Engel, S.M., Aase, H., Suren, P., Oie, M.G., Biele, G., Reichborn-Kjennerud, T., Caspersen, I.H., Hornig, M., Haug, L.S., Villanger, G.D., 2021. Metal and essential element concentrations during pregnancy and associations with autism spectrum disorder and attention-deficit/hyperactivity disorder in children. *Environ. Int.* 152, 106468.
- Smith, A.H., Arroyo, A.P., Mazumder, D.N., Kosnett, M.J., Hernandez, A.L., Beeris, M., Smith, M.M., Moore, L.E., 2000. Arsenic-induced skin lesions among Atacameño people in Northern Chile despite good nutrition and centuries of exposure. *Environ. Health Perspect.* 108, 617-620.
- Solomon, E., Davis-Anderson, K., Hovde, B., Micheva-Viteva, S., Harris, J.F., Twary, S., Iyer, R., 2021. Global transcriptome profile of the developmental principles of in vitro iPSC-to-motor neuron differentiation. *BMC molecular and cell biology* 22, 13.
- States, J.C., Barchowsky, A., Cartwright, I.L., Reichard, J.F., Futscher, B.W., Lantz, R.C., 2011. Arsenic toxicology: translating between experimental models and human pathology. *Environ. Health Perspect.* 119, 1356-1363.
- Steinbaugh, M., Turner, S., Wolen, A. 2017. stephenturner/annotables: Ensembl 90 (v0.1.90). Zenodo. <https://doi.org/10.5281/zenodo.996854>
- Steffens, A.A., Hong, G.M., Bain, L.J., 2011. Sodium arsenite delays the differentiation of C2C12 mouse myoblast cells and alters methylation patterns on the transcription factor myogenin. *Toxicol. Appl. Pharmacol.* 250, 154-161.
- Stern, M., Gierse, A., Tan, S., Bicker, G., 2014. Human Ntera2 cells as a predictive in vitro test system for developmental neurotoxicity. *Archives of Toxicology. Archiv für Toxikologie* 88, 127-36.
- Stifani, N., 2014. Motor neurons and the generation of spinal motor neurons diversity. *Frontiers in Cellular Neuroscience*, n/a.
- Szu, J., Wojcinski, A., Jiang, P., Kesari, S., 2021. Impact of the Olig Family on Neurodevelopmental Disorders. *Frontiers in neuroscience* 15, 659601.
- Tanaka, S., Kamachi, Y., Tanouchi, A., Hamada, H., Jing, N., Kondoh, H., 2004. Interplay of SOX and POU factors in regulation of the Nestin gene in neural primordial cells. *Mol. Cell. Biol.* 24, 8834-8846.
- Toda, T., Parylak, S.L., Linker, S.B., Gage, F.H., 2019. The role of adult hippocampal neurogenesis in brain health and disease. *Mol. Psychiatry* 24, 67-87.
- Trang, A., Khandhar, P.B., 2022. Physiology, Acetylcholinesterase. StatPearls Publishing.

- Tyler, C.R., Allan, A.M., 2013. Adult hippocampal neurogenesis and mRNA expression are altered by perinatal arsenic exposure in mice and restored by brief exposure to enrichment. *PLoS One* 8, e73720.
- Vahter, M., 2002. Mechanisms of arsenic biotransformation. *Toxicology* 181-182, 211-217.
- von Ehrenstein, O.S., Guha Mazumder, D.N., Hira-Smith, M., Ghosh, N., Yuan, Y., Windham, G., Ghosh, A., Haque, R., Lahiri, S., Kalman, D., Das, S., Smith, A.H., 2006. Pregnancy outcomes, infant mortality, and arsenic in drinking water in West Bengal, India. *Am. J. Epidemiol.* 163, 662-669.
- Wang, A., Holladay, S.D., Wolf, D.C., Ahmed, S.A., Robertson, J.L., 2006. Reproductive and developmental toxicity of arsenic in rodents: a review. *Int. J. Toxicol.* 25, 319-331.
- Wang, B., Liu, J., Liu, B., Liu, X., Yu, X., 2018. Prenatal exposure to arsenic and neurobehavioral development of newborns in China. *Environ. Int.* 121, 421-427.
- Wang, X., Meng, D., Chang, Q., Pan, J., Zhang, Z., Chen, G., Ke, Z., Luo, J., Shi, X., 2010. Arsenic inhibits neurite outgrowth by inhibiting the LKB1-AMPK signaling pathway. *Environ. Health Perspect.* 118, 627-634.
- Wasserman, G.A., Liu, X., Loiacono, N.J., Kline, J., Factor-Litvak, P., van Geen, A., Mey, J.L., Levy, D., Abramson, R., Schwartz, A., Graziano, J.H., 2014. A cross-sectional study of well water arsenic and child IQ in Maine schoolchildren. *Environ. Health* 13, 23-069X-13-23.
- Wisessaowapak, C., Visitnonthachai, D., Watcharasit, P., Satayavivad, J., 2021a. Prolonged arsenic exposure increases tau phosphorylation in differentiated SH-SY5Y cells: The contribution of GSK3 and ERK1/2. *Environ. Toxicol. Pharmacol.* 84, 103626.
- Wisessaowapak, C., Watcharasit, P., Satayavivad, J., 2021b. Arsenic disrupts neuronal insulin signaling through increasing free PI3K-p85 and decreasing PI3K activity. *Toxicol. Lett.* 349, 40-50.
- Witzemann, V. (2007). Choline acetyltransferase. *xPharm: The comprehensive pharmacology reference.*
- Wolfe, S.W. (2017). Traumatic Brachial Plexus Injury. *Green's Operative Hand Surgery.*
- Wu, T., Hu, E., Xu, S., Chen, M., Guo, P., Dai, Z., Feng, T., Zhou, L., Tang, W., Zhan, L., Fu, X., Liu, S., Bo, X., Yu, G., 2021. clusterProfiler 4.0: A universal enrichment tool for interpreting omics data. *Innovation (N. Y)* 2, 100141.
- Xiong, L., Huang, J., Gao, Y., Gao, Y., Wu, C., He, S., Zou, L., Yang, D., Han, Y., Yuan, Q., Zheng, Z., Hu, G., 2021. Sodium arsenite induces spatial learning and memory impairment associated with oxidative stress and activates the Nrf2/PPAR γ pathway against oxidative injury in mice hippocampus. *Toxicology research* 10, 277-283.

- Yadav, R.S., Chandravanshi, L.P., Shukla, R.K., Sankhwar, M.L., Ansari, R.W., Shukla, P.K., Pant, A.B., Khanna, V.K., 2011. Neuroprotective efficacy of curcumin in arsenic induced cholinergic dysfunctions in rats. *Neurotoxicology* 32, 760-768.
- Yen, Y.P., Tsai, K.S., Chen, Y.W., Huang, C.F., Yang, R.S., Liu, S.H., 2010. Arsenic inhibits myogenic differentiation and muscle regeneration. *Environ. Health Perspect.* 118, 949-956.
- Yu, G., Wang, L.G., Han, Y., He, Q.Y., 2012. clusterProfiler: an R package for comparing biological themes among gene clusters. *OMICS* 16, 284-287.

Figures



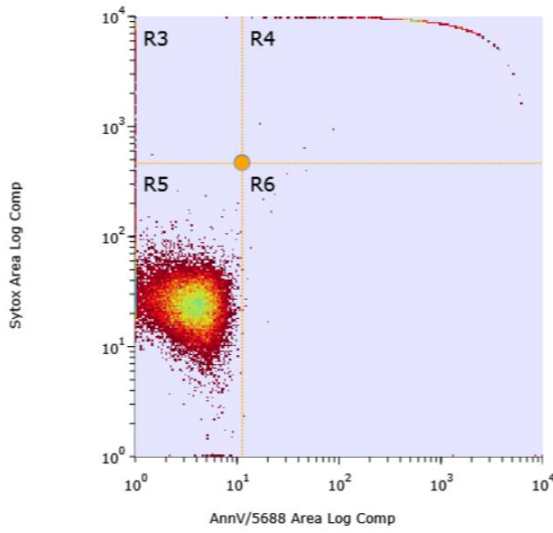
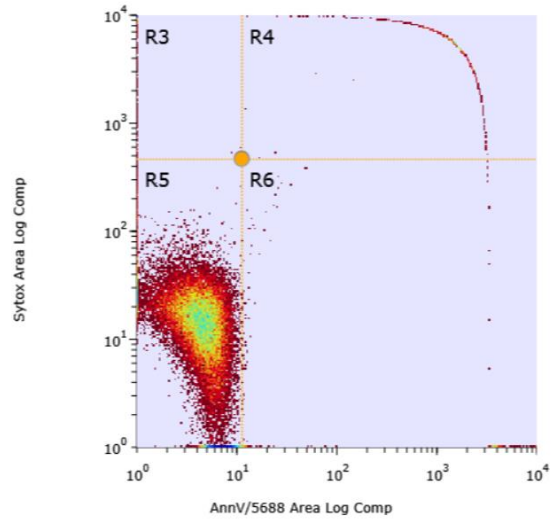
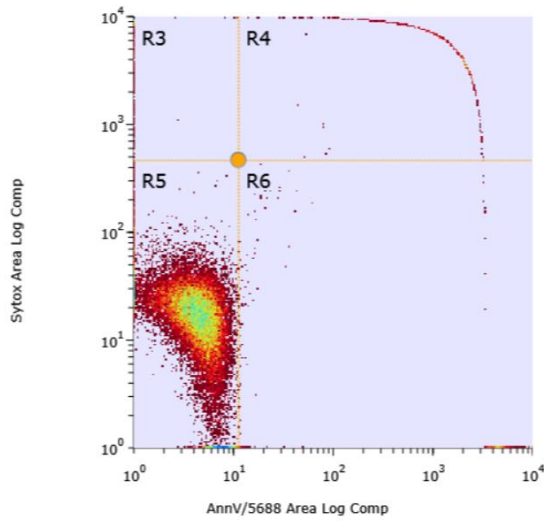
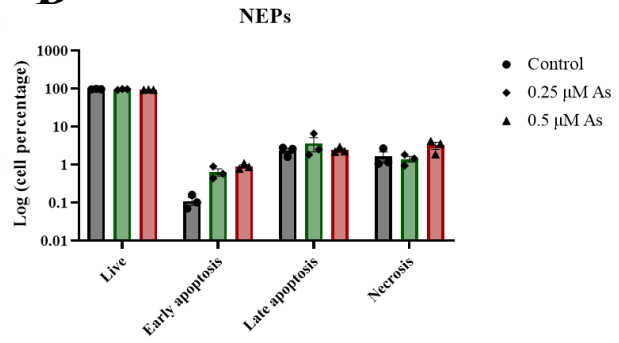
C**Control****0.25 μ M Arsenic****0.5 μ M Arsenic****D**

Figure 4.1. Low arsenic levels induce cell death in human iPS cells, but not in neuroepithelial progenitor cells (NEPs). (A) Representative images of human iPS cells exposed to 0, 0.1, 0.25 or 0.5 μM arsenic after four (left) and six (right) days. (B) Representative images of day 6 NEPs exposed to 0, 0.25, 0.5 or 0.75 μM arsenic. (C) Representative flow cytometry analysis of day 6 NEPs cells exposed to 0, 0.25 or 0.5 μM arsenic. Cells were stained with Annexin V and SyTox green to assess apoptosis. Percentage of live (R5), early apoptotic (R6), late apoptotic (R4) and necrotic (R3) cells is reported in each quadrant (D) Percentage of live, apoptotic, and necrotic NEPs cells exposed to 0, 0.25 or 0.5 μM arsenic ($n = 3$ per exposure group). Statistical differences were determined using two-way ANOVA followed by Tukey's multiple comparison test (*; $p \leq 0.05$).

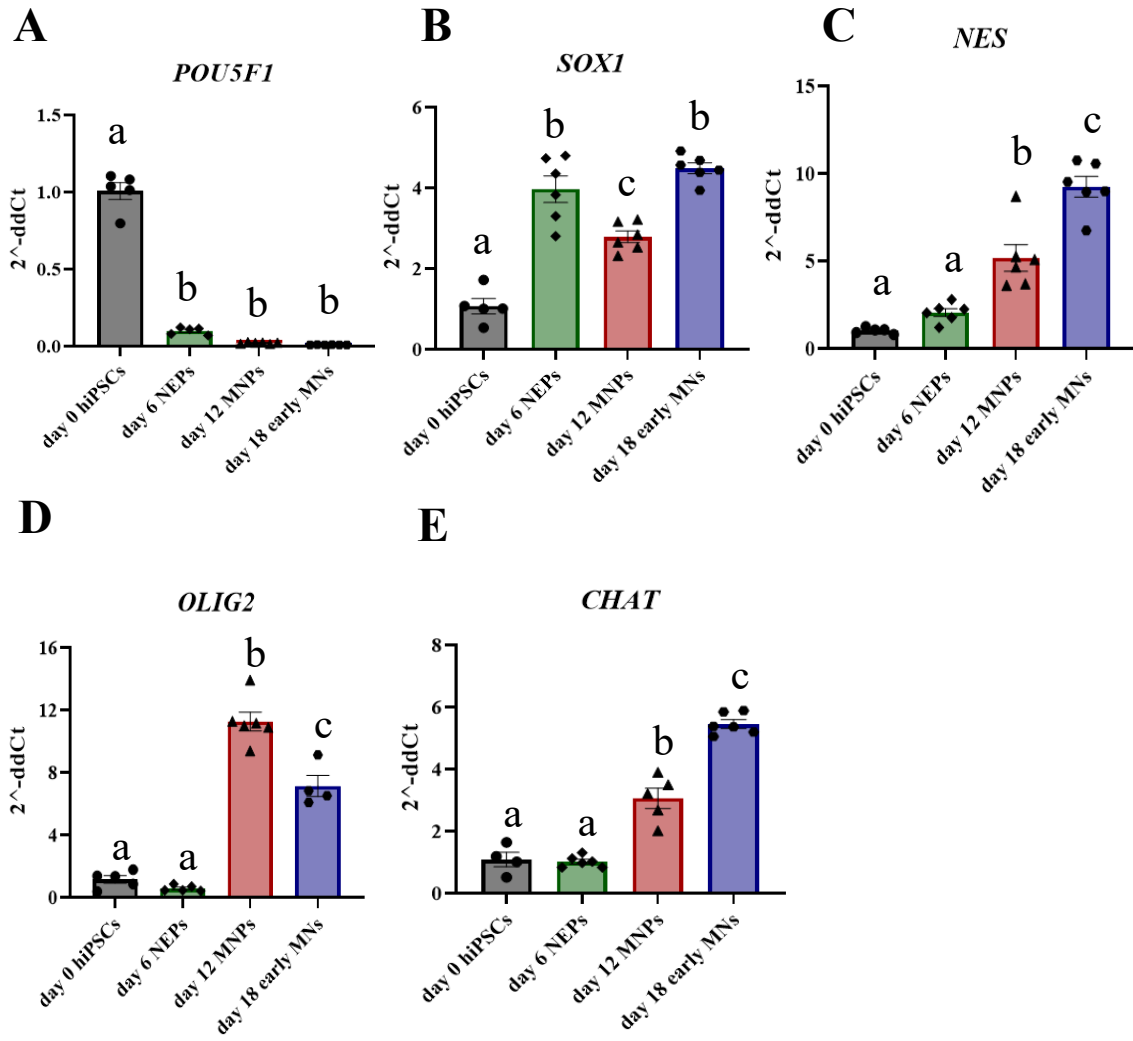
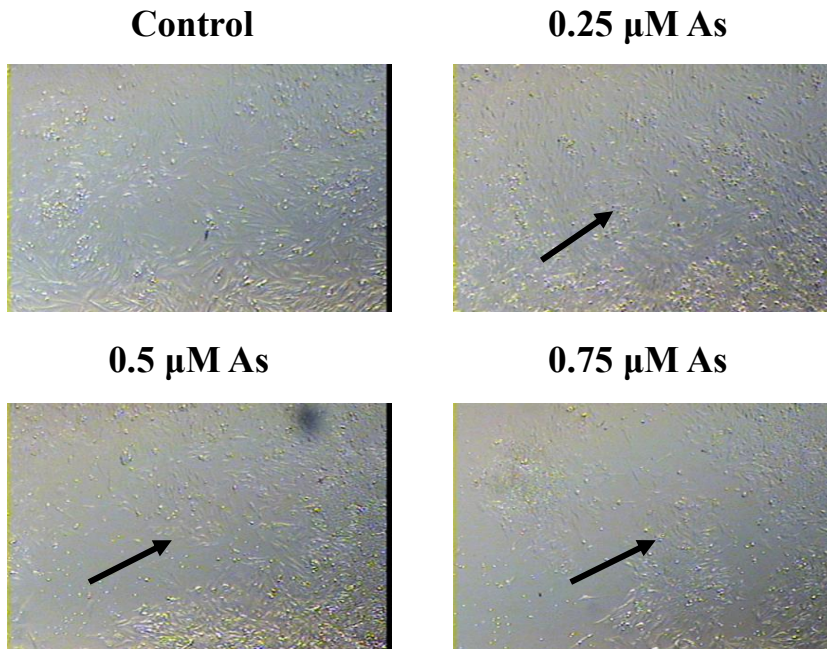
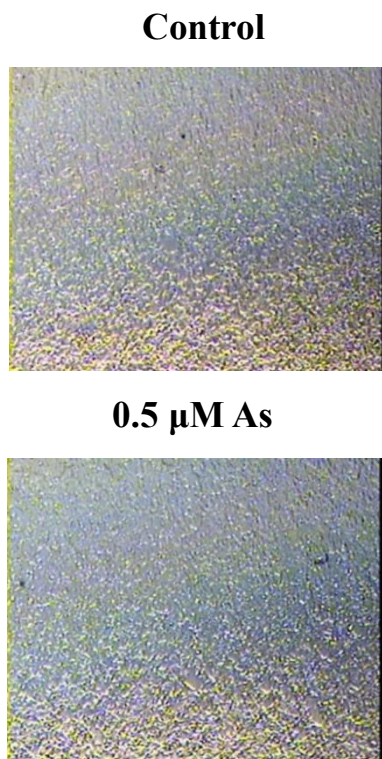


Figure 4.2. Differential gene expression of key markers during differentiation of human iPS cells into motor neurons. (A-E) Transcript levels of *POU5F1* (A), *SOX1* (B), *NES* (C), *OLIG2* (D) and *CHAT* (E) were assessed by qPCR in control samples from day 0 human iPS cells, day 6 NEPs, day 12 MNPs and day 18 early MNs. Fold change was determined using the ddCt method, and results were normalized to geometric mean of *Gapdh* and β 2-microglobulin. Statistical differences were determined using ANOVA followed by Tukey's multiple comparison test (*; $p \leq 0.05$) (n = 4-6 per exposure group).

A Day 12 MNPs



B Day 18 early MNs



C Day 28 mature MNs

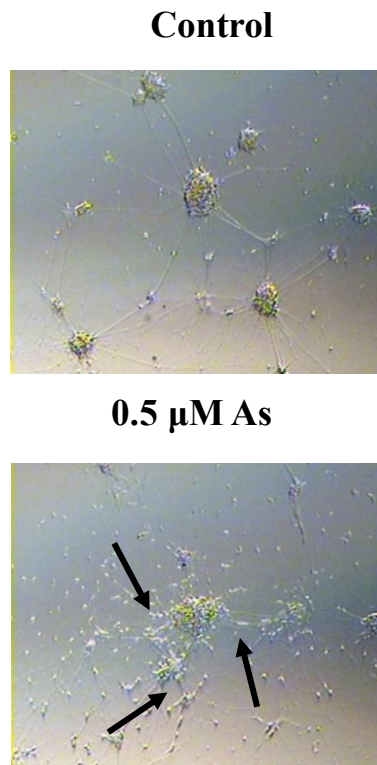
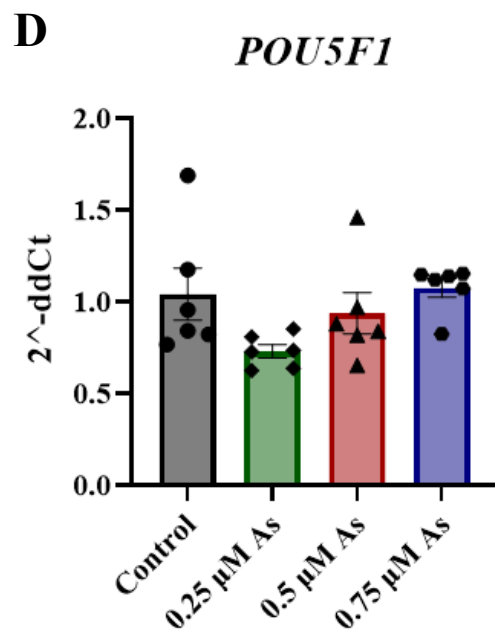
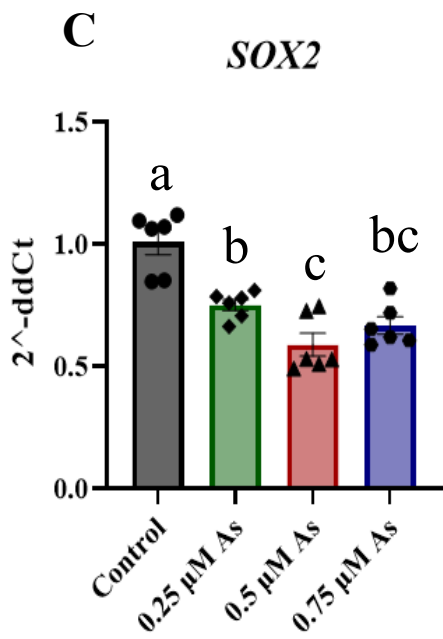
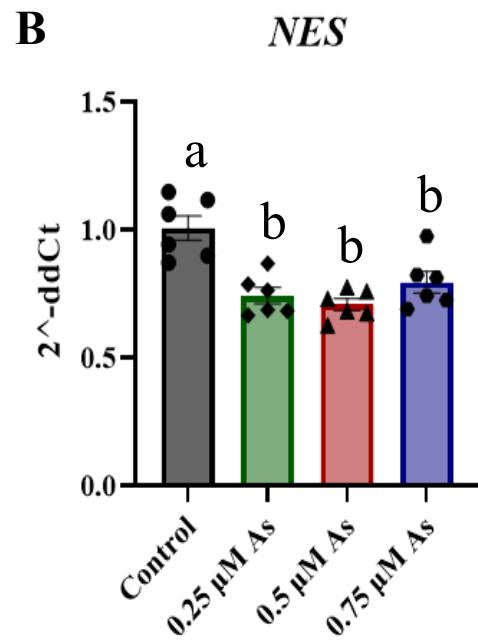
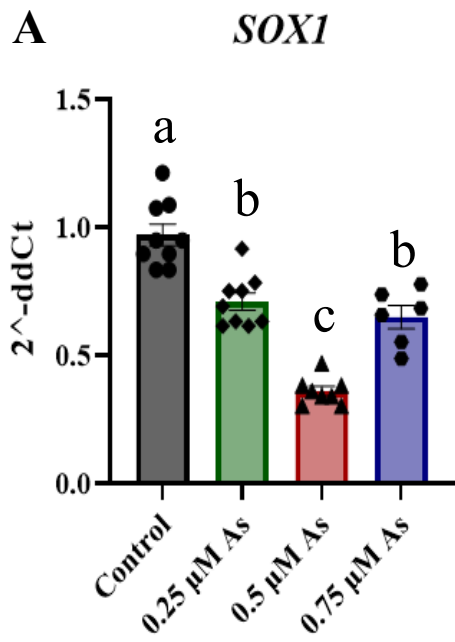


Figure 4.3. Arsenic exposure leads to morphological alterations of MNPs and mature MNs.

(A) Representative images of day 12 MNPs exposed to 0, 0.25, 0.5 or 0.75 μM arsenic. The arsenic-exposed MNPs have less concentric organization and fewer elongated MNPs (arrows). (B) Representative images of day 18 early MNs exposed to 0 or 0.5 μM arsenic. (C) Representative images of day 28 mature MNs exposed to 0 or 0.5 μM arsenic, showing reduced neurite length in the arsenic cells (arrows).



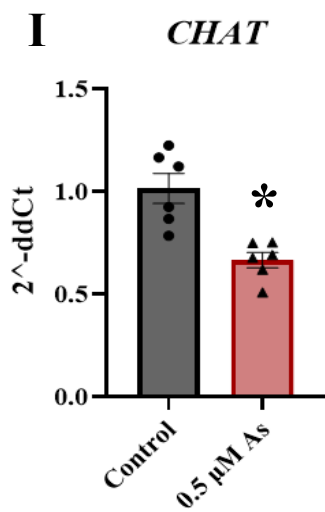
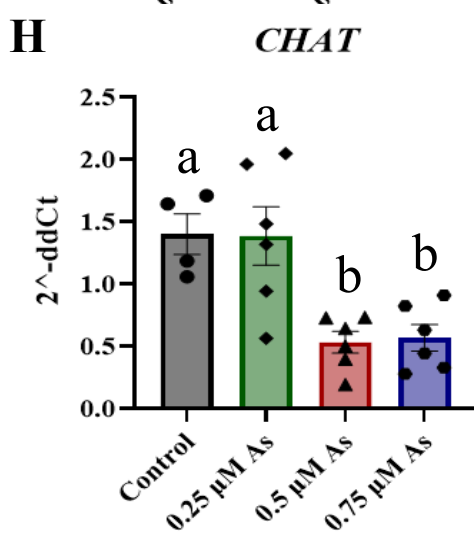
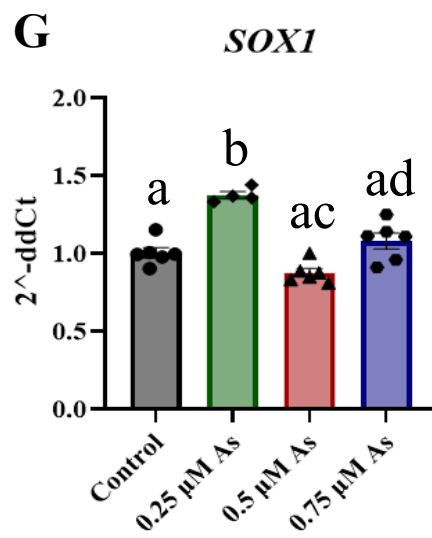
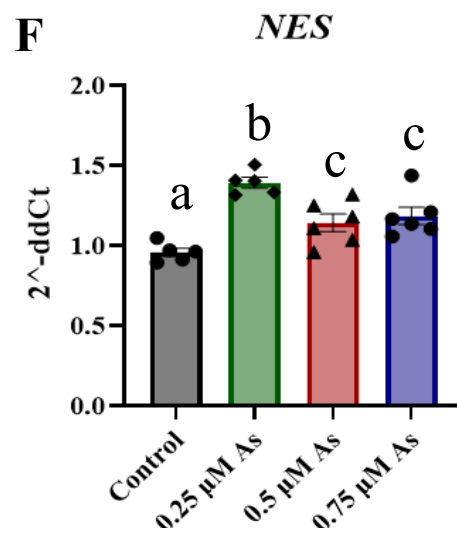
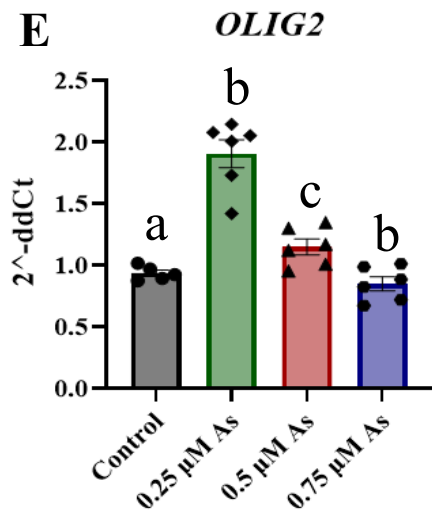
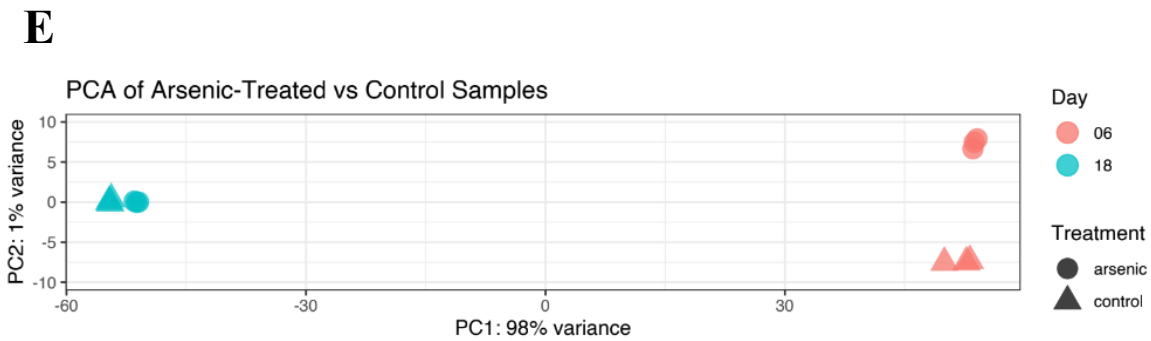
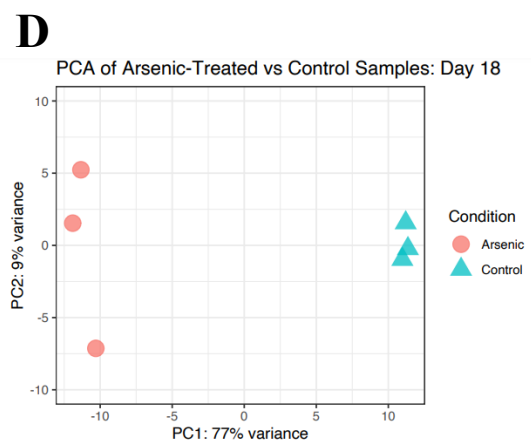
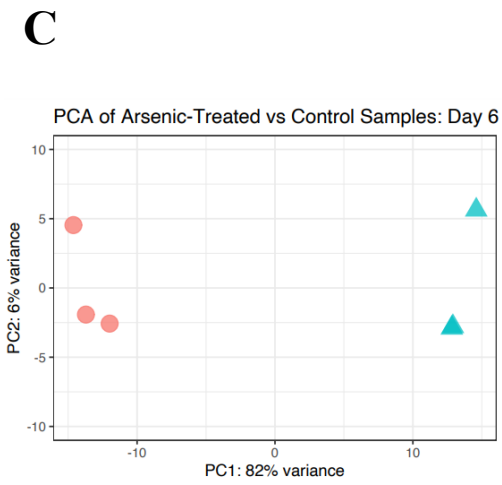
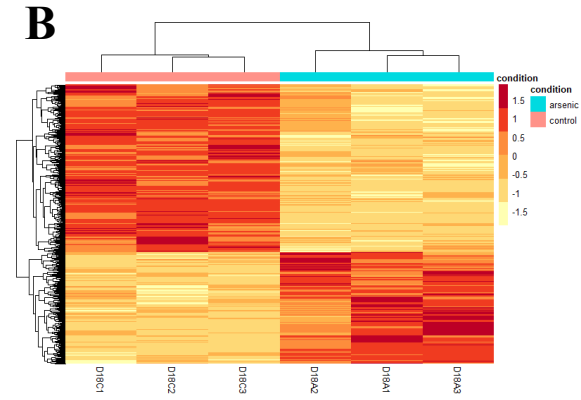
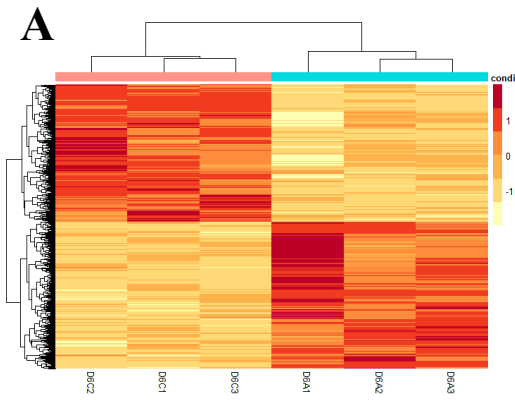
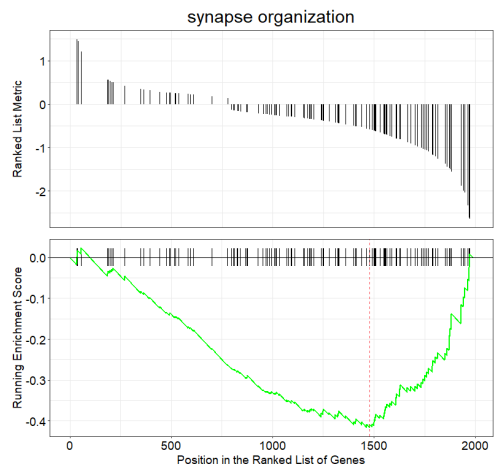
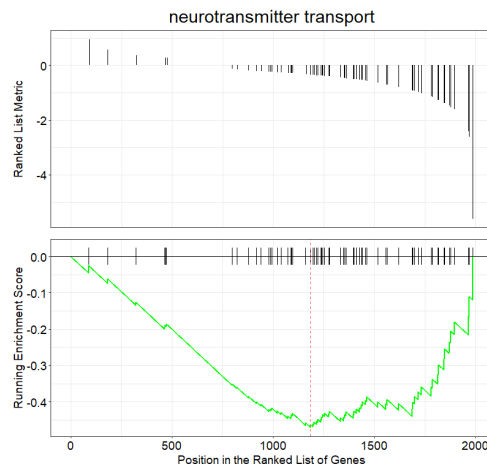
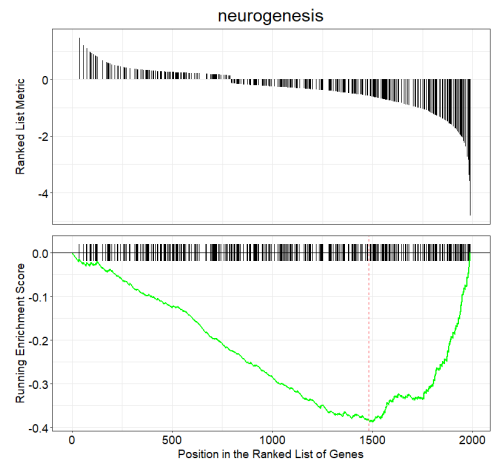
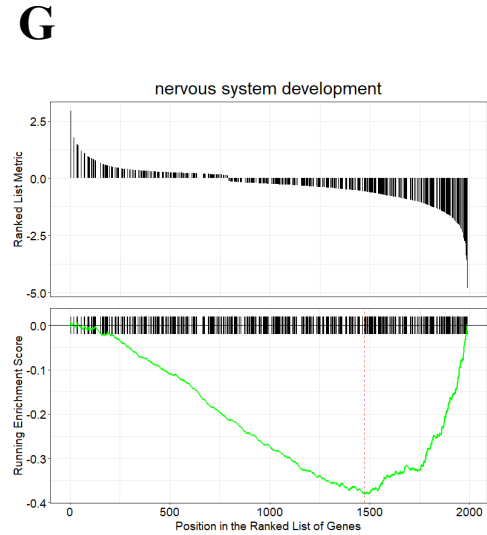
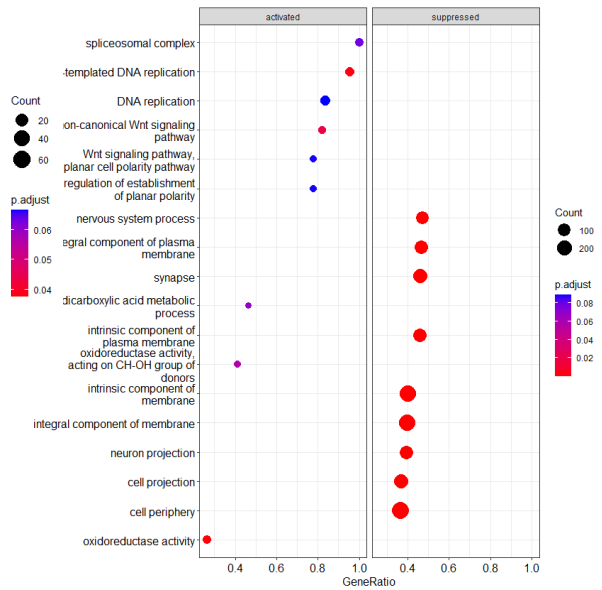
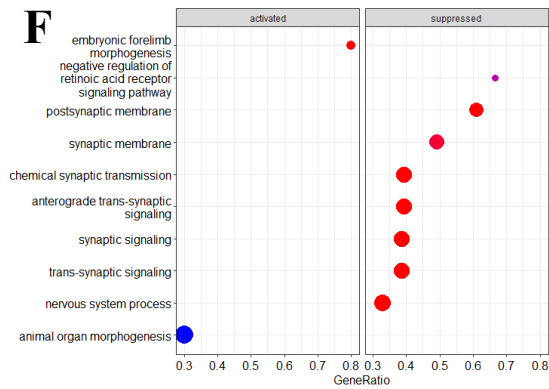


Figure 4.4. Arsenic exposure impairs transcript levels of motor neuron differentiation markers. (A-D) Transcript levels of *SOX1* (A), *NES* (B), *SOX2* (C) and *POU5F1* (D) were assessed in day 6 NEPs exposed to 0, 0.25, 0.5 or 0.75 μ M arsenic through qPCR analysis. (E-H) Transcript levels of *OLIG2* (E), *NES* (F), *SOX1* (G) and *CHAT* (H) were assessed in day 12 MNPs exposed to 0, 0.25, 0.5 or 0.75 μ M arsenic through qPCR analysis. (I) Transcript levels of *CHAT* were assessed in day 18 early MNs exposed to 0 or 0.5 μ M arsenic through qPCR analysis. Fold change was determined using the ddCt method and results were normalized to geometric mean of Gapdh and β 2-microglobulin. Statistical differences were determined using ANOVA followed by Tukey's multiple comparison test (*; $p \leq 0.05$) (n = 4-6 per exposure group).





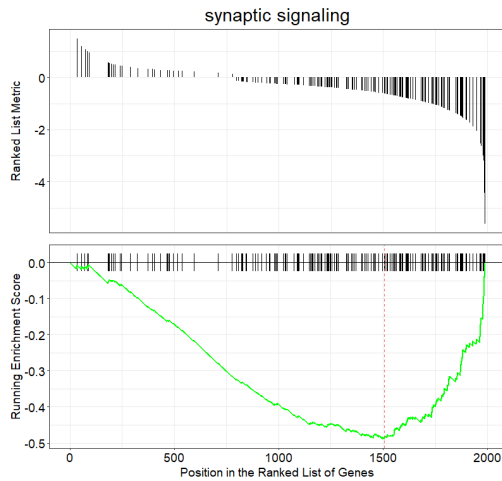


Figure 4.5. Arsenic exposure drives sample clustering in NEPs and early MNs, and disrupts biological processes related to nervous system development and synapses. (A-B) Heat map of normalized read counts of differentially expressed genes (DEGs) from day 6 NEPs (A) and day 18 early MNs (B) exposed to 0 (pink bars) or 0.5 μM arsenic (blue bars). (C-E) Principal component analysis (PCA) from day 6 NEPs (C), day 18 early MNs (D) and both day 6 NEPs and day 1 early MNs (E) exposed to 0 or 0.5 μM arsenic. The distance between the samples represents the differences in gene expression profile ($n = 3$ per exposure group). (F) Dot plot representing gene set enrichment analysis (GSEA) performed on DEGs of arsenic-treated day 6 NEPs (left) and day 18 early MNs (right). Dot plot shows activated and suppressed GO categories. (G) GSEA performed on DEGs of day 18 early MNs. Gene sets for nervous system development, neurogenesis, neurotransmitter transport, synapse organization and synaptic signaling were significantly enriched in day 18 MNs exposed to arsenic. The vertical black lines present on the x-axis represent the genes while the y-axis identified the enrichment score. Significance threshold was set at $\text{FDR} \leq 0.05$.

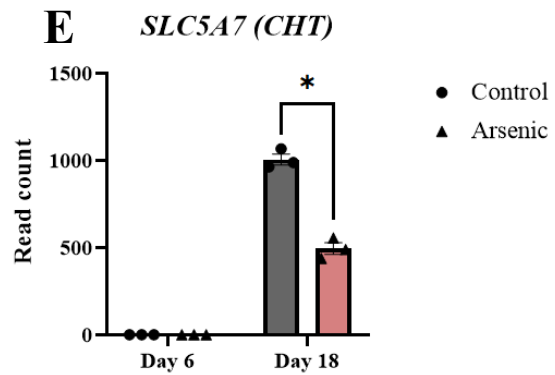
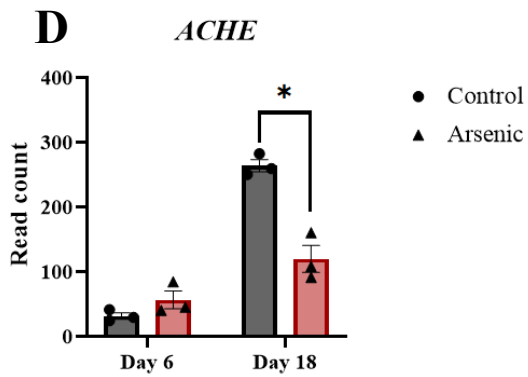
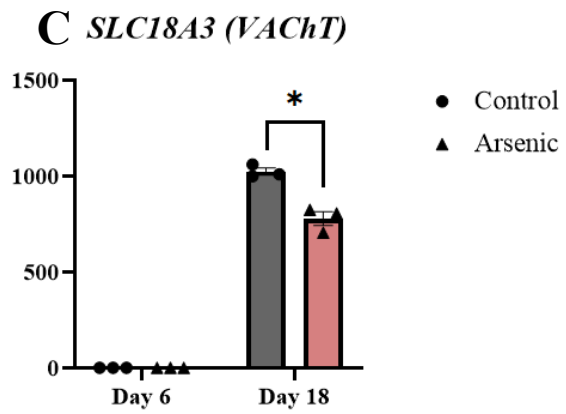
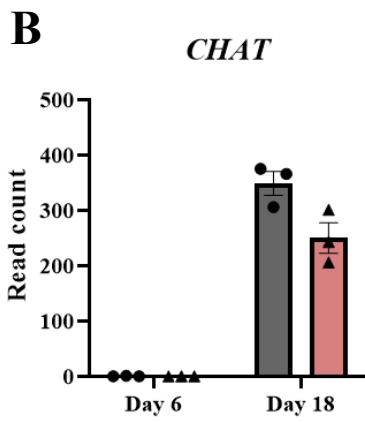
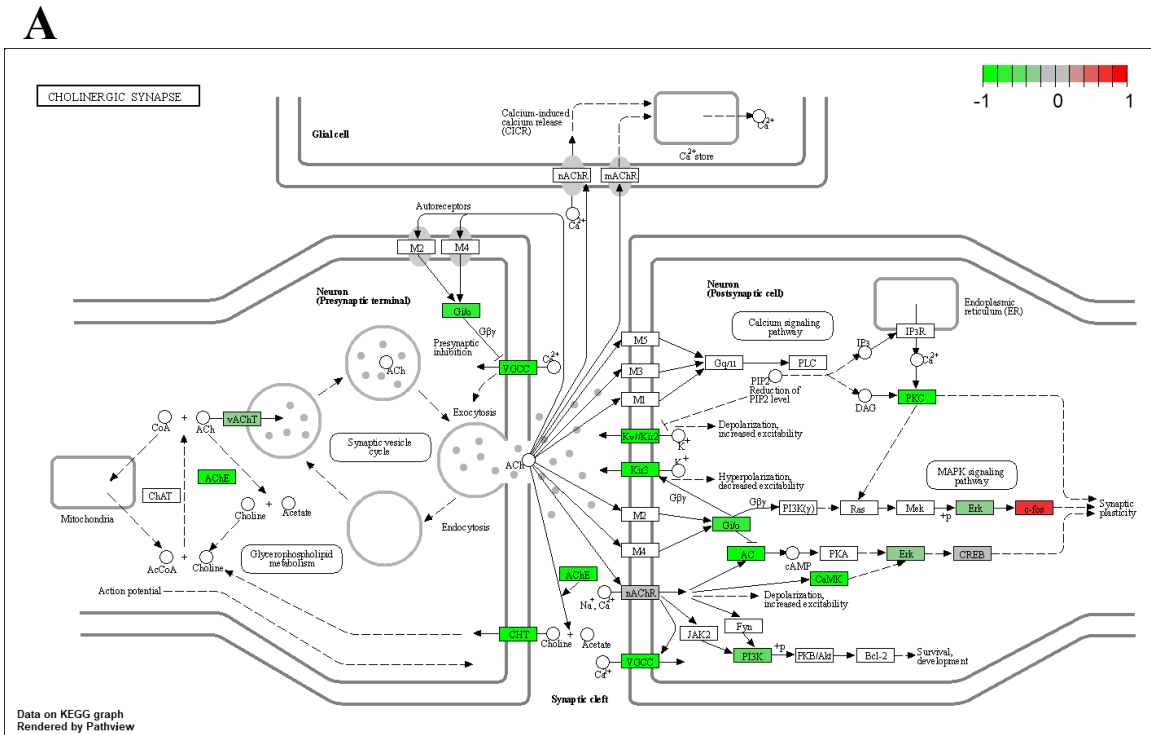


Figure 4.6. Arsenic exposure downregulates genes involved in acetylcholine synthesis, transport and degradation in day 18 early MNs. (A) KEGG pathway analysis shows several downregulated (green) genes of the cholinergic synapse pathway in arsenic-exposed day 18 early MNs. (B-F) RNA sequencing normalized read counts of *CHAT* (B), *SLC18A3* (C), *ACHE* (D) and *SLC5A7* (E) from day 6 NEPs and day 18 early MNs. Data is presented as read count \pm SE. Statistical differences (*) were determined by Student's t-test using the adjusted *p*-value (FDR \leq 0.05).

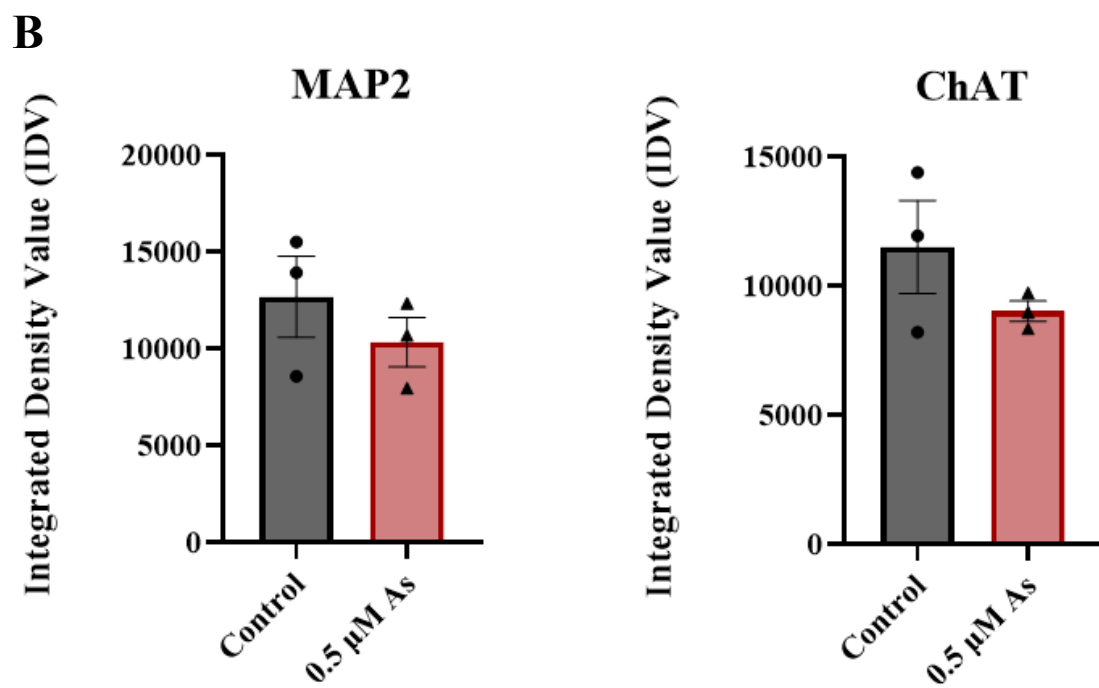
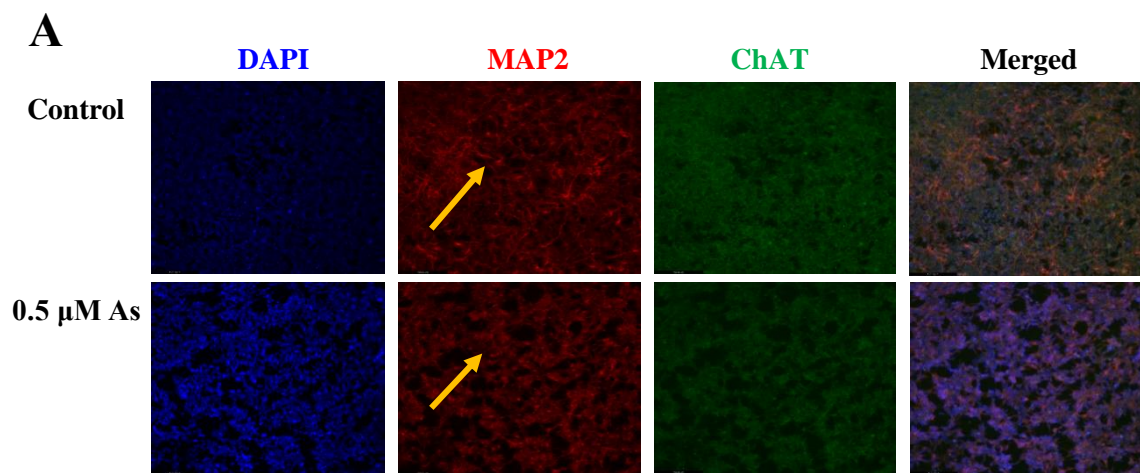
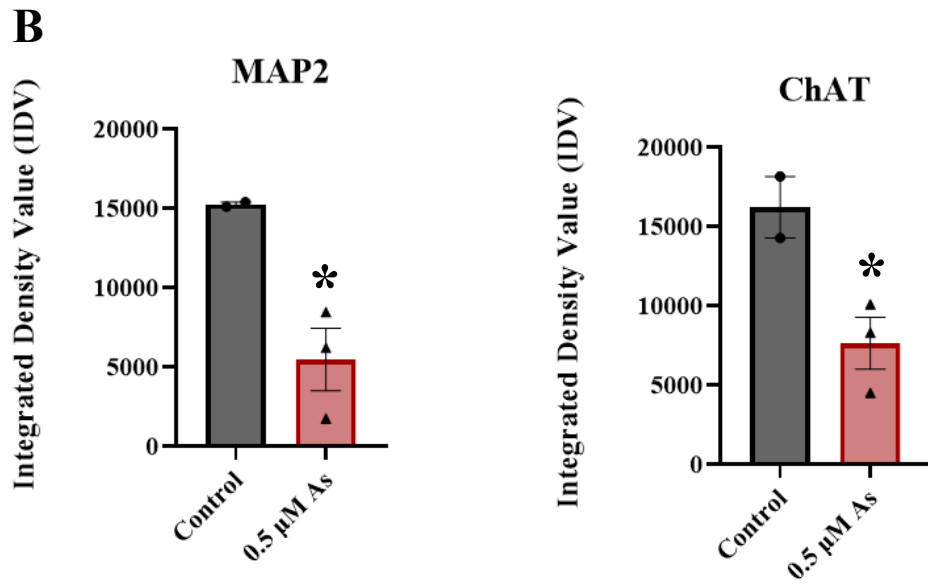
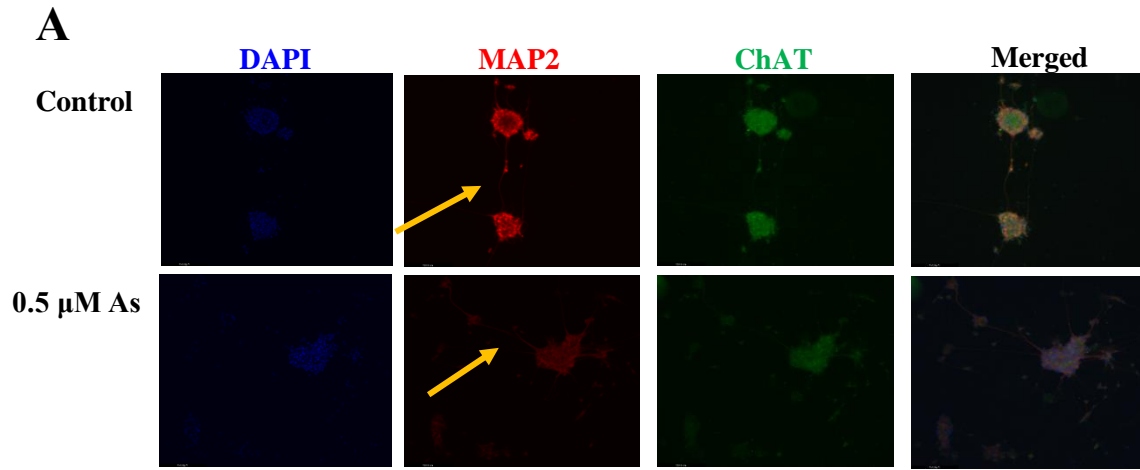


Figure 4.7. Arsenic exposure alters MAP2 pattern in day 18 early MNs. (A) Representative images of MAP2 (red) and ChAT (green) in control and 0.5 μ M arsenic-exposed day 18 early MNs. Arrows show differences in MAP2 pattern. (B) Relative fluorescence of MAP2 (left) and ChAT (right) was determined in ImageJ and is presented as integrated density value (IDV) \pm SE. (n = 3 per exposure group). Statistical differences were determined using Student's t-test (*; $p \leq 0.05$).



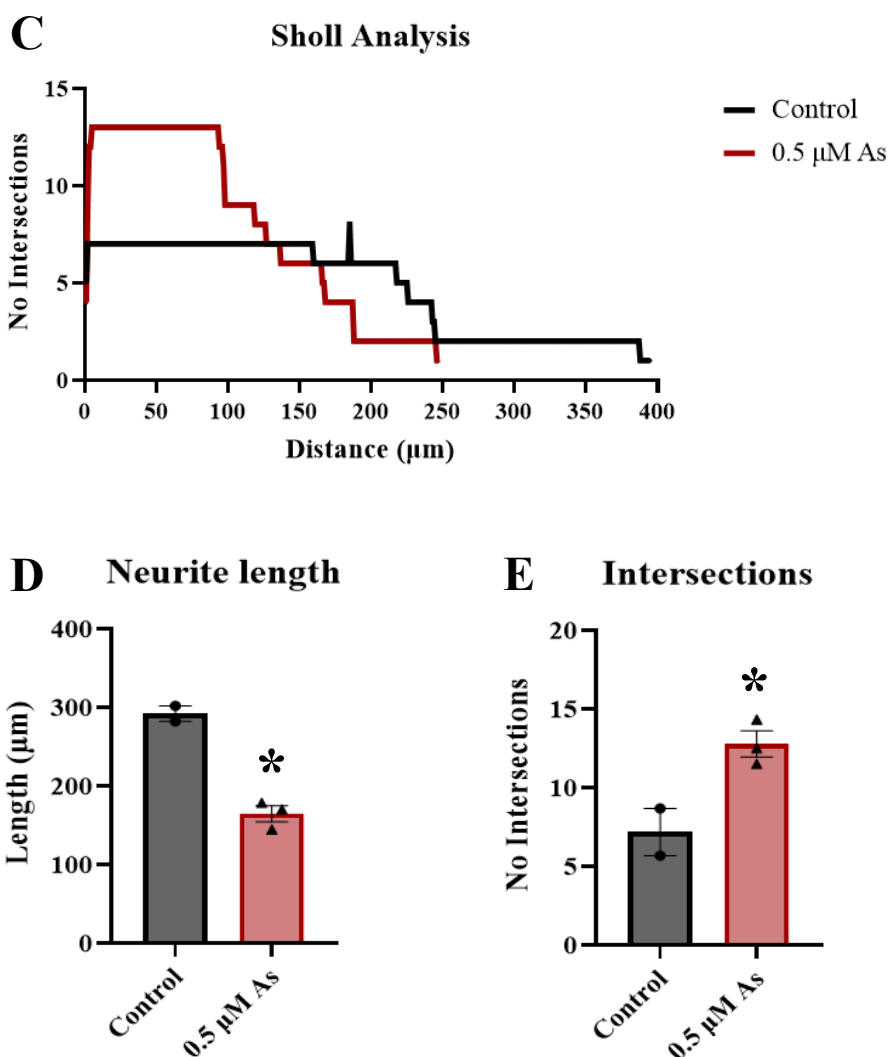


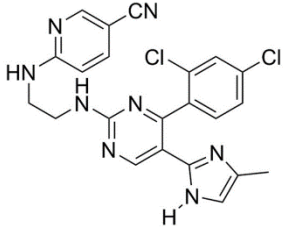
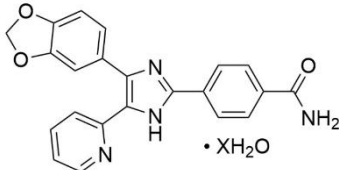
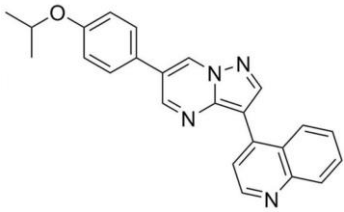
Figure 4.8. Arsenic exposure reduces neurite length and downregulates protein levels of MAP2 and ChAT in day 28 mature MNs. (A) Representative images of MAP2 (red) and ChAT (green) in control and 0.5 μM arsenic-exposed day 28 mature MNs. Arrows show differences in neurite length. (B) Relative fluorescence of MAP2 (left) and ChAT (right) in the cell aggregates was determined in ImageJ. Protein expression was assessed in two to six cell aggregates per biological replicate ($n = 3$ replicates per exposure group), and data are presented as integrated density value (IDV) \pm SE. Statistical differences were determined using Student's t-test (*; $p \leq$

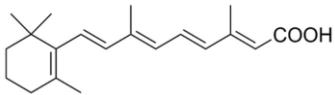
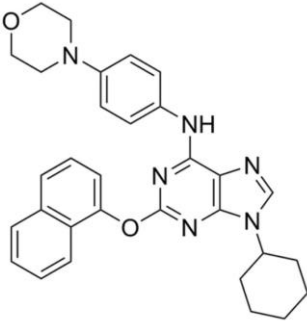
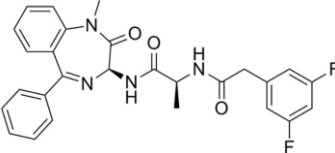
0.05). (C) Sholl analysis of neural processes of MAP2⁺ day 28 mature MNs was performed on one to two cells per biological replicate (n = 3 replicates per exposure group). (D) Average neurite length of neuronal processes of MAP2⁺ day 28 mature MNs. Analysis was performed on n = 3 per exposure group and one to two cells per biological replicas. (E) Average number of intersections obtained from C.

| Human iPS cells to NEPs (day 0 to day 6) | | | |
|---|----------------------|---|--------------------|
| Growth factor | Concentration | Role | Source |
| CHIR99021 | 3 μ M | Wnt signaling activator | StemCell |
| SB431542 | 2 μ M | TGF- β /Activin/NODAL signaling inhibitor | Sigma Aldrich |
| DMH-1 | 2 μ M | BMP signaling inhibitor | Tocris |
| NEPs to MNPs (day 6 to day 12) | | | |
| Growth factor | Concentration | Role | Source |
| CHIR99021 | 1 μ M | Wnt signaling activator | StemCell |
| SB431542 | 2 μ M | TGF- β /Activin/NODAL signaling inhibitor | Sigma Aldrich |
| DMH-1 | 2 μ M | BMP signaling inhibitor | Tocris |
| Retinoic acid | 0.1 μ M | Nuclear receptors RARs activator | Acros Organics |
| Purmorphamine | 0.5 μ M | SHH signaling agonist | Millipore Sigma |
| MNPs to early MNs (day 12 to day 18) | | | |
| Growth factor | Concentration | Role | Source |
| Retinoic acid | 0.5 μ M | Nuclear receptors RARs activator | Acros Organics |
| Purmorphamine | 0.1 μ M | SHH signaling agonist | Millipore Sigma |
| Early MNs to mature MNs (day 18 to day 28) | | | |
| Growth factor | Concentration | Role | Source |
| Retinoic acid | 0.5 μ M | Nuclear receptors RARs activator | Acros Organics |

| | | | |
|---------------|-------------|--|--------------------|
| Purmorphamine | 0.1 μ M | SHH signaling agonist | Millipore Sigma |
| Compound E | 0.1 μ M | Notch signaling inhibitor | Millipore Sigma |
| IGF-1 | 10 ng/ml | PI3K/Akt and Ras/ERK pathway activator | Sigma Aldrich |
| BDNF | 10 ng/ml | TrkB tyrosine kinase receptor activator | R&D systems |
| CNTF | 10 ng/ml | Neurotrophic and survival factor for embryonic motor neurons | R&D systems |

Table S4.1. Supplements and growth factors used during differentiation of human iPS cells into motor neurons

| Growth factor | Role | Chemical formula | Chemical structure |
|---------------|--|---|---|
| CHIR99021 | <p><u>Wnt signaling activator</u></p> <p>CHIR99021 is an aminopyrimidine derivative and a potent glycogen synthase kinase (GSK) 3 inhibitor. The serine/threonine kinase GSK3 is a key inhibitor of the WNT pathway; therefore, CHIR99021 functions as a Wnt signaling activator.</p> <p>In combination with SB431542, CHIR99021 generates and maintains primitive neural stem cells from human embryonic stem cells.</p> | C ₂₂ H ₁₈ Cl ₂ N ₈ |  |
| SB431542 | <p><u>TGF-β/Activin/NODAL signaling inhibitor</u></p> <p>SB431542 is a selective and potent inhibitor of the TGF-β/Activin/NODAL pathway. By competing for the ATP binding sites, it inhibits ALK5, ALK4 and ALK7.</p> <p>SB431542 promotes differentiation of neural progenitor cells from human pluripotent stem cells.</p> <p>SB431542 inhibits self-renewal and induces differentiation of human pluripotent stem cells, showing the importance of the TGF-β/Activin/NODAL pathway in the maintenance of pluripotent stem cells.</p> | C ₂₂ H ₁₆ N ₄ O ₃ • XH ₂ O |  |
| DMH-1 | <p><u>BMP signaling inhibitor</u></p> <p>DMH1 (dorsomorphin homolog 1) is a selective inhibitor of activin receptor-like kinase 2, which is a type I bone morphogenetic protein (BMP) receptor. Therefore, it inhibits BMP signaling.</p> | C ₂₄ H ₂₀ N ₄ O |  |

| | | | |
|---------------|---|--|---|
| | DMH-1 induces differentiation of human induced pluripotent stem cells to neural precursor cells expressing SOX1 and PAX6. | | |
| Retinoic acid | <p><u>Nuclear receptors RARs activator</u></p> <p>Retinoic Acid is a derivative of Vitamin A that functions as a ligand for the retinoic acid receptor (RAR). RARs heterodimerize with retinoid X receptors (RXRs) and bind to retinoic acid response elements (RAREs) in DNA acting as transcription factors and regulating gene expression.</p> <p>Retinoic acid promotes the differentiation of mouse and human pluripotent stem cells into motor neurons.</p> <p>Retinoic acid promotes the differentiation of neural stem cells into motor neurons</p> | C ₂₀ H ₂₈ O ₂ |  |
| Purmorphamine | <p><u>SHH signaling agonist</u></p> <p>Purmorphamine is a tri-substituted purine derivative that promotes the Hedgehog pathway activation by directly binding to Hedgehog receptor Smoothed and activating it.</p> <p>Purmorphamine promotes differentiation of human pluripotent stem cells into ventral spinal progenitors and motor neurons.</p> | C ₃₁ H ₃₂ N ₆ O ₂ |  |
| Compound E | <p><u>Notch signaling inhibitor</u></p> <p>Compound E is a potent, cell-permeable, selective inhibitor that blocks the cleavage of gamma-secretase and the Notch intracellular domain.</p> <p>Compound E promotes the differentiation of primitive</p> | C ₂₇ H ₂₄ F ₂ N ₄ O ₃ |  |

| | | | |
|--|--|--|--|
| | neural stem cells from human embryonic stem cells. | | |
|--|--|--|--|

Table S4.2. Roles and chemical structures of supplements and growth factors used during differentiation of human iPS cells into motor neurons.

| Gene Name | Primer Sequence | |
|-------------------------|------------------------|------------------------|
| | Forward (5'-3') | Reverse (5'-3') |
| <i>GAPDH</i> | CCCTTCATTGACCTCAACTACA | ATGACAAGCTTCCCGTTCTC |
| <i>β2-MICROGLOBULIN</i> | CCAGCGTACTCCAAAGATTCA | TGGATGAAACCCAGACACATAG |
| <i>SOX2</i> | GCTACAGCATGATGCAGGACCA | TCTGCGAGCTGGTCATGGAGTT |
| <i>POU5F14</i> | CCTGAAGCAGAAGAGGATCAC | AGATGGTCGTTTGGCTGAATA |
| <i>NANOG</i> | TGAAATCTAAGAGGTGGCAGAA | CCTGGTGGTAGGAAGAGTAAAG |
| <i>SOX1</i> | AATGTAGTAAGGCAGGTCCAAG | GGTGGTGGTGGTAATCTCTTT |
| <i>NES</i> | CACTTCAGTTTAGAGGCTAAGG | CCCTCTATGGCTGTTTCTTTCT |
| <i>OLIG2</i> | CAGAAGCGCTGATGGTCATA | CTCCCAAATCAACGAGAGACA |
| <i>CHAT</i> | GGAGTAAGAAAGCAACCAGAGA | CACAAAGAAGGGAGACCTACAG |

Table S4.3. Primer sequences of genes quantified by qPCR

| Correlation | | | |
|--------------------|-------------|---------------|--------------|
| | <i>SOX2</i> | <i>POU5F1</i> | <i>NANOG</i> |
| <i>SOX2</i> | 1 | 0.94 | 0.96 |
| <i>POU5F1</i> | 0.94 | 1 | 0.99 |
| <i>NANOG</i> | 0.96 | 0.99 | 1 |

Table S4.4. Correlation between transcript levels of *SOX2*, *POU5F1* and *NANOG* in human iPS cells exposed to 0, 0.1 or 0.5 μ M arsenic for six days.

| Correlation | | | |
|--------------------|-------------|-------------|------------|
| | <i>SOX1</i> | <i>SOX2</i> | <i>NES</i> |
| <i>SOX1</i> | 1 | 0.78 | 0.78 |
| <i>SOX2</i> | 0.78 | 1 | 0.76 |
| <i>NES</i> | 0.78 | 0.76 | 1 |

Table S4.5. Correlation between transcript levels of *SOX2*, *SOX1* and *NES* in day 6 NEPs exposed to 0, 0.25, 0.5 and 0.75 μ M.

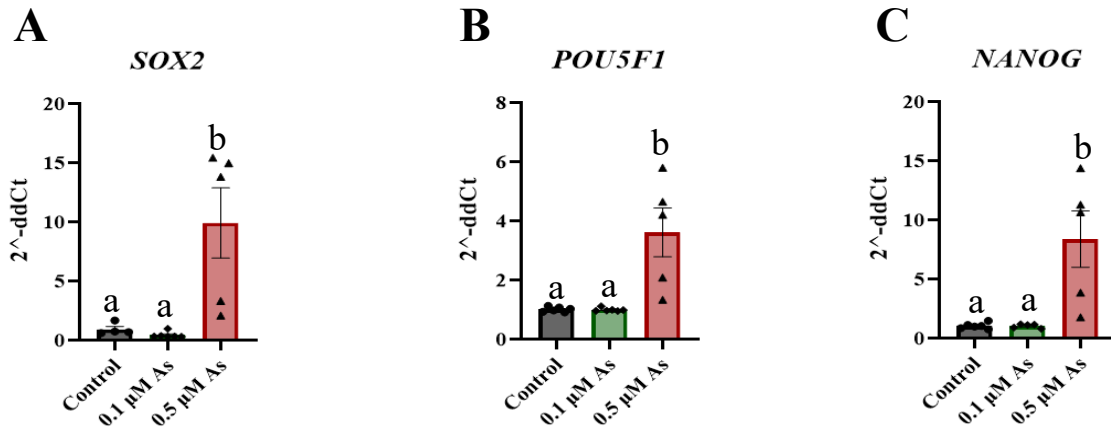
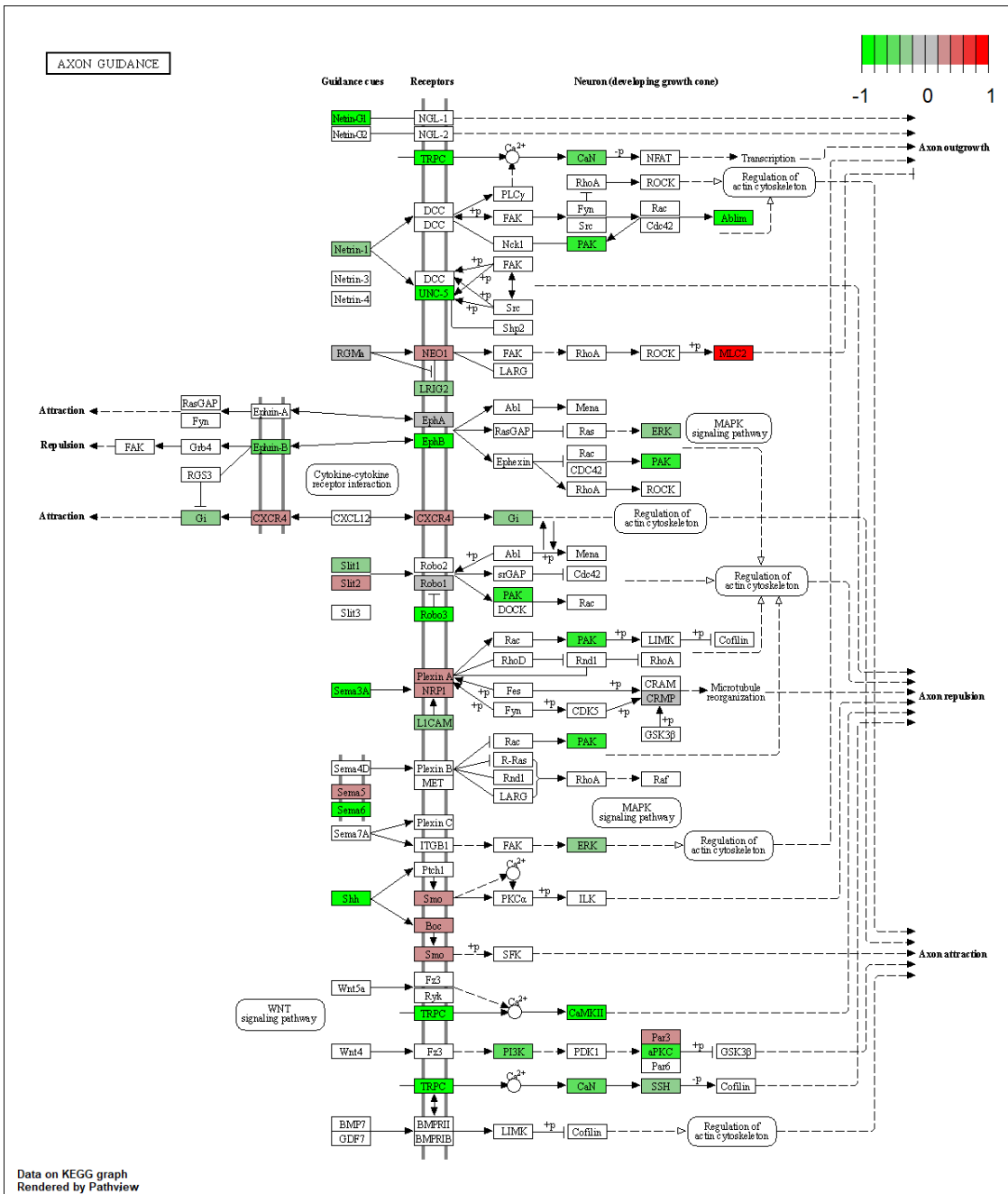
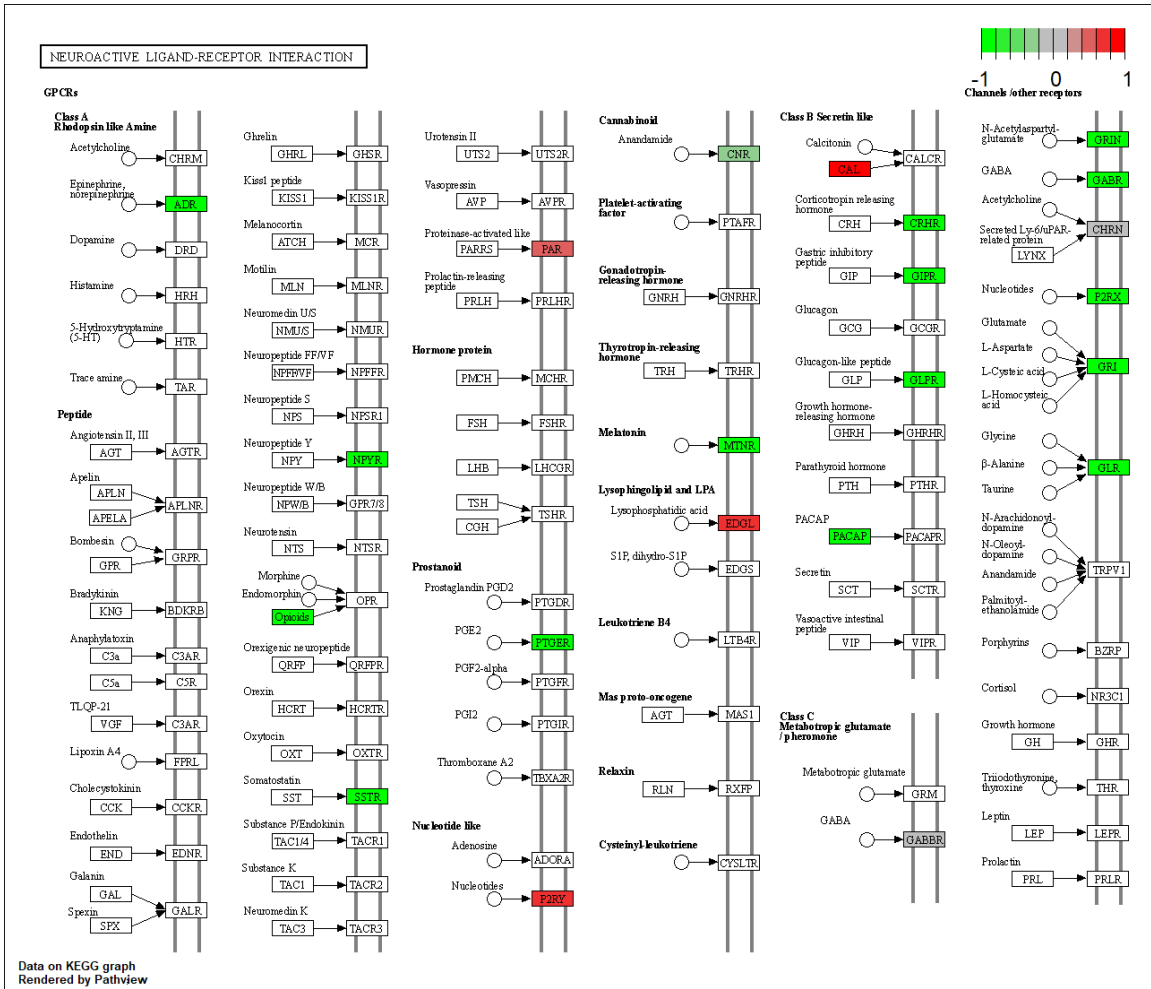


Figure S4.1. Arsenic increases transcript levels of pluripotency markers *SOX2*, *POU5F1* and *NANOG* in human iPS cells. Transcript levels of *SOX2* (A), *POU5F1* (B) and *NANOG* (C) were assessed by qPCR in human iPS cells exposed to 0, 0.1 or 0.5 μM arsenic for six days. Fold change was determined using the ddCt method and results were normalized to the geometric mean of *Gapdh* and β 2-microglobulin. Statistical differences were determined using ANOVA followed by Tukey's multiple comparison test (*; $p \leq 0.05$) (n = 5-6 per exposure group).

A



B



C

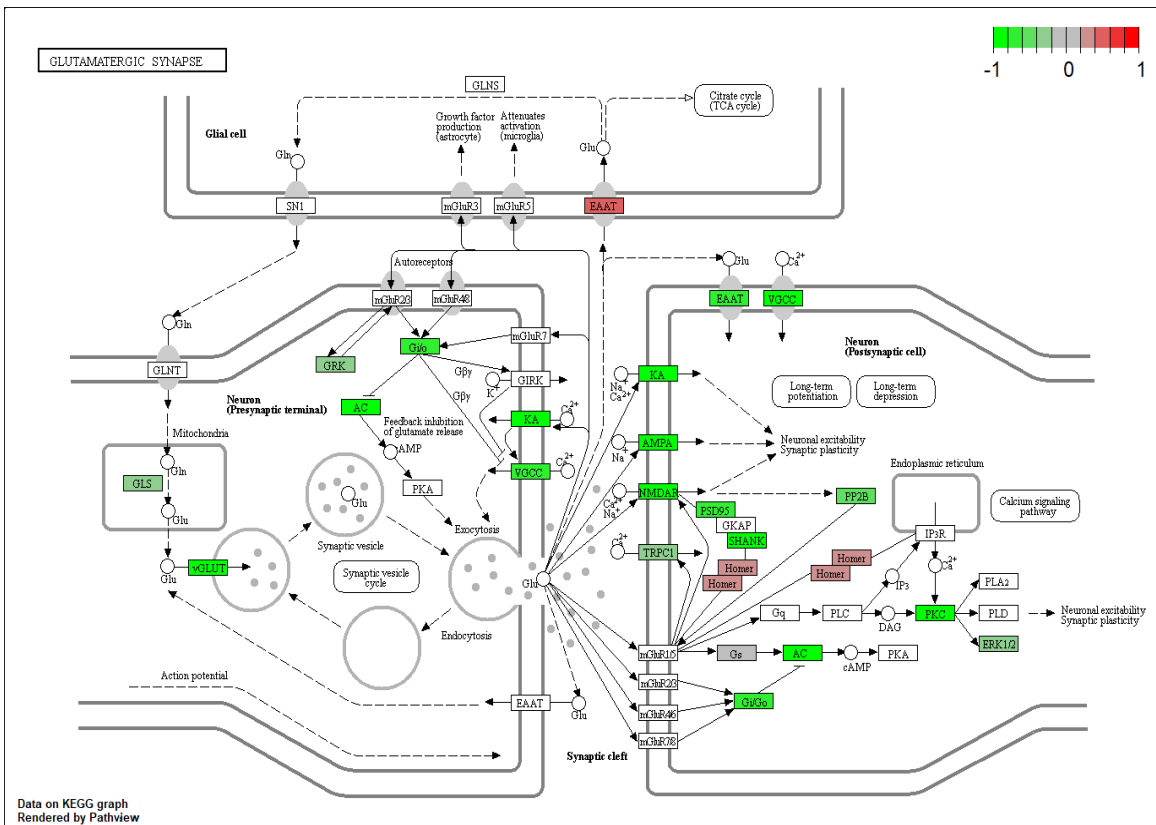


Figure S4.2. Arsenic exposure impairs glutamatergic synapse, axon guidance and neuroactive ligand-receptor interaction pathways. KEGG pathway analysis of pathways regulating axon guidance (A), neuroactive ligand-receptor interaction pathway (B) and glutamatergic synapse pathway (C) shows various downregulated (green) genes and a few upregulated (red) genes in arsenic-exposed day 18 early MNs.

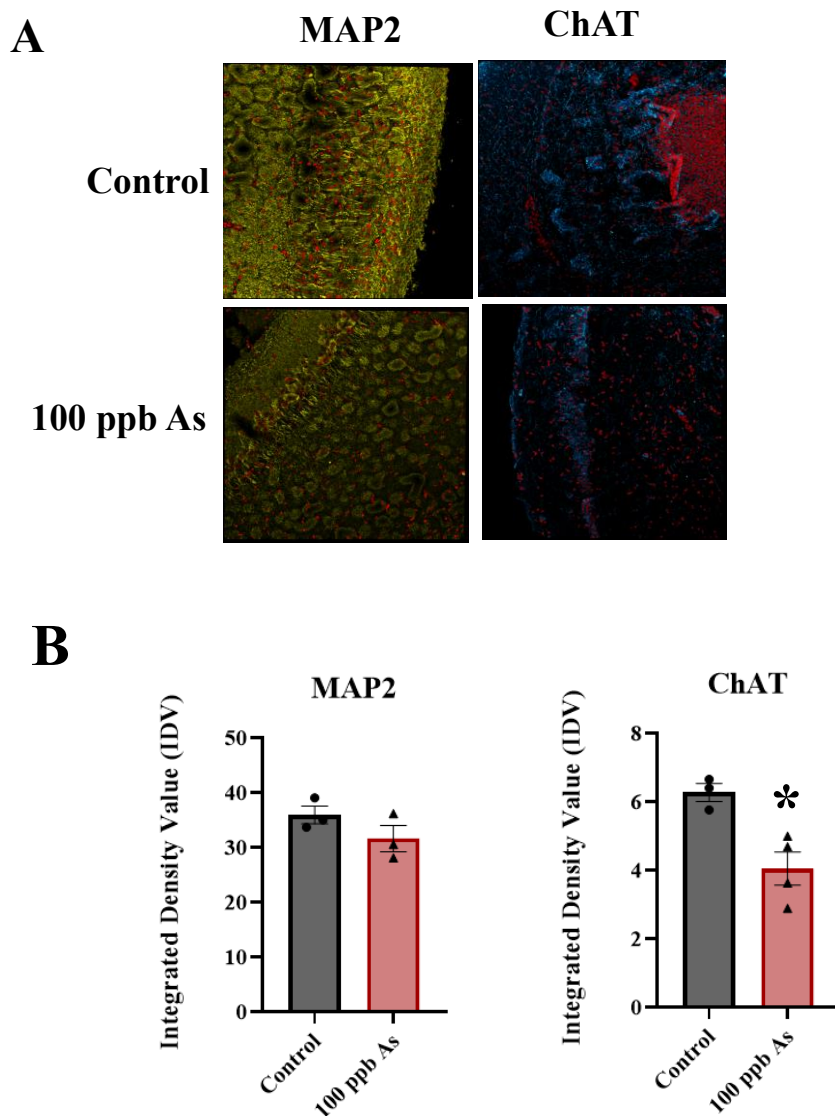


Figure S4.3. Arsenic exposure impairs ChAT protein levels in adult mice hippocampi. (A) Representative images of 3D z-stacked images of MAP2 (yellow) and ChAT (blue) in hippocampi harvested from adult mice exposed to 100 ppb of arsenic for five weeks. (B) Relative fluorescence of MAP2 (left) and ChAT (right) was determined in ImageJ and is presented as integrated density value (IDV) \pm SE (n = 3-4 per exposure group). Statistical differences were determined using Student's t-test (*; $p \leq 0.05$).

CHAPTER FIVE

CONCLUSION

Summary of the main findings

Previous studies in our lab have shown that acute exposure to 0.5 μM (37.5 ppb) arsenic inhibits skeletal muscle and neuronal differentiation in mouse embryonic stem cells (Hong and Bain, 2012; McCoy et al., 2015; Bain et al., 2016). However, little is known about the effects of chronic arsenic exposure on cellular differentiation. Therefore, we wanted to investigate impacts of exposing mouse embryonic stem (ES) cells to 0.1 μM (7.5 ppb) arsenic as sodium arsenite for 28 weeks. Importantly, 0.1 μM arsenic is a concentration not only environmentally relevant but it is also lower than the current drinking water standard of 10 ppb established by the World Health Organization and the U.S. Environmental Protection Agency. The results from Chapter 2 indicate that arsenic does hinder cellular differentiation and maintain pluripotency in mouse embryonic stem cells by enhancing levels of genes associated with pluripotency, such as *Sox2* and *Oct4*, and reducing levels of genes associated with cellular differentiation and neuronal progenitors, such as *Gdf3*. Additionally, we not only reported changes in transcript levels, but we also observed enhanced protein expression of SOX2 and its target N-cadherin starting at week 12 and 20, respectively. While no differences were seen in protein expression of the epithelial marker E-cadherin, increased expression of the mesenchymal marker N-cadherin is a hallmark of epithelial-mesenchymal transition (EMT). This data suggests that chronic low-level arsenic exposure might maintain pluripotency and delay neuronal differentiation through an EMT-like mechanism. Chapter 3 aimed to identify additional signaling pathways that might be impaired following chronic low-level arsenic exposure in mouse embryonic stem cells using RNASeq. One novel pathway identified as altered in arsenic-exposed cells was the Hippo signaling pathway. Interestingly, even after 24 weeks of exposure, no significant changes in the expression of the upstream key Hippo

pathway proteins MST and LATS were seen. Conversely, our results show that the ratio between nuclear (active) and cytoplasmic (inactive) of the main effector YAP and the main transcription factor TEAD were significantly increased in arsenic-exposed cells at week 16 and 28, along with increased expression of downstream targets *Ctgf* and *c-Myc*. This suggests that chronic low level arsenic exposure impairs the Hippo signaling pathway by enhancing the activation and nuclear translocation of the main effector YAP and the main transcription factor TEAD leading to upregulation of their downstream target genes. Chapter 4 aimed to investigate the effects of arsenic exposure on human iPS cells during their differentiation into motor neurons, as we have previously reported that arsenic inhibits cellular differentiation of skeletal muscle and sensory neurons (Hong and Bain, 2012; McCoy et al., 2015; Bain et al., 2016; McMichael et al., 2020). Further, we wanted to investigate whether the impairment of cellular differentiation we observed in mouse embryonic stem cells following arsenic exposure would also occur using human iPS cells, as significant differences in arsenic metabolism have been reported in murine and human species (Vahter, 2002; Drobná et al., 2010; States et al., 2011). We confirmed that arsenic exposure hinders motor neuron differentiation based on temporal changes in transcript levels of neuronal differentiation and pluripotency markers throughout the exposure. Additionally, we found that exposure to 0.5 μ M arsenic impairs the cholinergic synapse pathway in early motor neurons by inhibiting the expression of genes involved in acetylcholine synthesis, transport, and degradation. Changes in transcript levels of the gene involved in acetylcholine synthesis (*CHAT*) also result in changes in ChAT protein expression in mature motor neurons. This data suggests that arsenic exposure not only hinders the differentiation of human iPS cells into motor neurons, but it could also disrupt the acetylcholine cycle.

The importance of adequate drinking water standards

Several epidemiological studies have shown that *in utero* exposure to arsenic during embryonic and fetal development is linked to reduced birth weight, weight gain and impaired locomotor abilities along with neurodevelopmental changes including reduced IQ, impaired learning, memory and cognition (Rahman et al., 2009; Hamadani et al., 2011; Saha et al., 2012; Thomas, 2013; Wasserman et al., 2014; Tsuji et al., 2015). Importantly, arsenic can readily cross the blood-placenta barrier as previous studies have reported that arsenic levels in placental and cord blood are comparable with concentrations measured in maternal blood (Concha et al., 1998; Hall et al., 2007; Henn et al., 2016). For instance, Concha et al. (1998) reported average concentrations of 11 and 9 $\mu\text{g/L}$ arsenic in maternal blood and cord blood, respectively, in pregnant women exposed to 200 $\mu\text{g/L}$ through drinking water. The 0.1 μM arsenic concentration used in the Chapter 2 and 3 studies is equivalent to 7.5 $\mu\text{g/L}$ or 7.5 ppb. Therefore, it represents a realistic and highly relevant concentration to investigate the effects of arsenic during embryonic development. Further, this concentration is below the current drinking water standard of 10 $\mu\text{g/L}$.

In vitro exposure studies have shown that arsenic impairs neuronal differentiation via transcriptional alterations. For instance, Hong and Bain (2012) have reported that transcription factors involved in neuronal differentiation such as Neurogenin 1, Neurogenin 2 and NeuroD are reduced in mouse embryonic stem cells after a 9-day exposure to concentrations $\leq 1 \mu\text{M}$ arsenic. Similarly, McCoy et al. (2015) have shown reduced transcript levels of *NeuroD* along with decreased protein expression of Sox10, a marker of neural crest progenitor cells after 5 days of $\leq 1 \mu\text{M}$ arsenic exposure. Our chronic study used a 10-fold lower concentration (0.1 μM arsenic) for up to 28 weeks and also observed decreased expression of neuronal differentiation markers. These results might suggest that the current drinking water standard might not be completely protective of proper neurodevelopment.

Impairment of the Hippo signaling pathway might have a role in improper neurogenesis following arsenic exposure

Neurogenesis is a complex and highly regulated process by which a small number of cells, classified as neural stem cells, give rise to different neuronal cell type. These neural stem cells retain the ability to self-renew through symmetric division and have the capability to differentiate into specialized neuronal cell types, such as functional neurons, oligodendrocytes, and astrocytes (Niklison-Chirou et al., 2020). Various signaling pathways are involved in regulating the balance between cellular differentiation and proliferation and in maintaining a population of stem cells while also forming terminal differentiation neurons. Previous studies have shown that arsenic exposure impairs several of these pathways including Wnt/ β -catenin signaling pathway (Hong and Bain, 2012; Wang et al., 2017; Jatko et al., 2021) and TGF- β signaling pathway (Allison et al., 2013; Ji et al., 2014; McMichael et al., 2020). The Hippo signaling pathway also plays a prominent role in regulating cellular differentiation and stem cell renewal, but its involvement in arsenic-induced developmental toxicity has been largely overlooked.

While we did not confirm our hypothesis that arsenic enhances YAP activation and its nuclear translocation through a rescue experiment, we did observe enhanced transcription of YAP's target genes *c-Myc* and *Ctgf* along with increased protein expression of CTGF. While several studies have reported that arsenic exposure enhances c-MYC levels (Chen et al., 2001; Liu et al., 2006; Ruiz-Ramos et al., 2009; Nakareangrit et al., 2016; Jatko et al., 2021; Xiao et al., 2021), few studies have been conducted to investigate the changes in CTGF transcript and protein levels. The few that have examined CTGF have used concentrations in the ppm range, rather than ppb range. For instance, CTGF transcript levels were increased in the skin of mice following exposure to 100 ppm arsenic (Li et al., 2013) while its protein expression was enhanced in aortal tissues of rats following exposure to 50 ppm of arsenic for 90 days (Khuman et al., 2016). Additionally, our

results also suggest that TEAD activation and nuclear localization is increased following arsenic exposure. TEAD helps regulate the cellular localization, biological functions, and activity of YAP (Zhao et al., 2008; Lin et al., 2017). The ratio of nuclear to cytoplasmic TEAD and YAP were both increased, suggesting that the two work cooperatively to move to the nucleus and increase transcription of target genes. Further studies are needed to clarify the interplay between YAP and TEAD in arsenic-induced impairment of the Hippo signaling pathway following arsenic exposure.

The effects of arsenic on motor neuron differentiation

In addition to changes in neurogenesis, inhibition of transcription factors involved in myogenesis including myogenin, MyoD and Myf5 are seen in mouse ES cells exposed to $\leq 1 \mu\text{M}$ arsenic (Hong and Bain, 2012). Therefore, we hypothesized that arsenic could also disrupt cellular differentiation of motor neurons which are anatomically and physiologically connected to skeletal muscle. Interestingly, limited data is available regarding the effects of arsenic exposure on motor neurons. Nonetheless, a positive association have been recently reported between environmental arsenic exposure and higher risk of mortality associated with motor neuron disease (Sánchez-Díaz et al., 2018). Our results report an impairment of transcript levels of genes involved in neuronal differentiation and pluripotency maintenance throughout the differentiation process up to the day 18 early motor neurons stage. Because we had limited number of day 28 mature motor neurons, we were unable to quantify transcript levels of markers at this stage of the differentiation process. This would provide insight as to which markers are expressed in arsenic exposed mature motor neurons. Nonetheless, morphological and immunohistochemistry analysis revealed the presence of neuronal structures such as MAP+ neurites, and almost all cells co-expressed MAP2 and ChAT at day 28 in both control and arsenic samples, indicating that pluripotent cells were indeed differentiated into cholinergic neurons. However, transcript data obtained from control day 18 early motor neurons

indicate the presence of a heterogeneous population of neurons expressing both cholinergic markers and markers of progenitor cells. Further studies could investigate neuronal subpopulations in control and arsenic-treated samples through single cell sequencing analysis or flow cytometry analysis.

Notably, we continuously exposed cells to arsenic throughout the entire differentiation process. Further studies could therefore be conducted to identify critical periods of susceptibility by assessing changes in motor neuron gene patterns and functionality of cells only exposed to arsenic for the first 6 or 12 days. While I hypothesize that arsenic withdrawal could favor the recovery of motor neuron functions, the significant changes in gene expression patterns observed in arsenic-treated day 6 NEPs compared with their control counterpart suggest that early exposure to arsenic and the impairment of progenitor cells' proper differentiation could be sufficient to disrupt proper motor neuron differentiation and function at later time points.

RNAseq and KEGG pathway analyses of day 18 early motor neurons following arsenic exposure indicated that glutamatergic and cholinergic synapses terms were impaired following arsenic exposure including. Interestingly, it has been previously suggested that arsenic could disrupt the cholinergic system by inhibiting ChAT expression and reducing AChE activity (Yadav et al., 2011; Chandravanshi et al., 2019). Consistently, we reported downregulation of genes involved in the acetylcholine cycle including *CHAT*, *SLC18A3* (encoding for VACHT), *ACHE* and *SLC5A7* (encoding for ChT). Additionally, ChAT expression was reduced in day 28 mature motor neurons and in the hippocampi of adult mice exposed to 100 ppb arsenic for five weeks. We therefore hypothesized that arsenic-induced impairment of ChAT expression might lead to decreased synthesis of acetylcholine which might play a prominent role in the disruption of cholinergic synapse pathway reported in arsenic-exposed day 18 early MNs. As ChAT was still expressed in arsenic treated samples, we hypothesized that arsenic might impair the proper function

of the cholinergic synapses rather than its formation. While we did not evaluate the functionality of the mature motor neurons synapses, a co-culture of mature motor neurons with muscle cells, such as C2C12, followed by immunohistochemistry analysis to identify ChAT+ neurons and the neuromuscular junction using bungarotoxin staining, would provide insight to determine whether arsenic-exposed mature motor neurons and myoblasts would be able to form and develop neuromuscular junctions.

Arsenic might disrupt synaptic transmission of cholinergic synapses by impairing ion channels

Our results indicated that the cholinergic synapses were not only impaired at a presynaptic level by inhibiting genes involved in the acetylcholine cycle, but that several genes involved in the proper function of ion channels, including potassium and calcium channels, were also disrupted. Different types of ligand- and voltage-gated ion channels permeable to ions including sodium, potassium, and calcium, play a role in the regulation of the electrical activity of neurons and other excitable cells. While sodium and potassium ions are primarily involved in the transmission of the electric signal, calcium ion, whose entry into pre-synaptic and post-synaptic neuronal cells is regulated by voltage-gated calcium channels (VGCC) through depolarization, not only affect the membrane potential but also regulate gene transcription, neurite outgrowth and neurotransmitter release (Clapham et al., 2007; Wadel et al., 2007; Simms and Zamponi, 2014). Dysregulation of VGCC activity and impaired expression of genes involved in calcium functions has been associated with neurological disorders (Simms and Zamponi, 2014). We reported transcript levels reduction of potassium channels *KCNQ2,3*, encoding for $K_v7.2$ and $K_v7.3$, and *KCNJ6*, encoding for $K_{ir}3.2$. Voltage-gated potassium channels K_v7 are important regulators of neuronal and muscular excitability (Soldovieri et al., 2011; Baculis et al., 2020) and they have been involved in the onset

of neurodevelopmental disorders, neural plasticity, and memory and learning functions (Baculis et al., 2020). G protein-coupled inwardly rectifying potassium channel Kir3 functions by allowing potassium influx when the membrane is hyperpolarized and inhibiting potassium efflux when the membrane is depolarized mediating a background potassium conductance (Butt and Kalsi, 2006; Borin et al., 2014; Chen and Swale, 2018). This type of channels modulates various physiological processes including regulation of neuronal and muscle cells excitability (Borin et al., 2014). Considering the importance of these channels in neuronal excitability activity and proper neuronal functions, the effects of arsenic on these channels and on ions transport during neuronal transmission should be further investigated.

Conclusions

In conclusion, our studies were developed to determine whether exposure to environmentally relevant arsenic concentrations commonly found in maternal drinking water could impair neurogenesis of several types of neurons using mouse embryonic stem cells and human iPS cells and to investigate the mechanisms by which arsenic induces impairment of embryonic development. Our results suggest that neurodevelopmental and locomotor alterations observed following *in utero* arsenic exposure might be caused by arsenic-induced neuronal differentiation delay and disruption of proper cholinergic functions. Further studies investigating these mechanisms are needed to determine whether current drinking water and food standard are appropriate to protect developmental health.

References

- Allison, P., Huang, T., Broka, D., Parker, P., Barnett, J.V., Camenisch, T.D., 2013. Disruption of canonical TGFbeta-signaling in murine coronary progenitor cells by low level arsenic. *Toxicol. Appl. Pharmacol.* 272, 147-153.
- Baculis, B.C., Zhang, J., Chung, H.J., 2020. The Role of Kv7 Channels in Neural Plasticity and Behavior. *Frontiers in physiology* 11, 568667.
- Bain, L.J., Liu, J.T., League, R.E., 2016. Arsenic inhibits stem cell differentiation by altering the interplay between the Wnt3a and Notch signaling pathways. *Toxicol. Rep.* 3, 405-413.
- Borin, M., Fogli Iseppe, A., Pignatelli, A., Belluzzi, O., 2014. Inward rectifier potassium (Kir) current in dopaminergic periglomerular neurons of the mouse olfactory bulb. *Frontiers in Cellular Neuroscience*, n/a.
- Butt, A.M., Kalsi, A., 2006. Inwardly rectifying potassium channels (Kir) in central nervous system glia: a special role for Kir4.1 in glial functions. *J. Cell. Mol. Med.* 10, 33-44.
- Clapham, D.E., 2007. Calcium signaling. *Cell*, 131; 1047-1058
- Chandravanshi, L.P., Gupta, R., Shukla, R.K., 2019. Arsenic-Induced Neurotoxicity by Dysfunctioning Cholinergic and Dopaminergic System in Brain of Developing Rats. *Biol. Trace Elem. Res.* 189, 118-133.
- Chen, H., Liu, J., Zhao, C.Q., Diwan, B.A., Merrick, B.A., Waalkes, M.P., 2001. Association of c-myc overexpression and hyperproliferation with arsenite-induced malignant transformation. *Toxicol. Appl. Pharmacol.* 175, 260-268.
- Chen, R., Swale, D.R., 2018. Inwardly Rectifying Potassium (Kir) Channels Represent a Critical Ion Conductance Pathway in the Nervous Systems of Insects. *Scientific Reports (Nature Publisher Group)* 8, 1-13.
- Henn, B.C., Ettinger, A.S., Hopkins, M.R., Jim, R., Amarasiriwardena, C., Christiani, D.C., Coull, B.A., Bellinger, D.C., Wright, R.O., 2016. Prenatal Arsenic Exposure and Birth Outcomes among a Population Residing near a Mining-Related Superfund Site. *Environ. Health Perspect.* 124, 1308-1315.
- Concha, G., Vogler, G., Lezcano, D., Nermell, B., Vahter, M., 1998. Exposure to inorganic arsenic metabolites during early human development. *Toxicol. Sci.* 44, 185-190.
- Drobna, Z., Walton, F.S., Paul, D.S., Xing, W., Thomas, D.J., Styblo, M., 2010. Metabolism of arsenic in human liver: the role of membrane transporters. *Arch. Toxicol.* 84, 3-16.
- Hall, M., Gamble, M., Slavkovich, V., Liu, X., Levy, D., Cheng, Z., van Geen, A., Yunus, M., Rahman, M., Pilsner, J.R., Graziano, J., 2007. Determinants of arsenic metabolism: blood

- arsenic metabolites, plasma folate, cobalamin, and homocysteine concentrations in maternal-newborn pairs. *Environ. Health Perspect.* 115, 1503-1509.
- Hamadani, J.D., Tofail, F., Nermell, B., Gardner, R., Shiraji, S., Bottai, M., Arifeen, S.E., Huda, S.N., Vahter, M., 2011. Critical windows of exposure for arsenic-associated impairment of cognitive function in pre-school girls and boys: a population-based cohort study. *Int. J. Epidemiol.* 40, 1593-1604.
- Hong, G.M., Bain, L.J., 2012. Sodium arsenite represses the expression of myogenin in C2C12 mouse myoblast cells through histone modifications and altered expression of Ezh2, Glp, and Igf-1. *Toxicol. Appl. Pharmacol.* 260, 250-259.
- Jatko, J.T., Darling, C.L., Kellett, M.P., Bain, L.J., 2021. Arsenic exposure in drinking water reduces Lgr5 and secretory cell marker gene expression in mouse intestines. *Toxicol. Appl. Pharmacol.* 422, 115561.
- Ji, H., Li, Y., Jiang, F., Wang, X., Zhang, J., Shen, J., Yang, X., 2014. Inhibition of transforming growth factor beta/SMAD signal by MiR-155 is involved in arsenic trioxide-induced anti-angiogenesis in prostate cancer. *Cancer. Sci.* 105, 1541-1549.
- Khuman, M.W., Harikumar, S.K., Sadam, A., Kesavan, M., Susanth, V.S., Parida, S., Singh, K.P., Sarkar, S.N., 2016. Candesartan ameliorates arsenic-induced hypertensive vascular remodeling by regularizing angiotensin II and TGF-beta signaling in rats. *Toxicology* 374, 29-41.
- Li, C., Srivastava, R.K., Elmetts, C.A., Afaq, F., Athar, M., 2013. Arsenic-induced cutaneous hyperplastic lesions are associated with the dysregulation of Yap, a Hippo signaling-related protein. *Biochem. Biophys. Res. Commun.* 438, 607-612.
- Lin, K.C., Moroishi, T., Meng, Z., Jeong, H.S., Plouffe, S.W., Sekido, Y., Han, J., Park, H.W., Guan, K.L., 2017. Regulation of Hippo pathway transcription factor TEAD by p38 MAPK-induced cytoplasmic translocation. *Nat. Cell Biol.* 19, 996-1002.
- Liu, J., Benbrahim-Tallaa, L., Qian, X., Yu, L., Xie, Y., Boos, J., Qu, W., Waalkes, M.P., 2006. Further studies on aberrant gene expression associated with arsenic-induced malignant transformation in rat liver TRL1215 cells. *Toxicol. Appl. Pharmacol.* 216, 407-415.
- McCoy, C.R., Stadelman, B.S., Brumaghim, J.L., Liu, J.T., Bain, L.J., 2015. Arsenic and Its Methylated Metabolites Inhibit the Differentiation of Neural Plate Border Specifier Cells. *Chem. Res. Toxicol.* 28, 1409-1421.
- McMichael, B.D., Perego, M.C., Darling, C.L., Perry, R.L., Coleman, S.C., Bain, L.J., 2020. Long-term arsenic exposure impairs differentiation in mouse embryonal stem cells. *J. Appl. Toxicol.* .

- Nakareangrit, W., Thiantanawat, A., Visitnonthachai, D., Watcharasit, P., Satayavivad, J., 2016. Sodium arsenite inhibited genomic estrogen signaling but induced pERalpha (Ser118) via MAPK pathway in breast cancer cells. *Environ. Toxicol.* 31, 1133-1146.
- Niklison-Chirou, M.V., Agostini, M., Amelio, I., Melino, G., 2020. Regulation of Adult Neurogenesis in Mammalian Brain. *International journal of molecular sciences* 21.
- Rahman, A., Vahter, M., Smith, A.H., Nermell, B., Yunus, M., El Arifeen, S., Persson, L.A., Ekstrom, E.C., 2009. Arsenic exposure during pregnancy and size at birth: a prospective cohort study in Bangladesh. *Am. J. Epidemiol.* 169, 304-312.
- Ruiz-Ramos, R., Lopez-Carrillo, L., Rios-Perez, A.D., De Vizcaya-Ruiz, A., Cebrian, M.E., 2009. Sodium arsenite induces ROS generation, DNA oxidative damage, HO-1 and c-Myc proteins, NF-kappaB activation and cell proliferation in human breast cancer MCF-7 cells. *Mutat. Res.* 674, 109-115.
- Saha, K.K., Engström, A., Hamadani, J.D., Tofail, F., Rasmussen, K.M., Vahter, M., 2012. Pre- and Postnatal Arsenic Exposure and Body Size to 2 Years of Age: A Cohort Study in Rural Bangladesh. *Environ. Health Perspect.* 120, 1208-14.
- Sánchez-Díaz, G., Escobar, F., Badland, H., Arias-Merino, G., Manuel Posada de la Paz, Alonso-Ferreira, V., 2018. Geographic Analysis of Motor Neuron Disease Mortality and Heavy Metals Released to Rivers in Spain. *International Journal of Environmental Research and Public Health* 15, 2522.
- Simms, B.A., Zamponi, G.W., 2014. Neuronal voltage-gated calcium channels: structure, function, and dysfunction. *Neuron* 82, 24-45.
- Soldovieri, M.V., Miceli, F., Tagliatela, M., 2011. Driving with no brakes: molecular pathophysiology of Kv7 potassium channels. *Physiology (Bethesda, Md.)* 26, 365-376.
- States, J.C., Barchowsky, A., Cartwright, I.L., Reichard, J.F., Futscher, B.W., Lantz, R.C., 2011. Arsenic toxicology: translating between experimental models and human pathology. *Environ. Health Perspect.* 119, 1356-1363.
- Thomas, D.J., 2013. The die is cast: arsenic exposure in early life and disease susceptibility. *Chem. Res. Toxicol.* 26, 1778-1781.
- Tsuji, J.S., Garry, M.R., Perez, V., Chang, E.T., 2015. Low-level arsenic exposure and developmental neurotoxicity in children: A systematic review and risk assessment. *Toxicology* 337, 91-107.
- Vahter, M., 2002. Mechanisms of arsenic biotransformation. *Toxicology* 181-182, 211-217.
- Wadel, K., Neher, E., Sakaba, T., 2007. The coupling between synaptic vesicles and Ca²⁺ channels determines fast neurotransmitter release. *Neuron* 53, 563-575.

- Wang, Y., Wang, Z., Li, H., Xu, W., Dong, L., Guo, Y., Feng, S., Bi, K., Zhu, C., 2017. Arsenic trioxide increases expression of secreted frizzled-related protein 1 gene and inhibits the WNT/beta-catenin signaling pathway in Jurkat cells. *Exp. Ther. Med.* 13, 2050-2055.
- Wasserman, G.A., Liu, X., Loiacono, N.J., Kline, J., Factor-Litvak, P., van Geen, A., Mey, J.L., Levy, D., Abramson, R., Schwartz, A., Graziano, J.H., 2014. A cross-sectional study of well water arsenic and child IQ in Maine schoolchildren. *Environ. Health* 13, 23-069X-13-23.
- Xiao, T., Zou, Z., Xue, J., Syed, B.M., Sun, J., Dai, X., Shi, M., Li, J., Wei, S., Tang, H., Zhang, A., Liu, Q., 2021. LncRNA H19-mediated M2 polarization of macrophages promotes myofibroblast differentiation in pulmonary fibrosis induced by arsenic exposure. *Environ. Pollut.* 268, 115810.
- Yadav, R.S., Chandravanshi, L.P., Shukla, R.K., Sankhwar, M.L., Ansari, R.W., Shukla, P.K., Pant, A.B., Khanna, V.K., 2011. Neuroprotective efficacy of curcumin in arsenic induced cholinergic dysfunctions in rats. *Neurotoxicology* 32, 760-768.
- Zhao, B., Ye, X., Yu, J., Li, L., Li, W., Li, S., Yu, J., Lin, J.D., Wang, C.Y., Chinnaiyan, A.M., Lai, Z.C., Guan, K.L., 2008. TEAD mediates YAP-dependent gene induction and growth control. *Genes Dev.* 22, 1962-1971.